PHOTOELECTRON SPECTROSCOPY OF SOME POLYATOMIC MOLECULES

by

FOO-TIM CHAU

B.Sc., The Chinese University of Hong Kong, 1970

M.Sc., The Chinese University of Hong Kong, 1972

A THESIS SUBMITTED IN PARTIAL FULFILMENT OF

THE REQUIREMENTS FOR THE DEGREE OF

DOCTOR OF PHILOSOPHY

in the Department of

CHEMISTRY

We accept this thesis as conforming to the

required standard

THE UNIVERSITY OF BRITISH COLUMBIA

August, 1975

In presenting this thesis in partial fulfilment of the requirements for an advanced degree at the University of British Columbia, I agree that the Library shall make it freely available for reference and study. I further agree that permission for extensive copying of this thesis for scholarly purposes may be granted by the Head of my Department or by his representatives. It is understood that copying or publication of this thesis for financial gain shall not be allowed without my written permission.

Department of Chemistry

The University of British Columbia
2075 Wesbrook Place
Vancouver, Canada
V6T 1W5

Date 30, Oct, 1975

ABSTRACT

The photoelectron spectrum of a molecule displays the kinetic energy distribution of the ejected photoelectron by monochromatic radiation. From the fine structure on a photoelectron band, valuable information about the bonding properties of both the molecule and its cation, and the ionic geometry can be obtained.

The work described in this thesis falls into two main parts. The first is concerned with the quantitative application of the Franck-Condon principle to group VI hydrides, nitrous oxide and dihaloethylenes, by which the geometries of their molecular ions were obtained. An iterative method was devised to facilitate the computational procedure.

The second part of this thesis contains the results of photoelectron spectroscopic studies on several halogenated molecules, viz. fluorotribromomethane, fluorotrichloromethane, 1,2-dichloro-, 1,2 dibromo-, and 1,2 diiodoethanes and their perfluoro derivatives, 1,2 bromochloroethane, 1,2-dibromo-1,1-difluoroethane, cis and trans 1,2 difluoroethylenes, and 1,2 dibromocyclohexane. One electron models including spin orbital coupling, and through bond and through space interactions, are applied to most of these molecules as well as the dichloro-, dibromo-, and diiodoethylenes. The NMR chemical shifts, nuclear quadrupole coupling constants, electronegativity of the halogen atom and the force constants of the molecules studied are discussed in the light of the calculated molecular orbital parameters.

TABLE OF CONTENTS

LIST OF FIGURES

Figure - Page

Figure | Page

LIST OF TABLES

ACKNOWLEDGEMENTS

I wish to express my gratitude to Professor C.A. McDowell for his invaluable help, encouragement and guidance throughout the course of this work. I would also like to thank Professor D. C. Frost for his support and continuous interest in this work.

I also wish to express my appreciation to Dr. C. E. Brion, Dr. R. J. Boyd, Dr. J. C. Bunzli, Dr. M. Chiang, Dr. D. P. Chong, Dr. G. Pouzard, Dr. S. T. Lee, Prof. W. C. Lin, Dr. A. J. Merer, Dr. L. Weiler and Dr. N. P. C. Westwood for helpful discussions. Thanks are due to Drs. D. Solgadi and Y. Gounelle for providing me with the observed IP's of trans 1,2 dibromocyclohexane, Dr. K. Wittel for the Franck-Condon factors of the dihaloethylenes, and Dr. J. H. Calloman for a preprint of his work.

I take this opportunity to acknowledge the skilful technical assistance of the staff of the Electronic, Glass and Mechanical Workshops of the Chemistry Department at UBC. I am especially grateful to Mr. E. Matter and Mr. C. McCafferty for maintenance of the photoelectron spectrometer used in this work.

I am indebted to Dr. N. P. C. Westwood for a careful reading of this manuscript.

I am most grateful to my fiancee for her love and encouragement, and finally to my God of love for giving me this opportunity to study.

CHAPTER I

INTRODUCTION

Irradiation of a molecule by monochromatic light with sufficiently high energy may produce ionization amongst other processes by the following event

$$Mol + h\nu = Mol^{+} + e^{-} \qquad (1.1)$$

Measurement of the kinetic energy distribution of the ejected photoelectron yields the photoelectron spectrum of that molecule and hence also yields the ionization potentials (IP's) of the molecule studied.

The kinetic energy E_e of the ejected electrons in process (1.1) is related to the incident photon energy $h\nu$ by the equation,

$$E_e = h\nu - I_i^a - \Delta E_{vib} - \Delta E_{rot} - \Delta E_{trans} \qquad (1.2)$$

where ΔE_{vib}, ΔE_{rot} and ΔE_{trans} are; respectively; the change in the vibrational,

rotational, and translational energy, involved in the transition. I_i^a is the adiabatic IP which is the energy difference between the ground vibrational and rotational levels of the molecule and the corresponding states of the resulting ion; in contrast to the vertical IP, I_i^v, which corresponds to the most probable ionization transition from the ground state of the molecule. The translational energy of the ion is usually very small because conservation of momentum requires that the energy be almost completely transferred to the outgoing electrons. Under the present level of experimental resolution, rotational energy is usually not resolved (the exceptions are H_2[1], H_2O[2] and HF[3] where resolution better than 7 mev is required) and thus ΔE_{rot} is also neglected. Furthermore, the molecule is generally in the ground vibrational state. Therefore, eqn. (1.2) is reduced to

$$E_e = h\nu - I_i^a - E_{vib}^+ \qquad (1.3)$$

where E_{vib}^+ is the vibrational energy of the ion.

Depending upon the light source used to produce ionization, photoelectron spectroscopy can be classified into two categories. The first one involves the use of higher energy X-ray sources which enables one to study the core electrons. This technique is termed ESCA (Electron Spectroscopy for Chemical Analysis) by K. Siegbahn and his collaborators[4,5] and has been found to be a powerful analytical tool because of the sensitivity of the binding energy to the chemical environment. It is, of course, a surface technique for solids, although recently there has been increasing use of gas phase ESCA.

The second category, called molecular photoelecron spectroscopy[6-11] or simply photoelectron spectroscopy (PES), involves the use of vacuum ultra-

violet radiation and is applicable only to the ionization of valence shell electrons. This kind of spectroscopic technique was developed independently by two groups of Russian and English scholars[6-11] in the early 1960's. Since then, there has been an exponential growth of work in this field with the appearance of a considerable number of review articles[11-29]. So far, the He I resonance line (21.22 ev) is the most popularly used light source owing to its narrower line width and high intensity. However, there is a growing interest in utilizing the He II resonance line (40.8 ev)[30]. Other sources such as argon (11.83 and 11.62 ev) and neon (16.85 and 16.67 ev) resonance lines[31,32] have also been employed. This thesis is mainly concerned with PES using the He I radiation.

It is well known that the ionization process is governed by the Franck-Condon principle. Quantitative application of the principle[33-36] enables one to determine the ionic geometry which is usually not attainable by optical spectroscopy. However, the computation of ionic geometries requires knowledge of the ionic frequencies as well as vibrational transition probabilities. PES provides valuable information of this sort. This thesis will describe the current methods employed in the Franck-Condon factor calculations, and application to group VI hydrides, nitrous oxide and dihaloethylenes. In addition, a Huckel molecular orbital treatment is devised to deduce some intrinsic molecular orbital parameters of a number of halogenated organic molecules such as 1,2 dihaloethanes, 1,2 dihalotetrafluoroethanes, 1,2 bromochloroethane, 1,2-dibromo-2,2-difluoroethane, dihaloethylenes and 1,2 dibromocyclohexane, by making use of the experimental IP's derived from their PE spectra (invoking Koopmans' Theorem[37]). The relation between the cal-

culated molecular orbital parameters and other physical constants, for instance, bond lengths, force constants, electronegativity of the halogen, and NMR chemical shifts will also be discussed.

CHAPTER II

THEORETICAL ASPECTS OF PHOTOELECTRON SPECTROSCOPY

2.1 Interpretation of Photoelectron Spectra

2.1.1 General Comments

The PE spectrum of a molecule consists of several bands, each of which relates to an ionization potential of the molecule. The lowest energy band is usually associated with the ground ionic state, while the others correspond to excited ionic states. According to Koopmans' theorem[37], (see below), the i^{th} vertical IP is equal to the negative of the i^{th} orbital energy. Thus the PE spectrum is a direct display of the energies of the various molecular orbitals (MO's). This theorem has been used extensively in assigning the gross structure of the PE spectra.

The vibrational fine structure, band shapes and ionic frequencies associated with each IP usually provide fruitful information about the bonding nature of the corresponding orbital, and are also helpful in assigning the correct orbital sequence. The interpretations of the band shape is largely based on the application of the Franck-Condon principle which will be discussed in Section 2.1.3.

The assignment of the PE bands of a molecule is often accomplished with the aid of spectra from other related compounds[38-40]. Resonance, inductive and hyperconjugation effects as well as the electronegative nature of the substituent groups are frequently utilized in the study. The perfluoro effect[41,42] may sometimes be used to differentiate the nonbinding, the π and the σ orbitals in planar molecules. Recently, the stretching force constants and also the logarithm of bond lengths are found to correlate linearly with a large number of homologous series[43,44]. The relationship obtained should also be helpful in assignment of spectra.

In the assumption of the constancy of photoionization cross sections, the relative intensities of the PE bands reflect the degeneracy of the orbitals from which electrons are removed. In other words, degenerate orbitals are usually associated with higher intensity bands. However, this guideline should be used with caution because it has been found to be invalid in some cases[16]. Experimentally[45,46], the intensity of a band related to an orbital with mainly s character, tends to increase with respect to that with mainly p character when higher energy light sources are used. Several theoretical investigations[47-53] using a plane wave approximation have been attempted to study the energy dependence of the photoionization cross sections and the bonding character of

orbitals, with some success. This approach may become a useful assignment criterion in the near future.

Since PES is not a threshold technique, the spectra are generally not complicated by the autoionization process. However, because of its resonant nature, autoionization in PES can usually be identified by using different light sources, and often leads to valuable information about the autoionizing states.

It should be mentioned that the light source used in PES is not truly monochromatic. Each of the spurious lines adds its spectrum to the total and errors in interpretation may occur[54-57]. Under normal conditions, the 21.22 ev He I line of the helium resonance lamp is accompanied in low intensities by lines at 40.82 ev (He II), 23.1 ev (He Iβ), 12.09 ev (Lyman β), 10.93 ev (NI), and 10.21 ev (Lyman α)[55-57].

2.1.2 Koopmans' Theorem

Koopmans' theorem, as mentioned before, states that the i^{th} orbital energy is related to the vertical IP, I_i^v according to the equation,

$$I_i^v = -\varepsilon_i^e \qquad (2.1)$$

with $$\varepsilon_i^e = H_{ii} + \sum_j^n \{2J_{ij} - K_{ij}\} \qquad (2.2)$$

H_{ii} is the expectation value of the one electron core hamiltonian corresponding to the orbital. J_{ij} and K_{ij} are known as the coulomb integral and exchange integral, respectively. Eqn. (2.1) can be derived from eqn. (2.2) by assuming that there is no reorganization energy[58,59] and no alteration in correlation energy between the molecule and its cation. Hence, the validity of Koopmans'

theorem depends on the delicate balance between these two energy terms. Usually, the IP's calculated are too large. For closed shell molecules, calculations near Hartree-Fock accuracy of valence shell orbital energies are often too high by~8%. Semi-empirical MO methods such as the CNDO/2[59] or INDO[59] methods usually give predicted IP's about 4 ev larger than the experimental values. Though the agreement is not perfect, in many cases, the calculated result is sufficient to assign unambiguously PE bands to ionizations from specific MO's in the molecules.

Despite the general success of Koopmans' theorem for closed shall molecules, its breakdown in predicting the correct ordering of the ionic states is not uncommon. In general, the theorem is more likely to fail when large orbital reorganization is involved in the ionization process. This includes the cases when the electron being removed is localized in one region of the molecule[60], either for symmetry reasons, or by virtue of it being a 'lone pair' electron. In the same manner, molecules containing electron-rich atoms like fluorine[61] tend to deviate from the prediction of Koopmans' theorem. Caution should also be made in the case where two or more orbitals lie close together, leading to doubts in assigning the experimental IP's.

Various theoretical methods have been attempted to reproduce the observed IP's. One approach is to carry out separate Hartree-Fock calculations for the molecule and its cation and to obtain IP's by their difference. Other approaches[62-69] involve the use of many-body techniques of second quantization[70,71] by which the vertical IP's are directly related to the poles of the one-particle Green's function[72]. Very recently, Chong, Herring and McWilliams[73,74] of this Department have employed Rayleigh-Schrodinger perturbation theory[75] to estimate the correlation energy of a closed shell

molecule and also the correlation and reorganization energies of the cation. Basis sets of double or one and a half zeta Slater orbitals are used in the computation. The calculated IP's reproduce well the experimental values within ±0.5 ev.

2.1.3 Franck-Condon Principle

The Franck-Condon principle states that an electronic transition takes place so rapidly that a vibrating molecule does not change its internuclear geometry appreciably during the transition.

The transition moment $P_{\underline{m}\,\underline{n}}$ for a vibronic transition between the $\underline{n}^{th}$ vibrational level in the neutral ground state and the $\underline{m}^{th}$ vibrational level of the ionic state can be expressed[76] as,

$$P_{\underline{m}\,\underline{n}} = \langle \Psi'_{\underline{m}}(Q') \mid M \mid \Psi_{\underline{n}}(Q) \rangle \qquad (2.3)$$

with $$M = \langle \phi'(\underline{q}', \underline{Q}') \mid \Sigma \underline{p}_n \mid \phi(\underline{q}, \underline{Q}) \rangle \qquad (2.4)$$

and $$\underline{m} = \Pi_i m_i \qquad (2.5)$$

in the Born-Oppenheimer approximation. The quantity with a line underneath denotes that the quantity is a matrix or column vector, $\underline{p}_n$ represents the momentum operator summed over all elctrons n, $\Psi(\underline{Q})$ and $\phi(\underline{q}, \underline{Q})$ are the total vibrational and electronic wavefunctions respectively. M is the electronic transition moment and the quantities $\underline{q}$ and $\underline{Q}$ designate the total electronic and normal vibrational coordinates of the molecule.

If the electronic transition moment varies slowly with the nuclear configuration, the intensity of the vibrational components within a progression

will be proportional to the Franck-Condon factor (FCF), the square of the overlap integral $\langle \psi_m' | \psi_n \rangle$. In general, the FCF is appreciable only when the maxima or minima of the two wavefunctions lie on top of each other, i.e. at the same Q_i (element of matrix $\underline{Q}$) and these maxima or minima for the higher vibrational levels appear near classical turning points of the motion. Therefore, the vertical electronic transitions are usually the most favorable.

Fig. 1 shows qualitatively the influence of the Franck-Condon principle on the vibrational patterns and the band shapes observed in the PE spectrum of a diatomic molecule. The shaded area called the Franck-Condon region which can be defined in terms of the maximum and minimum internuclear distance where observable transitions can occur. The fine structures of a band are determined by the potential curve of the resultant ion, which is in turn determined by the equilibrium distance r_e' and vibrational frequency ν' of the ion. r_e' may be greater, smaller or almost the same if the ejected photoelectron came from a bonding, antibonding or nonbonding orbital. The band shape may be further complicated by dissociation or predissociation of the ion. The general features of a PE spectrum for transitions from the neutral ground state to different ionic states are described in Fig. 1.

A further indication of the bonding character of the electron removed may be obtained by comparing the vibrational frequencies ν' in the ion with the corresponding frequencies ν in the neutral molecule. In diatomic molecules, these frequencies are related to the stretching force constant K by

$$\frac{\nu}{\nu'} = \left(\frac{K}{K'}\right)^{1/2} \tag{2.6}$$

THE FRANCK-CONDON PRINCIPLE IN PHOTOELECTRON SPECTROSCOPY

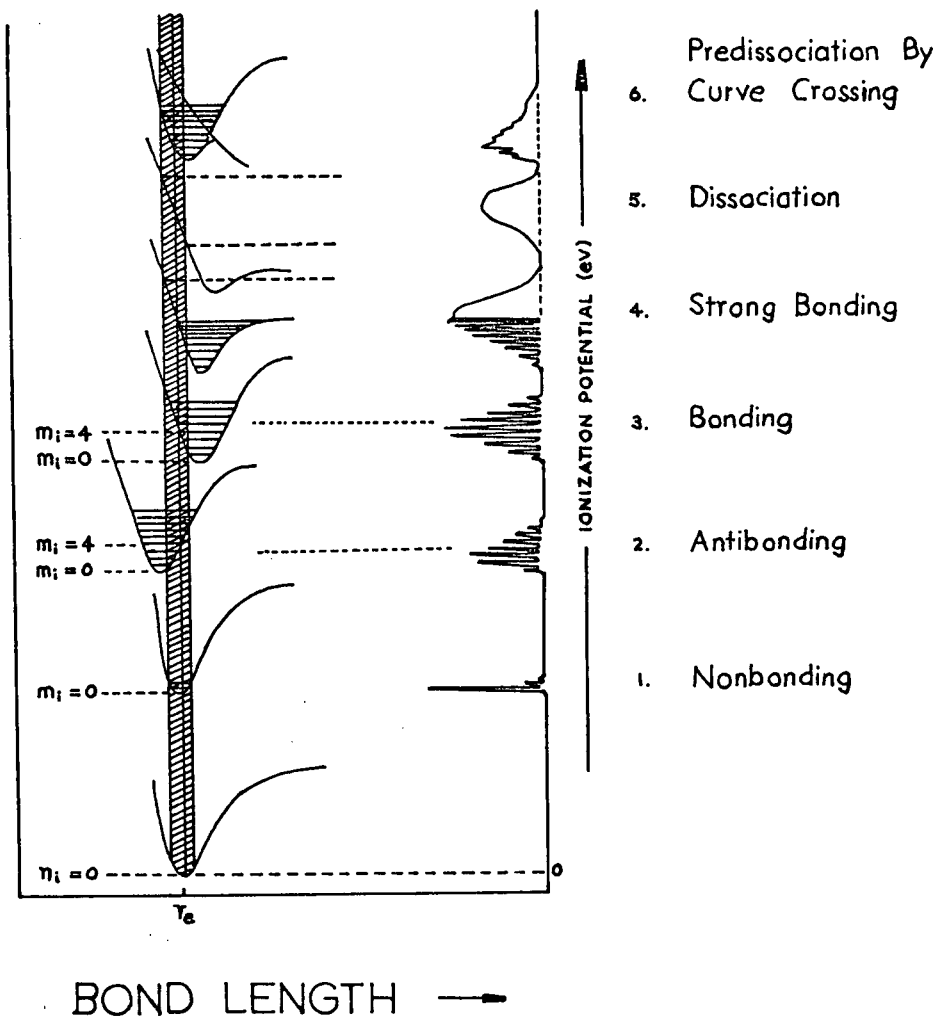

FIGURE 1

Thus if a nonbonding electron is removed, there will be practically no change in force constant and frequency, whereas if a bonding electron is removed, both quantities of the ion should be less than those of the parent molecule and vice versa for the removal of an antibonding electron.

With regard to polyatomic molecules, the above arguments for deducing bonding character from band shape and vibrational frequency should be used with care since one is now dealing with multidimensional potential surfaces, and changes in bond angle as well as bond length are involved. Nevertheless, the same ideas as given above for the diatomic case may be used as a guide to bonding character.

2.1.4 Through Bond and Through Space Interactions

Although the delocalized molecular orbitals obtained from a self-consistent-field calculation present a fairly accurate picture of the electronic structure of a molecule, it is usually easier to understand and interpret a PE spectrum in terms of the more familiar localized orbitals. For instance, a halogen lone pair molecular orbital (LPMO) means that most of the electron density resides on the halogen atom, but there are also contributions from other atomic orbitals in the molecule.

According to Hoffmann and his coworkers[77-78], localized orbital may interact with each other via two distinct symmetry-controlled mechanisms: (1) a through space interaction or (2) a through bond interaction. The former perturbation arises from the spatial overlap between the localized orbitals and the magnitude d_{ij} between the i^{th} and j^{th} orbitals can be

approximated as[79]

$$d_{ij} = k_d \, S_{ij} \, (\varepsilon_i \varepsilon_j)^{1/2} \tag{2.7}$$

where S_{ij} is the Mulliken overlap integral[80]. ε_i and ε_j are the Coulomb energies for the i^{th} and j^{th} orbitals respectively. The constant k_d is set equal to unity in this work[81].

In addition, localized orbitals can mix with each other indirectly through the intervening σ bonds of the same symmetry. This through bond interaction between the i^{th} orbitals, l_i , and the j^{th} σ orbital, σ_j , may be described quantitatively by using the second order perturbation method[82] in the approximation of zero differential overlap as,

$$E_i = \varepsilon_i + \frac{|\langle l_i | H' | \sigma_j \rangle|^2}{\varepsilon_i - \varepsilon_j} \tag{2.8}$$

$$E_j = \varepsilon_j + \frac{|\langle l_i | H' | \sigma_j \rangle|^2}{\varepsilon_j - \varepsilon_i} \tag{2.9}$$

with H' the perturbed hamiltonian. In this work, the second terms on the right hand side of eqns. (2.6 and 2.7) are parametized as S_i and are determined from experimental IP's. Since S_i is inversely proportional to the factor $(\varepsilon_i - \varepsilon_j)$, significant mixing between localized orbitals and σ orbitals occurs only for a small energy gap between the two interacting orbitals.

The concept of through bond and through space interactions has been used extensively in molecules with π bonds[83-87], and with nitrogen atoms [88,89]. This observation in PE or ultraviolet spectroscopy is used in deducing the orbital sequence of the frontier occupied orbitals. So far, these interactions

are considered qualitatively only. In chapter four of this thesis, PE spectra of a series of halogenated compounds will be given and both the through bond and through space interactions between the halogen LPMO's and σ orbitals are treated quantitatively. Fruitful information is obtained on the bonding properties of the molecules studied.

2.1.5 Spin Orbit Coupling

Consider a halide molecule RX (with X the halogen atom) in which the bond R - X coincides with an n-fold axis of the system ($n \geq 3$). Removal of an electron from a π type halogen LPMO will give rise to an ion in a doublet spin state. Because of the spin orbit coupling interaction, the $^2\Pi$ term is split into two levels $^2\Pi_{3/2}$ and $^2\Pi_{1/2}$ with an energy difference given by,

$$\mathcal{E}(^2\Pi_{3/2}) - \mathcal{E}(^2\Pi_{1/2}) = \Delta \qquad (2.10)$$

The magnitude of the splitting Δ can be estimated by using the following spin orbit operator[93]

$$H_{SO} = \sum_{\substack{\text{all} \\ \text{electrons}}} \zeta(r_i)\, \vec{l}_i \cdot \vec{s}_i \qquad (2.11)$$

with $$\zeta(r_i) = \frac{e}{2 m_e^2 c^2 r_i} \left(\frac{\partial V(r_i)}{\partial r_i}\right) \qquad (2.12)$$

where e is the electronic charge

m_e is the mass of the electron

c is the velocity of light

r_i is the distance of the i^{th} electron from the nucleus

$V(r_i)$ is the potential at the electron arising from the nucleus

$\vec{l}_i^{\circ}$ is the orbit operator for the i^{th} electron

$\vec{s}_i^{\circ}$ is the spin operator for the i^{th} electron

If an electron is removed from the π type LPMO's l_λ (angular momentum quantum number), $\lambda = +1$ or -1 which is centered entirely on the halogen atom of RX, i.e. $l_\lambda = p_\lambda$, then we should expect, according to eqn. (2.10), that the corresponding band in the PE spectrum will exhibit two components with an energy gap (assuming Koopmans' theorem[37] to hold),

$$I^v_{3/2} - I^v_{1/2} = \Delta \tag{2.13}$$

$I^v_{3/2}$ and $I^v_{1/2}$ are the vertical IP's corresponding to the $^2\pi_{3/2}$ and $^2\pi_{1/2}$ states respectively. Δ is equal to $-\zeta_x$, which is 2/3 of the spin orbit coupling constant of X.

If, on the other hand, the LPMO l_λ where ionization takes place is not strictly localized on X, but is a linear combination (in the zero differential overlap approximation)

$$l_\lambda = C_x p_x + \sum_{K \neq X} C_K \phi_\lambda(K) \tag{2.14}$$

with $\phi_\lambda(K)$ being the basis atomic orbitals localized in the alkyl group. Then ζ in equn. (2.10) should now be given by,

$$\zeta = C_x^2 \zeta_x + \sum_{K \neq X} C_K^2 \zeta_K \tag{2.15}$$

Hence the splitting Δ between the two $^2\pi$ components is a sensitive probe for the relative participation of the orbitals p_λ and $\phi_\lambda(K)$ in the LPMO l_λ.

Recently, Heilbronner and his coworkers[94,95] have recorded the PE spectra of some alkyl bromides (some with low symmetry e.g. C_s) and they found that the splittings Δ obtained from these spectra have the full value of ζ_x in spite of appreciable mixing between orbitals of the alkyl group and the bromine atom. To explain these observations, a one electron model was proposed with the inclusion of conjugative interaction between orbitals of bromine and the alkyl group as well as spin orbit coupling between the LPMO's of bromine itself. Under the assumption that the ejected electron has β spin (this yields the inverse order $E(^2\Pi_{1/2}) > E(^2\Pi_{3/2})$), one obtains the following matrix elements:

$$\begin{aligned}
&\langle p_x | H_{so} | p_x \rangle = \langle p_y | H_{so} | p_y \rangle = 0 \\
&\langle p_z | H_{so} | p_y \rangle = \langle p_z | H_{so} | p_y \rangle = 0 \\
&\langle p_z | H_{so} | p_z \rangle = 0 \\
&\langle p_x | H_{so} | p_y \rangle = -i\zeta/2 \\
&\langle p_y | H_{so} | p_x \rangle = i\zeta/2
\end{aligned} \qquad (2.16)$$

The same spin orbit operator is used in the one electron models devised to interpret the PE spectra of halogenated compounds (in chapter 4).

2.1.6 Jahn-Teller Splitting

The Jahn-Teller theorem[96] states that a non-linear molecule in a degenerate electronic state is unstable towards nuclear distortions which lower the molecular symmetry, and thereby remove the electronic degeneracy.

When this effect is active in a PE spectrum, a band may be split into several components, sometimes separated by as much as 1 ev[97]. The effect is largest when the degenerate orbital concerned is strongly involved in the bonding and is minimal for degeneracy in nonbonding orbitals. However, there is no direct way of predicting the magnitude of this effect that may be observed.

Quantitative treatment of the Jahn-Teller effect on PE spectra of methyl halides[98], ammonia[99] and methane[100] has been carried out to attain a better understanding of the structure of their respective cations. The corresponding effect in degenerate orbitals of linear molecules is called the Renner-Teller effect and has been observed in the case of water[101] and hydrogen sulphide[102].

2.2 Quantitative Application of the Franck-Condon Principle in Photoelectron Spectroscopy

2.2.1 Method of Franck-Condon Factor Calculation

(a) General Description of the Method

The relative arrangement of the nuclei of a molecule at vibrational equilibrium is often simply called its structure. In general, the structure of an ion differs from its parent molecule, and the deviation therefrom depends upon the nature of the orbital involved in the ionization process. The geometry of neutral polyatomic molecules can be determined by various physical methods such as electron diffraction, ultraviolet, infrared, Raman and microwave spectroscopy. However, structural data are available for only a small number of ions[76] e.g. CO_2^+, COS^+, N_2O^+. Rotational fine structure in the

vibronic bands of an ultraviolet absorption system occasionally yields information of this kind. Therefore, the Franck-Condon principle offers the only alternative method of obtaining information about the ionic geometry.

Assuming the validity of the Born-Oppenheimer Approximation, and the constancy of the electronic transition moment, the vibrational transition probability or intensity $I_{\underline{m}\underline{n}}$ is given as,

$$I_{\underline{m}\underline{n}} = H_n |\langle \psi'_{\underline{m}} | \psi_{\underline{n}} \rangle|^2 \tag{2.17}$$

The constant H_n includes those contributions from the electronic transition moment as well as the design of the PE spectrometer[103]. In the harmonic oscillator approximation, each vibrational wavefunction $\psi(Q)$ may be expressed as a product of 3N-6 (for linear molecules 3N-5) θ_i, Hermite orthogonal functions[82]. N is the number of atoms in the molecule. Then the overlap integral in eqn. (2.17) can be separated into 3N-6 components

$$\begin{aligned} b_{\underline{m}\underline{n}} &= \langle \psi'_{\underline{m}} | \psi_{\underline{n}} \rangle \\ &= \Pi_i^{3N-6} b_{m_i n_i} \end{aligned} \tag{2.18}$$

with $$b_{m_i n_i} = \langle \theta'_{m_i}(Q'_i) | \theta_{n_i}(Q_i) \rangle \tag{2.19}$$

To evaluate the integral $b_{m_i n_i}$, the coordinates of the ionic state must be expressed as functions of the coordinates in the ground state. This can be accomplished by a linear transformation[104]

$$\underline{Q'} = \underline{J}\,\underline{Q} + \underline{d} \tag{2.20}$$

where $\underline{J}$ is a (3N-6) x (3N-6) square matrix and $\underline{d}$, a column vector of order 3N-6, having elements d_i representing the separation of the origins of the two coordinates. A similar expression can be written in terms of the internal symmetry displacement coordinates or simply by the symmetry coordinates (section 2.2.3a) $\underline{S}$ and $\underline{S'}$ as

$$\underline{S'} = \underline{S} + \underline{\Delta S} \tag{2.21}$$

Upon employing the transformation from symmetry to normal coordinates,

$$\underline{S'} = \underline{L'_s}\ \underline{Q} \quad ; \quad \underline{S} = \underline{L_s}\ \underline{Q} \tag{2.22}$$

we obtain

$$\underline{Q'} = (\underline{L'_s})^{-1}\ \underline{L_s}\ \underline{Q} + (\underline{L'_s})^{-1}\ \underline{\Delta S} \tag{2.23}$$

A comparison of eqns. (2.23) and (2.20) yields the definition

$$\underline{J} = (\underline{L'_s})^{-1}\ \underline{L_s} \tag{2.24}$$

$$\underline{d} = (\underline{L'_s})^{-1}\ \underline{\Delta S} \quad \text{or} \quad \underline{\Delta S} = \underline{L'_s}\ \underline{d} \tag{2.25}$$

The off diagonal elements of matrix $\underline{J}$ are different from zero only when the i^{th} and j^{th} normal coordinates have the same symmetry unless changes in molecular symmetry occur upon ionization. d_i is nonzero for totally symmetric vibrations only.

From eqn. (2.25), a knowledge of $\underline{d}$ can be related to $\underline{S'}$, from which the change in internal coordinates (changes in interatomic distances or in the angles between chemical bonds or both) is in turn calculated.

The Ls and Ls′ matrices are readily obtained through a normal coordinate analysis, (see section 2.2.3) or a force constant analysis using the vibrational frequencies in the corresponding state. However, the number of observed vibrational frequencies in the ionic state is usually not large enough to carry out a normal coordinate analysis. In such a case, we use Ls instead of Ls′ .

Making use of the property of Hermite polynomials and relation (2.18), $b_{m_j n_j}$ was expressed by Ansbacher[105] in the form,

$$b_{m_j n_j} = a_{m_j n_j} \left(\frac{1-\beta_j^2}{1+\beta_j^2}\right)^{\frac{m_j+n_j}{2}} \sum_{l=0}^{[m_j,n_j]} \left(\frac{4\beta_j}{1-\beta_j^2}\right)^{l} \frac{(-1)^{m_j-l}}{l!\,(m_j-l)!\,(n_j-l)!} \times H_{m_j-l}\left[i\beta_j^2\gamma_j(1-\beta_j^4)^{-1/2}\right] H_{n_j-l}\left[-\beta_j\gamma_j(1-\beta_j^4)^{-1/2}\right] \tag{2.26}$$

where

$$a_{m_j n_j} = (m_j!\,n_j!)^{1/2}\, 2^{-(m_j+n_j-1)/2} \left(\frac{\beta_j}{1+\beta_j^2}\right)^{1/2} \exp\left[-\frac{\gamma_j^2\beta_j^2}{2(1+\beta_j^2)}\right] \tag{2.27}$$

and $[\, m_j , n_j \,]$ denotes the smaller of the two integers m_j and n_j . In this formula, H_{m_i} is the Hermite polynomial of degree m_i , $\beta_j = \alpha_j/\alpha_j' = (\nu_j/\nu_j')^{1/2}$, $\gamma_j = \alpha_j' d_j$ and $\alpha_j^2 = 4\pi^2\nu_j c/h$ with h as Planck's constant. Now, the relative transition probabilities for overtones may be given as,

$$\frac{b_{m_j 0}}{b_{00}} = \frac{2^{-m_j/2}(-1)^{m_j}}{(m_j!)^{1/2}} \left(\frac{1-\beta_j^2}{1+\beta_j^2}\right)^{m_j/2} H_{m_j}\left[i\beta_j^2\gamma_j(1-\beta_j^4)^{-1/2}\right] \tag{2.28}$$

according to eqns. (2.26) and (2.27), or

$$b_{m_j 0} = \frac{\beta_j^{1/2} (m_j!)^{1/2}}{[2^{m_j-1}(1+\beta_j^2)]^{1/2}} \exp\left[-\frac{1}{2}\gamma_j^2 \left(\frac{\beta_j^2}{1+\beta_j^2}\right)\right]$$

$$\times \sum_{l\geq 0}^{m_j} \left(-\frac{2\gamma_j \beta_j}{1+\beta_j^2}\right)^l \frac{1}{l!\left(\frac{m_j-l}{2}\right)!} \left(\frac{\beta_j^2-1}{\beta_j^2+1}\right)^{\frac{m_j-l}{2}} \tag{2.29}$$

according to Heilbronner and his coworkers[106]. The summation extends only over even (odd) indices l in the interval $0 \leq l \leq m_j$ if m_j is even (odd). With the aid of the recursion formula for the Hermite polynomials[82], it can be shown that

$$\frac{b_{m_j+1,0}}{b_{m_j 0}} = \frac{\sqrt{2}\,\beta_j^2 \gamma_j}{(1+\beta_j^2)(m_j+1)^{1/2}} + \left(\frac{m_j}{m_j+1}\right)^{1/2} \frac{b_{m_j-1,0}}{b_{m_j 0}} \left(\frac{1-\beta_j^2}{1+\beta_j^2}\right) \tag{2.30}$$

The Hermite polynomials rapidly become complicated as m_j increases, but the recursion formula (2.28) allows one to calculate numerical values of $b_{m_j 0} / b_{00}$ up to any desired value of m_j with comparative ease.

So far,, the treatment is restricted to a one-dimensional problem i.e. d_i is determined separately. The method (hereafter referred to as method A) enjoys the popularity for the ease in computation. Using the generating function technique, Rosenstock and his coworkers[35] have developed a method to calculate FCF of overtones and combination bands of several vibrational frequencies at the same time. The derivation of this method (method B) is similar to the former one. Briefly, in the Born-Oppenheimer approximation, assuming constancy of the electronic transition moment,

harmonic oscillator approximation and linear relationship (2.20), we get,

$$\sum_m \sum_n \underline{T_f}^m \underline{U_f}^n \, (2^m 2^n / \underline{m}\,!\,\underline{n}\,!) \, I_{\underline{m}\,\underline{n}} \tag{2.31}$$

$$= I_o \exp \left[\left(\underline{T_f}^t \, \underline{A} \, \underline{T_f} + \underline{T_f}^t \, \underline{B} \right) + \left(\underline{U_f}^t \, \underline{C} \, \underline{U_f} + \underline{U_f}^t \, \underline{D} \right) + \underline{U_f}^t \, \underline{E} \, \underline{T_f} \right]$$

where
$$I_o = \left[\det \left(\underline{\Gamma} \, \underline{\Gamma}' \right)^{4\mu} \right]^{1/4} \left[\det \left(\underline{J}^t \, \underline{\Gamma}' \, \underline{J} + \underline{\Gamma} \right) \right]^{-1/2} \tag{2.32}$$

$$\times \exp \left[-\tfrac{1}{2} \, \underline{d}^t \, \underline{\Gamma}' \, \underline{d} + \tfrac{1}{2} \, \underline{d}^t \, \underline{\Gamma}' \, \underline{J} \left(\underline{J}^t \, \underline{\Gamma}' \, \underline{J} + \underline{\Gamma} \right)^{-1} \underline{J}^t \, \underline{\Gamma}' \, \underline{d} \right]$$

$$\underline{A} = 2 \, \underline{\Gamma}'^{1/2} \, \underline{J} \left(\underline{J}^t \, \underline{\Gamma}' \, \underline{J} + \underline{\Gamma} \right)^{-1} \underline{J}^t \, \underline{\Gamma}'^{1/2} - \underline{1} \tag{2.33}$$

$$\underline{B} = -2 \, \underline{\Gamma}'^{1/2} \left[\underline{J} \left(\underline{J}^t \, \underline{\Gamma}' \, \underline{J} + \underline{\Gamma} \right)^{-1} \underline{J}^t \, \underline{\Gamma}' - \underline{1} \right] \underline{d} \tag{2.34}$$

$$\underline{C} = 2 \, \underline{\Gamma}^{1/2} \left(\underline{J}^t \, \underline{\Gamma}' \, \underline{J} + \underline{\Gamma} \right)^{-1} \underline{\Gamma}^{1/2} - \underline{1} \tag{2.35}$$

$$\underline{D} = -2 \, \underline{\Gamma}^{1/2} \left(\underline{J}^t \, \underline{\Gamma}' \, \underline{J} + \underline{\Gamma} \right)^{-1} \underline{J}^t \, \underline{\Gamma}' \, \underline{d} \tag{2.36}$$

$$\underline{E} = 4 \, \underline{\Gamma}^{1/2} \left(\underline{J}^t \, \underline{\Gamma}' \, \underline{J} + \underline{\Gamma} \right)^{-1} \underline{J}^t \, \underline{\Gamma}'^{1/2} \tag{2.37}$$

μ is dimension of matrices $\underline{\Gamma}$, $\underline{d}$ etc. with value less or equal to 3N-6. $\underline{\Gamma}$ is the diagonal matrix of frequencies $4\pi^2\nu_i/h$. The superscript t indicates the Hermitian conjugate of a matrix (which is, for a real matrix, the transpose). $\underline{T_f}$ and $\underline{U_f}$ are the dummy variables for the ionic and neutral ground states respectively. The individual overlap integrals $I_{\underline{m}\underline{n}}$ are now obtained by expanding the right hand side of eqn. (2.31) and equating coefficients of appropriate powers of $\underline{T_f}$ and $\underline{U_f}$. General expressions for calculating FCF's of overtones, combination levels and hot bands are well documented in refs. 35 and are not repeated here. It should be mentioned that both methods A and B cannot be applied to ionization process with changes in the vibrational degrees of freedom between a molecule and its ion.

(b) Method of Calculation

The general procedure in FCF calculations with the application of method A is outlined below.

1. The intensities $I_{\underline{m}\underline{n}}$ of the fine structure components in a PE band are measured. In the approximation of the intensities they are assumed to be proportional to the heights of the fine structure maxima, i.e. under the implicit assumption of a constant half width of the components. Usually, the maximum FCF is arbitrarily set to be 1 unit and the other FCF's are scaled accordingly.

2. For each observed vibrational mode, the FCF's are evaluated at a series of d_i values or by means of a least square fit method (section 2.2.2). The best d_i value is then chosen on the basis of two citeria:- (i) the overall

qualitative features of the experimental FCF's from the experimental FCF's is a minimum. For those vibrational modes not observable in the spectrum, the corresponding d_i's are set equal to zero.

3. A normal coordinate analysis is performed on the ground state of the molecule studied, using vibrational frequencies determined from infrared and Raman spectroscopy. Hence the $\underline{Ls}$ matrix is obtained.

4. Through expression (2.25) and $\underline{Ls}$ used instead of $\underline{Ls}'$, $\underline{d}$ is employed to calculate $\underline{\Delta S}$ and hence the change in internal coordinates. Since the sign of each d_i is undetermined, there are 2^{n_s} possible ionic state models consistent with the observed FCF's, where n_s is the number of vibrational modes of the same symmetry excited. If the geometry of the ionic state studied is known, the sign of Δr_i, the difference in bond lengths in the ionic state and the ground state, is simply chosen in accordance with observation. However, this kind of information is not available for most polyatomic molecules. Therefore, the following cirteria are usually used to determine the sign:

(i) the change in a bond length during an ionization process is related in a reverse manner to the bonding character of the bond, and hence the orbital from which an electron is removed,

(ii) the sign of Δr_i agrees with that of $f_i - f_i'$, the difference in force constants or $\nu_i - \nu_i'$, the difference in vibrational frequencies, and finally,

(iii) the change in bond distance parallels the difference in the overlap population, or bond order of the bond, between the neutral molecule and its cation.

With regard to a change in bond angle, there are no definite guidelines given in the literature for choosing the appropriate sign. This promotes us to propose a criterion to do so by making use of the concept of anodal repulsive force[107]. For instance, the highest occupied molecular orbital of gem dihaloethylene possesses C-C π bonding but C-X antibonding

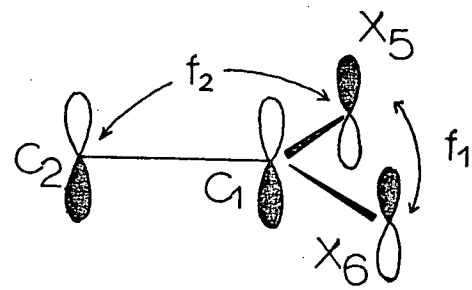

character. The force f_1 is attractive while f_2 is repulsive in the molecule. The interaction between X_5 and H_3 is neglected for large internuclear distances. If an electron is removed from this orbital, both f_1 and f_2 are weakened and hence the angle $X_5C_1X_6$ is increased. The opposite is true for angle $C_2C_1X_5$. The angle changes should more or less depend on the overlap population between nonbonded atoms. The CCH angle change cannot be predicted in this case because the coefficients of hydrogen atomic orbitals are zero.

5. If the number of ionic frequencies observed is not sufficient to carry out a force constant analysis, the structural parameters obtained from (4) are regarded as the geometry of the ion. If not, the structure obtained is

used to calculate $\underline{Ls'}$ and also a new $\underline{\Delta S}$. This process is repeated until the $\underline{Ls'}$ do not change significantly. Usually, one or two cycles are enough. Even for H_2O^+ in the $^2A_1$ state with geometry deviating largely from that of the neutral molecule, only three cycles are required to obtain a consistent $\underline{Ls'}$ matrix (section 3.1.3c).

Determination of the ionic geometry using method B is mainly carried out by a FORTRAN program (appendix I) written for the IBM 370 computer. Input data required are the dimension μ , frequencies ν and ν' , $\underline{\Delta S}$, $\underline{Ls}$ and $\underline{Ls'}$ matrices as well as the number of overtones and combination levels desired in the calculation, while the transition probabilities of overtones and combination bands are printed after the computation. The theoretical intensity distribution can be displayed graphically upon request. $\underline{\Delta S}$ is varied in a trial and error manner until the criteria mentioned before are satisfied. The calculated result by using this program was checked against that of Botter and Rosenstock[108] with good agreement.

2.2.2 Iterative Method in Franck-Condon Factor Calculation

In all the current FCF calculations (method A), evaluation of d_i from the observed overlap integrals for overtones OIO (square root of FCF) $b_{m_i 0}$ is done in a trial and error manner. First a value of d_i is chosen arbitrarily and thus γ_i and β_i are computed. A set of OIO's is then evaluated up to the desired number of m_i and these are compared with the observed OIO's. γ_i is adjusted until agreement is reached. However, the treatment becomes more and more tedious to handle for increasing numbers of overtones observed, as well as for large changes in geometry upon ionization. In this

section, an iterative method is proposed by which the value of d_i will be refined automatically to match the observed OIO's by a least squares fit adjustment.

Computation of d_i requires the knowledge of at least two observed OIO's within a progression. If only two OIO's are available experimentally, d_i can be determined uniquely. However, in many cases, the number of overtones observed is greater than two and the least squares fit technique is required to obtain a value of d_i that gives the best fit between the observed and calculated OIO's. The general outline of the treatment used in this work is as follows:-

(a) An estimated value of d_i, d_i° is used to calculate a set of $b_{m_i o}$, $\underline{b}$. Then these calculated OIO's are compared with the observed ones $\underline{b^{obs}}$, and the error vector $\underline{\Delta b}$ is defined as,

$$\underline{\Delta b} = \underline{b^{obs}} - \underline{b} \tag{2.38}$$

The weighted sum of squares deviation is given as,

$$S_d = \underline{\Delta b}^t \, \underline{W} \, \underline{\Delta b} \tag{2.39}$$

$\underline{W}$ is a diagonal matrix with elements giving the statistical weights of the observed OIO's, $W_{ii} = b_{m_i o}^{n_w}$. n_w can be any real number and is fixed to be -2.0 throughout this work since the weighting factor enables one to fit the observed OIO's on a percentage basis.

(b) Assuming that there is a linear relationship between $\underline{\Delta b}$ and Δd_i, the correction for d_i, then we obtain,

$$\underline{\Delta b} = \underline{J P} \, \Delta d_i \tag{2.40}$$

where $\underline{JP}$ is a column vector with element $JP_{m_i} = d\, b_{m_i o}/d\, d_i$, i.e. derivative of $b_{m_i o}$ with respect to d_i. JP_{m_i} is related to $b_{m_i o}$, β_i and γ_i in the following way:-

$$JP_{m_i} = -\frac{2\beta_i^2}{1+\beta_i^2}\,\gamma_i\, b_{m_i o} + \frac{2\beta_i^{1/2}\,(m_i!)^{1/2}}{\gamma_i\,[2^{m_i-1}(1+\beta_i^2)]^{1/2}}\,\exp\left[-\frac{\beta_i^2\,\gamma_i}{2(1+\beta_i^2)}\right]$$

$$\times \sum_{l\geq 0}^{m} \left(-\frac{2\gamma_i\beta_i}{1+\beta_i^2}\right)^l \frac{1}{(l-1)!\,\left(\frac{m_i-l}{2}\right)!} \left(\frac{\beta_i^2-1}{\beta_i^2+1}\right)^{\frac{m_i-p}{2}} \tag{2.41}$$

from eqn. (2.29). Then Δd_i is computed through the expression (2.42)

$$\underline{JP}^t\ \underline{W}\ \underline{JP}\ \Delta d_i = \underline{JP}\ \underline{W}\ \underline{\Delta b} \tag{2.42}$$

(c) A new d_i is obtained through the relation

$$\underline{d_i^{new}} = \underline{d_i^{old}} + C_a\,\Delta d_i \tag{2.43}$$

where C_a is an arbitrary scaling factor for damping purposes, and d_i thus obtained is used over again until the desired number of reiterations are completed.

A FORTRAN program (appendix II) based on the method described above has been written for the IBM 370 computer. The $\underline{b^{obs}}$, C_a and d_i° comprise the input while the calculated $\underline{b}$, d_i and S_d are printed out after each iteration.

The least squares fit method mentioned above has been tested for two cases. Transitions from the ground state to the $A\,^2\Pi_u$ states of CS_2,

and the $^2A_1$ state of $CFBr_3$ where the corresponding OIO's are given in ref. 11 and section 4.1 respectively. In these transitions, excitation of only one vibrational mode is observed.

The results of the calculations indicate that even for a poor approximation of d_i° (about 30-40% off from the best value of d_i for a certain ion), it is always possible to know roughly where the best value of d_i is by adjusting the factor C_a in expression (2.43). Then, a better approximation of d_i° can be made for the next calculation. Once a good estimation of d_i° is made (within 90% of the best value of d_i obtained), d_i will keep on increasing or decreasing with the value of S_d decreasing first, passing through a minimum and then increasing very slowly afterward. Fig. 2 shows the general trend of the iterative process. The best value of d_i obtained for the $^2A_1$ state of $CFBr_3$ and the $A\ ^1\Pi_u$ state of CS_2 are 1.8700 and 0.7349 x 10^{-20} $gm^{1/2}$ cm respectively, and the calculated OIO's for these molecules from these d_i values are shown in Table 1. Theoretically, Δd_i should approach to zero in the iterative process. However, in fact, this is not true, which is probably due to the validity of the linear relation (2.41) as well as the accuracy of the intensity of the components within a progression which are overlapping with each other.

Up to now, little attention has been paid by previous workers with regard to the criteria necessary in choosing a value of d_i. Here, we have proposed the weighted sum of squares deviation as one of the criteria, since in such a treatment there is no discrimination on the low intensity components within a progression.

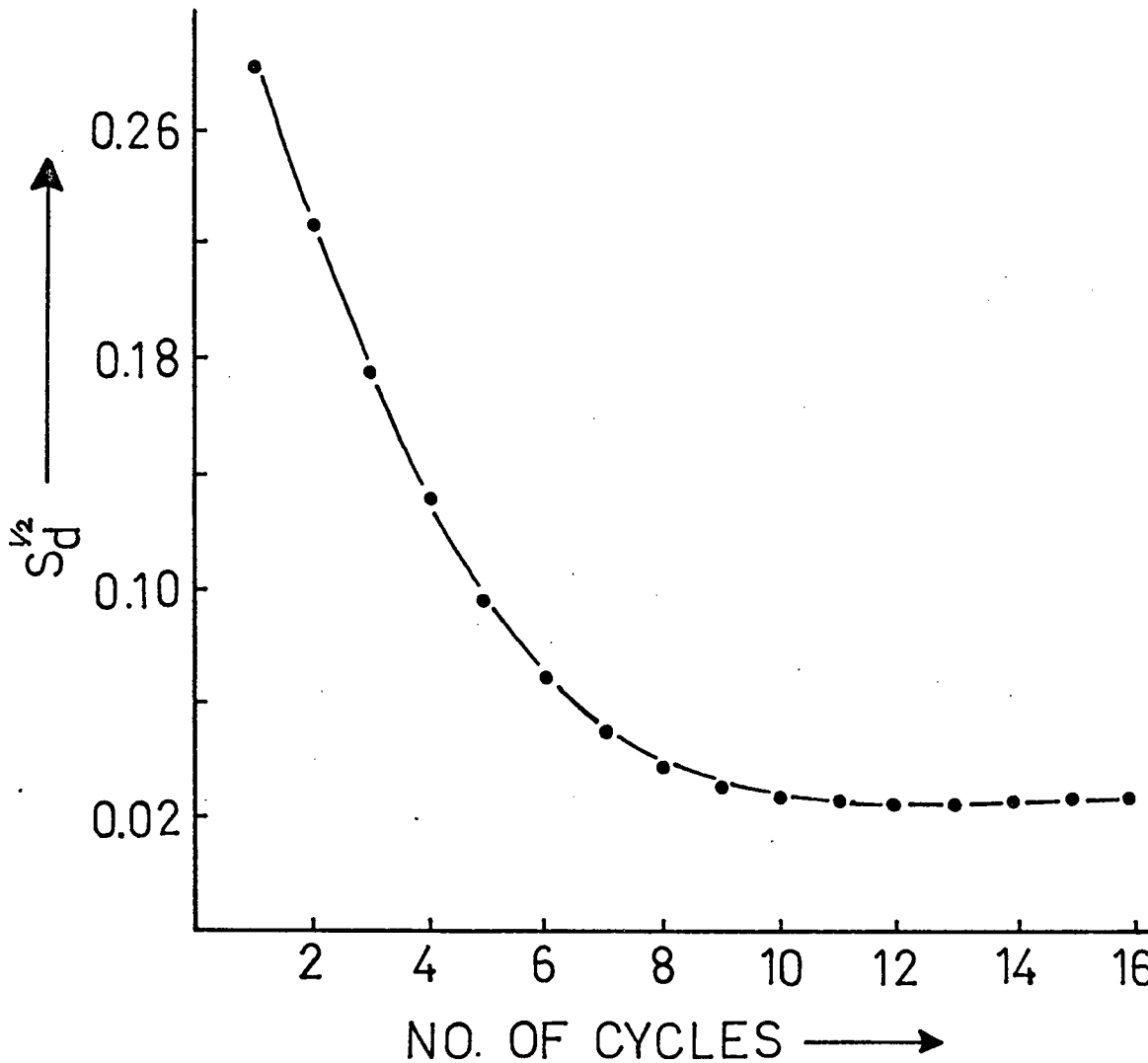

Figure 2. Plot of the weighted sum of squares deviation against the number of cycles for the $^1\Sigma_g^+ \longrightarrow A\,^2\Pi_u$ transition of CS_2 during the iterative process (n_w = -2, C_a = -5.0 and d_i° = 0.5 x 10^{-20} $gm^{\frac{1}{2}}$ cm).

Table 1. Calculated and Observed Overlap Integral (OIO) For the $^2A_1$ State of $CFBr_3$ and the A $^3\Pi_u$ state of CS_2

m_i	$CFBr_3$		CS_2	
	Obs. OIO[a]	Cald. OIO	Obs. OIO[b]	Cald. OIO
0	—	0.15	0.65	0.55
1	0.42	0.41	0.93	0.98
2	0.59	0.62	1.00	1.00
3	0.79	0.80	0.87	0.89
4	0.92	0.94	0.70	0.70
5	1.00	1.00	0.53	0.51
6	0.98	0.99	0.35	0.34
7	0.90	0.91	0.22	0.21
8	0.77	0.79		
9	0.64	0.65		
10	0.53	0.51		

[a] Obs. OIO is estimated from Table 14. The maximum OIO is arbitrarily set to be one unit.

[b] Obs. OIO is obtained from ref. 11.

2.2.3 Normal Coordinate Analysis

(a) General Principles

A molecule or an ion may be considered as a system of atoms elastically coupled together. The forces between them are electrostatic in nature. When the nuclei are displaced from their equilibrium positions, restoring forces due to the potential field of the electrons and nuclei will act on the system. This kind of potential field is described in terms of the force constants associated with the restoring forces. Since force constants always provide valuable information about the bonding nature of the species studied, it is desirable to obtain these constants from the observed properties such as vibrational frequencies.

This is usually accomplished by calculating the frequencies, assuming a suitable set of the force constants. If the agreement between the observed and calculated frequencies is satisfactory, this particular set of force constants is adopted as a representation of the potential energy of the system. The Ls matrix deduced gives the correlation between the symmetry coordinate and the normal coordinate.

To evaluate the force constants, it is necessary first to express both the potential and kinetic energies of the molecule in terms of some common coordinates. Changes in bond lengths and bond angles can be used to provide a set of displacement coordinates, the internal coordinates, R_i. These coordinates are unaffected by translation or rotation of the molecule as a whole. The corresponding force constants have a clearer physical meaning than those expressed in terms of other coordinates since they are characteristic of the bond stretchings and the angle deformations

involved. The number of internal coordinates is equal to or, if redundant coordinates exist, greater than 3N-6.

In terms of the internal coordinates, the following secular determinant can be obtained[109]

$$|\underline{G}\,\underline{F} - \underline{\Lambda}| = 0 \tag{2.44}$$

or

$$\underline{G}\,\underline{F}\,\underline{L} = \underline{L}\,\underline{\Lambda} \tag{2.45}$$

where $\underline{G}$ is the inverse kinetic energy matrix in internal coordinates

$\underline{F}$ is the force constant matrix in internal coordinates

$\underline{\Lambda}$ is a diagonal matrix with element λ_i

$$\lambda_i = 4\pi^2 c^2 \nu_i^2 \tag{2.46}$$

The $\underline{G}$ matrix is a function of the molecular geometry only, and the methods for constructing this matrix have been described in detail by Wilson et al[109] and will not be given here.

The time required to solve the vibrational secular determinant (2.45) increases rapidly with increasing order of the determinant. An efficient way to reduce it is to use symmetry coordinates which transform as certain irreducible representations of the molecular point group. They are related to the internal coordinates by the orthonormal transformation matrix $\underline{U}$

$$\underline{S} = \underline{U}\,\underline{R} \tag{2.47}$$

The projection operator[110] or the method given by Wilson et al[109] may be used to generate the symmetry coordinates. In terms of these coordinates,

the secular equations (2.44) and (2.45) are factored to the maximum extent and can be expressed as,

$$\underline{G_s}\,\underline{F_s} - \underline{\Lambda} = \underline{0} \tag{2.48}$$

or

$$\underline{G_s}\,\underline{F_s}\,\underline{L_s} = \underline{L_s}\,\underline{\Lambda} \tag{2.49}$$

where $\underline{Gs}$ and $\underline{Fs}$ are respectively the inverse kinetic energy matrix and the force constant matrix in the symmetry coordinates. $\underline{0}$ is the null matrix.

(b) Molecular Force Field

As discussed in the previous section, the molecular force field of a polyatomic molecule is described by the $\underline{F}$ matrix if internal coordinates are used. Such a force field is generally with no inherent assumptions at all if there is no redundant coordinate and is called the general valence force field (GVFF). Methematically, it is given by

$$\begin{aligned} 2V = {} & \Sigma_i f_{r_i} (\Delta r_i)^2 + \Sigma_{i<j} f_{\alpha_{ij}} (r_{ij} \Delta\alpha_{ij})^2 + \\ & \Sigma_{i\neq j} [f_{rr}^{ij} (\Delta r_i)(\Delta r_j) + f_{r\alpha}^{ij} (\Delta r_i)(r_{ij} \Delta\alpha_{ij})] + \\ & \Sigma_{i\neq j\neq k} [M_f^{ijk} (\Delta r_i)(r_{jk} \Delta\alpha_{jk}) + N_f^{ijk} (r_{ij} \Delta\alpha_{ij})(r_{ik} \Delta\alpha_{ik}) + \\ & \Sigma_{i\neq j\neq k\neq l} P_f^{ijkl} (r_{ij} \Delta\alpha_{ij})(r_{kl} \Delta\alpha_{kl}) \end{aligned} \tag{2.50}$$

where V is the potential energy function, r_i the bond length, α_{ij} the bond angle between the two adjacent i^{th} and j^{th} bonds and r_{ij} represents $(r_i r_j)^{\frac{1}{2}}$. f_r and f_α are the stretching and bending force constants respectively while f_{rr}, $f_{r\alpha}$, M_f, N_f, and P_f are the interaction force constants. In the most general case, a $\underline{F}$ matrix of order n will contain

$n(n + 1)/2$ distinct force constants. For molecules possessing higher symmetry than C_1, it contains a smaller number of independent force constants.

The number of general valence force constants of a molecule always exceeds the number of vibrational frequencies. Consequently, a unique set of force constants cannot be obtained. One of the methods to overcome this difficulty is to assume the same set of force constants for the isotopic isomers of the molecule. In the other approach, some of the interaction force constants are neglected prejudicially. Since the factors determining which interaction force constants to be neglected are not simple, various model force fields have therefore been proposed[109]. Among these force fields, the Urey-Bradley force field[111-113] (UBFF) has been widely used.

The general form of the Urey-Bradley force field corrected to the second order is given by[112]

$$
\begin{aligned}
V = {} & \tfrac{1}{2} \Sigma_i \left[K_i + \Sigma_{j(\neq i)} \left(t_{ij}^{a2} F_{ij}' + s_{ij}^{a2} F_{ij} \right) \right] (\Delta r_i)^2 \\
& + \tfrac{1}{2} \Sigma_{i<j} \left[H_{ij} - s_{ij}^{a} s_{ji}^{a} F_{ij}' + t_{ij}^{a} t_{ji}^{a} F_{ij} \right] (r_{ij} \Delta \alpha_{ij})^2 \\
& + \Sigma_{i<j} \left[- t_{ij}^{a} t_{ji}^{a} F_{ij}' + s_{ij}^{a} s_{ji}^{a} F_{ij} \right] (\Delta r_i)(\Delta r_j) \\
& + \Sigma_{i<j} \left[t_{ij}^{a} s_{ji}^{a} F_{ij}' + t_{ji}^{a} s_{ij}^{a} F_{ij} \right] (r_j / r_i)^{1/2} (\Delta r_i)(r_{ij} \Delta \alpha_{ij})
\end{aligned}
\tag{2.51}
$$

where

$$
\begin{aligned}
s_{ij}^{a} &= (r_i - r_j \cos \alpha_{ij}) / q_{ij} \\
s_{ji}^{a} &= (r_j - r_i \cos \alpha_{ij}) / q_{ij} \\
t_{ij}^{a} &= (r_i \sin \alpha_{ij}) / q_{ij} \\
t_{ji}^{a} &= (r_i \sin \alpha_{ij}) / q_{ij} \\
q_{ij} &= r_i^2 + r_j^2 - 2 r_i r_j \cos \alpha_{ij}
\end{aligned}
\tag{2.52}
$$

K and H are the bond stretching and angle bending force constants respectively. F and F′ are both the nonbonded repulsive force constants, and F′ is usually taken as -0.1 F with the assumption that the repulsive energy between nonbonded atoms is proportional to $1/r^9$ [114].

The number of force constants in a Urey-Bradley force field is, in general, much smaller than those in a general valence force field. In addition, the Urey-Bradley force constants (UBFC) have a clearer physical meaning and also they are often transferable from molecule to molecule[113,114]. This latter property of the Urey-Bradley force constants is highly useful in calculations for complex molecules. However, ignorance of the interactions between stretching vibrations as well as between bending vibrations in the force field sometimes causes difficulties in adjusting the force constants to fit the observed frequencies. In such a case, it is possible to improve the results by introducing more force constants[113,114].

(c) Force Constant Calculation

The procedure in force constant calculations may be summarized as follows:-

1. Choose the appropriate internal coordinates of the molecule or ion under investigation.

2. Construct the proper symmetry coordinates so as to obtain the transformation matrix U. If the number of internal coordinates exceeds the number of vibrational degrees of freedom, instead of discarding some of the internal coordinates, all these coordinates are still used to construct the symmetry coordinates. The removal of the redundant symmetry coordinates

can be accomplished simply by discarding them all[109].

3. Construct the $\underline{G}$ and $\underline{F}$ matrices by the standard method[109] in the internal coordinate representation according to the symmetry of the molecule.

4. Use the $\underline{U}$ matrix to transform $\underline{G}$ and $\underline{F}$ to $\underline{G_s}$ and $\underline{F_s}$.

The problem now is to find a set of general valence force constants or Urey-Bradley force constants which satisfies,

$$\underline{L_s^{-1}}\ \underline{G_s}\ \underline{F_s}\ \underline{L_s} = \underline{\Lambda_{cal}} \cong \underline{\Lambda_{obs}} \tag{2.53}$$

The elements of $\underline{\Lambda_{cal}}$ and $\underline{\Lambda_{obs}}$ are the calculated and the observed values of the λ's respectively. Various methods have been proposed to obtain such a set, e.g. Newton's method[115], Herranz and Castanz"s method[116] and a least squares fit method[117,118]. Among these the least squares fit method has been widely used. Briefly the procedure of this method is outlined below.

1. A set of estimated force constants $\underline{\Phi}$ is used to calculate a set of theoretical frequencies, the error vector $\underline{\Delta\Lambda}$ ($\underline{\Lambda_{obs}} - \underline{\Lambda_{cal}}$), and the Jacobian matrix $\underline{JZ}$. The Jacobian matrix is defined[117] as

$$\underline{JZ} = \underline{L_s^t}\ \underline{Z_s}\ \underline{L_s} \tag{2.54}$$

where $\underline{Z_s}$ is defined by the relation

$$\underline{F_s} = \underline{Z_s}\ \underline{\Phi} \tag{2.55}$$

2. A linear relationship is assumed between the corrections to the initial force constants $\underline{\Delta\Phi}$ and $\underline{\Delta\Lambda}$ such that

$$\underline{\Delta\Lambda} = \underline{JZ}\ \underline{\Delta\Phi} \tag{2.56}$$

If the number of force constants m is smaller than the number of observed frequencies n, the first-order correction to the force constants $\underline{\Delta\Phi}$ can be calculated[119] from the normal equation

$$\underline{\Delta\Phi} = (\underline{JZ}^t \underline{W} \underline{JZ})^{-1} \underline{JZ} \underline{W} \underline{\Delta\Lambda} \qquad (2.57)$$

where the weighting matrix $\underline{W}$ is usually taken to be $\underline{\Lambda}^{-2}$, which enables one to fit the observed frequencies on a percentage basis[118]. If m = n, a unique solution will be obtained for eqn. (2.56). If m > n, a unique solution will not be possible. In such a case, some of the force constants have to be constrained, or simply set to zero so that the number of force constants refined is equal to or less than the number of observed frequencies. However, which force constants are to be constrained depends on the individual case.

3. The variations in $\underline{\Phi}$ are used to give a new set of force constants

$$\underline{\Phi}^{new} = \underline{\Phi}^{old} + C_a \underline{\Delta\Phi} \qquad (2.58)$$

The force constants are renewed after each iteration until the desired number of iterations is completed or the desired accuracy is obtained.

A program based on the method described above was written in Hong Kong[120] for an ICL 1904A computer and revised for the IBM 370 computer at the University of British Columbia. The $\underline{Gs}$, $\underline{Zs}$, $\underline{\Lambda}_{obs}$ and the assumed force constants $\underline{\Phi}$ comprise the input. The calculated frequencies and the force constants are printed out after each iteration, while the $\underline{Ls}$ matrix and the $\underline{Ls}^{-1}$ matrix appear after the desired number of iterations.

2.2.4 Change in Electronic Transition Moment

In the conventional FCF calculation mentioned in section 2.2.1, the electronic transition moment is assumed to vary slowly with the nuclear configuration. Therefore, the vibrational intensity distribution within a progression in a PE band is proportional to the FCF's. However, recent work on the PE spectra of the hydrogen molecule, and its deuterated derivatives[121-123] show that the electronic transition moment is not constant. A theoretical treatment[123] with variation in vibrational cross section and with the use of a Morse potential function was employed to interpret the PE spectra of hydrogen and nitrogen molecules. However, the same approach cannot be applied to most polyatomic molecules owing to an insufficient amount of data available in the ionic states. In the following paragraph, a simple method with the inclusion of variation in the electronic transition moment will be described.

The electronic transition moment may be written approximately in terms of Q_i to the first order[76,124] as

$$M = M_o + \Sigma_i (\partial M/\partial Q_i)_o Q_i \qquad (2.59)$$

with $(\partial M/\partial Q_i)_o$, the derivative of M with respect to the i^{th} normal coordinate and M_o the electronic transition moment at the equilibrium position. For instance, in a linear unsymmetric triatomic molecule, if only two of the bond stretching normal coordinates Q_1 and Q_2 are active in changing the transition moment, eqn. (2.59) becomes

$$M = M_o + (\partial M/\partial Q_1)_o Q_1 + (\partial M/\partial Q_2)_o Q_2 \qquad (2.60)$$

and according to eqn. (2.3), the vibrational intensity $I_{\underline{m}\,\underline{n}}$ is

$$I_{\underline{m}\,\underline{n}} \propto |\langle \psi'_{\underline{m}} | M | \psi_{\underline{n}} \rangle|^2$$

$$= M_o |\langle \theta'_{m_1}\ \theta'_{m_2} | 1 + \tau_1 Q_1 + \tau_2 Q_2 | \theta_{n_1}\ \theta_{n_2} \rangle|^2$$

$$\times |\langle \theta'_{m_3} | \theta'_{n_3} \rangle|^2 \tag{2.61}$$

with $$\tau_i = \left(\frac{\partial M}{\partial Q_i}\right)_o / M_o \tag{2.62}$$

The integral $\langle \theta'_{m_3} | \theta_{n_3} \rangle$ in expression (2.61) is equal to unity for $m_3 = n_3 = 0$.

Using the harmonic oscillator wavefunction and the property of a Hermite polynomial, it can be shown that

$$\langle \theta'_{m_1}\ \theta'_{m_2} | 1 + \tau_1 Q_1 + \tau_2 Q_2 | \theta_{o_1}\ \theta_{o_2} \rangle$$

$$= M_o \left[\langle \theta'_{m_1} | \theta_{o_1} \rangle \langle \theta'_{m_2} | \theta_{o_2} \rangle + \frac{\tau_1}{\sqrt{2}\,\alpha_1} \langle \theta'_{m_1} | \theta_{1_1} \rangle \langle \theta'_{m_2} | \theta_{o_2} \rangle \right.$$

$$\left. + \frac{\tau_2}{\sqrt{2}\,\alpha_2} \langle \theta'_{m_1} | \theta_{o_1} \rangle \langle \theta'_{m_2} | \theta_{1_2} \rangle \right] \tag{2.63}$$

where the subscript O_2 means the vibrational quantum of the second mode is zero. The integrals in eqn. (2.63) are evaluated using the expressions (2.29).

2.3 Experimental

All the spectra in this thesis were taken on a spectrometer described by A. Katrib[125] which is shown schematically in Figs. 3 and 4.

The He I 21.22 ev resonance radiation is generated by a low pressure microwave discharge in unpurified helium (Canadian Liquid Air). The discharge takes place in a quartz tube within a resonant cavity[126] (Fig. 3) and the power is supplied by a microtron-200 generator (Electro-Medical Supplies) with a maximum output of 200 watts at 2450 MHz. The radiation produced passes through a collimating capillary tube into the collision chamber. Differential pumping is applied between the quartz discharge tube and the collimating capillary to remove unwanted helium.

The sample vapor is introduced through a Granville Philips leak valve to the collision chamber until the pressure in the whole system is about 3×10^{-6} torr. The photoelectrons produced by bombarding the molecule with the He I radiation pass through an exit hole at 90° to the photon beam. This hole is drilled in the center of the collision chamber.

Under the collision chamber, a lens element (Fig. 3) with a circular aperture is used in focussing the photoelectrons upon the entrance slit to the analyzer. This lens is electrically isolated from the chamber by a teflon washer and during operation applied voltage is varied until the best resolution and maximum intensity of the signal is attained.

A 180° hemispherical electrostatic analyzer with a mean radius of 10 cm has been used in the present work. The capability of the hemi-

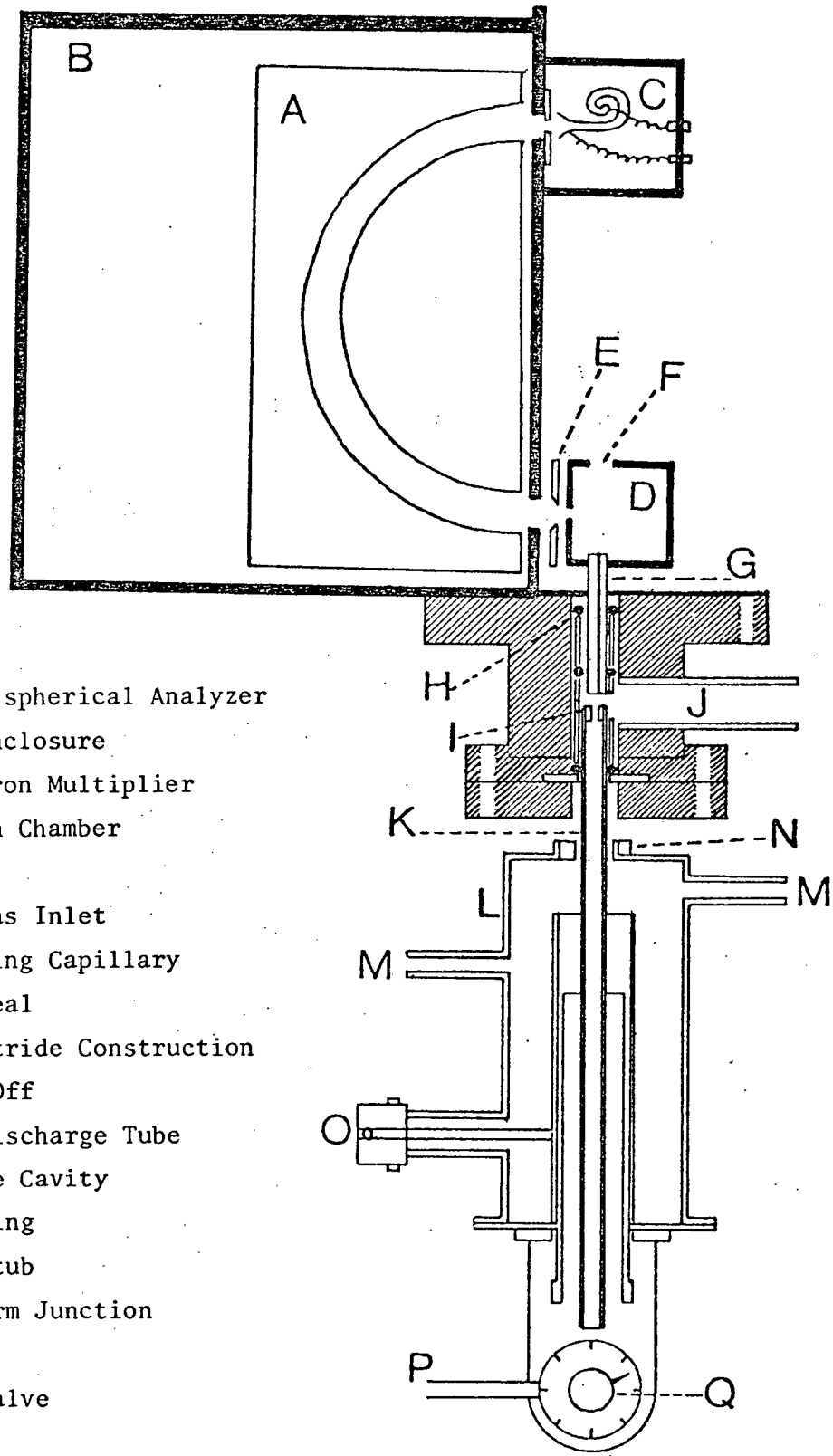

A - 180° Hemispherical Analyzer
B - Vacuum Enclosure
C - Channeltron Multiplier
D - Collision Chamber
E - Lens
F - Sample Gas Inlet
G - Collimating Capillary
H - O-Ring Seal
I - Boron Nitride Construction
J - He Pump Off
K - Quartz Discharge Tube
L - Microwave Cavity
M - Air Cooling
N - Tuning Stub
O - Microtherm Junction
P - He Inlet
Q - Needle Valve

Figure 3. Light source and 180° hemispherical analyzer unit.

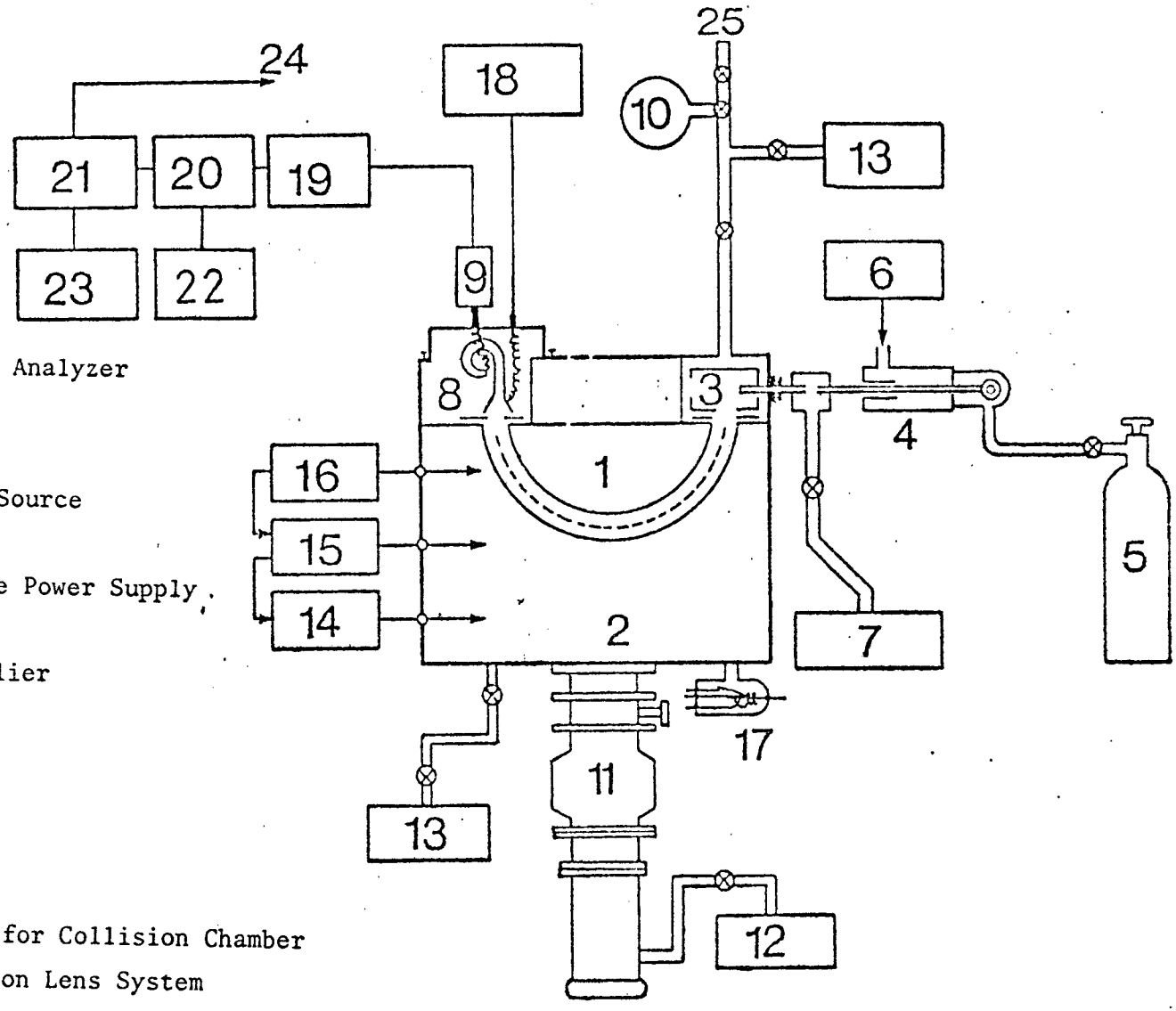

1. 180° Hemispherical Analyzer
2. Vacuum Enclosure
3. Collision Chamber
4. Vacuum U.V. Light Source
5. He Cylinder
6. Microwave Discharge Power Supply
7. Rotary fore pump
8. Channeltron Multiplier
9. Head Amplifier
10. Argon Reservoir
11. Diffusion Pump
12. Rotary Fore Pump
13. Rotary Fore Pump
14. Scanning Potential for Collision Chamber
15. Controls for Electron Lens System
16. Controls for Energy Analyzer
17. Ion Gauge
18. Acceleration Voltage
19. Pulse Amplifier
20. Discriminator
21. Fabriteck 1000 Chan. Analyzer
22. Chart Recorder
23. X-Y Plotter
24. Ramp to Energy Analyzer
25. Sample Inlet

Figure 4. Scheme of the PE spectrometer.

spherical analyzer to accept a relatively large solid angle permits transmission of a relatively high electron flux. The electrode surfaces exposed to the electron trajectory are treated with Aquadaq in order to minimize any field distortion and to minimize stray scattered electrons. Theoretically, the energy resolution of this type of analyzer can be approximated by

$$\Delta E_{1/2} / E_e = \omega_a / 2 R_a \qquad (2.64)$$

where ω_a is the diameter of the entrance and exit apertures

R_a is the radius of the electron path

$\Delta E_{1/2}$ is the energy spread at half maximum of the signal measured

However, practically, the resolution is worse than the theoretical value owing to the undesired magnetic fields originating from various sources in and out of the laboratory and also from the earth's magnetic field in the region of the analyzer. Three pairs of Helmholtz coils mounted at right angles to each other are used to reduce these fields. Other factors[127,128] such as the Doppler effect arising from the motion of the molecules and electrons with respect to the stationary detector, surface charges on the walls of the collision chamber and analyzer, slit widths, self-absorption in the light source and also the nature of the molecule under investigation also influence the resolution of the spectrometer. The best working resolution of the spectrometer on the argon doublet is of the order of 19 mev, but under normal operating conditions, and for the work described in this thesis, the resolution varied between 20 - 40 mev.

The detector chamber (fig. 4) consists of a circular lens with a central hole at earth potential. The ejected photoelectrons are accelerated into a Mullard electron multiplier (Channeltron). Each electron produces a pulse, which is first preamplified and then passes to a EMI LA2 amplifier-discriminator and finally to a EMI RM1 rate meter. The output signal produced is porportional to the number of counts per second and can be plotted out directly on a chart recorder or accumultated in a Fabri-Tek model 1062 multichannel analyzer.

The spectrum is scanned by varying the potential applied between the collision chamber and the analyzer. The scanning potential is obtained by amplifying a 4 volt ramp originating from the multichannel analyzer.

The enclosure shown in Fig. 4 is evacuated by using rotary pumps (Duo-Seal model 1402). The main chamber is pumped by an oil diffusion pump (C.E.C. type MCF 60) which is backed by a Duo-Seal rotary pump (model 1402). A Veeco ionization gauge RG 75K situated below the chamber is used to measure the pressure. The base pressure measured in the system is of the order of 5×10^{-7} torr.

Finally, all the chemicals used in this study were commercially available, of the highest available purity, and were used as received. The IP scale was calibrated by comparison with IP's of argon, xenon and methyl iodide because these are well known.

CHAPTER III

MOLECULAR CONSTANTS OF SOME POLYATOMIC MOLECULAR IONS

3.1 Group VI Hydrides

3.1.1 Introduction

The group VI hydrides have long been a subject of discussion because of their importance in chemistry. Techniques such as electron impact ionization[129-134], photoionization[135-141] and photoelectron spectroscopy[2,9,101,102,142-147] have been employed in deducing useful information concerning the bonding nature of the states of several molecular ions. In recent years, there has been a growing

interest in investigation of ionic states[148,149] by using optical spectroscopy. The better resolution in the latter method enables one to observe fine structure[148], such as that arising from centrifugal distortion. Using data obtained from electron spectroscopy, molecular constants, e.g. geometries, force constants, centrifugal distortion constants and mean square parallel amplitudes of vibrations of the ions H_2O^+ and D_2O^+ in their $^2B_1$ and $^2A_1$ states as well as H_2S^+, D_2S^+, H_2Se^+ and H_2Te^+ in the $^2B_1$ state can be evaluated and the constants obtained are compared with observed data if available.

3.1.2 Gs and Fs Matrices

All the molecules and ions under investigation are of C_{2V} symmetry. The structural parameters[76,107,150,151] and observed frequencies[125,151-159] of these species used in the present calculation are given in Tables 2 - 4.

The symmetry distribution of the normal vibrations of a bent triatomic XY_2 molecule is given by

$$\Gamma(\text{vibration}) = 2a_1 + b_1 \qquad (3.1)$$

The symmetry coordinates used were[160]

a_1 species:

$$S_1 = (\Delta r_1 + \Delta r_2)/\sqrt{2}$$
$$S_2 = r\,\Delta\alpha \qquad (3.2)$$

b species:

$$S_3 = (\Delta r_1 - \Delta r_2)/\sqrt{2} \qquad (3.3)$$

Table 2. Structural Parameters of Group VI Hydrides and their Molecular Ions in Various States

Molecule	State	Bond Length (A)	Bond Angle (deg.)
H_2O	$^1A_1$ [a]	0.9572	104.52
H_2O^+	$^2B_1$ [b]	0.995	109
	$^2A_1$	0.9577	166.1
D_2O	$^1A_1$ [a]	0.9575	104.47
	C [c]	1.023	109.9
	D	1.024	113.1
D_2O^+	$^2B_1$ [b]	0.995	109
	$^2A_1$	0.9586	166.7
H_2S	$^1A_1$ [d]	1.3455	93.3
H_2S^+	$^2B_1$	1.3676	94.6
D_2S	$^1A_1$ [d]	1.345	92.3
D_2S^+	$^2B_1$	1.364	92.5
H_2Se	$^1A_1$ [d]	1.46	91
H_2Se^+	$^2B_1$	1.48	91.3
H_2Te	$^1A_1$ [d]	1.7	89.5
H_2Te^+	$^2B_1$	1.72	89.7

[a] Ref. 151. [b] Ref. 108. [c] $r = 1.002$ Å and $\alpha = 108.7$ from rotational analysis (ref. 169). [d] Ref. 150.

Table 3. The Observed Frequencies (cm^{-1}) of H_2O, H_2O^+, D_2O and D_2O^+ in Various States

	H_2O			H_2O^{+a}		D_2O			D_2O^{+a}	
	$^1A_1$ [b]	C [c]	D [c]	$^2B_1$ [d]	$^2A_1$ [e]	$^1A_1$ [b]	C [c]	D [c]	$^2B_1$ [d]	$^2A_1$ [e]
ν_1 (a_1)	3656.7	3179	3268	3195	3680	2671.5	2338	2381	2295	2648[f]
ν_2 (a_1)	1594.6	1407	1631	1400	975	1178.3	1041	1223	1015	715
ν_3 (b_1)	3755.8	3060[g]	2958[g]	3150	3812[g]	2788.1	2247[g]	2175[g]	2310	2842[g]

[a]The uncertainties in observed frequencies for the ions are estimated to be within ± 50 cm^{-1}, except ν_3, ± 100 cm^{-1} and ν_1 for $^2A_1$ state of H_2O.

[b]Ref. 151. [c]Ref. 170. [d]Refs. 102 and 152. [e]Refs. 2 and 101.

[f]From product rule. [g]From normal coordinate analysis.

Table 4. Observed Frequencies[a] (cm^{-1}) of H_2S, D_2S, H_2Se and H_2Te in the Ground State and the $^2B_1$ States of the Molecular Ions

	$H_2S(^1A_1)$[b]	$H_2S^+(^2B_1)$[c]	$D_2S(^1A_1)$[b]	$D_2S^+(^2B_1)$[c]	$H_2Se(^1A_1)$[d]	$H_2Se^+(^2B_1)$[e]	$H_2Te(^1A_1)$[f]	$H_2Te^+(^2B_1)$[e]
$\nu_1(a_1)$	2614.6	2540	1896.4	1830	2344.5	2260	2000	2100
$\nu_2(a_1)$	1182.7	1250	855.5	950	1034.2	----	861	----
$\nu_3(b_1)$	2666.	2185[g]	1926	1569[g]	2357.8	----	2000	----

[a]The uncertainties in observed frequencies of all the ions are within ± 40 cm^{-1}, except that of H_2Te^+ in $^2B_1$ state ± 200 cm^{-1}.

[b]From refs. 76, 150-156. [c]Ref. 125. [d]Refs. 157 and 158.

[e]Ref. 147. [f]Ref. 159. [g]From normal coordinate analysis.

The internal coordinates are defined as follows: r = X - Y bond distance and α = Y-X-Y angle.

The inverse kinetic energy matrix Gs as well as the force constant matrix Fs in GVFF were set up by Wilson's GF formalism[109] and are listed in Table 5. They are the same as those given in ref. 160. f_r and f_α and are respectively the bond stretching and angle bending force constants while f_{rr} and $f_{r\alpha}$ are the bond stretch-bond stretch and bond stretch-angle bending interaction force constants respectively. μ_X and μ_Y are respectively the reciprocal of the atomic weights of the X and Y atoms.

In the most general valence force field, there are totally four force constants f_r, f_α, f_{rr} and $f_{r\alpha}$. However, at most, only three frequencies can be observed for each hydride or its ion. To circumvent this difficulty, we adopt the conventional assumption that the force constants are the same for both the molecule (or ion) and its deuterated derivative.

Normal coordinate analysis was carried out by the least squares fit program mentioned in section 2.2.3 to obtain a set of refined force constants as well as the Ls matrices for the conventional FCF calculation. Method A is utilized throughout this work.

3.1.3 Results and Discussion

(a) $^2B_1$ State of H_2O^+ and D_2O^+

The ground state configuration of group VI hydrides is represented as,[11]

$$(1a_1)^2\ (2a_1)^2\ (1b_2)^2\ (3a_1)^1\ (1b_1)^2 \qquad {}^1A_1$$

Table 5. The Gs and Fs Matrix Elements of a Bent Symmetric Triatomic Molecule XY_2

Sym. Species	Gs Matrix		Fs Matrix[a]	
a_1	G_{11}	$\mu_Y + \mu_X(1+\cos\alpha)$	F_{11}	$f_r + f_{rr}$
	G_{12}	$-\sqrt{2}\,\mu_X \sin\alpha$	F_{12}	$2\,f_{r\alpha}$
	G_{22}	$2[\mu_Y + \mu_X(1-\cos\alpha)]$	F_{22}	f_α
b_1	G_{33}	$\mu_Y + \mu_X(1-\cos\alpha)$	F_{33}	$f_r - f_{rr}$

[a] In GVFF.

Ionization of an electron from the nonbonding $1b_1$ orbital will leave the ion in $^2B_1$ state. The geometries of H_2O^+ and D_2O^+ in this ionic state have been discussed in detail by Rosenstock and his coworkers[108,161] and are listed in Table 2. By using the structural parameters[108] and observed frequencies[101,152] of the two ions (Table 3), a normal coordinate analysis was carried out and the calculated frequencies were found to converge to within 1% after five iterations. The force constants obtained are given in Table 6.

In view of the large uncertainty in the measurement of vibrational frequencies by the electron spectroscopy technique, and also the anharmonic effect on these frequencies, force constant analysis of the two ions was again carried out by using the following sets of frequencies: (i) 50 cm^{-1} was added to every ν', but 100 cm^{-1} to every ν_3' (hereafter referred to as set (1)), and (ii) a value $(\omega_i - \nu_i)$ was added to every ν' (set 2) where ω_i are the harmonic frequencies[151] in the ground state. The result of the calculation shows that the valence force constants f_r and f_α augment by 10% with a 5% increase in frequencies. Also the interaction force constants f_{rr} and $f_{r\alpha}$ are very sensitive to the frequencies used.

Though a unique set of force constants cannot be obtained because of the large uncertainties in observed ionic frequencies, f_r and f_α are definitely smaller in the ions than in the molecules. This implies that the nonbonding $1b_1$ orbital possesses some O-H bonding character.

The off-diagonal elements of the $\underline{Ls'}$ matrix, just like the constants f_{rr} and $f_{r\alpha}$ are sensitive to the frequencies used. However, the diagonal elements, which have values much greater than that of off-

Table 6. Valence Force Constants (mdyn/Å) of Group VI Hydrides and their Molecular Ions in Various States

	State	f_r	f_{rr}	f_α	$f_{r\alpha}$
H_2O	$^1A_1$	7.775	-0.081	0.712	0.122
	C	5.490[a]	0.301	0.552	0.001
	D	5.464[a]	0.688	0.731	0.010
H_2O^+	$^2B_1$	5.601	0.164	0.538	-0.038
	Set 1	5.943	0.093	0.584	0.123
	Set 2	6.180	0.174	0.571	0.042
	$^2A_1$	7.543[a]	0.577	0.251	0.000
H_2S	$^1A_1$	4.038	-0.073	0.409	-0.052
H_2S^+	$^2B_1$	3.241[a]	0.499	0.471	-0.049
H_2Se	$^1A_1$	3.242	-0.055	0.345	-0.189
H_2Se^+	$^2B_1$	3.021[b]			
H_2Te	$^1A_1$	2.348	-0.002	0.225	0.123
H_2Te^+	$^2B_1$	2.587[b]			

[a]Estimated from Badger's rule[171,172].

[b]From approximate method (see appendix III).

diagonal elements are essentially unchanged. In addition, the diagonal elements are quite inert to geometrical change. For example, in the $^2A_1$ state (section 3.1.3c), these quantities change by only 3 to 4% compared to those in the ground state even though there is a dramatic increase in bond angle in this state. This may explain the rapid convergence of the cycling process in method A. The constancy of the Ls matrix is not unreasonable because the contributions of the normal coordinates to a symmetry coordinate are nearly the same in both the molecule and its cation.

The structural parameters, Ls' matrix and the inverse force constants in symmetry coordinates obtained the last cycle, and also the observed frequencies are used to compute distortion rotational constants[162-164] and mean square amplitudes of vibration[165] for the two ions. The results of the calculation are given in Table 7. The agreement between the calculated and observed distortion constants[148] for the H_2O ion is satisfactory in view of the fact that the fundemental frequencies instead of the harmonic frequencies are used. The distortion constants for the ion differ only slightly from the neutral molecule[166,167]. The mean square amplitudes of vibrations are found to be larger in both H_2O and D_2O ions than in their parent molecules[165]. The greater flexibility of the constituted atoms in the ions again indicates O-H bonding character of the $1b_1$ orbital.

It has been pointed out by some authors[102] that the $^2B_1$ and the C and D Rydberg states[168-170] of water are very similar to one another. FCF calculations were carried out on these two Rydberg states of H_2O and D_2O. Unfortunately, divergence was obtained during the refinement of force constants. This is due to an unknown value for the ν_3' frequency. A set of force constants (Table 6) is chosen in such a way that values of

Table 7. Distortion Rotational Constants (cm^{-1}) and Mean Square Amplitudes of Vibrations ($Å^2$) at 298° K of H_2O, D_2O, H_2S and D_2S and their Molecular Ions in Various States

	$H_2O^+(^2B_1)$	$D_2O^+(^2B_1)$	$D_2O(C)$	$H_2S^+(^2B_1)$	$D_2S^+(^2B_1)$
D_J	0.0010 (0.0008)[a]	0.0003	0.0002	0.0004	0.0001
D_K	0.0348 (0.045)	0.0107	0.0096	0.0020	0.0005
D_{JK}	-0.0045 (0.004)	-0.0013	-0.0010	-0.0007	-0.0002
R_5	0.0011	0.0003	0.0002	0.0001	0.0000
R_6	-0.0001	0.0000	0.0000	0.0000	0.0000
δ_J	0.0005	0.0001	0.0001	0.0002	0.0001
l^2_{x-Y}	0.00561	0.00410		0.00735	0.00527
l^2_{x-Y}	0.01576	0.01136		0.02030	0.01411

[a]Experimental data from ref. 148 in parentheses.

f_r equal to that predicted from Badger's rule[171,172]; viz. 5.490 and 5.464 $^{mdyn}/_{Å}$ for the C and D states respectively. Badger's rule states that the logarithm of stretching force constants f_{AB} of a series of molecules is related linearly to the logarithm of the corresponding bond length r_{AB}. The resultant geometry of D_2O in the C and D states is given in Table 2 and the calculated bond lengths of the C state differs appreciably from experimental values[169]. The fundamental frequencies used instead of the harmonic frequencies in the calculation cannot account for such a large deviation. Therefore, method A including the variation in electronic transition moment (section 2.2.4) is applied to this state and the calculated structural parameters and intensities are the same as the experimental data[169] with τ_{OH} and τ_{HOH} equal to 6.65 and 1.20 x 10^{20} $g^{-½}\,cm^{-1}$ respectively. The quantity τ_{OH} becomes smaller for lower values of the observed intensity used for m_i = 1 (in this case, the error limit is ± 0.2!).

Using the calculated Coriolis coupling constants[163,164] (which describe interations between rotation and vibration) from this work and observed g values[169] of the C state of D_2O, the inertia defect[173] is found to be 0.075 amu Å², in comparison to the experimental value[169], 0.074 amu Å². Inertia defects of H_2O and D_2O in the $^2B_1$ states are predicted to be 0.089 and 0.117 amu Å² respectively by assuming that the contribution from the electronic defect is negligible.

(b) $^2B_1$ State of the Molecular Ions, H_2S, D_2S, H_2Se and H_2Te.

Determination of the geometry of the H_2S and D_2S ions requires knowledge of d as well as Ls and Ls'. The frequencies (Table 4) and intensities of peaks observed in the corresponding PE bands[125] were employed to

compute d. Ls and Ls′ matrices were generated from a normal coordinate analysis. For the neutral molecules, convergence in calculated frequencies to within 1 cm^{-1} was obtained. However, this is not the case for the ions again because ν_3' is not available. So Badger's rule[171,172] is used as a criterion for choosing a set of force constants which reproduce well the observed frequencies. The structural parameters (Table 2) obtained for the two ions are nearly the same as their parent molecules. Centrifugal distortion constants and mean amplitudes of vibrations of the ions were evaluated and are listed in Table 7.

The $^2B_1$ states of H_2Se^+ and H_2Te^+ have been studied by PES[147]. Only excitation of symmetric stretching frequencies was observed in the PE spectra. No electron spectra were reported for their deuterated derivatives. In this case, a force constant analysis for these ions is not applicable since the number of unknown force constants (even in the simple valence force field, SVFF, with only diagonal force constants being considered) exceeds the number of observed frequencies. Therefore, Ls′ is assumed to be equal to Ls. Values of f_r given in Table 6 for H_2Se and H_2Te ions were approximated by the method described in appendix III. Owing to insufficient observed data for these two ions, no computation of distortion constants or mean square amplitudes of vibration was carried out.

(c) $^2A_1$ State of the Molecular Ions H_2O and D_2O

The PE spectra of H_2O and D_2O corresponding to the $^2A_1$ state have been obtained by Brundle et al[101], Asbrink et al[2] and Potts et al[147]. It has been mentioned by Potts et al[147] that the vibrational structures of both ions displayed in the spectra differ from those of other hydrides

of the same group by their rather constant spacings in a progression of ν_2' . This led the authors to conclude that these ions are probably linear in this state. Using the observed frequencies[2,101], and the estimated intensities of various peaks in the spectra, bond angles of the two ions are found to be close to 180° (Table 2).

It has been mentioned by Botter and Rosenstock[108] that if there is a large change in geometry of a molecule during ionization, there is no longer a one to one correlation between the symmetry coordinates of an ion and its parent molecule, i.e. expression (2.21) is invalid, but they are related to each other by

$$\underline{S'} = \underline{Z_a}\,\underline{S} + \underline{\Delta S} \tag{3.4}$$

where the off diagonal elements of the transformation matrix $\underline{Z_a}$ measures the mixing of the symmetry coordinates. The matrix $\underline{J}$ is now given by,

$$\underline{J} = (\underline{L_s'})^{-1}\,\underline{Z_a}\,\underline{L_s} \tag{3.5}$$

From the result of the calculation, the off-diagonal elements of the $\underline{Z_a}$ matrix, and hence $\underline{J}$ have values comparable to diagonal elements. This indicates that mixing between symmetry coordinates of the same symmetry is appreciable.

3.2 Nitrous Oxide

3.2.1 Introduction

The conventional FCF calculation (method B)[174] has been applied to the $X\,^2\Pi$ and $A\,^2\Sigma^+$ states of the molecular ion of N_2O without success owing to the large discrepancy between observed and calculated FCF's. Recently, the two ionic states have been studied by using the optical

technique[175] by which force constants f_i' , vibrational frequencies ν_i' and geometries of the ions (both are found to be linear) are obtained. In light of the data available, we have reinvestigated the differences in bond lengths Δr_i of N_2O between the ground states and the $X\,^2\Pi$ and $A\,^2\Sigma^+$ states by utilizing the FCF's derived from its PE spectrum[11] and the generating function method[35]. However, only the experimental values in the $A\,^2\Sigma^+$ state can be reproduced. With regard to the $X\,^2\Pi$ state, the treatment is modified by including the variation of electronic transition moment. Both τ_{NN} and τ_{NO} in expression (2.62) are adjusted to give a value of d_i and, hence, Δr_{NN} , Δr_{NO} and calculated intensities that match well with the observed values. The Ls and Ls′ matrices and force constants (in GVFF) of both molecules and ions are generated from a normal coordinate analysis by utilizing the observed frequencies[175-178] of $N_2^{16}O$ and $N_2^{18}O$ in various electronic states. The symmetry coordinates, Gs and Fs matrices used in the present calculation are the same given in ref. 160.

3.2.2 Results and Discussion

(a) Geometry of N_2O^+ in the $X\,^2\Pi$ and $A\,^2\Sigma^+$ States

Physical constants such as force constants[179], vibrational frequencies[175-178] adopted in the conventional FCF calculation, together with the bond angle α and bond length[180] r_i and Δr_i in the ground state as well as the two ionic states are given in Table 8. Here f_{NN} and f_{NO} denote the stretching force constant of the N-N and N-O bonds respectively, f_{NNO} the bending force constant and $f_{NN,NO}$ the bond stretch-bond stretch interaction force constant. FCF's thus deduced using parameters given in Table 9 agree well with experimental values. Large

Table 8. Calculated Force Constants (mdyn/Å), Bond lengths (Å), Observed Vibrational Frequencies (cm^{-1}) and Structural Parameters of N_2O in the $X\ ^1\Sigma^+$, and the Molecular Ions in the $X\ ^2\Pi$ and $A\ ^2\Sigma^+$ States

	N_2O	N_2O^+	
	$X\ ^1\Sigma^+$	$X\ ^2\Pi$	$A\ ^2\Sigma^+$
f_{NN}	18.01[a]	12.43	18.70
f_{NO}	11.33[a]	8.06	14.41
f_{NNO}	0.486[a]	0.29	0.53
$f_{NN,NO}$	1.41[a]	2.28	-0.06
ν_1	2223.76[b]	1737.65[c]	2451.70[c]
ν_2	1284.91[b]	1126.47[c]	1345.52[c]
ν_3	588.77[b]	456.80[c]	614.10[c]
$\angle$ NNO	180 [b]	180 [c]	180 [c]
Δr_{NN}^{obs} [d]		0.0259[c]	0.0113[c]
Δr_{NO}^{obs}		-0.0062[c]	-0.0496[c]
Δr_{NN}^{cald}		0.0174[e] (0.0259)[f]	0.0068[e]
Δr_{NO}^{cald}		0.0048[e] (-0.0062)[f]	-0.0391[e]

[a]Ref. 179. [b]Ref. 176. [c]Ref. 175. [d] $\Delta r_i = r_i' - r_i$.

[e]From conventional FCF calculation. [f]From method involving change in electronic transition moment with τ_{NN} and τ_{NO} -1.704 and 0.515 x 10^{20} $gm^{1/2}cm^{-1}$ respectively.

Table 9. Calculated and Observed Franck-Condon Factors in the $X\ ^2\Pi$ and $A\ ^2\Sigma^+$ States of N_2O^+

Vibrational Level			$X\ ^2\Pi$			$A\ ^2\Sigma^+$	
m_1	m_2	m_3	Obs. FCF[a]	Cald FCF[a]	Cald FCF[c]	Obs. FCF[a]	Cald FCF[b]
0	0	0	0.91	0.91[d]	0.91[d]	0.749	0.749[d]
1	0	0	0.03	0.03	0.03	0.073	0.069
2	0	0		0.01	0.01	0.004	0.001
0	1	0	0.05	0.05	0.05	0.164	0.169
0	2	0	0.01	0.01	0.00		0.013
1	1	0	0.01	0.00	0.00	0.008	0.012

[a]Ref. 11. [b]From conventional FCF calculation (method B).

[c]From calculation including change in electronic transition moment with τ_{NN} and τ_{NO} -1.704 and 0.515 x 10^{20} $gm^{-1/2}$ cm^{-1} respectively.

[d]Assigned to have value same as observed intensity.

discrepancies obtained between calculated and observed FCF's for the $X \longrightarrow \Pi$ transition by the previous worker[174] are mainly due to the use of incorrect force constants and also neglect of variation in electronic transition moment as well (see discussion later).

Determination of Δr_i by means of the current methods[33-35] in FCF calculations gives only the magnitude but not the sign of the change. For example, application of method B to the $X\,^1\Sigma^+ \longrightarrow X^2\Pi$ transition gives two sets of parameters, with Δr_{NN} and Δr_{NO} respectively, 0.0174 and 0.0048 Å, and 0.0090 and -0.0244 Å which can reproduce well the observed FCF's. Since some physical properties in the two ionic states studied are known experimentally[175], it is worthwhile to test the criteria given in section 2.2.1b.

According to these criteria, the sign of Δr_{NN} and Δr_{NO} in the $X\,^2\Pi$ is predicted to be (i) positive and negative respectively from a CNDO/2 calculation[59], (ii) both positive from the variation in force constants or vibrational frequencies, and (iii) same as (ii) in accordance with the bond order change[181]. Also, bond lengthening for both r_{NN} and r_{NO} in the $A\,^2\Sigma^+$ state in comparison with that of the ground state is expected from the first two criteria. However, surprisingly, none of the above guidelines explains the experimental result satisfactorily. This is somewhat unexpected especially for the second criteria where the magnitude of the force constants derived should indicate the bond strength in both the ground and ionic states.

(b) Variation in Electronic Transition Moment in the $X\,^1\Sigma^+ \rightarrow X\,^3\Pi$ Transition

The conventional FCF calculation on the $X\,^3\Pi$ state does not give the correct value of Δr_{NO}. The deviation cannot be explained by merely the anharmonicity effect. This leads us to reinvestigate the problem by introducing the change of electronic transition moment. The method used in computation has been described in section 2.2.4. Only one set of τ_i's, -1.704 and 0.515 x 10^{20} $g^{-1/2}$ cm^{-1} for τ_{NN} and τ_{NO} respectively are used, which yields Δr_i's and the calculated intensities in good agreement with experimental data (Tables 8 and 9). The absolute value of τ_{NN} is found to be larger than that of τ_{NO} owing to the large value of one of the off-diagonal elements in the Ls' matrix and parallels the greater change in the NN bond length compared to the NO bond.

It is interesting to note that the magnitude of the transition probability for the i^{th} vibrational mode with vibrational quantum number equal to two decreases with diminishing values of τ_i but is rather insensitive to other τ's. The physical significance of the sign of τ_i obtained is not clear, and little work has been done on this aspect.

(c) Force Constants in the Molecule and the Ions of N_2O

It has been shown that[182] the interaction force constant $f_{NN,NO}$ is important in deducing correct bond stretching force constants for the neutral molecule. A normal coordinate analysis in GVFF gives values 18.01 and 11.33 mdyn/Å for f_{NN} and f_{NO} respectively[179] while the same treatment in SVFF (this work) gives values 14.09 and 14.30 mdyn/Å for f_{NN} and f_{NO} respectively, which is obviously wrong. Also the off-diagonal

elements of the Ls matrix differ appreciably from those using GVFF. The quantity $f_{NN,NO}$ reflects the resonance effect between the NO and NN bonds.

The interaction force constants as mentioned by Jones[183] may provide valuable information about the bonding character of a species. The interaction displacement coordinate $(S_{NN})_{NO}$, the change in N-N bond length to minimize the energy after a unit positive change in NO bond distance, is related to f_{NN} by

$$f_{NN,NO} = -(S_{NN})_{NO} f_{NN} \qquad (3.6)$$

The quantity $(S_{NN})_{NO}$ is found to be -0.08, -0.18 and 0.00 Å for the $X\ ^1\Sigma^+$, $X\ ^2\Pi$ and $A\ ^2\Sigma^+$ states respectively. This indicates that the resonance effect is greater in the $X\ ^2\Pi$ state, which agrees with the result of a CNDO/2 calculation[59] that the highest occupied nonbonding π orbital possesses weak NN bonding and NO antibonding character and the highest σ orbital indicates strong NN and NO bonding character.

Application of the modified Urey-Bradley force field[112] with six force constants, K_{NN}, K_{NO}, H_{NNO}, $f_{NN,NO}$, F and F′ has been attempted to obtain more information about the potential energy surface in the two ionic states studied. However, no convergence in the force constant refinement was obtained owing to large correlations between them.

3.3 Dihaloethylenes

3.3.1 Introduction

Today, the application of FCF calculations is usually limited to triatomic or tetraatomic molecules owing to the overlapping nature of the

PE bands of the molecule, the small number of ionic frequencies observed, the large uncertainty associated with these frequencies, the dimension of the matrices handled in the normal coordinate analysis, and also criteria in choosing a reasonable set of calculated structural parameters. In this section, we report the FCF calculations on the geometry of all the gem and cis and trans 1,2 dihaloethylenes $C_2H_2X_2$ molecular ions (except gem diiodoethylene) in some ionic states. The choice of calculated ionic geometry is based on the bonding properties of the neutral molecules. From the result obtained, the operation of various mechanisms proposed by Coulson and Luz[184] on structural changes upon ionization are discussed.

In the course of this work, we found that most force constant analyses[185-187] with few exceptions[188-190] on the in-plane vibration of dihaloethylenes are carried out on the assumption of the transferability of force constants among these molecules in either the Urey-Bradley force field or, in general valence force field. Some of the calculated force constants contradict each other[186,189,190]. Therefore, force constants of all the dihaloethylenes are recalculated by using the modified Urey-Bradley force field to obtain consistent results, and also different sets of force constants are used for different isomers of the same dihaloethylene.

3.3.2 Method of Calculation

The gem, cis and trans 1,2 dihaloethylenes studied are found to be planar[150,191-195] with symmetry C_{2V}, C_{2V} and C_{2h} respectively. The symmetry distribution of the in-plane vibrations is $5a_1 + 4b_1$ for both cis and gem isomers, and is $5\ a_g + 4\ b_u$ for trans. A representative of each type of internal coordinate for a general, planar ethylene molecule is shown in Fig. 5.

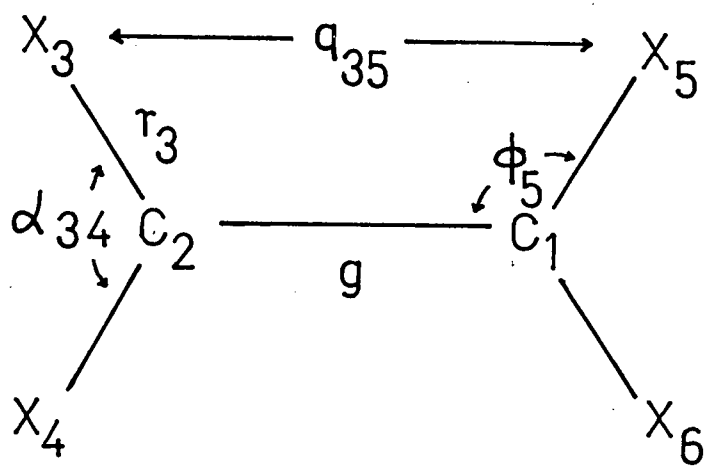

Figure 5. Internal coordinates of substituted ethylene.

The symmetry coordinates used for cis, 1,2 difluoroethylenes in the present calculation are similar to those given by Ziomek et al[196] and are given as,

$$
\begin{aligned}
a_1 : \quad S_1 &= \frac{1}{\sqrt{2}}(\Delta r_4 + \Delta r_6) \\
S_2 &= \Delta g \\
S_3 &= \frac{1}{2\sqrt{3}}(\Delta\phi_3 + \Delta\phi_4 + \Delta\phi_5 + \Delta\phi_6 - 2\Delta\alpha_{34} - 2\Delta\alpha_{56}) \\
S_4 &= \frac{1}{\sqrt{2}}(\Delta r_3 + \Delta r_5) \\
S_5 &= \frac{1}{2}(-\Delta\phi_3 + \Delta\phi_4 - \Delta\phi_5 + \Delta\phi_6) \\
S_R &= \frac{1}{\sqrt{6}}(\Delta\phi_3 + \Delta\phi_4 + \Delta\phi_5 + \Delta\phi_6 + \Delta\alpha_{34} + \Delta\alpha_{56}) \equiv 0
\end{aligned}
\qquad (3.7)
$$

$$
\begin{aligned}
b_1 : \quad S_6 &= \frac{1}{\sqrt{2}}(\Delta r_4 - \Delta r_6) \\
S_7 &= \frac{1}{\sqrt{2}}(\Delta r_3 - \Delta r_5) \\
S_8 &= \frac{1}{2\sqrt{3}}(\Delta\phi_3 + \Delta\phi_4 - \Delta\phi_5 - \Delta\phi_6 - 2\Delta\alpha_{34} + 2\Delta\alpha_{56}) \\
S_9 &= \frac{1}{2}(-\Delta\phi_3 + \Delta\phi_4 + \Delta\phi_5 - \Delta\phi_6) \\
S_R' &= \frac{1}{\sqrt{2}}(\Delta\phi_3 + \Delta\phi_4 - \Delta\phi_5 - \Delta\phi_6 + \Delta\alpha_{34} - \Delta\alpha_{56}) \equiv 0
\end{aligned}
$$

where r_4 and r_6 denote the C-H bond lengths and r_3 and r_4 the C-F bond lengths.

With regard to trans 1,2 difluoroethylene, the symmetry coordinates used are identical to those of cis except that a_1 and b_1 are replaced by a_g and b_u respectively and also the subscripts 5 and 6 for the internal coordinates interchange. In this case, r_4 and r_5 are the C-H bond lengths while r_3 and r_6 are the C-F bond lengths.

The symmetry coordinates used for gem difluoroethylene are different from cis or trans 1,2 difluoroethylene and are in the form[197]

$$
\begin{aligned}
a_1 : \quad S_1 &= \frac{1}{\sqrt{2}} (\Delta r_3 + \Delta r_4) \\
S_2 &= \Delta q \\
S_3 &= \frac{1}{\sqrt{6}} (2\Delta\alpha_{34} - \Delta\phi_3 - \Delta\phi_4) \\
S_4 &= \frac{1}{\sqrt{2}} (\Delta r_5 + \Delta r_6) \\
S_5 &= \frac{1}{\sqrt{6}} (2\Delta\alpha_{56} - \Delta\phi_5 - \Delta\phi_6)
\end{aligned} \qquad (3.8)
$$

$$
\begin{aligned}
b_2 : \quad S_6 &= \frac{1}{\sqrt{2}} (\Delta r_3 - \Delta r_4) \\
S_7 &= \frac{1}{\sqrt{2}} (\Delta r_5 - \Delta r_6) \\
S_8 &= \frac{1}{\sqrt{2}} (\Delta\phi_3 - \Delta\phi_4) \\
S_9 &= \frac{1}{\sqrt{2}} (\Delta\phi_3 - \Delta\phi_6)
\end{aligned}
$$

Here r_3 and r_4 are the C-H bond distances and r_5 and r_6 the C-F bond distances.

As for dichloro-, dibromo- and diiodoethylenes, the symmetry coordinates adopted in the present calculation are the same as those given by expressions (3.7) and (3.8) except that S_7 and S_8 interchange with each other.

The modified Urey-Bradley force field (MUBFF) employed in this work can be written as

$$V_{MUBFF} = V_{UBFF} + V_A \qquad (3.9)$$

The complete expression for V_{UBFF} in terms of internal coordinates is given by[198]

$$
\begin{aligned}
2\,V_{UBFF} = {} & K_{cc}(\Delta q)^2 + 2K'_{cc}(q\,\Delta q) + \sum_{i=3}^{i=6} K_{cx_i}(\Delta r_i)^2 + \\
& 2\sum_{i=3}^{i=6} K'_{cx_i}(r_i\,\Delta r_i) + \sum_{i=3}^{i=6} H_{cx_i}(r_i^2)(\Delta\phi_i)^2 + \\
& H_{x_3x_4}(r_3\,r_4)(\Delta\alpha_{34})^2 + H_{x_5x_6}(r_5\,r_6)(\Delta\alpha_{56})^2 + \\
& \sum_{i=3}^{i=6} F_{cx_i}(\Delta q_i)^2 + 2\sum_{i=3}^{i=6} F'_{cx_i}(q_i\,\Delta q_i) + \\
& F_{x_3x_4}(\Delta q_{34})^2 + F_{x_5x_6}(\Delta q_{56})^2 + \\
& 2F'_{x_3x_4}(q_{34}\,\Delta q_{34}) + 2F'_{x_5x_6}(q_{56}\,\Delta q_{56}) + \\
& C_{x_3x_5}(\Delta q_{35})^2 + C_{x_4x_6}(\Delta q_{46})^2 + \\
& 2C'_{x_3x_5}(q_{35}\,\Delta q_{35}) + 2C'_{x_4x_6}(q_{46}\,\Delta q_{46})
\end{aligned}
\qquad (3.10)
$$

with C and C′ as nonbonded repulsive force constants. C′ is related to[198] C by a factor -0.1. The interaction potential function V_A is

$$
\begin{aligned}
2\,V_A = {} & h_{HH}(\Delta r_{cH})(\Delta r'_{cH}) + h_{xx}(\Delta r_{cx})(\Delta r'_{cx}) + \\
& \sum_{i\neq j} e_{ij}(\Delta\phi_i)(\Delta\phi_j)\,g\,(r_i\,r_j)^{1/2}
\end{aligned}
\qquad (3.11)
$$

where h_{HH}, h_{xx} and e_{ij} are the interaction force constants. The addition of h_{HH} and e_{ij} accords with other work[186,199] and the second term in eqn. (3.11) should be important in dihaloethylenes owing to the conjugative effect between carbon π orbitals and halogen lone pairs.

The inverse kinetic energy matrix Gs and the force constant matrix Fs using symmetry coordinates (3.7) and (3.8) are obtained by standard methods[109,200].

The force constant calculation was carried out by the least squares fit program described earlier to reproduce observed frequencies[185-187, 201-207] of the molecules and their deuterated derivatives. The initial sets of force constants used in the iterative method were estimated from previous work[185-189,197].

The FCF calculations are carried out using method A, and Ls is used instead of Ls' since the ionic frequencies observed are not sufficient to perform a normal coordinate analysis. The FCF's of the molecules studied are derived from refs. 208 and 209 as well as from section 4.5. Some ionic geometries of dihaloethylenes obtained are shown in Table 10. It should be mentioned that the geometries derived are based on the planarity of the ions. The perturbations on FCF's arising from spin orbit coupling and variation in electronic transition moment is neglected in this treatment.

3.3.3 Results and Discussion

(a) Modified Urey-Bradley Force Constants of Dihaloethylenes

Convergence was obtained only for some of the dihaloethylenes. With regard to others, force constants were obtained in a trial and error fashion to give a good frequency fit (within 3.2%) as well as to agree with Badger's rule[171,172] qualitatively, i.e. shorter bond lengths are associated with greater stretching force constants. e_{HH} and e_{XX} in cis 1,2 dihaloethylenes and e_{HX}^{cis} in gem dihaloethylenes are fixed to be zero for

Table 10. Geometrical Changes in Dihaloethylene upon Ionization

Ionic State	Δr_{CH}(Å)	Δr_{CC}(Å)	Δr_{CX}(Å)	$\Delta\alpha_{HCX}$	$\Delta\phi_X$	$\Delta\phi_H$	$\Delta\alpha_{XCX}$	$\Delta\alpha_{HCH}$
Cis 1,2 $C_2H_2F_2$								
$2\,^2B_1$	-0.001	0.110	-0.055	7.2	-3.7	-3.6		
$5\,^2A_1$	0.004	0.022	0.027	-0.5	-0.7	1.3		
$3\,^2B_2$	0.050	-0.016	0.005	2.5	0.2	-2.7		
Cis 1,2 $C_2H_2Cl_2$								
$2\,^2B_1$	0.015	0.120	-0.001	2.3	-1.5	-0.8		
or	0.012	0.081	-0.081	4.2	-0.2	-0.4		
$1\,^2A_2$	0.002	0.025	0.052	-1.3	-0.8	2.1		
Cis 1,2 $C_2H_2Br_2$								
$2\,^2B_1$	0.015	0.076	-0.084	4.0	0.1	-4.1		
$1\,^2A_2$	0.001	0.013	0.039	-0.3	-0.6	0.9		
Cis 1,2 $C_2H_2I_2$								
$2\,^2B_1$	0.003	0.042	-0.055	1.2	0.2	-1.4		
Trans 1,2 $C_2H_2F_2$								
$2\,^2A_u$	-0.004	0.133	-0.087	4.6	-1.4	-3.2		
$5\,^2A_g$	-0.009	0.020	0.051	-4.9	7.4	-2.5		
$4\,^2B_u$	0.045	0.022	0.019	2.5	-1.9	-0.7		
Trans 1,2 $C_2H_2Cl_2$								
$2\,^2A_u$	0.009	0.202	-0.046	17.8	-10.0	-7.8		
$5\,^2A_g$	0.007	0.028	0.033	2.3	-3.2	0.8		
$1\,^2B_g$	0.009	0.033	0.038	2.7	-3.7	1.0		
Trans 1,2 $C_2H_2Br_2$								
$4\,^2B_u$	0.004	0.004	0.049	2.1	-3.9	1.8		
$1\,^2B_g$	0.005	0.004	0.062	1.9	-3.5	1.6		
Trans 1,2 $C_2H_2I_2$								
$4\,^2B_u$	0.004	0.005	0.027	1.5	-2.2	0.6		
Gem $C_2H_2F_2$								
$2\,^2B_1$	0.013	0.142	-0.033		-1.8	-3.0	3.7	6.1
or	0.017	0.128	-0.065		-2.4	-4.0	4.8	7.9
$5\,^2A_1$	-0.056	0.013	-0.022		-0.9	9.2	1.7	18.5
Gem $C_2H_2Cl_2$								
$2\,^2B_1$	-0.023	0.067	-0.057		-1.5	-8.8	3.0	-17.6
Gem $C_2H_2Br_2$								
$2\,^2B_1$	-0.011	0.071	-0.063		-1.7	-6.2	3.5	12.4

convenience in calculation owing to their smallness in value and insignificance in improving the frequency fit. As for cis 1,2 diiodoethylene, only vibrational frequencies[206,207] of one isotopic species are observed. Therefore, only eleven force constants are determined with F_{CH} and H_{CCH} transferred from trans 1,2 diiodoethylene. The calculated force constants for all their dihaloethylenes are listed in Table 11. Using force constants given in Table 11, the in-plane vibrational modes of cis 1,2 $C_2D_2I_2$ are predicted to be 2242, 1475, 779, 480 and 81 cm^{-1} for the a_1 species and 2212, 1064, 590 and 391 cm^{-1} for the b_1 species.

It has been mentioned[210] that the introduction of interaction force constants between angles with one side as a C-C bond is necessary to account for the higher energy of the b_{1g} rocking mode and the lower energy of the b_{2u} mode of ethylene. In their study of bromoethylenes[186], Scherer and Overend found that only the interaction between trans CH bending coordinates is important. However, this is not realistic judging by our results (Table 11) for a series of dihaloethylenes. The trans interaction cross term e_{ij} is always found to be necessary to reproduce the observed frequencies.

The absolute value of h_{xx} is found to be smaller in the trans isomers than in the gem or cis isomers. This is related to a lesser amount of electron delocalization between halogen atoms in the former isomer, and is also consistent with a smaller difference between the symmetric ν_s and the asymmetric ν_{as} C-X stretching frequency observed in the trans isomer[211]. When ν_s of the trans isomer is plotted against ν_{as}, a good straight line is obtained which can be represented by the equation (in cm^{-1})

$$\nu_{as} = 1.5\ \nu_s + 545 \qquad (3.12)$$

Table 11. Urey-Bradley Force Constants (mdyn/Å) of Dihaloethylenes

	K_{CC}	K_{CX}	K_{CH}	H_{CCX}	H_{XCH}	H_{XCX}	H_{CCH}	H_{HCH}	F_{CX}	F_{XX}	F_{CH}	F_{HH}	F_{HX}	C_{HX}	C_{HH}	C_{XX}	h_{HH}	e_{HH}	e_{HX}^{trans}	e_{HX}^{cis}	e_{XX}	h_{XX}
Cis 1,2 CHFCHF	7.312	5.688	4.911	0.485	0.074		0.191		0.600		0.398		0.943		0.102	-0.159	-0.100	0.0	0.098		0.0	-0.428
Cis 1,2 CHClCHCl	6.814	3.556	5.262	-0.172	0.258		0.410		1.604		-0.075		-0.225		0.064	0.156	-0.043	0.0	-0.069		0.0	0.0
Cis 1,2 CHBrCHBr	6.481	2.648	5.658	0.179	0.417		0.486		1.625		-0.119		-0.878		0.079	-0.075	0.009	0.0	-0.026		0.0	0.500
Cis 1,2 CHICHI	6.402	2.021	4.502	0.102	0.004		0.240		0.418		0.537		0.299		0.005	0.151						
Trans 1,2 CHFCHF	7.123	5.655	5.315	0.002	0.202		0.241		0.266		0.700		0.369	0.625			-0.278	0.105		-0.592	0.257	-0.502
Trans 1,2 CHClCHCl	6.903	3.511	5.416	-0.081	0.187		0.008		0.093		-0.624		0.398	0.624			-0.250	0.156		-0.588	-0.039	0.096
Trans 1,2 CHBrCHBr	6.648	2.744	5.302	0.235	0.542		0.356		0.986		0.649		-0.982	-0.156			0.059	-0.173		0.550	0.532	0.125
Trans 1,2 CHICHI	6.157	2.212	5.308	0.133	0.538		0.239		1.168		0.537		-1.032	-0.137			0.115	0.261		0.009	-0.152	0.146
Gem CHFCHF	7.693	5.702	5.376	0.130		0.689	0.163	0.788	1.562	0.598	0.822	-0.871			-0.152		0.304		-0.017	0.0		-0.539
Gem CHClCHCl	7.052	3.581	4.885	0.128		0.130	0.249	0.247	0.293	-1.924	-0.624	0.698			0.624		-0.397		0.0	0.0		-0.418
Gem CHBrCHBr	6.603	2.559	4.502	-0.036		0.447	0.126	0.183	0.402	-1.861	0.110	0.685			0.240		-0.328		0.191	0.0		-0.431

(b) Geometries of the Dihaloethylene Molecular Ions

The sign of d_i determined from the FCF method A discussed previously is not known because it is derived from the square root of the FCF's. The choice of sign for bond lengths and bond angles is based on the bonding property of the neutral molecule (criteria given in section 2.2.1 b). Table 12 lists the overall change in bond length and angle of difluoro- and dibromoethylenes estimated from the results of a CNDO/2 calculation[59]. The bonding property of dibromo- and diiodoethylene should be similar to dichloroethylene. In Table 12, a positive sign means bond lengthening or angle widening. Those changes in internal coordinates which cannot be predicted from the criteria are denoted by question marks.

The geometric changes given in Table 10 are chosen to reproduce the expected sign varation given in Table 12 as close as possible. Sometimes, two sets of parameters may fit the same criteria. In this case, both sets are listed. In general, the agreement is good for the ground ionic states. The discrepancy in sign between calculated and predicted change in bond angle is probably due to modification of the repulsive force between nonbonding atoms during the alteration of bond distances.

Ionization of an electron from the highest occupied π orbital results in a large change in the C-C bond and sometimes in the C-X bond also. Δr_{cc} is largest for dichloroethylenes, and is smaller for dibromoethylenes, and then diiodoethylenes, while the opposite is true for Δr_{cx} (except trans 1,2 dihaloethylenes). This agrees with the fact that the conjugative effect is more important, as well as $\varepsilon_{c=c}$ (sections 4.5 and 4.6) becoming larger for heavier halogen atoms in the halogenated ethylenes studied. Δr_{cc} of difluoroethylenes is found to be the same or even less than that

Table 12. Predicted Changes[a] in Geometry of Dihaloethylenes upon Ionization

Ionic State	Δr_{CH}	Δr_{CC}	Δr_{CX}	$\Delta\alpha_{HCX}$	$\Delta\Phi_X$	$\Delta\Phi_H$	$\Delta\alpha_{XCX}$	$\Delta\alpha_{HCH}$
Cis 1,2 $C_2H_2F_2$								
$2\,^2B_1$	?	+	-	?	-	?		
$5\,^2A_1$	+	+	+	?	+	-		
$3\,^2B_2$	+	-	+	?	+	-		
Cis 1,2 $C_2H_2Cl_2$								
$2\,^2B_1$	?	+	-	?	-	?		
$1\,^2A_2$	?	-	+	?	-	?		
Trans 1,2 $C_2H_2F_2$								
$2\,^2A_u$	?	+	-	?	-	?		
$5\,^2A_g$	+	+	+	+	-	-		
$4\,^2B_u$	?	-	+	?	-	?		
Trans 1,2 $C_2H_2Cl_2$								
$2\,^2A_u$	?	+	-	?	-	?		
$5\,^2A_g$	+	-	+	?	-	-		
$4\,^2B_u$	+	+	+	+	-	?		
$1\,^2B_g$	?	-	+	?	-	?		
Gem $C_2H_2F_2$								
$2\,^2B_1$	?	+	-		-	?	+	?
$5\,^2A_1$	+	+	-		-	-	+	+
Gem $C_2H_2Cl_2$								
$2\,^2B_1$	?	+	-		-	?	+	?

[a]Positive sign means bond lengthening or angle widening. Question mark denotes that the change in internal coordinate cannot be estimated from the treatment of nodal repulsive force.

of dichloroethylenes. This is unexpected from the above reasoning for the other dihaloethylenes, and is probably due to reorganization of electron distribution in the compounds on ionization.

At first glance, it may be surprising to find that $\Delta\gamma_{CH}$ and $\Delta\phi_H$ are nonzero in the ground ionic state. This arises from the nonvanishing value of the off-diagonal elements in the Ls matrix used in the calculation.

The ionic frequency of the dihaloethylenes deduced from the PE band (refs. 208, 209 and section 4.5 also) is sometimes midway between the two ground state fundamentals, and it is difficult to decide on the correct assignment. Results from the FCF calculation are useful in assigning the frequency. For example, the frequencies 1360, 992 and 1185 cm^{-1} respectively observed in the first, second and fourth PE band of cis 1,2 difluoroethylene are assigned to come from ν_4', ν_4', and ν_3' from the result of the FCF treatment. In the same manner, 1234 and 1125 cm^{-1} respectively obtained in the fine structure of the first and fourth PE band of trans 1,2 difluoroethylene are attributed to excitation of ν_3' and ν_4' modes.

(c) Origin of the Geometrical Change on Ionization

Three mechanisms have been proposed by Coulson and Luz[184] to describe the difference in geometry of C_2Cl_4 in the ground neutral state and the lowest ionic state. They are (i) change in bond order, (ii) change in electrostatic interaction, and (iii) change in repulsive exchange forces. The last mechanism is not clear since the available wavefunctions are not good enough. In the following paragraph, we are going to discuss the importance of mechanisms (i) and (ii) operating on the ground ionic state of difluoro- and dichloroethylenes.

In the dihaloethylenes, the highest occupied MO possesses C-C π bonding and C-X antibonding character. Hence, the removal of an electron from this orbital weakens the C-C bond (lowers the bond order) but strengthens the C-X bond. Quantitatively, the changes in C-C and C-Cl bonds are related to the bond order change Δu by

$$\Delta r_{cc}^{cal} = -0.16\,\Delta u_{cc} / (1 + 0.24\,\Delta u_{cc}) \qquad (3.13)$$

$$\Delta r_{ccl}^{cal} = -0.205\,\Delta u_{ccl} / (0.77 + 0.235\,\Delta u_{ccl}) \qquad (3.14)$$

from equation[184,212] originally derived for hydrocarbons. Thus Δr_{cc}^{cal} is found to have a value 50% or less of Δr_{cc} from the FCF calculation for both difluoro- and dichloroethylenes given in Table 10. However, Δr_{ccl}^{cal}'s of cis, trans 1,2 and gem isomers are respectively -0.06, -0.06 and -0.05 Å, compared with Δr_{ccl}'s -0.08 (or 0.00), -0.05 and -0.06 Å. This indicates that mechanism (i) is important in altering the C-X bond rather than the C-C bond. Qualitatively, the bond order approach for bond angle changes is good for all the dihaloethylenes as mentioned before. However, a calculation on the bond order change in the ClCCl angle in gem dichloroethylene gives $\Delta\alpha_{ClCCl}^{cal}$ 0.9° which is much smaller than that in Table 10, 3.0°.

In addition to mechanism (i) described, electrostatic forces[184] between carbon and halogen atoms, or carbon and carbon, as well as halogen and halogen themselves in the ion may be active in the rearrangement of molecular coordinates (mechanism (ii)). Assuming the localization of the π electron in the carbon skeleton, removal of an electron from the π orbital leaves $+\frac{1}{2}e$ charge on each carbon nucleus. Hence, there are coulombic attractive forces between carbon and halogen atoms. Using the same treatment as Coulson and Luz[184] on C_2Cl_4, Δr_{CF}^{cal} and $\Delta\alpha_{FCF}^{cal}$ for gem difluoroethylene have values of -0.03 Å and 3.0° respectively, in good agreement with

-0.033 Å and 3.7° from the FCF method. The C-F bond dipole moment used is 1.43 Debyes from vinyl fluoride[213] and the force constants are adopted from Table 11. In the case of gem dichloroethylene, the C-Cl dipole moment is taken to be 1.44 Debyes from C_2H_3Cl[214]. The values of Δr_{CCl}^{cal} and $\Delta\alpha_{ClCCl}^{cal}$ obtained, -0.03 Å and 1.34° deviate quite large from those given in Table 10. As mentioned before[184], mechanism (ii) is predicted to be more important for C_2F_4 than for C_2Cl_4 and the result of our calculation supports this statement.

Adopting the naive assumption that we have $+\frac{1}{2}e$ charge on each carbon nucleus in the ion, then Δr_{CC}^{cal} is found to be about 50% of Δr_{CC}. It seems that both mechanisms (i) and (ii) are active in C-C bond length changes. It should be mentioned that the two mechanisms predict that Δr_{CC} becomes larger for more electronegative halogen atoms in dihaloethylenes owing to the variation of the coefficient of the carbon atomic orbitals in the occupied π orbital, as well as the diversity of the electron cloud in the C-C bond length.

Because of the success of mechanisms (i) and (ii) in the estimation of structural changes in fluoroethylenes, a FCF calculation was carried out also on the ground ionic state of C_2F_4 with FCF's derived from ref. 215 and the $\underline{Ls}$ matrix from ref. 216. On the assumption of the planarity of the ion, Δr_{CC}, Δr_{CF} and $\Delta\alpha_{FCF}$ are found to be 0.133 Å, -0.062 Å and 4.7° respectively. Δr_{CC}^{cal} is predicted to be 0.04 Å from mechanism (i) while Δr_{CC}^{cal}, Δr_{CF}^{cal} and $\Delta\alpha_{FCF}^{cal}$ are 0.04 Å, -0.04 Å and 4.8° respectively from mechanism (ii). The force constants used are taken from ref. 217.

It seems that the widening of the fluorine-carbon-fluorine bond angle is mainly due to electrostatic forces between the carbon and fluorine atoms.

CHAPTER IV

PHOTOELECTRON SPECTROSCOPY OF SOME HALOGENATED COMPOUNDS

4.1 Fluorotrichloromethane and Fluorotribromomethane

4.1.1 Introduction

The first four highest occupied MO's, a_1, a_2, e′ and e″ (C_{3v} symmetry), of the trihalomethanes CHX_3, and their fluoro-substituted derivatives CFX_3 (X = Cl,Br) are mainly contributed to from the formally nonbonding ρ orbitals of the halogen atom. The relative orderings of these orbitals have been the subject of several discussion.

Potts et al[30] suggested the electronic structures for chloroform and bromoform to be $(e'')^4\ (e')^4\ (a_1)^2\ (a_2)^2$ and $(e'')^4\ (a_1)^2\ (e')^4\ (a_2)^2$ respectively, in order of decreasing energy. To distinguish between the first two highest occupied e orbitals, e' and e'' are chosen in such a way that they transform as different representations in the limit of a planar CX_3 group. A different assignment, $(e')^4\ (a_1)^2\ (e'')^4\ (a_2)^2$, was given by Dixon et al[218] for both molecules. Recently, CNDO/2 calculations on the chloromethanes were reported by Katsumata and Kimura[219] and their results gave the ordering of the orbitals as $(e'')^4\ (a_2)^4\ (e')^4\ (a_1)^2$. In planar molecules, the perfluoro effect[41,42] has been found to be active in lowering the σ and π orbital energies (within one ev for π orbitals but greater than two ev for σ orbitals) upon fluorine substitution of hydrogen in the molecules. A similar kind of effect may also operate on chloro- and bromoform with replacement of the hydrogen by a fluorine atom, in which large energy separations exist between σ and lone pair orbitals. We have therefore measured the PE spectra of fluoro-substituted $CHBr_3$ and $CHCl_3$, i.e. $CFBr_3$ and $CFCl_3$, from which the energetic ordering of the nonbonding orbitals of the trihalomethane can be deduced. The observed IP's for the two compounds and their assignment (which are justified later) are given in Table 13.

4.1.2 Interpretation of the Spectra

$CFBr_3$

The He I PE spectrum of $CFBr_3$ is shown in Fig. 6. Bands with IP's below 13 ev are assigned as arising from the bromine lone pairs (a_2, e'', e' and a_1 orbitals in order of increasing IP) on the basis of the intensities of these bands, as well as for reasons given below. The first sharp peak in the spectrum reflects the nonbonding character of the a_2 orbital from

Table 13. Observed Vertical Ionization Potentials in the Photoelectron Spectra of Fluorotribromomethane and Fluorotrichloromethane

Orbital	$CFCl_3$[a] (ev)	$CFBr_3$[a] (ev)
$1a_2$	11.77 (1)	10.67 (1)
5e''	12.16 (1)	11.14[b] (1)
4e'	12.95 (1)	11.81[b] (1)
$5a_1$	13.46 (1)	12.38 (1)
3e'	15.04 (2)	13.96 (2)
$4a_1$	18.44 (2)	17.59 (7)

[a]The reproductibility of the last digit is shown inside the bracket.

[b]Mean of the fine structure components.

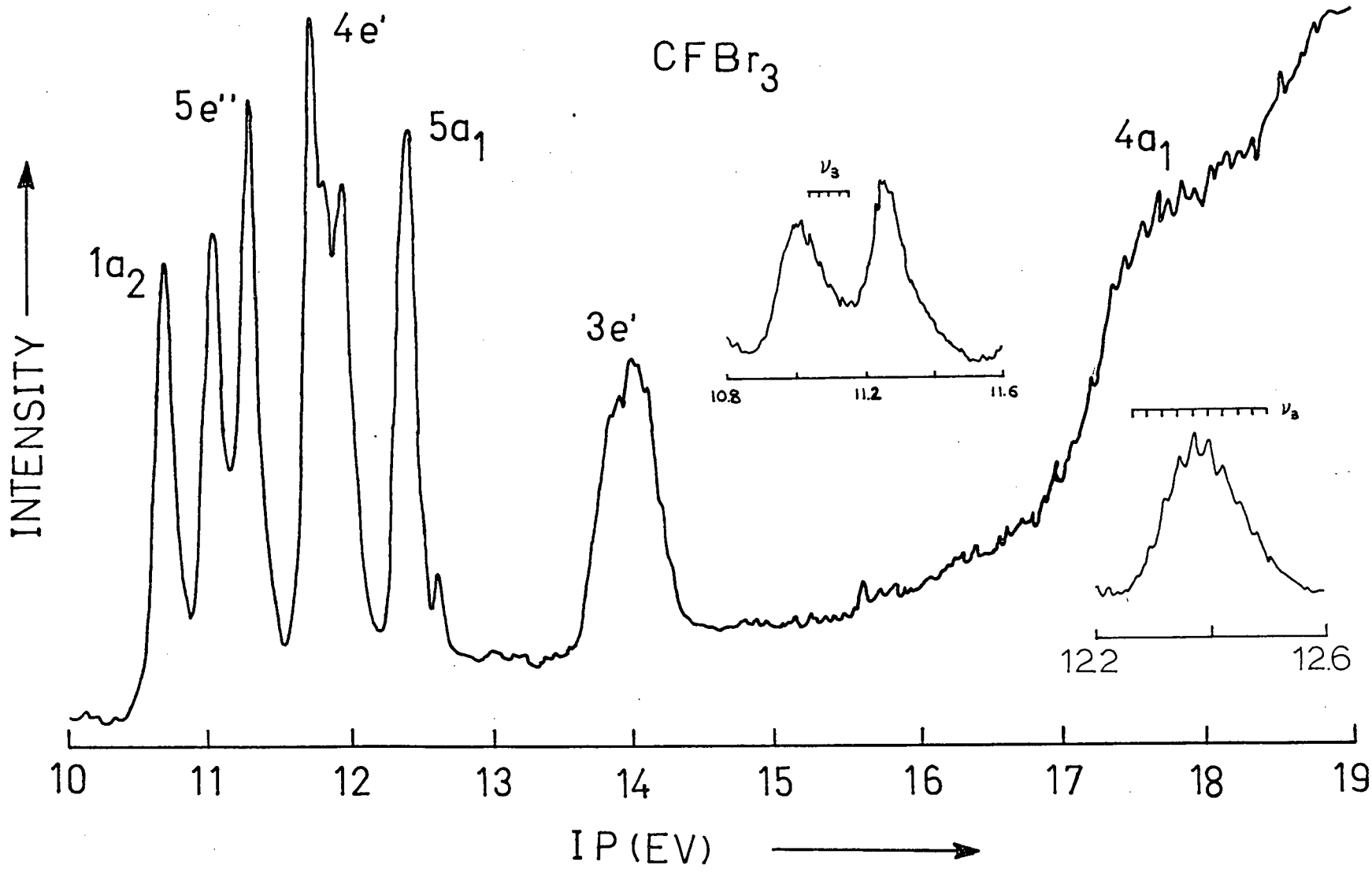

Figure 6. The PE spectrum of fluorotribromomethane.

which the electron is removed. The IP of this orbital is shifted to a higher value by 0.2 ev with respect to bromoform. The fourth band (with vertical IP 12.38 ev) exhibits well resolved vibrational structure (Fig. 6) starting at 12.28 ev. The result of a FCF calculation (method A) using FCF's given in Table 14 indicates that the fine structure arises from a single progression of ν_3* rather than from a composite of ν_2 and ν_3. The C-F and C-Br bonds, and the BrCBr angle are found to be increased by 0.11, 0.017 Å, and 3°, respectively, during the ionization process.

The second and third bands in the spectrum, relating to the loss of electrons from the e orbitals, consist of well-resolved doublets with separations of 0.25 and 0.21 ev respectively. The splitting of the first band is 0.25 ev, compared to that observed for PBr_3[30], 0.2; $CHBr_3$[30], 0.14; $OPBr_3$[97], 0.25 and $SPBr_3$[97], 0.22 ev. Single quantum excitations of ν_3 (213 cm^{-1}) and ν_1 (874 cm^{-1}) are also observed in the first as well as the second E band.

The result of a CNDO/BW calculation[221] shows that there is a weak C-Br antibonding character in the e'' orbital, and there is weak C-Br bonding character in the e' orbital although these two highest occupied e orbitals are essentially nonbonding. The vibrational spacings in ν_3 indicate that the first E band is derived from the e'' orbital.

Recently we have measured the PE spectrum of chloroform, which has been recorded by Potts et al[30] with a lower resolution spectrometer. The right hand shoulder of the second E band (Fig. 7) exhibits two well

* The vibrational modes ν_1 (C-F stretch), ν_2 ($C-Br_3$ symmetric stretch), and ν_3 ($C-Br_3$ symmetric bending) have values of 1069, 398 and 218 cm^{-1} respectively in the neutral molecule[220].

Table 14. Franck-Condon Factors of $CFBr_3$ in the $^2A_1$ Ionic State

m_3	Energy(ev)	FCF[a]	cald FCF	Vibrational Spacings (mev)
0	12.251[b]		0.03	
1	12.277	0.18	0.21	23
2	12.300	0.35	0.45	28
3	12.328	0.62	0.72	26
4	12.354	0.85	0.92	26
5	12.380	1.00	1.00	29
6	12.406	0.96	0.92	26
7	12.432	0.81	0.74	27
8	12.459	0.59	0.53	25
9	12.484	0.41	0.35	26
10	12.510	0.28	0.20	

[a]The intensity of a peak is assumed to be proportional to the height of the fine structure maximum. The value listed in the Table is chosen in such a way that the intensity of the highest peak is one unit.

[b]The value obtained by extrapolation.

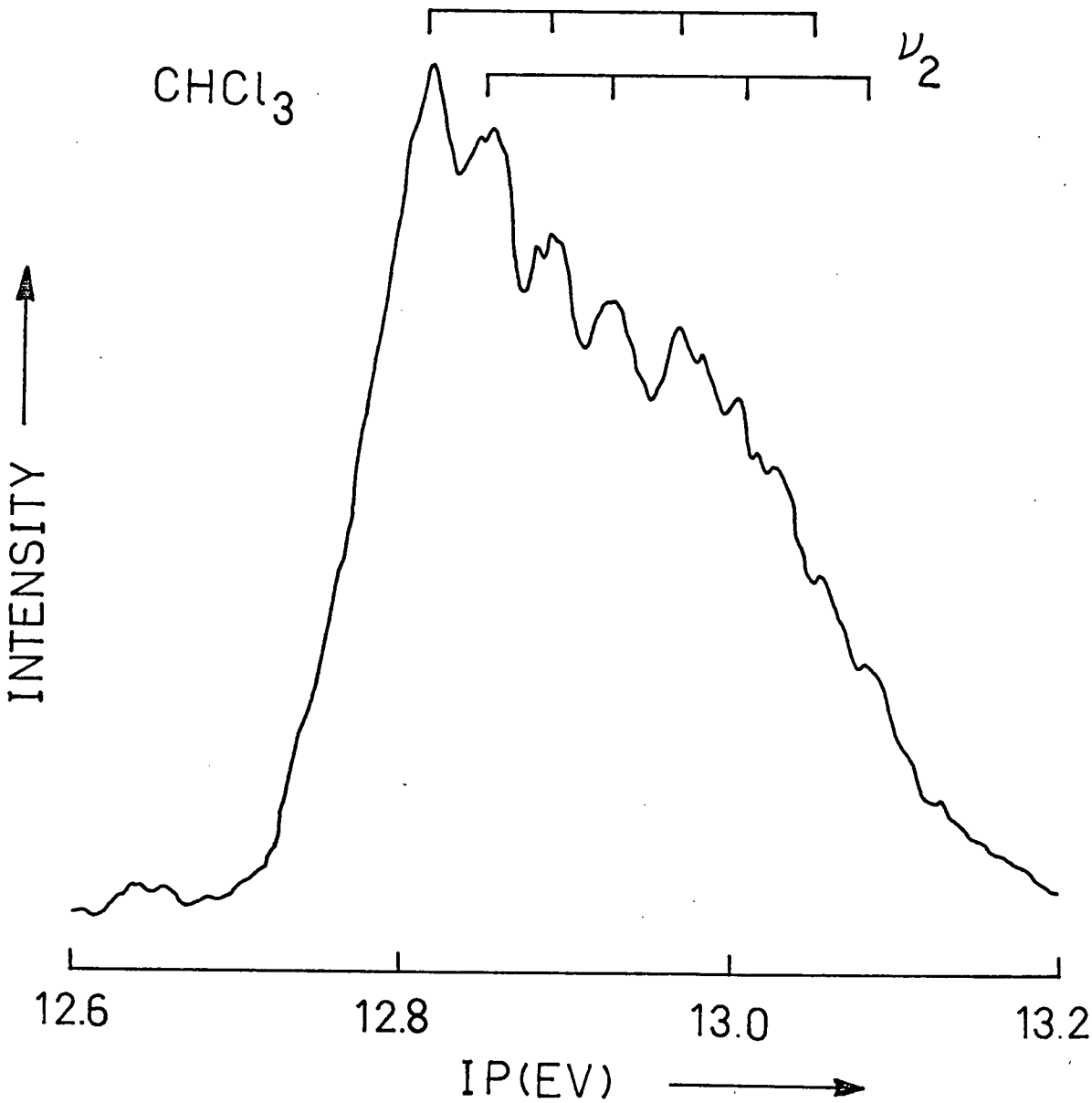

Figure 7. The second PE band of chloroform.

resolved progressions in ν_2 , the C-Br_3 symmetric stretching mode with values slightly less than that of the neutral molecule[76]. The same result was obtained for deuterated chloroform. This supports our assignment that the second PE band of $CFBr_3$ is related to the e' orbital.

The last two PE bands of $CFBr_3$ in the 13-18 ev region are readily assigned to the e' and a_1 orbitals according to the MO calculation. It is interesting to note that the e' orbital is destabilized by about 0.8 ev with respect to the corresponding band of $CHCl_3$. This reflects the antibonding character of the e' orbital for the CF bond. The observation parallels the result of MO calculations on this molecule.

$\underline{CFCl_3}$

The PE spectrum of $CFCl_3$ is shown in Fig. 8 and thus the IP's obtained are given in Table 13. The relative areas of the first bands reflect the degeneracies of the levels involved and thus their ordering is likely to be a, e, e, a. These orbitals contain a major contribution from the chlorine p orbitals. The first band at 11.77 ev can readily be assigned as arising from the a_2 nonbonding orbital. The next two bands are fairly broad and asymmetrical with nonresolvable vibrational fine structure. The assignment of these two bands is somewhat ambiguous. Assuming the orbital ordering to be the same as that of $CFBr_3$, the experimental IP's at 12.16 and 12.96 ev correspond to the e'' and e' orbitals. However, the alternative assignment that the e' is associated with a higher IP than e'' cannot be definitely rulted out. In the fourth band, the vibrational spacings $\approx$ 1011, 641 and 303 cm^{-1} can be deduced. This suggested that all the three totally symmetric vibrational modes ν_1 , ν_2 and ν_3 (1085, 535 and 350 cm^{-1} respectively in the ground state[222]) are excited during

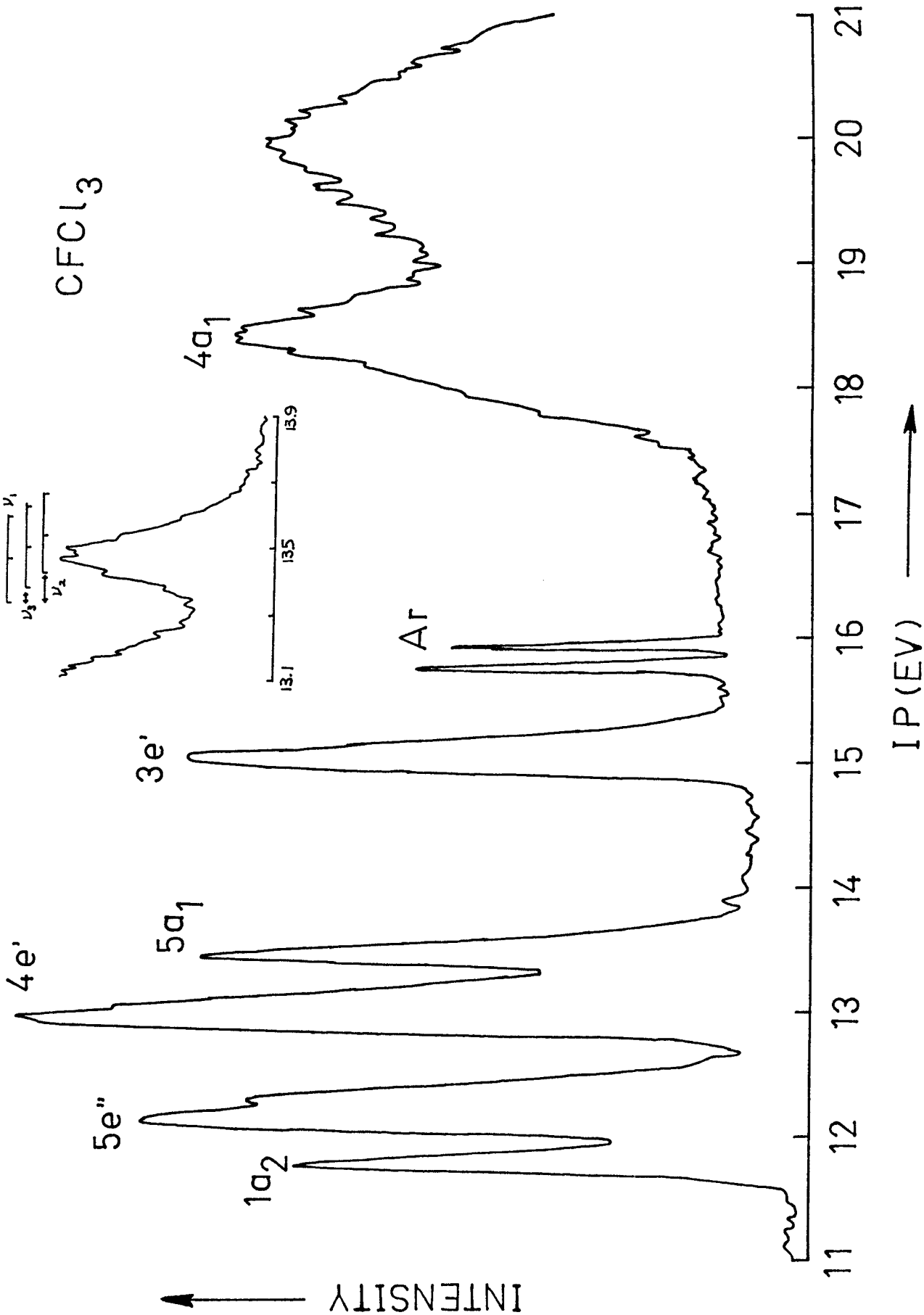

Figure 8. The PE spectrum of fluorotrichloromethane.

the ionization process.

The last two bands are related to electron loss from the e' and a_1 orbitals, and parallel to those in $CHCl_3$ and $CFBr_3$ mentioned previously. The e' orbital again shifts to lower energy with respect to $CHCl_3$ presumably for the same reasons as we offered in explaining the downshift for the corresponding e' orbital in $CFBr_3$. The structure at 19.98 ev comes from low energy scattered electrons in the spectrometer itself.

4.1.3 Discussion

From the analysis of the fluorotribromomethane spectrum, the e' orbital is found to have a higher bonding energy than the e'' orbital in this molecule. Following the assignment on the experimental IP's of $CHBr_3$ given by Potts et al[30], the e' orbital is stabilized by $\approx$ 0.9 ev while the e'' orbital is destabilized by $\approx$ 0.7 ev from $CHBr_3$ to $CFBr_3$. The trends and the magnitudes of these shifts in energies in nonbonding orbitals as influenced by the effect upon fluorine substitution of hydrogen seem to be too large in comparison to those shifts in the π orbitals of planar molecules[41,42]. Because of this, Dixon et al's assignment[218] on $CHBr_3$ is preferred. When similar arguments are applied to $CHCl_3$, the relative ordering of e' and e'' orbitals is found to agree with that proposed by Dixon et al[218] and by our work on chloroform.

The correlation diagram (Fig. 9) shows that the energy levels of $CFBr_3$ and $CFCl_3$ have the same ordering with the former being uniformly shifted towards lower energies by $\approx$ 1 ev. The same observation applies to chloroform and bromoform, and phosphoryl chloride and bromide[97]. This reflects the fact that the first five or six highest occupied orbitals are mainly built up from halogen p atomic orbitals.

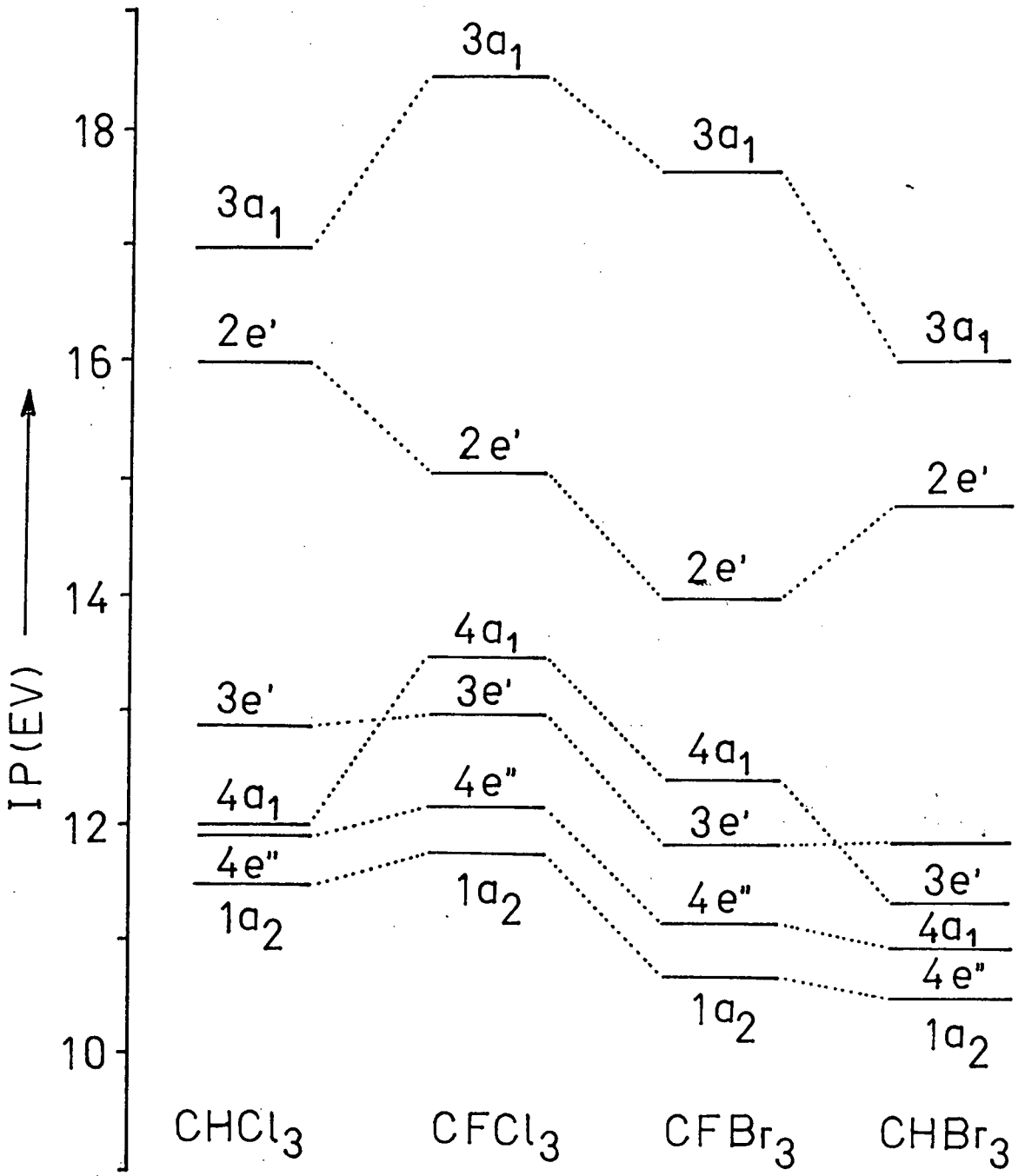

Figure 9. Correlation diagram for the first six highest occupied orbitals of CHX_3 and CFH_3 (X = Cl, Br). The data for $CHCl_3$ and $CHBr_3$ are from Dixon et al[218] and Potts et al[30].

In Fig. 10, the vertical IP's of the non bonding orbitals $1a_2$ or $1a_2'$ of CFX_3[30*], CHX_3[30,218], OPX_3[97,223], BX_3[30] and PX_3[30] (X = F, Cl, Br or I) are plotted against the Pauling electronegativity values of the halogen atoms. Straight lines are obtained. The predicted IP's for $1a_2$ orbitals of CF_3I and OPI_3, and for the $1a_2'$ orbital of PI_3 are 9.45, 10.28 and 9.36 ev respectively. Following arguments similar to those by Kimura et al[224], the gradients of these lines in the plots indicate the contributions of halogen p atomic orbitals in the trihalo compounds. It is interesting to note that the gradients in the two series CHX_3 and OPX_3 (Fig. 10) are nearly the same.

It should be noted that our assignments of the first four nonbonding orbitals of $CHCl_3$ disagrees with that based on the CNDO/2 calculation[219]. However, it is well recognized that[219] the resulting orbital sequences of the chloromethanes depend greatly on the selection of parameter values for the chlorine atoms. The fact that no comparison was made between IP's of related compounds may also lead to a different assignment.

While this work was near completion, Doucet et al[225] presented a communication in which they reported the PE spectrum of $CFCl_3$. Their data is in good agreement with ours, although they did not offer a complete assignment of the observed IP's.

4.2 1,2 Dichloro-, 1,2 Dibromo- and 1,2 Diiodoethane

4.2.1 Introduction

Compounds with a C-C single bond such as the 1,2 dihaloethanes $(CH_2X)_2$ (X = Cl, Br and I), exist in the vapor state as equilibrium mixtures of the gauche (C_2) and trans (C_{2h}) conformers because of rotation about the

* For CF_4, the vertical IP of the $1a_2$ orbital is considered the same as that of t_1 which under C_{3v} symmetry splits into a_2 and e.

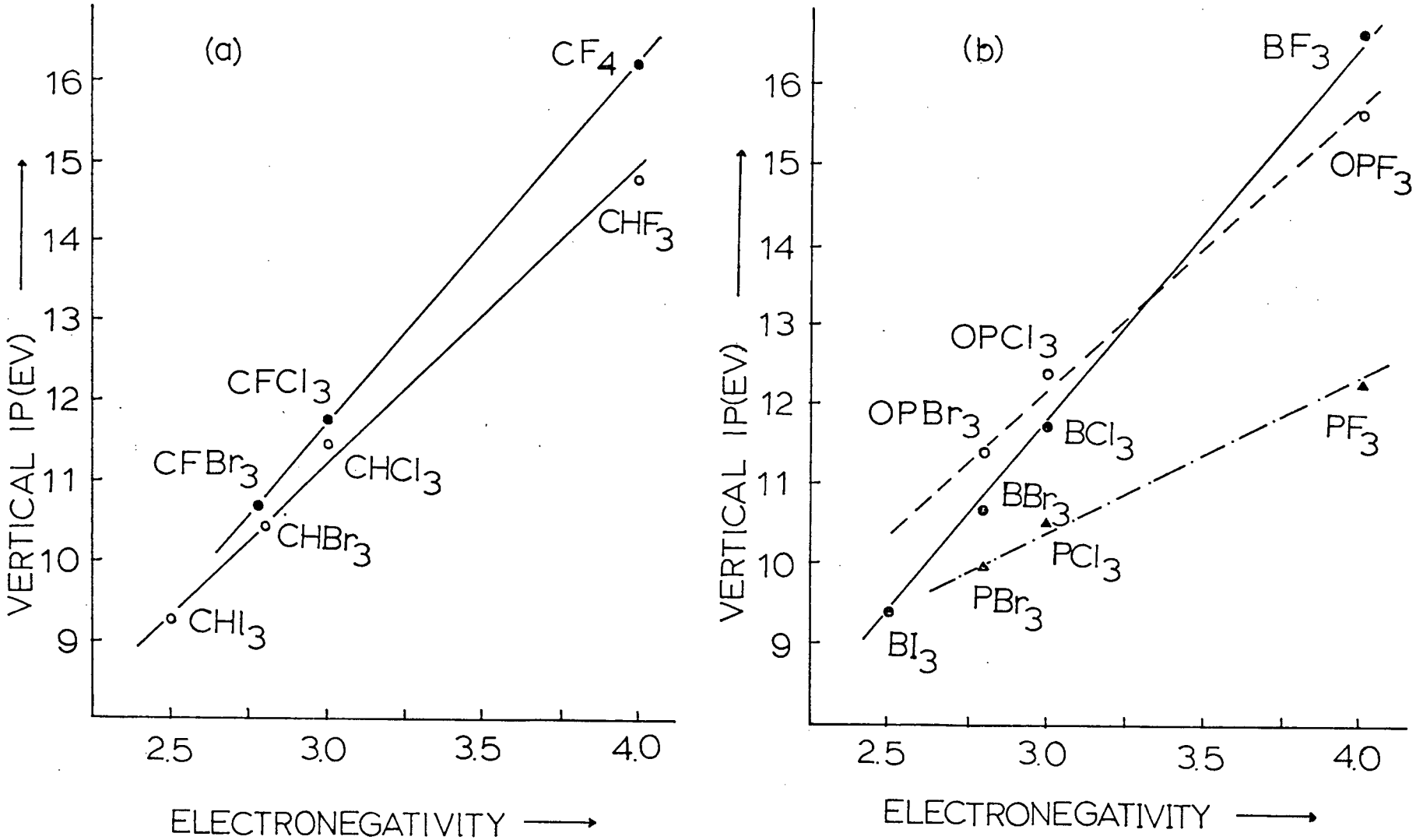

Figure 10. Plot of vertical IP's of (a) the $1a_2$ orbitals of CFX_3[30] and CHX_3[30,218], (b) the $1a_2$ orbitals of OPX_3[97,223] and the $1a_2'$ orbitals of BX_3[30] amd PX_3[30] with X = F, Cl, Br or I, against the Pauling electronegativity of the halogen atom.

C-C bond. Various physical methods such as infrared and Raman spectroscopy[226-228], electron diffraction[229,230], microwave spectroscopy[231,232], and X-ray diffraction[233] have been used extensively to determine the molecular structures, populations and conformational energies of the conformers of the disubstituted ethanes. The trans isomers are generally found to be more stable than the gauche by 1.09 (77%)* and 1.68 kcal/mole (90%) for $(CH_2Cl)_2$ and $(CH_2Br)_2$ respectively. Although no information of this sort is available for $(CH_2I)_2$, the stability and population of the trans form of this molecule should be at least equal or even greater than that of $(CH_2Br)_2$, in view of the larger nonbonded repulsions between the halogen atoms in the former molecule[226-228].

In spite of the large amount of experimental data accumulated concerning the molecular structure of the dihaloethanes, little work has been done on elucidation of the electronic structures, and the nature of the bonding in these molecules. In this section, we present the He I high resolution spectra of the 1,2-dihaloethanes, and discuss the interaction between the halogen LPMO's in these molecules, the enthalpy difference between the isomeric trans and gauche ions, as well as the geometry of the $(CH_2Cl)_2$ ion in the first ionic state. Moreover, a correlation between IP's and certain physical properties will be mentioned.

The PE spectra of 1,2-dichloro-, 1,2-dibromo-, and 1,2-diiodoethane are shown in Figs. 11 - 13. The observed IP's are summarized in Table 15.

* Number in parenthesis refers to the concentration of the trans isomer in gas phase as determined by infrared spectroscopy[228].

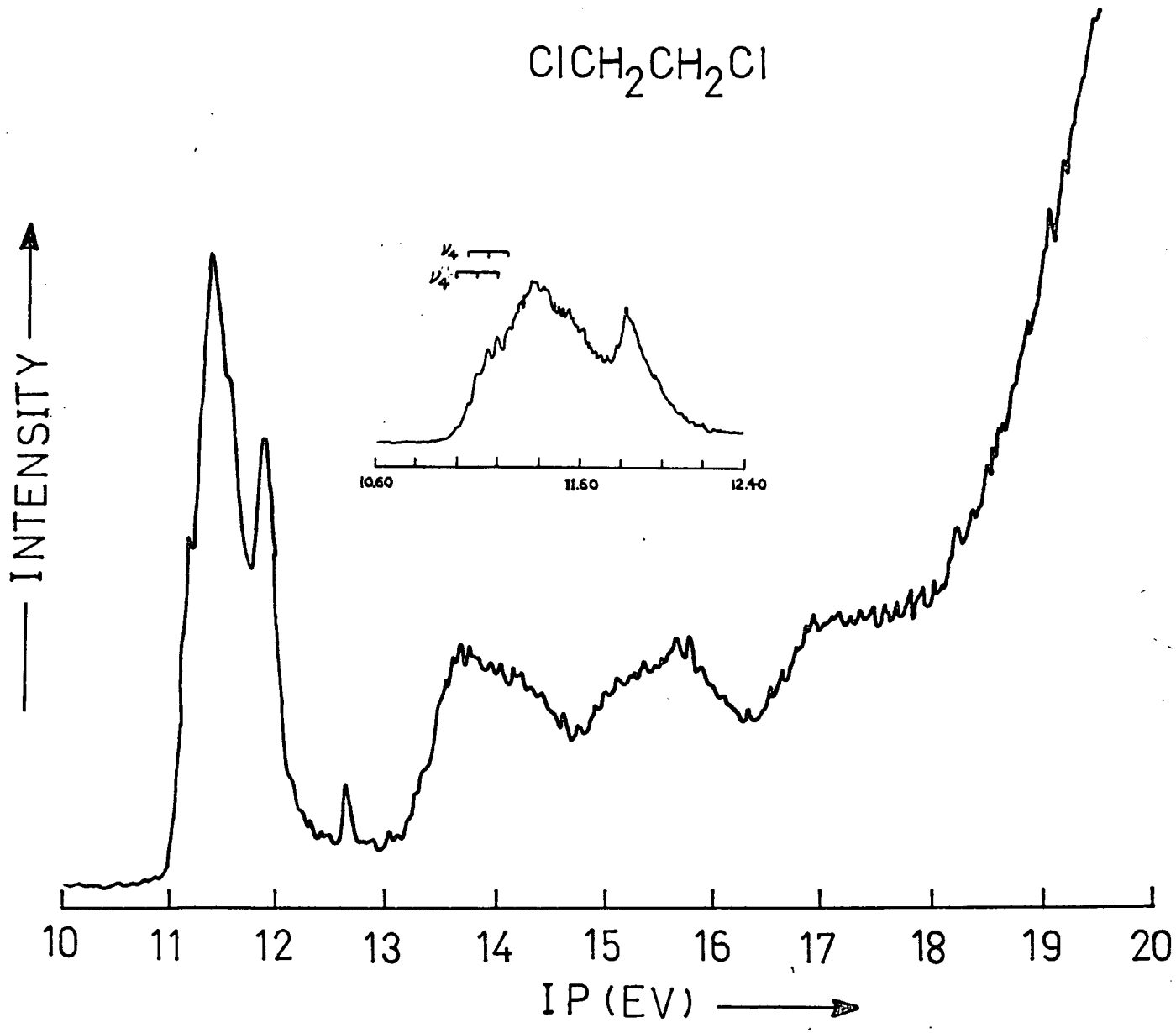

Figure 11. The PE spectrum of dichloroethane.

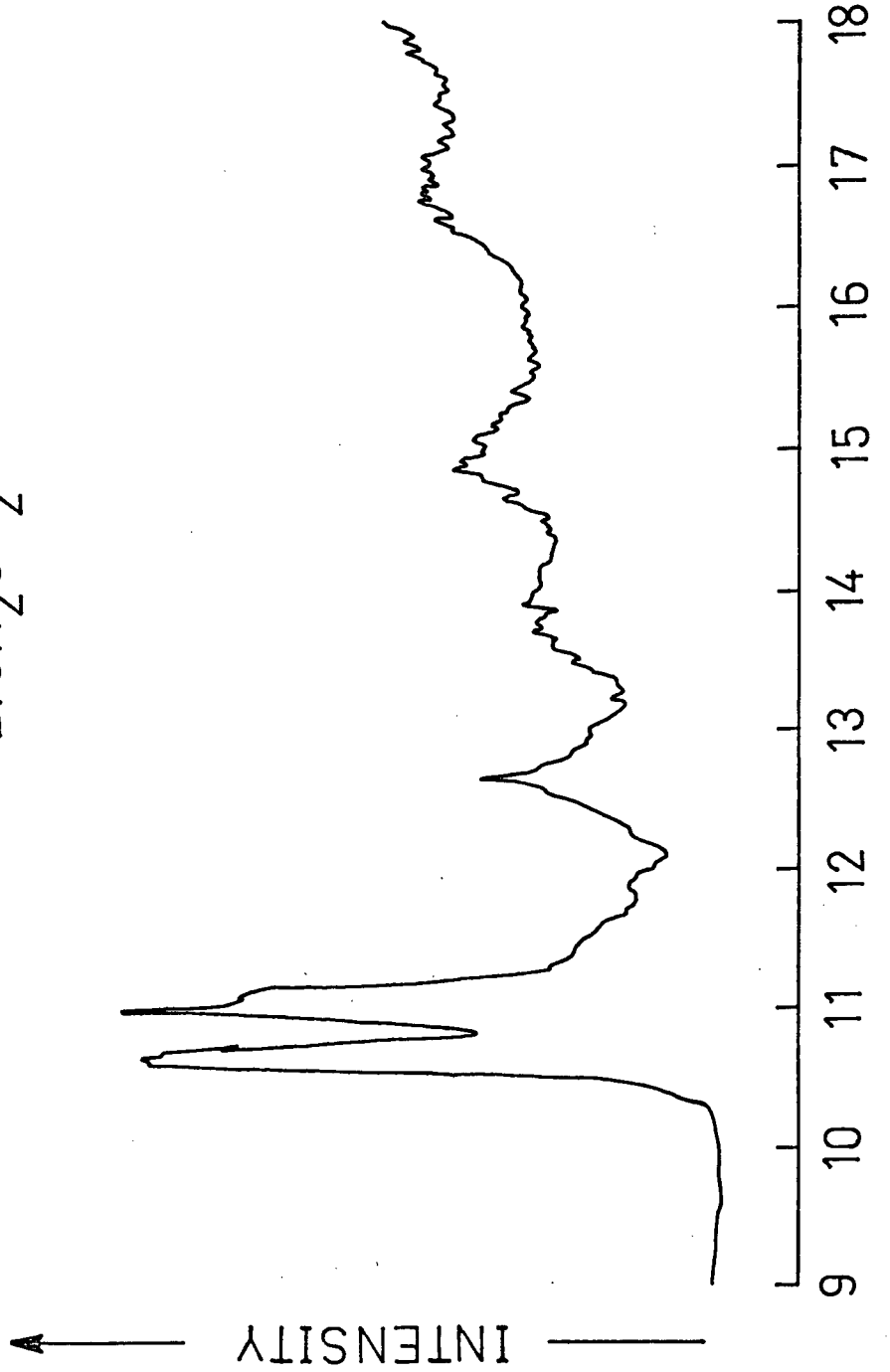

Figure 12. The PE spectrum of dibromoethane.

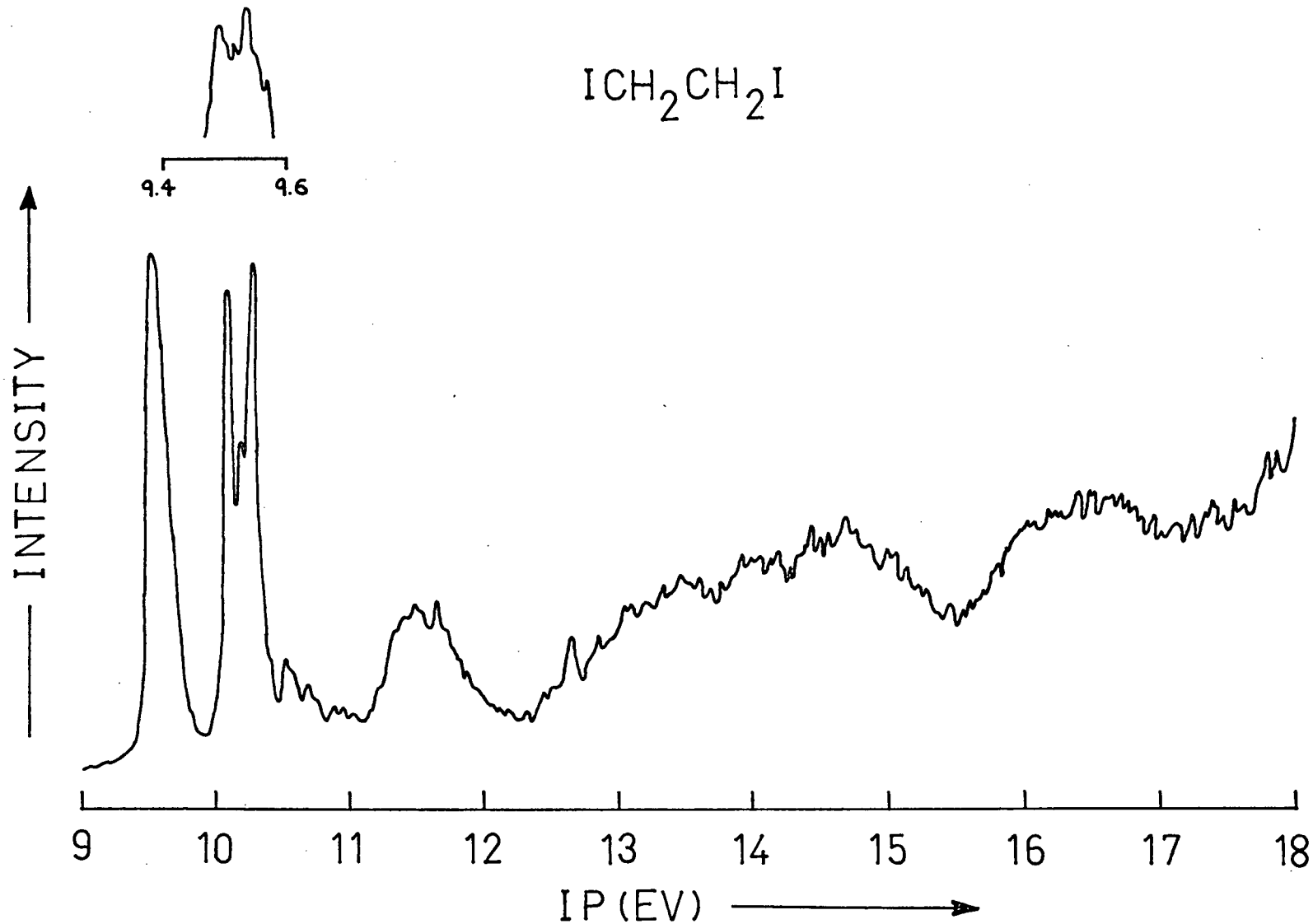

Figure 13. The PE spectrum of diiodoethane.

Table 15. Observed and Calculated Vertical IP's (ev) of 1,2 Dihaloethanes[a]

Orbital	$(CH_2Cl)_2$		$(CH_2Br)_2$		$(CH_2I)_2$	
	Obs.	Cald.[b]	Obs.	Cald.[b]	Obs.	Cald.[b]
χ_1[c]	11.22	11.22	10.57	10.58	9.50	9.49
χ_2	11.39	11.39	10.63	10.63	9.56	9.55
χ_3	11.55	11.55	10.96	10.95	10.08	10.08
χ_4	11.83	11.83	11.08	11.07	10.26	10.27
σ_{4a_g}	13.68	13.68	12.61	12.60	11.50	11.51
σ_{3b_u}	14.39	14.39	13.84[b]	13.87	13.19	13.18
σ_{1b_g}	15.28	15.28	14.88	14.85	14.69[d]	14.68
σ_{3a_g}	16.97[d]		16.87[d]		16.34[d]	

[a] Experimental error within ± 0.02 ev.

[b] These IP's are calculated from values of parameters given in Table 16.

[c] χ_i is the i^{th} halogen LPMO.

[d] Experimental error ± 0.05 ev.

4.2.2 Results and Discussion

(a) One Electron Model for the Lone Pair Orbitals of Trans 1,2-dihaloethanes (C_{2h})

Classically, non-bonding electrons of halogen atoms in molecules can be considered to be localized as lone pairs in the p orbitals. For example, in the ethyl halides EtX[94,95,224,234], the two highest occupied molecular orbitals are found to have an appreciable amount of halogen p character and may be regarded as LPMO's of the halogen atom. As the local cylindrical symmetry at the halogen atom is disturbed to a negligible extent by, say, a methyl group[95], removal of electrons from these orbitals give rise to two intense sharp peaks in the PE spectra, with separations roughly equal to ζ_x [94]. In a trans dihaloethane, if there is no interaction between the LPMO's of the halogen atoms, its PE spectrum should be similar to that of the corresponding ethyl halide. In fact, each of the two PE bands relating to ionization from the LPMO's shows a double maximum (Fig. 11 - 13) with the separation being greater in the one associated with the higher IP. This clearly indicates that there is an appreciable amount of mixing between these LPMO's. The observation can be explained using a one electron model similar to that employed by Brogli and Heilbronner[44] (section 2.1.5) for the case of the alkyl bromides where both spin orbit coupling between the halogen LPMO's, and also the mixing between these orbitals and the σ orbitals (section 2.1.4) are taken into consideration. It is, of course, assumed that Koopmans' theorem[37] can be applied in these cases. Throughout this work, the trans conformer is considered to give rise to the main features in the PE spectra.

Assuming that there is no interaction between the LPMO's of dihaloethane (Fig. 14, case a), then all these orbitals are degenerate. However, if a direct spatial overlap between these LPMO's, that is, a through space interaction[77,78] is present, the degeneracy of the orbital is removed (Fig. 14, case b). The four LPMO's will combine with each other to give MO's of a_g, a_u, b_g and b_u symmetry (Fig. 15) under the C_{2h} point group. The through space parameter d_{xx} which measures the degree of the interaction between the orbitals themselves is a sensitive function of the X...X distance ($\simeq 3$ Å) and is estimated from expression (2.7).

There is another kind of interaction called through bond interaction[77,78] by which LPMO's mix indirectly with each other through σ MO's, providing all of them belong to the same symmetry class. In other words, orbitals of the same symmetry repel one another. The degree of perturbation is inversely proportional to the energy separation of the two interacting orbitals. As a result of this through bond interaction, all LPMO's except l_{2a_u} are destabilized, and the parameters S_{a_g}, S_{b_g} and S_{b_u} are used to describe the interaction. In view of the large energy difference between l_{2a_u} and σ_{1a_u} (IP > 21 ev), the quantity S_{a_u} is small and may be assumed to be zero.

It should be mentioned that the σ orbital sequence given in Fig. 14 as well as in Table 15, namely, σ_{4a_g}, σ_{3b_u}, σ_{1b_g} and σ_{3a_g} in order of increasing IP, is chosen in the following way. According to the CNDO calculations[59,221], the σ MO ordering is σ_{4a_g}, σ_{1b_g}, σ_{3a_g}, and σ_{3b_u}. If this is true, then S_{b_g} should be greater than S_{b_u} because the through bond interaction is inversely proportional to the energy

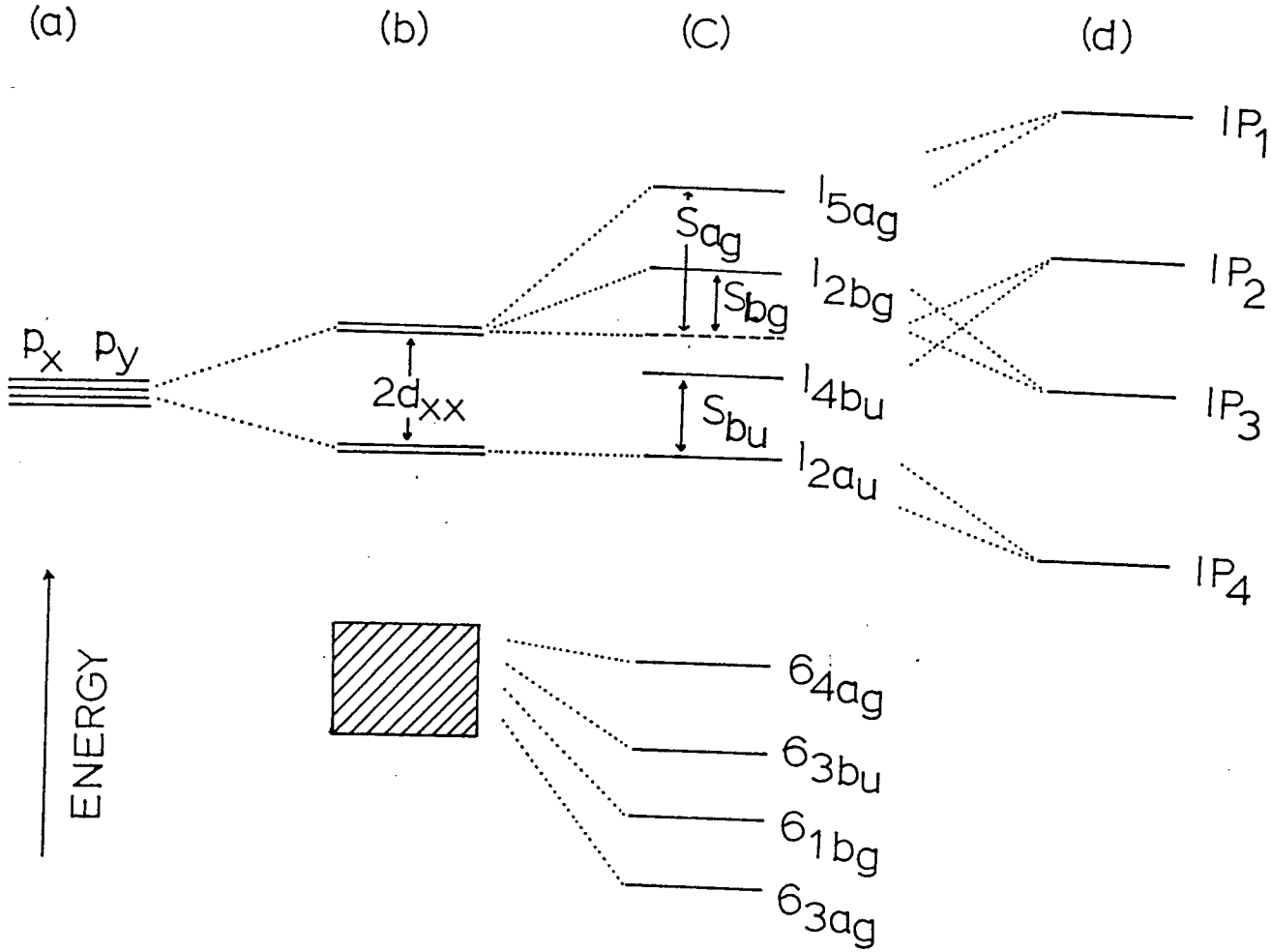

Figure 14. Effect of interaction on the molecular orbitals of XCH_2CH_2X
(a) no perturbation; (b) through space interaction;
(c) through bond interaction added; and (d) spin orbit coupling added.

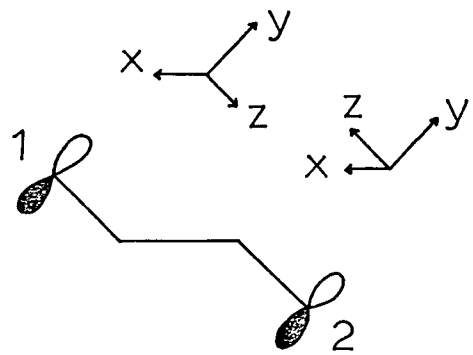

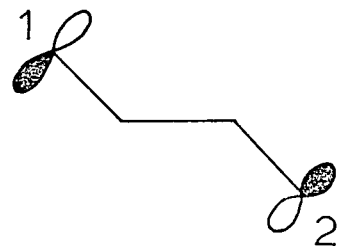

$$^1b_u = \frac{1}{\sqrt{2}} (p_{y_1} + p_{y_2})$$

$$^1a_g = \frac{1}{\sqrt{2}} (p_{y_1} - p_{y_2})$$

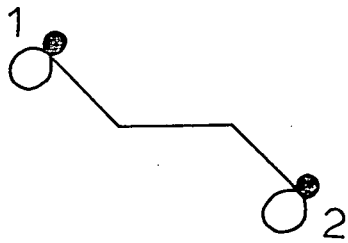

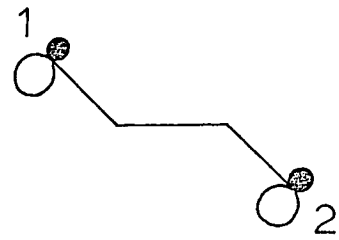

$$^2a_u = \frac{1}{\sqrt{2}} (p_{x_1} + p_{x_2})$$

$$^2b_g = \frac{1}{\sqrt{2}} (p_{x_1} - p_{x_2})$$

Figure 15. The lone pair orbitals of the halogen atoms in XCH_2CH_2X.

difference between two interacting orbitals (section 2.1.4), in contrast to our observation (see discussion later). Because of this we put 6_{3b_u} above 6_{1b_g}, this assignment, being confirmed by the following calculation on the relative magnitudes of the through bond and through space interactions.

In addition to the through space and through bond interactions mentioned above, spin orbit coupling may also play an important part between LPMO's, according to the investigations of Heilbronner and his coworkers[94,95] (Fig. 14, case d). Using the spin orbit coupling operator described in section 2.1.5, the following secular equation corresponding to the MO model can be obtained:

$$\begin{vmatrix} \varepsilon_p + d_{xx} - \varepsilon & 0 & i\zeta/2 & 0 & S'_{a_g} & 0 & 0 \\ 0 & \varepsilon_p - d_{xx} - \varepsilon & 0 & i\zeta/2 & 0 & 0 & S'_{b_u} \\ -i\zeta/2 & 0 & \varepsilon_p + d_{xx} - \varepsilon & 0 & 0 & S'_{b_g} & 0 \\ 0 & -i\zeta/2 & 0 & \varepsilon_p - d_{xx} - \varepsilon & 0 & 0 & 0 \\ S'_{a_g} & 0 & 0 & 0 & \varepsilon_{a_g} - \varepsilon & 0 & 0 \\ 0 & 0 & S'_{b_g} & 0 & 0 & \varepsilon_{b_g} - \varepsilon & 0 \\ 0 & S'_{b_u} & 0 & 0 & 0 & 0 & \varepsilon_{b_u} - \varepsilon \end{vmatrix} = 0 \qquad (4.1)$$

for the interactions involving the 1_{5a_g}, 1_{4b_u}, 1_{2b_g}, 1_{2a_u}, 6_{4a_g}, 6_{1b_g} and 6_{3b_u}. The through bond interaction for 1_{5a_g} and 6_{3a_g} is not included here. ε_p, ε_{a_g}, ε_{b_g}, and ε_{b_u} are the energies of the unperturbed LPMO's, 6_{4a_g}, 6_{1b_g} and 6_{3b_u} respectively. ζ, the spin orbit coupling constant for the halogen atom is estimated from refs. 94 and 235,

and S_i' , the interaction energy between l_i and σ_i is related to S_i approximately by expression (4.2) with a plus sign for l_{5a_g} and

$$S_i'^2 = S_i (S_i + \varepsilon_p - \varepsilon_i \pm d_{xx}) \qquad (4.2)$$

l_{2b_g} and a minus sign for l_{4b_u} and l_{2a_u} .

Theoretically, all the seven parameters, ε_p , S_i''s and ε_i's can be exactly solved through eqn. (4.1) because there are a sufficient number of observed IP's known. However, the values of these quantities are actually obtained in a trial and error fashion because of the high order of the secular determinant. Those listed in Table 16 for dichloro-, dibromo- and diiodoethane are chosen in such a way that they reproduce the experimental data within the experimental error limit (see Table 15).

The quantity ε_p for a dihaloethane possesses a greater value in comparison with that of the ethyl halide ε_p' [$(I_1)_{av}$ from ref. 234]. Their difference $\varepsilon_p' - \varepsilon_p$ represents the inductive substituent effect of the halogen.

(b) Relative Stability of Isomeric Trans and Gauche Ions

Up to now, the PE spectra corresponding to LPMO's are interpreted in terms of the trans conformation only. This treatment is at least justified for $(CH_2Br)_2$ and $(CH_2I)_2$ in which the concentration of the gauche isomer is very low[226-228]. On the high IP edge of the PE band of $(CH_2Br)_2$ at around 10.6 ev, a small shoulder at about 870 cm^{-1} from the second maximum is observed, and this is probably due to excitation of the C-C stretching or CH_2 twisting mode. Similarly, peaks occuring on the right hand side of the first band and also on the second band of $(CH_2I)_2$ (ca. 710 cm^{-1} and 986 cm^{-1} respectively from the band center) could be associated with

Table 16. Calculated MO Parameters (ev)[a] of $(CH_2X)_2$

	$(CH_2Cl)_2$	$(CH_2Br)_2$	$(CH_2I)_2$
β	0.070	0.330	0.630
S_{xx}	0.0003	0.0005	0.0006
d_{xx}	0.007	0.011	0.012
ε_p	-11.82	-10.99	-10.11
ε'_p	-11.01	-10.44	-9.63
$\varepsilon'_p - \varepsilon_p$	0.81	0.55	0.48
S'_{ag}	-1.05	-0.73	-0.77
S'_{bu}	-0.96	-0.64	-0.91
S'_{bg}	-1.06	-0.93	-1.12
ε_{ag}	-13.09	-12.28	-11.07
ε_{bu}	-13.95	-13.57	-12.77
ε_{bg}	-15.02	-14.75	-14.50
S_{ag}	0.59	0.33	0.43
S_{bu}	0.37	0.15	0.28
S_{bg}	0.32	0.22	0.27

[a]Reproduced Observed IP's within $\pm$ 0.03 ev.

excitations of C-C stretching and CH_2 deformation modes respectively, or, may be due to the presence of CH_3I[235], 9.6 and 10.2 ev. Two peaks at around 10.52 and 10.57 ev fall off in intensity after a period of time, and are unknown impurities. For $(CH_2Cl)_2$, the ratio of the population of the trans and gauche forms is about three to one in the vapor phase[228]. Therefore, among the dihaloethanes it is most likely that this molecule will provide information about the stability of the two isomeric ions, providing that the photoionization cross sections and energies of the LPMO's* are the same for both rotamers.

The relative magnitudes of the IP's for the trans and gauche forms, namely IP_t and IP_g, respectively, depend on the enthalpy differences, ΔH_{mol} and ΔH_{ion} of the isomers and their corresponding ions (Fig. 16). The relationship between IP's and enthalpy differences is given by eqn. (4.3) when the gauche ion is more stable

$$IP_t - IP_g = \Delta H_{mol} + \Delta H_{ion} \qquad (4.3)$$

and IP_t is always greater than IP_g irrespective of values of ΔH_{mol} and ΔH_{ion}; or eqn. (4.4) when the trans ion is more stable

$$IP_t - IP_g = \Delta H_{mol} - \Delta H_{ion} \qquad (4.4)$$

In the PE spectrum of $(CH_2Cl)_2$ (Fig. 11) no peak with an intensity about one-third that of the broad peak at 11.40 ev is observable on the low IP side. (A small peak at 12.6 ev comes from impurities (may be H_2O)

* The assumption is justified by the fact that the predominantly through bond interaction is rather independent of C-C rotation[77,78], and the calculations indicate the energy increase due to a larger through space interaction in the gauche conformer is about 0.1 ev.

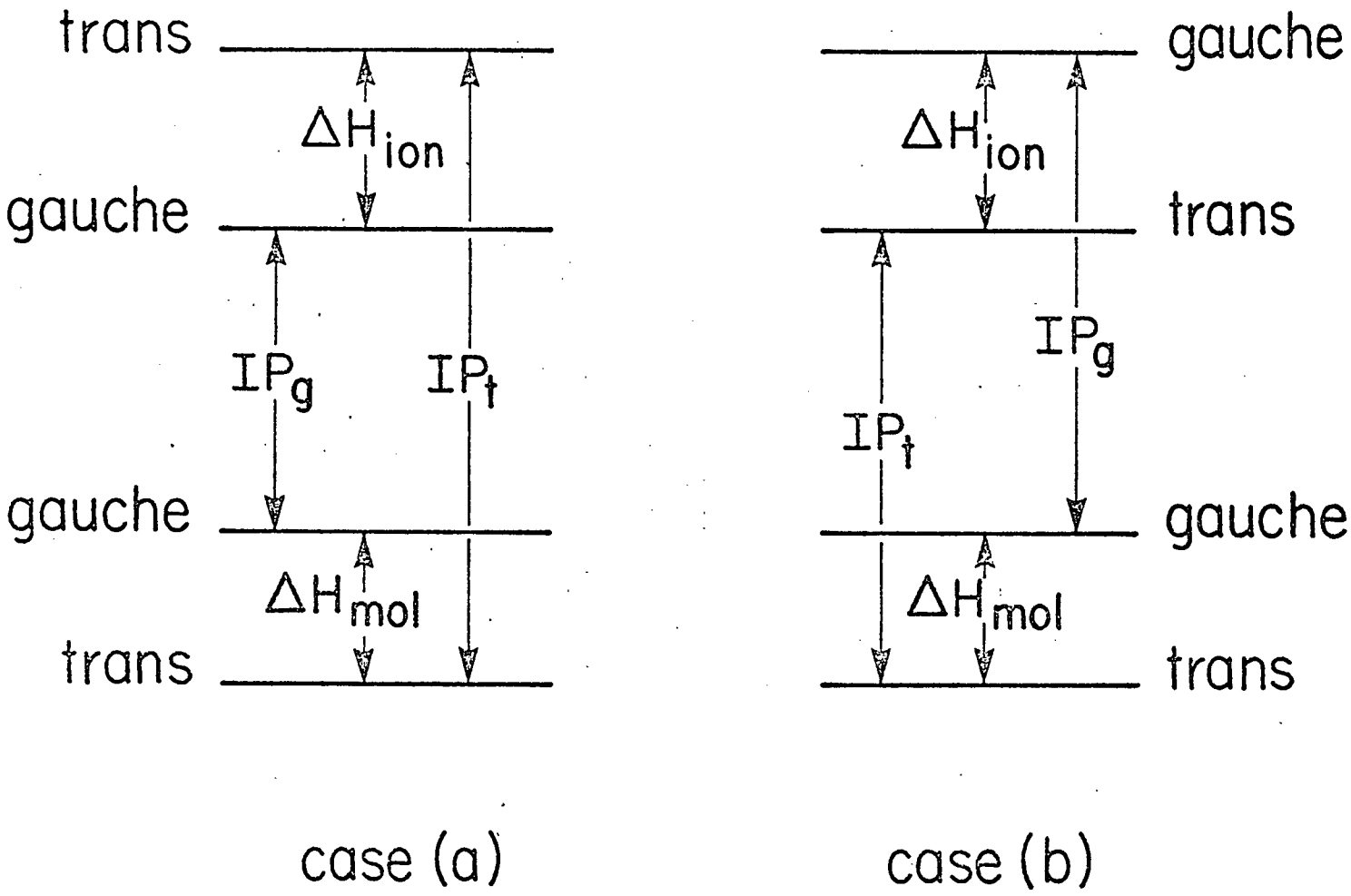

Figure 16. Effect of stability of the trans and gauche conformers and their ions on the relative magnitude of IP_t and IP_g: Case (a) where the gauche ion is more stable, and Case (b), where the trans ion is more stable.

in the spectrometer.) This indicates that ΔH_{ion} is greater than ΔH_{mol} even if the difference, $IP_t - IP_g$, is not known. The stronger dipole-dipole interaction between the chlorine atom in the gauche ion than in the neutral gauche molecule agrees with this observation. The extra electrostatic interaction energy for the gauche ion is estimated to be 0.30 ev by assuming that the energy is proportional to the reciprocal of the Cl...Cl non-bonded distance, and also that the Cl atoms are very small and have charge $+\frac{1}{2}e$. Therefore, we conclude that the trans conformer is still more stable in the ionic state as is the case in the neutral ground state. This is further supported by the work on 1,2-diiodotetrafluoroethane (section 4.3).

(c) Geometry of the $ClCH_2CH_2Cl$ Molecular Ions

Among all the PE spectra obtained for the dihaloethanes, only that of the first band of $(CH_2Cl)_2$ exhibits resolvable fine structure. Analysis of the vibrational spacings indicates that the ν_4 (C-C stretching), and ν_6 (CCCl deformation) are excited and have frequencies of 826 and 360 cm^{-1}, respectively, as compared with those in parent molecule[236] of 1052 and 300 cm^{-1}.

A FCF calculation to determine the ionic geometry of $(CH_2Cl)_2$ has been carried out by using method A. Assuming the separability of the C-H vibrations from other deformations, the constructed symmetry coordinates[226] are

$$\begin{aligned} S_4 &= \Delta q \\ S_5 &= (\Delta r + \Delta r')/2 \\ S_6 &= (\Delta\alpha + \Delta\alpha')\, r/2 \end{aligned} \qquad (4.5)$$

where g and r are C-C and C-Cl bond lengths and α is the CCCl bond angle. The transition intensities of combination bands or overtones are simply taken to be proportional to the heights of the fine structure maxima. The changes in structural parameters of the C-C and C-Cl bonds and the CCCl angle are found to be, respectively 0.136 A, -0.068 A and -8° according to the criteria mentioned in section 2.2.1b. These values seem to be quite large for a geometrical change of a nonbonding orbital. This may be due to, (i) the simplified symmetry coordinates used in the calculation, (ii) neglect of the perturbation in intensity due to spin orbit coupling and (iii) overestimation of intensities of individual components in the progressions which are seriously overlapped by bands originating from the second highest occupied orbital of the trans conformer or the LPMO's of the gauche isomer, and so the errors on the estimated vibrational intensities are quite high.

(d) Relation Between the Observed Ionization Potentials and Some Physical Properties of XCH_2CH_2X.

In the halogen acids[237], and alkyl halides[234], the first IP's have been found to vary linearly with the electronegativities of the halogen atoms. The gradient of these lines is approximately related to the magnitude of the contribution of the halogen p orbitals[234]. The same kind of dependence is obtained in plotting the halogen electronegativities against the first IP's as well as the two highest occupied σ MO's (mainly localized in the C-X bond) of the dihaloethanes (Fig. 17).

The ionization potential of a molecule is a measure of the difference between the heat of formation of the molecule and the corresponding

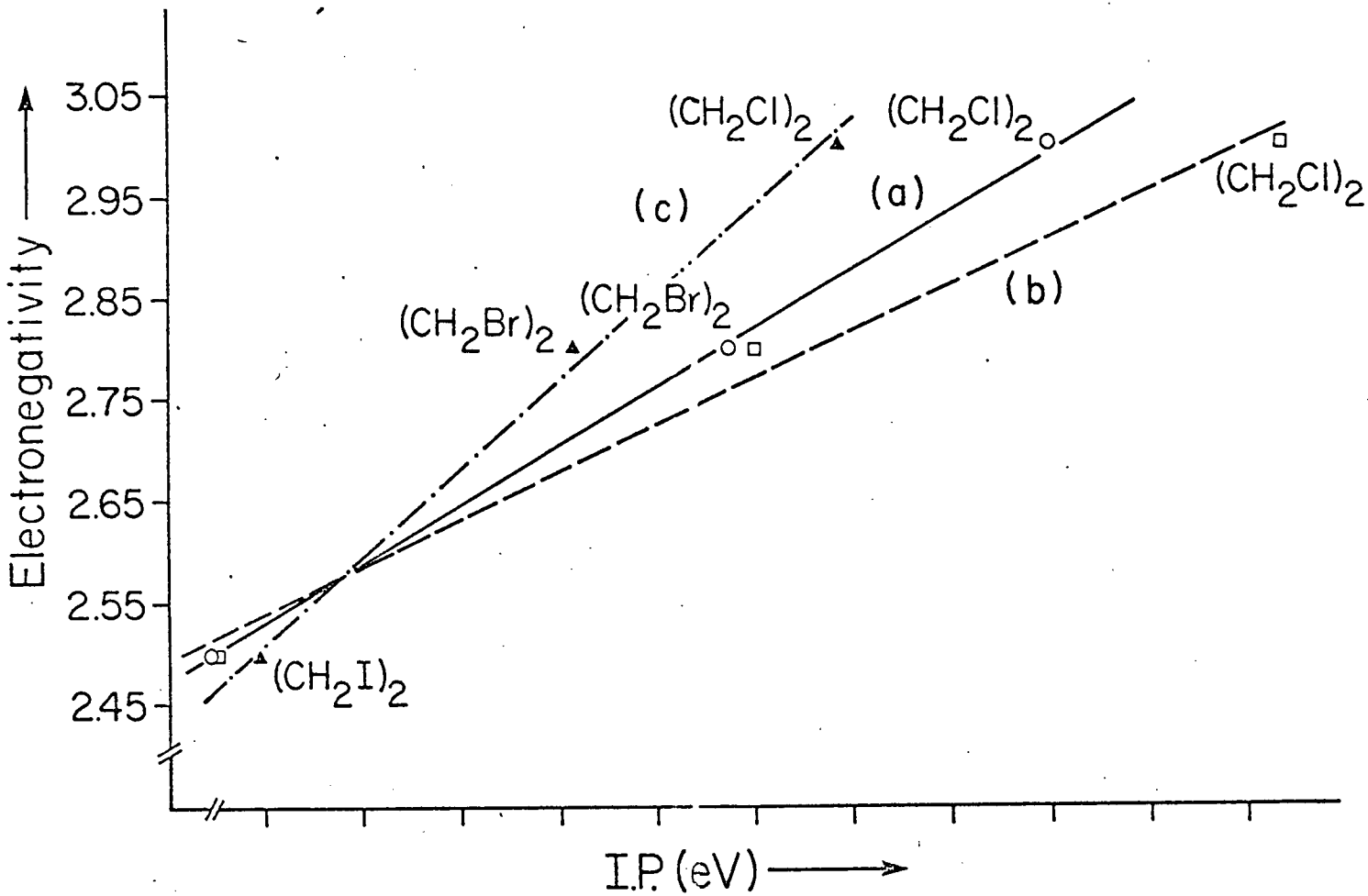

Figure 17. Plot of the Pauling electronegativity of the halogen atom against (a) the first halogen lone pair, (b) the first sigma ionization potential, and (c) the second sigma ionization potentials of XCH_2CH_2X: A different scale for the IP's is used for different orbitals.

ion. Fig. 18 shows graphically the IP's corresponding to removal of electrons from the first three outer orbitals plotted against the heats of formation[238], ΔH_f which are deduced from the reaction scheme (4.6)

$$C_2H_4\,(gas) + X_2\,(gas) = C_2H_4X_2\,(gas) \qquad (4.6)$$

It is interesting to note that a linear relationship is obtained for the heat of reaction ΔH_r of (4.6) and the first two σ IP's.

Force constants have long been regarded as a measurement of the rigidity of a bond in a molecule. Ionization of an electron from the MO's which are localized in a certain bond, e.g. the C-X bond, will change the energy of that bond. Hence the corresponding IP gives information about the C-X bond strength. Fig. 19 shows a plot of the first two σ IP's of the XCH_2CH_2X molecules plotted against the C-X stretching force constants[228*] K_{CX}. A good approximation to a linear plot is obtained.

According to Badger's rule[171,172], K_{CX} is related to the C-X bond length r_{CX} by eqn. (4.7) where a and b are constants.

$$K_{CX} = a r_{CX}^{-b} \quad \text{or} \quad \log K_{CX} = \log a - b \log r_{CX} \qquad (4.7)$$

In light of the correlation obtained between the IP's and K_{CX}, the log (IP) of the first two σ MO's is plotted against log r_{CX}, and again straight lines are obtained (Fig. 20).

In view of the correlation obtained for the observed IP's, force

* K_{CI} is estimated from the C-I stretching frequency[239] by using the approximate method[226] mentioned previously in the FCF calculation on $(CH_2Cl)_2$.

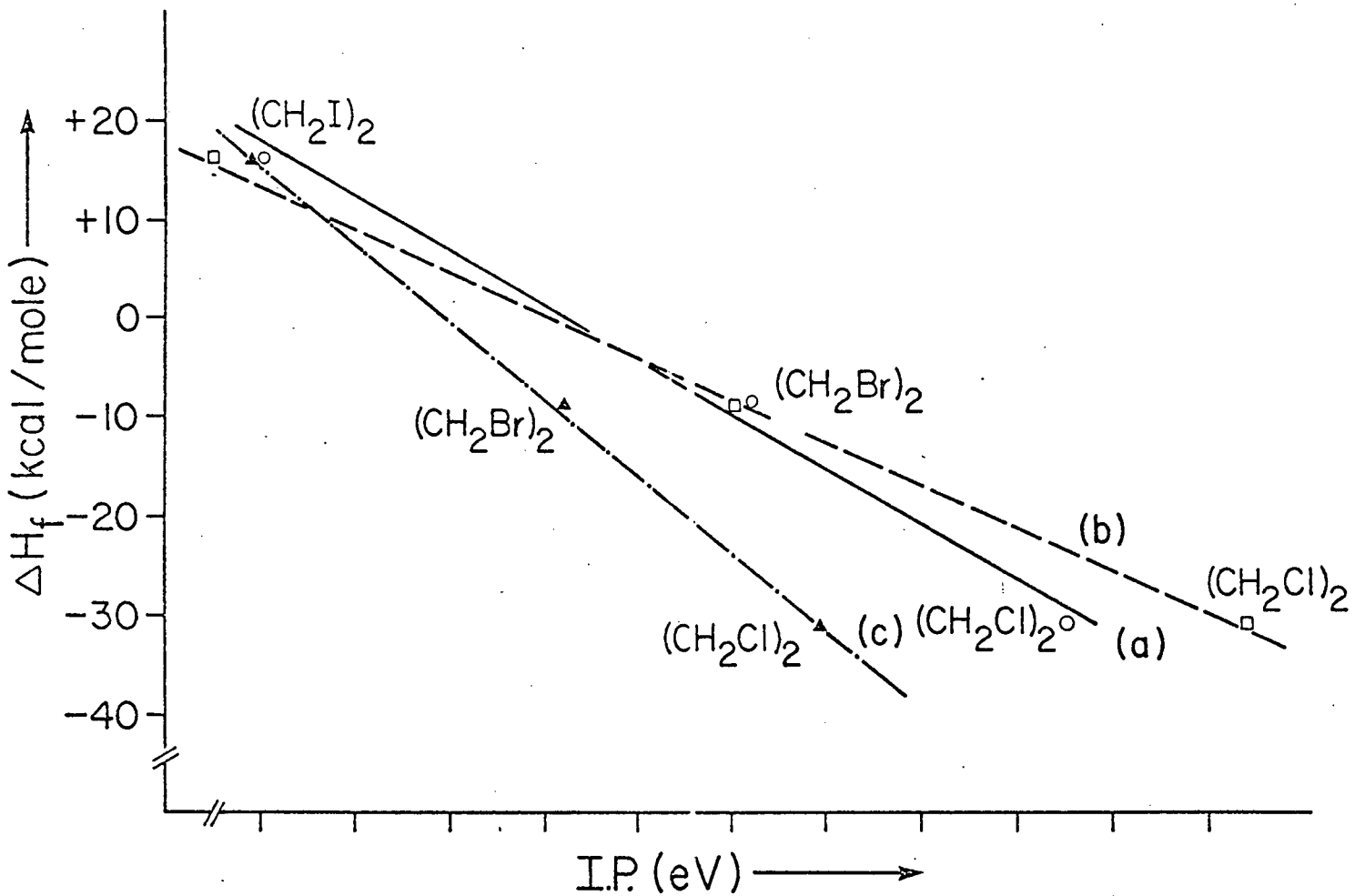

Figure 18. Plot of the heat of formation (ΔH_f°) against (a) the first halogen lone pair, (b) the first sigma, and (c) the second sigma ionization potentials of XCH_2CH_2X. A different scale for IP's is used for the different orbitals.

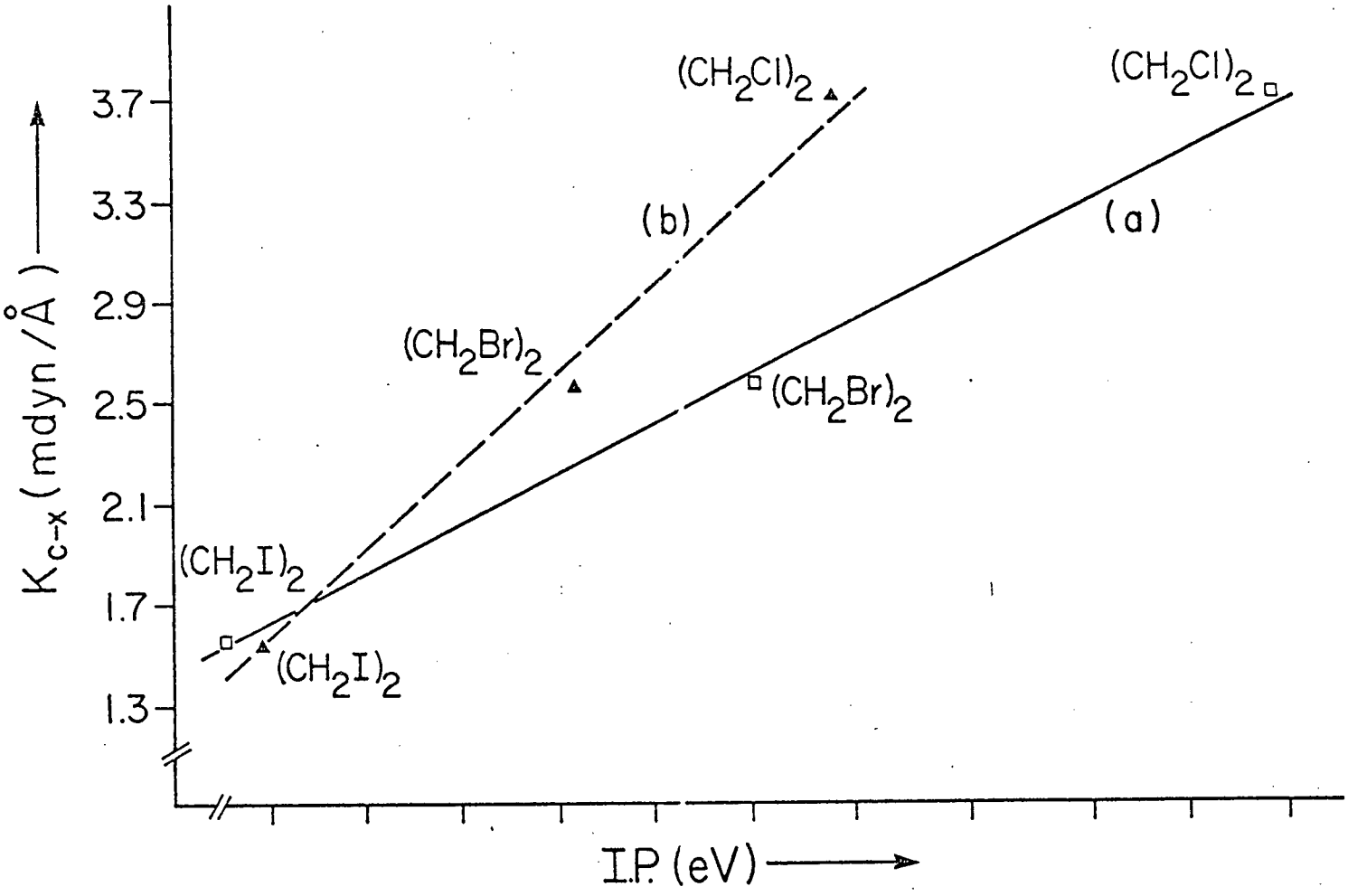

Figure 19. Plot of the C-X stretching force constant K_{cx} against (a) the first sigma ionization potentials, and (b) the second sigma ionization potentials of XCH_2CH_2X. A different scale for IP's is used for different orbitals.

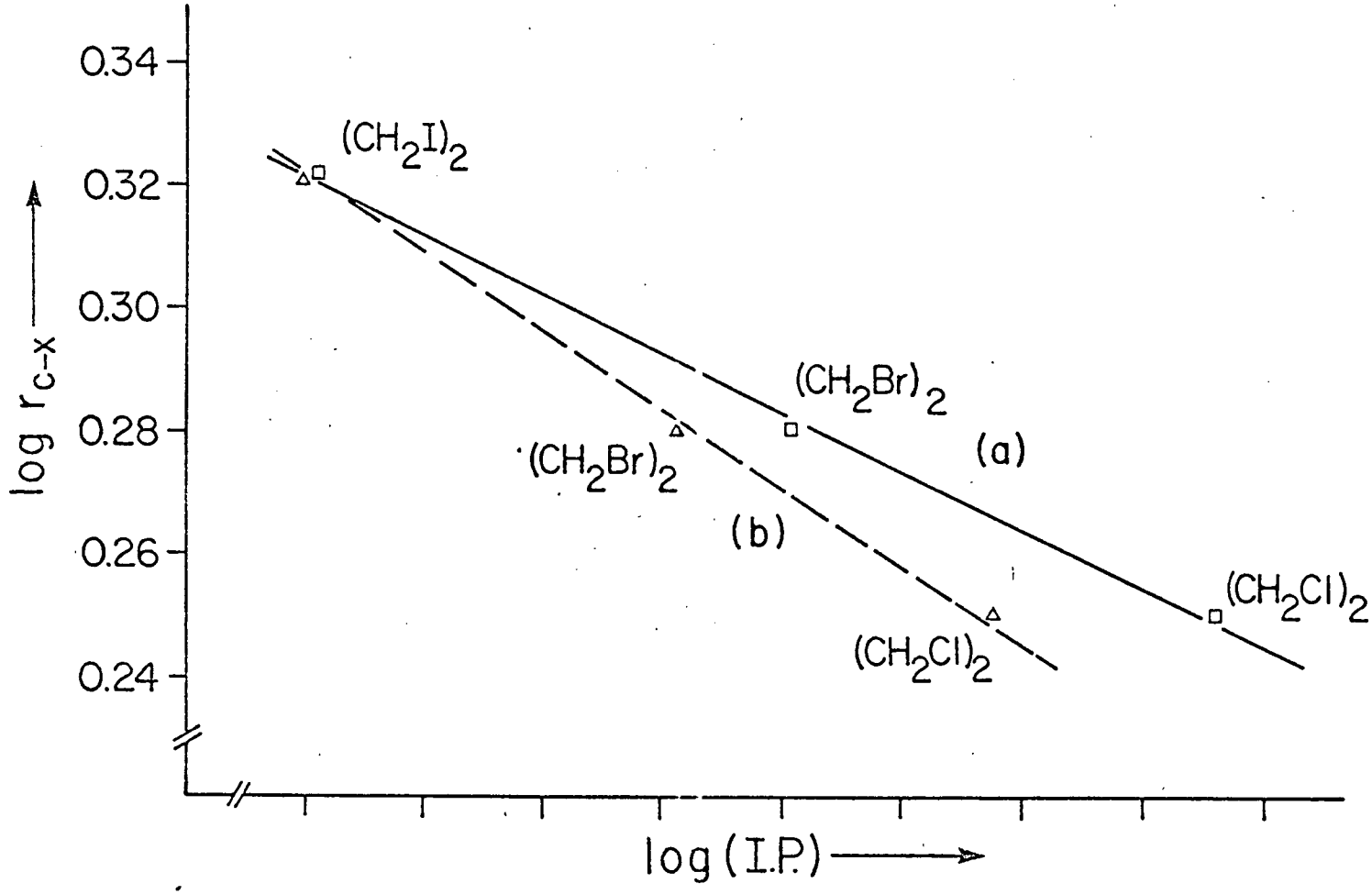

Figure 20. Plot of log Y_{cx} against log IP of (a) the highest occupied and (b) the next highest occupied sigma orbitals of XCH_2CH_2X. (The values for Y_{cx} are obtained from ref. 150.)

constants, and bond distances of the XCH_2CH_2X series, we have attempted to investigate whether the same kind of relationship holds for other molecules. Figs. 21 - 24 show the plot of the stretching force constants[43, 106, 109, 240-244] K_{AB} of the bond A-B of X_2, HX and BrX (X = F, Cl, Br, I), CY_2, OCY, SCY and H_2Y (Y = O, S, Se, Te), WH_3 (W = N, P, As), BX_3, CH_3X, CX_4, YF_6 and HCCX, against observed IP's[11,12,30,147,235,245-247] * corresponding to the removal of electrons from orbitals mainly localized on the A-B bond. Good linear plots are observed in each case.

By plotting the result of CNDO/BW calculations[221,248,249] for the hydrogen halides (not shown here), we have observed a linear relationship between the calculated as well as the observed stretching force constants and the calculated total energy. A similar correlation exists between the force constants and all occupied valence orbital energies. This supports the experimental observations of Figs. 21 and 22, i.e. that the plot of IP versus force constant is linear. Thus, the exact similarity between the experimental and the theoretical plots (provided Koopmans' theorem holds) supports the validity of the correlation. At this stage, no obvious explanation can be offered to explain all the correlations observed in Figs. 21 - 24.

It should be mentioned that from the correlation of observed IP's with force constants as well as bond lengths for a series of molecules, IP's for compounds which are not available can thus be estimated. For instance, the fourth lowest IP of CI_4 is predicted to be about 14 ev.

* Second lowest IP (LIP) of SeF_6 and TeF_6, and third LIP's of SF_6, SeF_6 and TeF_6 were estimated from spectra in ref. 30.

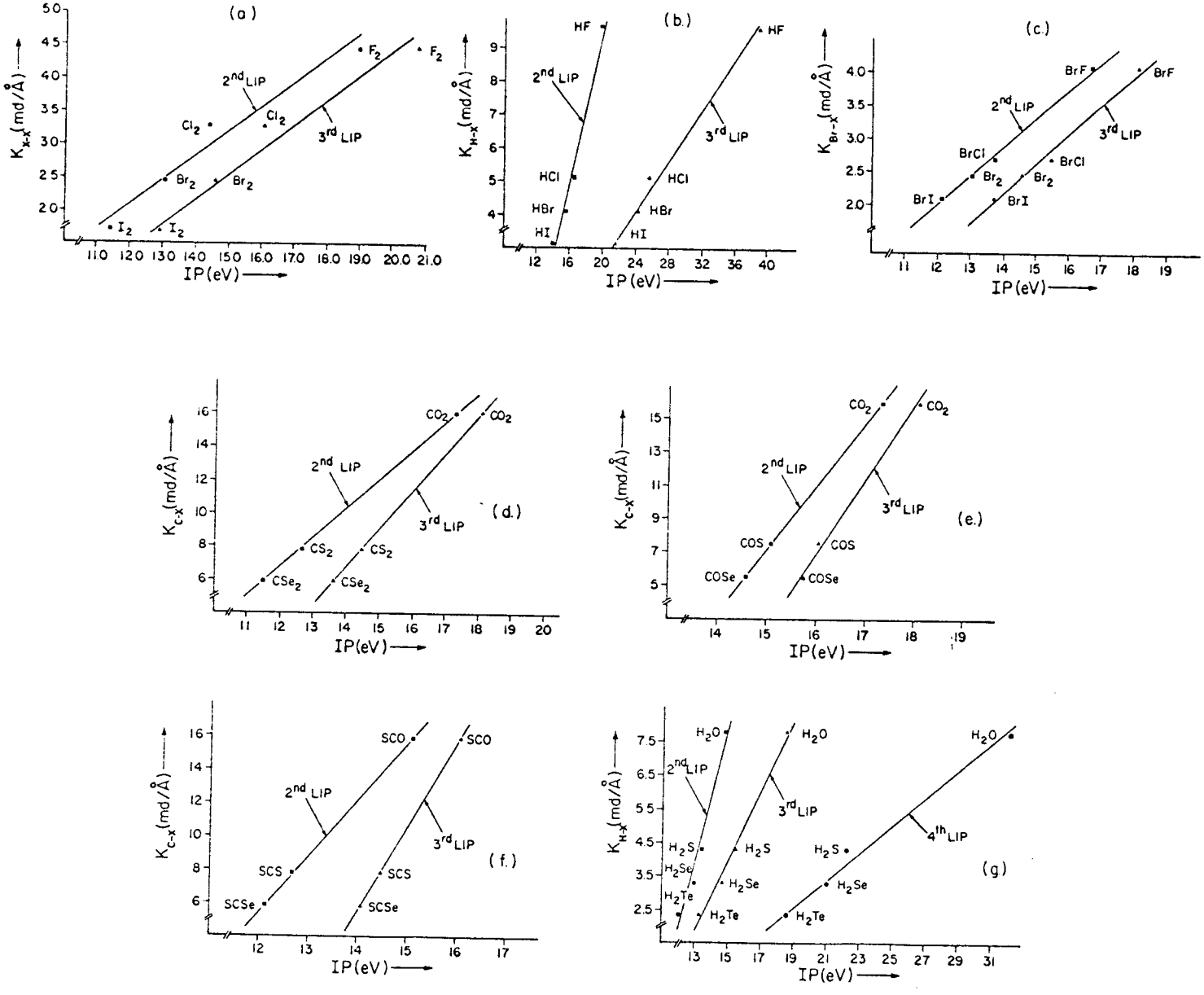

Figure 21. Plot of some ionization potentials of (a) X_2, (b) HX, (c) BrX (X = F, Cl, Br, I), (d) CY_2, (e) OCY, (f) SCY and (g) H_2Y (Y = O, S, Se, Te) against the stretching force constants.

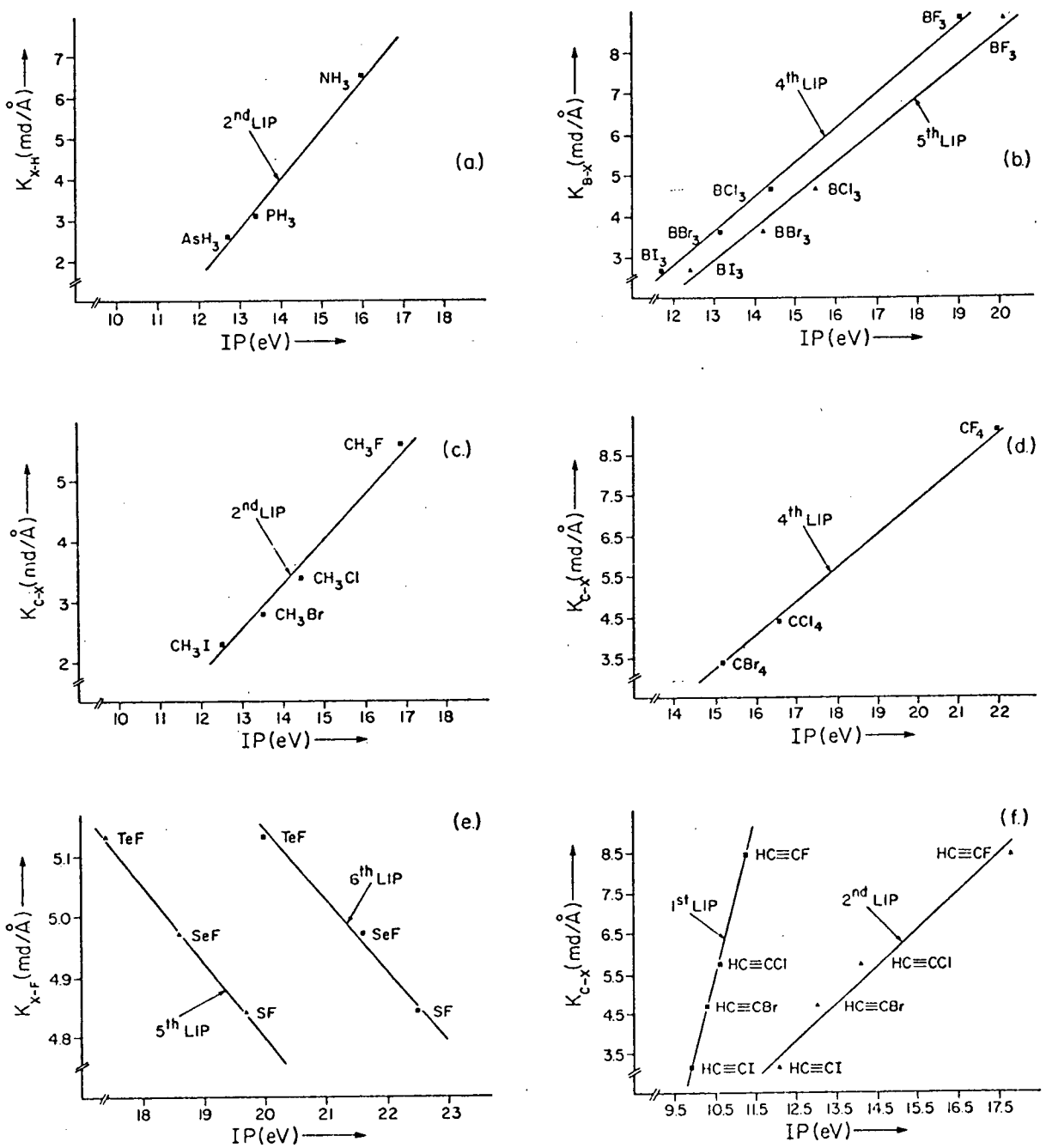

Figure 22. Plot of some ionization potentials of (a) WH_3 (W = N, P, As), (b) BX_3, (c) CH_3X, (d) CX_4 (X = F, Cl, Br, I), (e) YF_6 (Y = S, Se, Te) and (f) HCCX against the stretching force constants.

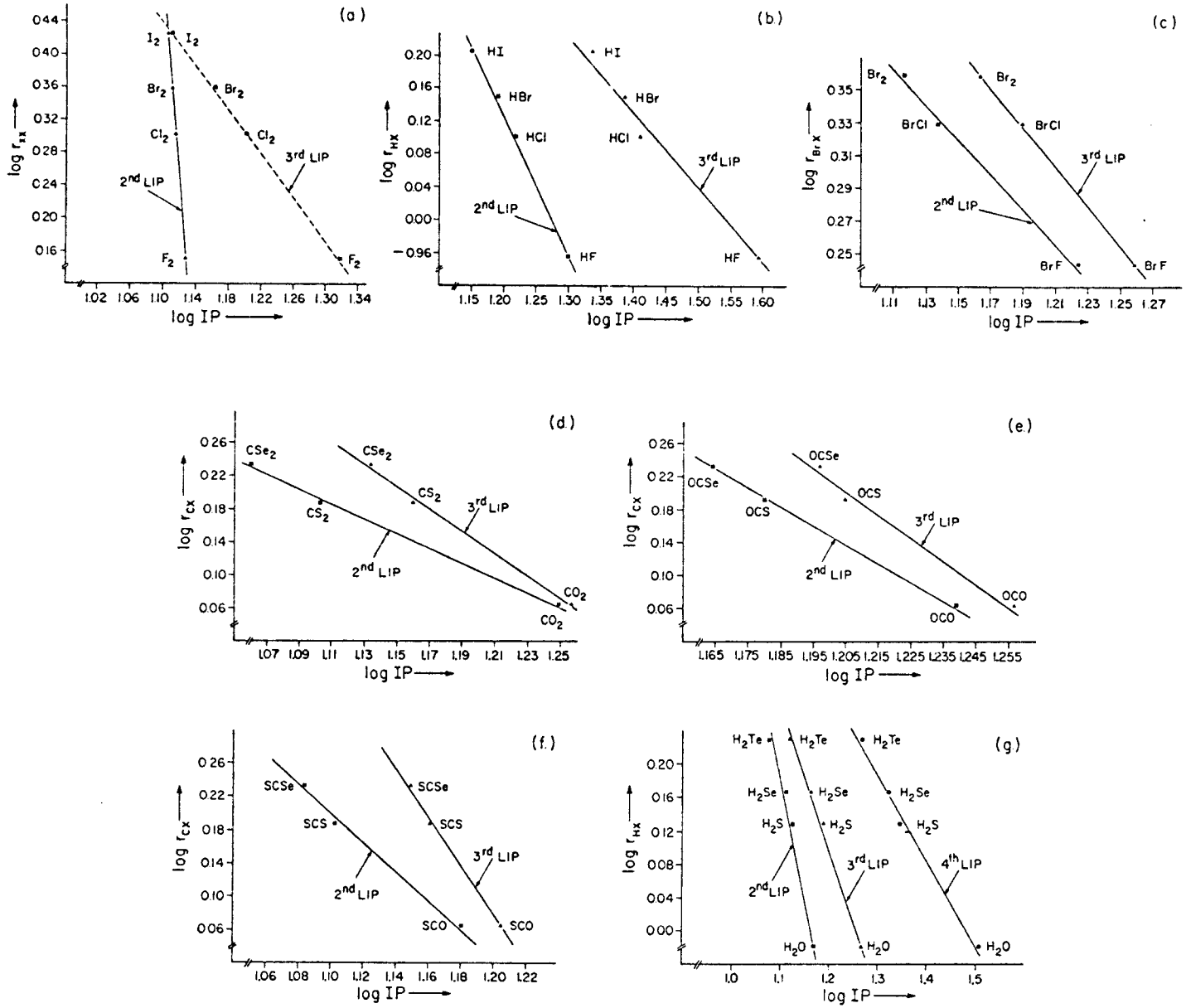

Figure 23. Plot of the logarithm of some ionization potentials of (a) X_2, (b) HX, (c) BrX (X = F, Cl, Br, I), (d) CY_2, (e) OCY, (f) SCY and (g) H_2Y (Y = O, S, Se, Te) against the logarithm of bond lengths.

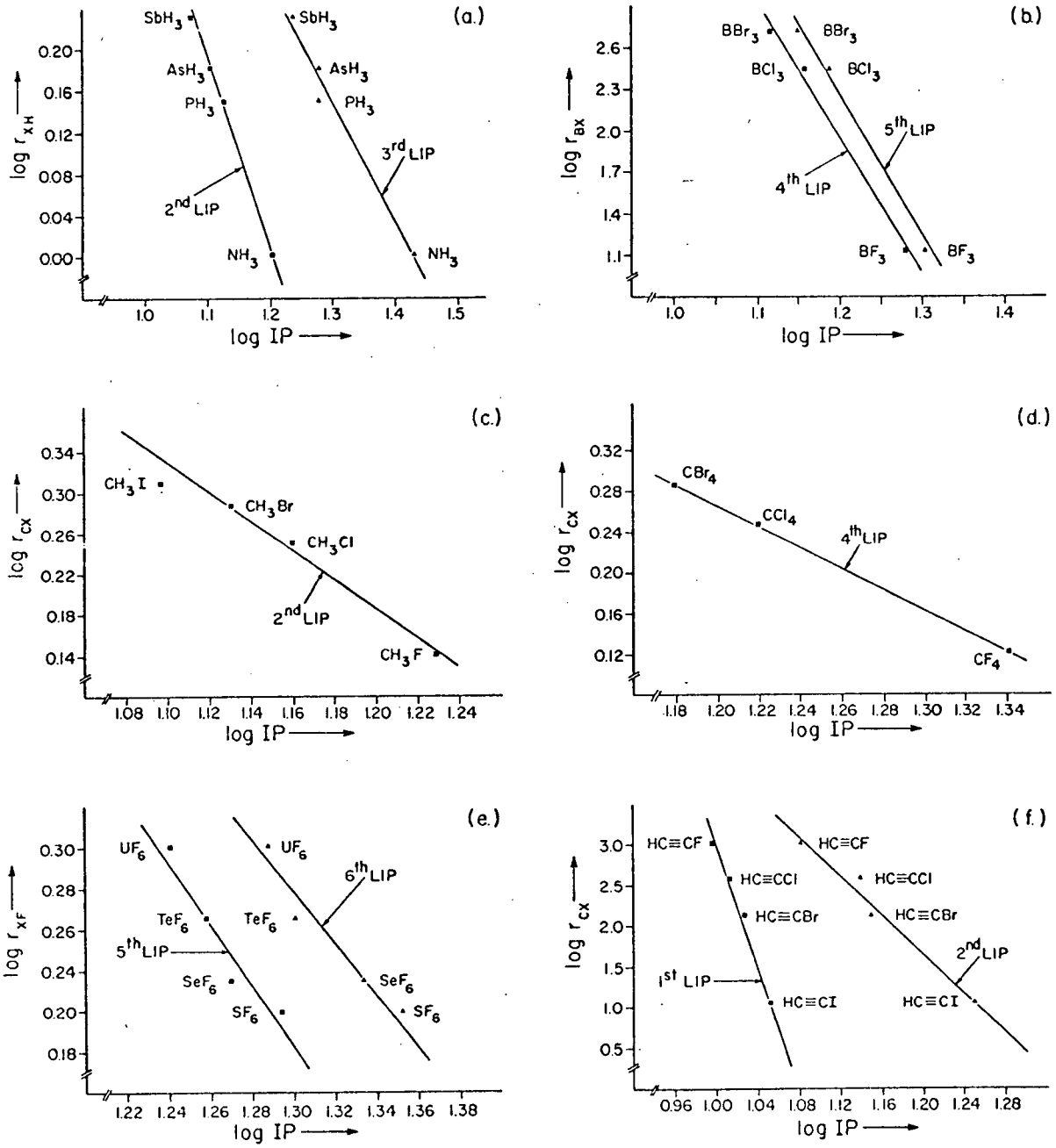

Fig. 24. Plot of the logarithm of some ionization potentials of (a) WH_3 (W = N, P, As), (b) BX_3 (c) CH_3X, (d) CX_4 (X = F, Cl, Br, I), (e) YF_6 (Y = S, Se, Te) and (f) HCCX against the logarithm of bond lengths.

4.3 1,2 Dichloro-, 1,2 Dibromo- and 1,2 Diiodotetrafluoroethane, 1,2-Dibromo-1,1-difluoroethane and 1,2-Bromochloroethane.

4.3.1 Introduction

Rotational isomers of substituted ethanes such as $(CF_2Cl)_2$, $(CF_2Br)_2$, $(CF_2I)_2$, CF_2BrCH_2Br and CH_2ClCH_2Br have been studied by infrared and Raman spectroscopy[227,228,251-253], ultrasonic techniques[254] and microwave spectroscopy[255,256] and the trans form of these compounds is found to be more stable than the gauche with conformational energy differences ΔH_{mol} of 0.44, 0.95, 1.03 and 1.43 Kcal/mole for $(CF_2Cl)_2$[256], $(CF_2Br)_2$[227], CF_2BrCH_2Br[251] and CH_2ClCH_2Br[228] respectively. The percentages of the trans forms of $(CF_2Cl)_2$[256] and CH_2ClCH_2Br[228] are respectively 52 and 85%, while those of $(CF_2Br)_2$ and CF_2BrCH_2Br are estimated to be 71 and 74% respectively by considering the relation[227] between ΔH_{mol} and the population of the isomers. Even though such data is unavailable for $(CF_2I)_2$, the trans isomer should still be more stable than the gauche owing to both steric and electrostatic effects in this molecule.

The PE spectra of the five substituted ethanes are given in Figs. 25 and 26 and the observed IP's are summarized in Table 17. MO treatment similar to the one described in section 4.2 is employed and will be mentioned below. Throughout this work, the trans isomer of all the molecules studied except $(CF_2Cl)_2$ is considered to give the main feature in their PE spectra.

4.3.2 Method of Calculation

(a) One Electron Model for Trans 1,2 Dihalotetrafluoroethane (C_{2h})

The four halogen LPMO's of trans $(CF_2X)_2$ are of the same energy if they are free from any kind of perturbation (Fig. 27 case a). However,

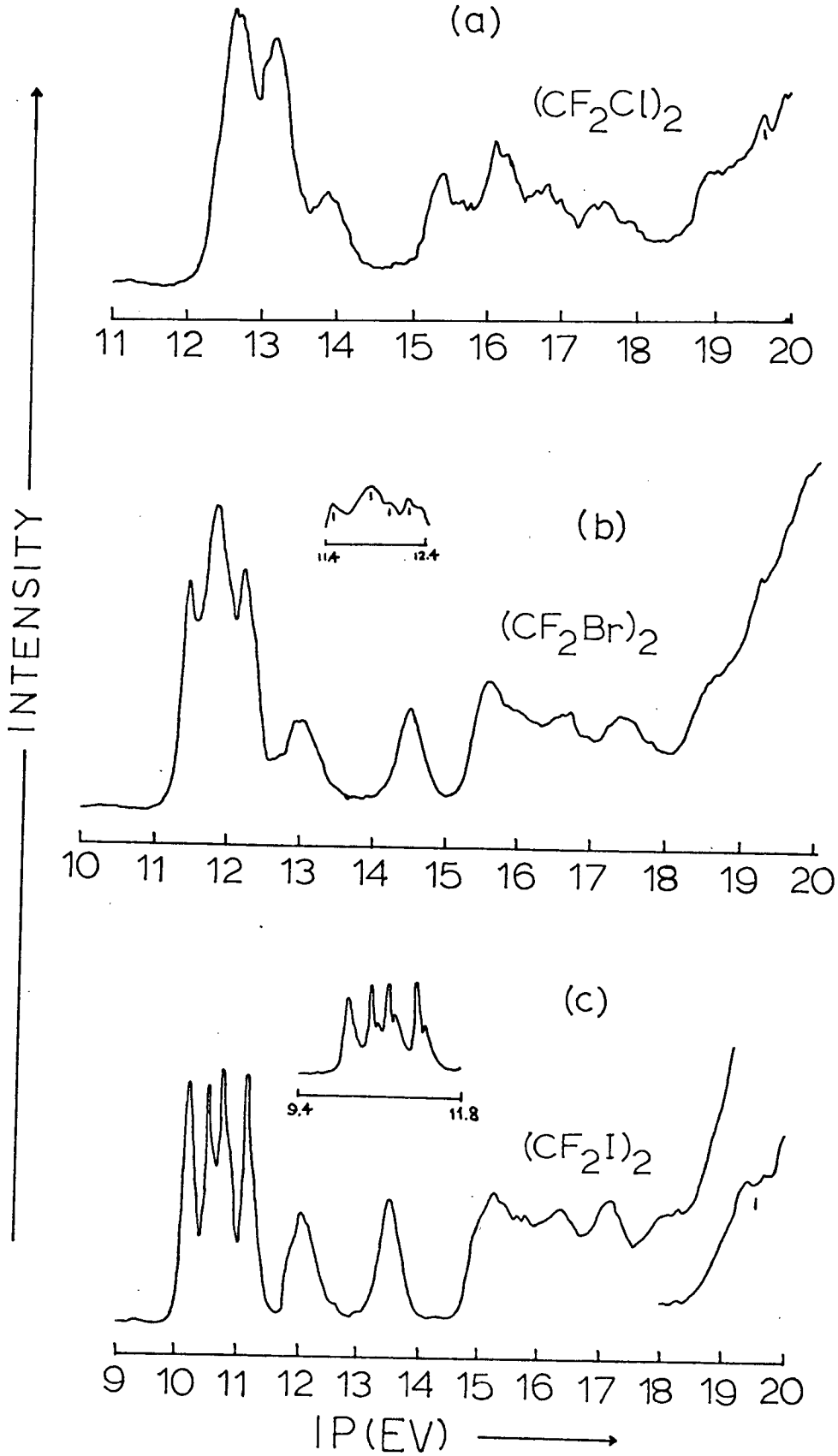

Figure 25. The PE spectra of (a) 1,2 dichloro-, (b) 1,2 dibromo-, and (c) 1,2 diiodotetrafluoroethane.

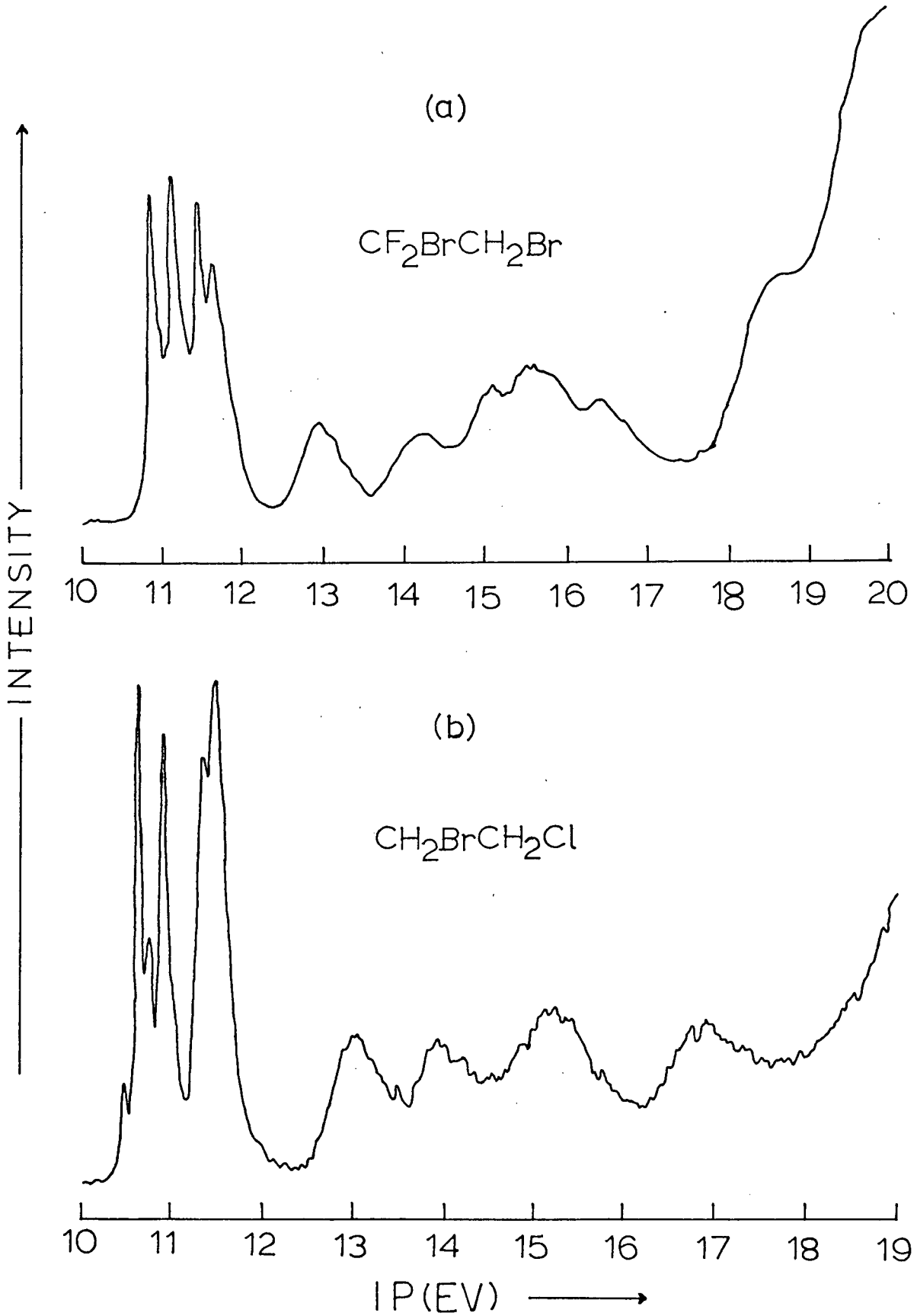

Figure 26. The PE spectra of (a) 1,2 dibromo-1,1-difluoroethane and (b) 1,2 bromochloroethane.

Table 17. Experimental IP's of $(CF_2Cl)_2$, $(CF_2Br)_2$, $(CF_2I)_2$, CF_2BrCH_2Br and CH_2BrCH_2Cl

	$(CF_2Cl)_2$	$(CF_2Br)_2$	$(CF_2I)_2$		CF_2BrCH_2Br		CH_2BrCH_2Cl
χ_1	12.47[b]	11.44	10.11	χ_1	10.86	χ_1	10.65
χ_2	12.82[b]	11.83	10.44	χ_2	11.14	χ_2	10.94
χ_3	13.06	12.11	10.69	χ_3	11.46	χ_3	11.40
χ_4	13.19	12.21	11.10	χ_4	11.65	χ_4	11.52
σ_{7a_g}	13.88	13.00[b]	12.02	$\sigma_{10a'_-}$	12.96[c]	$\sigma_{6a'_+}$	13.05
σ_{6b_u}	15.43	14.53	13.49	$\sigma_{9a'_+}$	14.21[c]	$\sigma_{2a''_-}$	13.94
σ_{6a_g}	16.13	15.62	15.24	$\sigma_{8a'_-}$	15.06	$\sigma_{5a'_-}$	15.24[c]
σ_{4b_g}	16.81	15.99	15.67	$\sigma_{5a''_-}$	15.51	$\sigma_{4a'_+}$	16.85
σ_{4a_u}	17.54	16.61[c]	16.31	$\sigma_{4a'_+}$	16.43		
σ_{3b_g}	18.93	17.43[c]	17.13	$\sigma_{3a''_-}$	18.63		
σ_{3a_u}	19.6 ?	18.66[c]	18.05	$\sigma_{7a'_-}$	19.88		
σ_{5b_u}			19.37				

[a] Experimental error ± 0.01 ev. [c] Experimental error ± 0.02 ev.

[b] Uncertainty not known.

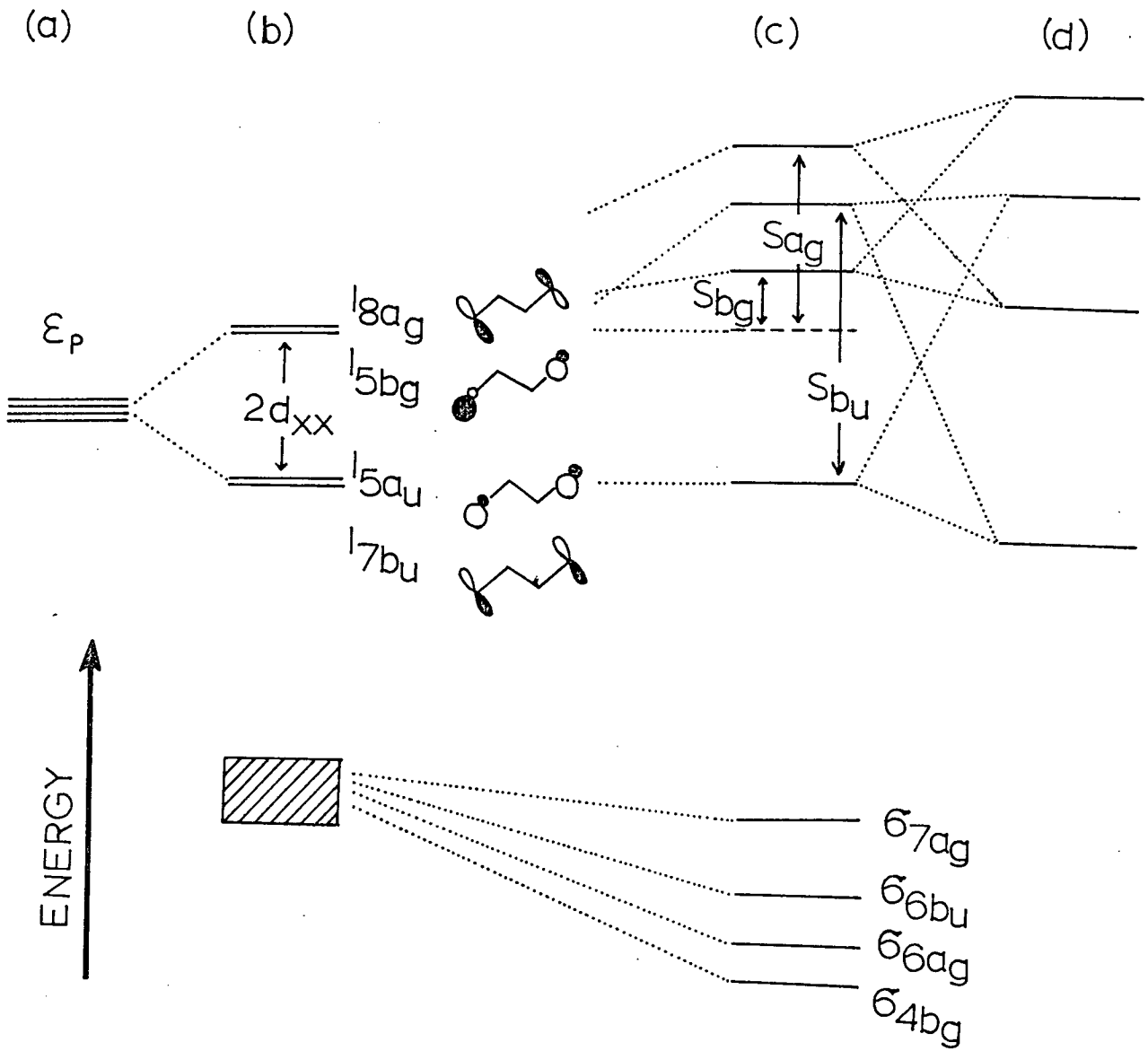

Figure 27. Qualitative MO diagram of trans $(CF_2X)_2$, (a) no perturbation, (b) through space interaction, (c) through bond interaction added, and (d) spin orbit coupling added.

these orbitals are shifted to a different extent by both the through sapce and the through bond interaction[77,78]. According to a CNDO/2 calculation[59] on $(CF_2Cl)_2$, the first four highest occupied σ orbitals are σ_{7a_g}, σ_{6b_u}, σ_{6a_g} and σ_{4b_g} in order of increasing IP. Since only orbitals of the same symmetry can undergo through bond interactions, only the LPMO's l_{8a_g}, l_{7b_u} and l_{5b_g} are considered to be destabilized by the amount, S_{a_g}, S_{b_u} and S_{b_g} respectively. To simplify the calculation, the influence on l_{8a_g} by σ_{6a_g} is neglected. The through space interaction parameter d_{xx} is evaluated from expression (2.7).

In addition, the LPMO's can mix with each other through spin orbit coupling. Using the same spin orbit coupling operator described in section 2.1.5, the following secular equation can be set up in accord with the overall interactions for l_{8a_g}, l_{7b_u}, l_{5b_g}, l_{5a_u}, σ_{7a_g}, σ_{4b_g} and σ_{6b_u} respectively. ε_{a_g}, ε_{b_g} and ε_{a_u} are the unperturbed energies

$$\begin{vmatrix} \varepsilon_p + d_{xx} - \varepsilon & 0 & i\zeta/2 & 0 & S'_{a_g} & 0 & 0 \\ 0 & \varepsilon_p - d_{xx} - \varepsilon & 0 & i\zeta/2 & 0 & 0 & S'_{b_u} \\ -i\zeta/2 & 0 & \varepsilon_p + d_{xx} - \varepsilon & 0 & 0 & S'_{b_g} & 0 \\ 0 & -i\zeta/2 & 0 & \varepsilon_p - d_{xx} - \varepsilon & 0 & 0 & 0 \\ S'_{a_g} & 0 & 0 & 0 & \varepsilon_{a_g} - \varepsilon & 0 & 0 \\ 0 & 0 & S'_{b_g} & 0 & 0 & \varepsilon_{b_g} - \varepsilon & 0 \\ 0 & S'_{b_u} & 0 & 0 & 0 & 0 & \varepsilon_{a_u} - \varepsilon \end{vmatrix} = 0 \qquad (4.8)$$

of σ_{7a_g}, σ_{4b_g} and σ_{6b_u} respectively. The value of ζ in $(CF_2X)_2$ should be smaller than that in the corresponding $(CH_2X)_2$ owing to the mixing of the LPMO's with those of fluorine. In fact, a very small

splitting is observed in the first PE band of CF_3CF_2Cl[256]. Since the number of unknown variables, ε_p, $S_{a_g'}$, $S_{b_u'}$, $S_{b_g'}$, ε_{a_g}, ε_{b_u} and ε_{b_g} in eqn. (4.8) is equal to that of observed IP's, ζ is fixed to have values 0, $\zeta_x/2$ and ζ_x. (This, therefore, includes the limits of ζ and the mean value.) The other parameters given in Table 18 are obtained in a trial and error fashion to give good fit with experimental data.

(b) <u>One Electron Model for Trans CH_2BrCH_2Cl and Trans CF_2BrCH_2Br (C_s)</u>

Fig. 28 shows the qualitative MO diagram for trans CH_2BrCH_2Cl. In this molecule, the Coulomb energy of bromine ε_{Br} and chlorine ε_{Cl} are different with $\varepsilon_{Cl} < \varepsilon_{Br}$. The two pairs of doubly degenerate LPMO's (Fig. 28 case a) can combine to give orbitals $l_{7a'_-}$, $l_{4a''_+}$, $l_{8a'_+}$ and $l_{3a''_+}$. The subscripts + and − mean the in phase and out of phase combination of the LPMO's. The coordinate system used for this compound is the same as that for the dihaloethanes (Fig. 15). d_{BrCl} is again estimated from expression (2.5).

According to a CNDO/BW calculation[221] on the molecule, the first four σ IP's are related to $\sigma_{6a'_+}$, $\sigma_{2a''_-}$, $\sigma_{5a'_-}$ and $\sigma_{4a'_+}$ with increasing IP. These σ orbitals can interact with LPMO's of the same symmetry[77,78]. Since the energy gap between the LPMO's, and $\sigma_{5a'_-}$ and $\sigma_{4a'_+}$ is large, only $\sigma_{6a'_+}$ and $\sigma_{2a''_-}$ are considered to mix appreciably with the LPMO's. Under the operation of this perturbation, the orbital sequence of LPMO's in increasing IP is of symmetry (i) a''_-, a'_-, a'_+ and a''_+, (ii) a''_-, a'_+, a'_- and a''_+, or (iii) a'_+, a''_-, a'_- and a''_+. Furthermore, these LPMO's interact with each other by spin orbit coupling,

Table 18. Calculated MO Parameters (ev)[a] of Trans $(CF_2X)_2$

	$(CF_2Cl)_2$	$(CF_2Br)_2$			$(CF_2I)_2$		
ζ	0.00,0.035,0.070	0.00	0.165	0.330	0.00	0.315	0.630
S_{xx}	0.0003	0.0007	0.0007	0.0007	0.0010	0.0010	0.0010
d_{xx}	0.008	0.017	0.017	0.017	0.022	0.022	0.022
ε_p	-13.18	-12.20	-12.19	-12.13	-11.08	-11.04	-10.91
S'_{ag}	-0.70	-0.78	-0.78	-0.75	-0.95	-0.93	-0.84
S'_{bu}	-0.92	-0.94	-0.90	-0.76	-1.25	-1.19	-0.90
S'_{bg}	-0.66	-0.52	-0.52	-0.26	-1.29	-1.24	-1.21
ε_{ag}	-13.18	-12.26	-12.26	-12.31	-11.07	-11.12	-11.35
ε_{bu}	-15.05	-14.14	-14.18	-14.28	-12.83	-12.91	-13.17
ε_{bg}	-16.69	-15.92	-15.92	-15.97	-15.31	-15.34	-15.36
S_{ag}	0.70	0.74	0.74	0.74	0.94	0.88	0.94
S_{bu}	0.38	0.39	0.35	0.39	0.66	0.59	0.66
S_{bg}	0.12	0.07	0.07	0.07	0.36	0.33	0.36

[a]Reproduce observed IP's within ± 0.02 ev.

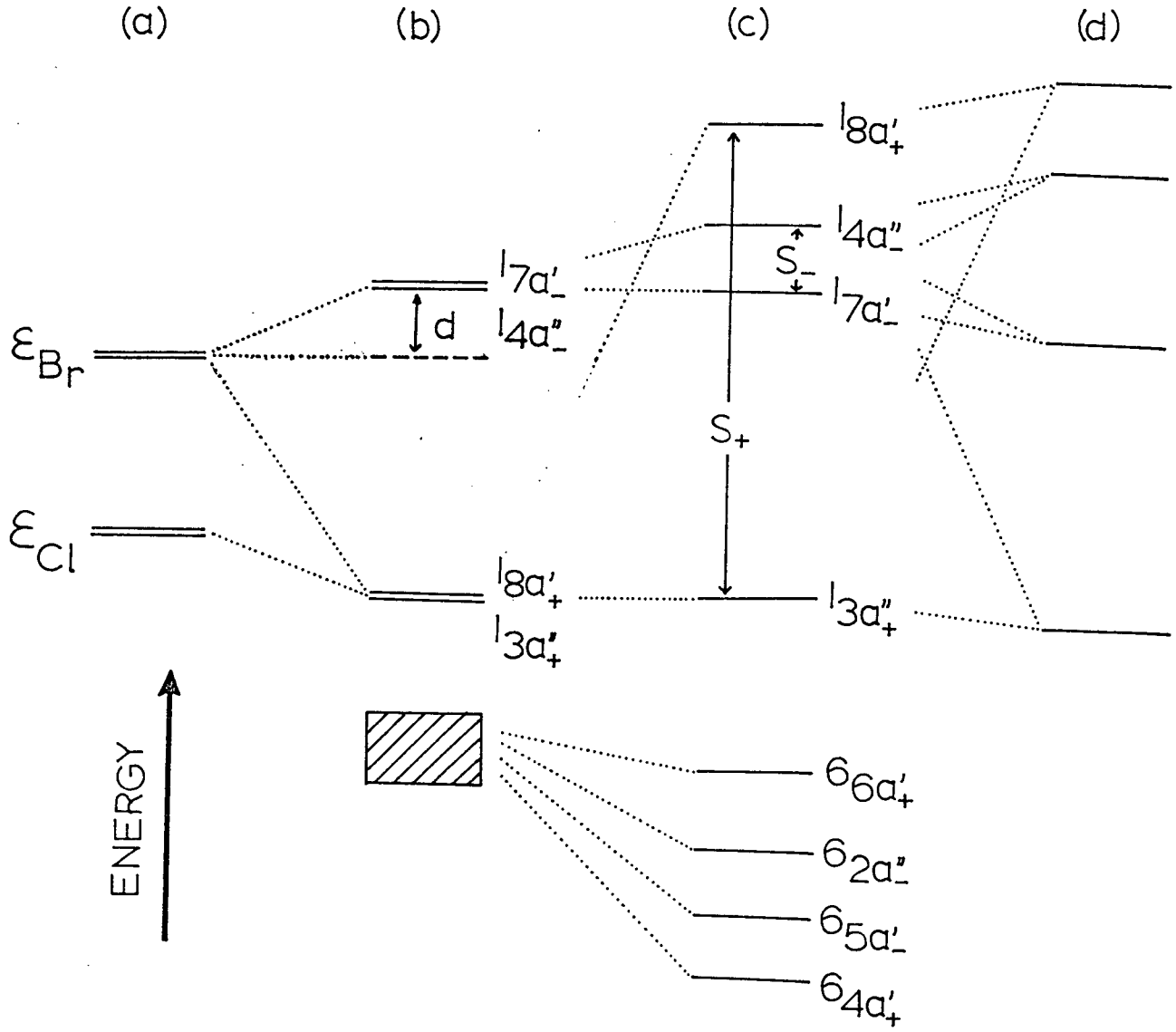

Figure 28. Qualitative MO diagram of trans CH_2BrCH_2Cl, (a) no perturbation, (b) through space interaction, (c) through bond interaction added, and (d) spin orbit coupling added.

and the coupling constants are different for chlorine ς_{Cl} and ς_{Br}, with $\varsigma_{Br} > \varsigma_{Cl}$. In ethyl bromide and chloride[95,234], their first PE bands give a splitting almost equal to ς_x of bromine and chlorine atoms. This reflects that the LPMO's of the halogen atom in the ethyl halides are only slightly perturbed by the σ moiety. This should also be true in CH_2BrCH_2Cl. Therefore ς_{Cl} and ς_{Br} are assigned to have the full value of ς_x, i.e. 0.07 and 0.33 ev respectively in the treatment. On the assumption that the election ejected from a LPMO has β spin only, then the secular determinant corresponding to the above MO model can be written as,

$$\begin{vmatrix} \varepsilon_{Br} + d_{Br,Cl} - \varepsilon & 0 & i(c_{11}^2\varsigma_{Br} + c_{12}^2\varsigma_{Cl})/2 & 0 & 0 & 0 \\ 0 & \varepsilon_{Cl} - d_{Br,Cl} - \varepsilon & 0 & i(c_{12}^2\varsigma_{Br} + c_{11}^2\varsigma_{Cl})/2 & S_+' & 0 \\ -i(c_{11}^2\varsigma_{Br} + c_{12}^2\varsigma_{Cl})/2 & 0 & \varepsilon_{Br} + d_{Br,Cl} - \varepsilon & 0 & 0 & S_-' \\ 0 & -i(c_{12}^2\varsigma_{Br} + c_{11}^2\varsigma_{Cl})/2 & 0 & \varepsilon_{Cl} - d_{Br,Cl} - \varepsilon & 0 & 0 \\ 0 & S_+' & 0 & 0 & \varepsilon_{a_+'} - \varepsilon & 0 \\ 0 & 0 & S_-' & 0 & 0 & \varepsilon_{a_-''} - \varepsilon \end{vmatrix} = 0 \qquad (4.9)$$

for $l_{7a'_-}$, $l_{8a'_+}$, $l_{4a''_-}$, $l_{3a''_+}$, $\sigma_{6a'_+}$ and $\sigma_{2a''_-}$ respectively. c_{11} and c_{12} in the determinant come from the through space interaction. Since c_{11} is found to be much greater than c_{12} in the calculation, c_{11} is simply set equal to unity and c_{12} to zero. Table 19 lists the calculated MO parameters that reproduce the observed IP's within experimental error. Although there are three possible orderings in the LPMO's as mentioned previously, the eigenvectors of eqn. (4.9) indicate that they all give the same ordering of (iii) ultimately. The calculated MO parameters are given in Table 19.

Table 19. Calculated MO Parameters (ev)[a] of Trans CF_2BrCH_2Br, Trans CH_2BrCH_2Cl and Gauche $(CF_2I)_2$

Trans CF_2BrCH_2Br			Trans CH_2BrCH_2Cl		Gauche $(CF_2I)_2$		
β_{Br_H}	0.00	0.165	0.330	β_{Br}	0.33	β	0.00	0.315	0.63
β_{Br_F}	0.00	0.165	0.165	β_{Cl}	0.07	ε_p	-11.17	-11.17	-11.19
S_{BrBr}	0.001	0.001	0.001	S_{BrCl}	0.001	S_{a-}	0.19	0.19	0.22
d_{BrBr}	0.002	0.002	0.001	d_{BrCl}	0.000	S_{b-}	0.79	0.79	0.79
ε_{Br_H}	-11.46	-11.46	-11.44	ε_{Br}	-11.37	S_{a+}	0.91	0.91	0.94
ε_{Br_F}	-11.65	-11.64	-11.64	ε_{Cl}	-11.52				
S'_+	-1.14	-1.12	-1.12	S'_+	-0.95				
S'_-	-0.95	-0.94	-0.91	S'_-	-1.33				
$\varepsilon_{a'_+}$	-13.71	-13.72	-13.72	$\varepsilon_{a'_+}$	-12.46				
$\varepsilon_{a'_-}$	-12.36	-12.37	-12.41	$\varepsilon_{a'_-}$	-13.24				
S_+	0.50	0.49	0.49	S_+	0.59				
S_-	0.60	0.59	0.55	S_-	0.69				

[a]Reproduce observed IP's within experimental error.

With regard to CF_2BrCH_2Br, the interactions between the LPMO's themselves, as well as the σ orbitals are essentially the same as that in CH_2BrCH_2Cl. In CF_2BrCH_2Br, the Coulomb energy ε_{Br_H} for bromine with hydrogen attached to the same carbon is expected to be higher than ε_{Br_F} for bromine with fluorine attached to the carbon, owng to the electron withdrawing nature of fluorine. In addition, ζ_{Br_H} is greater than ζ_{Br_F} for the same reason. Since both ζ's are not known for this molecule, ζ_{Br_H} and ζ_{Br_F} are assigned to have values 0, $\zeta_x/2$ and ζ_x (Table 19).

A CNDO/BW calculation[221] on CF_2BrCH_2Br indicates that the two highest occupied MO's are $\sigma_{10a'}$ and $\sigma_{9a'}$. The repulsive forces exerted by these orbitals destabilizes $l_{11a'}$ and $l_{12a'}$. Hence, there are also three possible orbital sequences in the LPMO's, the same as those given for CH_2BrCH_2Cl. However, in this case, It is difficult to determine the orderings owing to an appreciable amount of mixing between the orbitals. The set of parameters employed to reproduce the observed IP's is given in Table 19.

4.3.3 Results and Discussion

(a) Interpretation of the Spectra

$(CF_2Cl)_2$, $(CF_2Br)_2$, $(CF_2I)_2$ and CF_2BrCH_2Br

The He I PE spectra of these compounds (figs. 25 and 26a) are similar to each other. Each of the spectra consists of a high intensity band accompanied by seven or eight broad overlapping bands. These low intensity bands correspond to ionization of electrons from σ orbitals. The assignment of these IP's (Table 17) is based on the relative intensity

of the PE bands, as well as the result of CNDO/2[59] or CNDO/BW[321] calculations. The former MO calculations[59] also indicates that 6_{4b_g}, 6_{4a_u}, 6_{3b_g} and 6_{3a_u} of $(CF_2X)_2$ are mainly composed of fluorine LPMO's.

The first PE band of each molecule derives from the four combinations of halogen LPMO's which are mixed with each other through the possible interactions mentioned previously. If the relative population of the trans isomer is very large compared to the gauche isomer in the vapor phase, this band will give approximately four maxima. However, the spectrum may become more complicated with an increasing population of the gauche form. In $(CF_2Cl)_2$, the concentration of the trans rotamer is only slightly higher than that of the gauche. The lowest IP band exhibits a double maxima with not well resolved structure instead of four distinct bands. The IP's given in Table 17 for these peaks are obtained from a band shape analysis which assumes that the trans isomer still gives the main features of the spectrum. However, the uncertainties associated with these two IP's are not known. With regard to $(CF_2Br)_2$ or CF_2BrCH_2Br, the situation is less complicated owing to the lower concentration of the gauche form. The first PE band gives four maxima. However, it is impossible to observe any peaks due to the gauche isomer,and these may be buried under those from the trans isomer.

Among all the dihalotetrafluoroethanes studies, only $(CF_2I)_2$ gives well resolvable structure in the first PE band (Fig. 25c). The four sharp and intense peaks can readily be assigned to derive from the iodine LPMO's of the trans isomer. Each of these peaks is accompanied by a small peak

with IP's of 10.21, 10.55, 10.81 and 11.22 ev (experimental error ± 0.01 ev). A band shape analysis shows that the intensities of these peaks are almost constant with intensity 43 ± 4% of the main peaks. Excitation of vibrational modes cannot account for such a consistently high intensity on four separate LPMO's. This leads us to suggest that these peaks are mainly contributed from the gauche conformer of $(CF_2I)_2$. Assuming the constancy of the photoionization cross sections for both isomers, as well as the temperature of the collision chamber (300°K), ΔH_{mol} is found to be 0.92 ± 0.05 Kcal/mole, compared to 0.95 Kcal/mole for $(CF_2Br)_2$. The magnitude of ΔH_{mol} should be greater in the former molecule than in the latter, owing to both steric and electrostatic effects[227]. However, the difference should not be large due to the electronegative nature of the fluorine atoms in these molecules.

CH_2BrCH_2Cl

The He I spectrum of CH_2BrCH_2Cl (Fig. 26 b) is almost the same as that of the dihaloethanes (Fig. 11 - 13). Only four peaks are observable in the region 12 - 18 ev. These can be attributed to ionization of electrons from σ orbitals. The IP's of these orbitals are somewhere between those of 1,2 dichloro- and 1,2 dibromethanes (Table 15). The first PE band of this molecule is similar to that of $(CF_2I)_2$ and has resolvable fine structure. The four sharp major peaks come from the LPMO's of the trans isomer. The small peak at 10.50 ev cannot arise from the gauche form of this molecule, in accordance with the observation of a higher energy for this form in 1,2 dichloroethane (section 4.2.2b) and $(CF_2I)_2$, but rather from an impurity which may possibly be Br_2[11]. However, the assignment of

the peak at 10.79 ev is not so obvious. The intensity of this peak may be due partly to the excitation of CH_2 mode or from the LPMO of the gauche form. On the assumption of the constancy of photoionization cross sections for both isomers, the intensity ratio of the PE bands of trans and gauche is calculated to be 1 to 0.2. In fact, a band shape analysis gives a ratio 1 to 0.3.

(b) Orbital Energy of Gauche CF_2ICF_2I

There are totally four LPMO's π_3', π_3'', π_8' and π_8'' in the gauche form of $(CF_2I)_2$. They can combine spatially (Fig. 29) with each other to give,

$$\begin{aligned} l_{12a_+} &= \tfrac{1}{2}(\pi_3' + \pi_8' + \pi_3'' + \pi_8'') \\ l_{13a_-} &= \tfrac{1}{2}(\pi_3' + \pi_8' - \pi_3'' - \pi_8'') \\ l_{12b_+} &= \tfrac{1}{2}(\pi_3' - \pi_8' + \pi_3'' - \pi_8'') \\ l_{11b_-} &= \tfrac{1}{2}(\pi_3' - \pi_8' - \pi_3'' + \pi_8'') \end{aligned} \tag{4.10}$$

with

$$\begin{aligned} \pi_3' &= p_{x_3} \\ \pi_3'' &= \tfrac{1}{3} p_{y_3} - \tfrac{2\sqrt{2}}{3} p_{z_3} \\ \pi_8' &= -\tfrac{1}{2} p_{x_8} + \tfrac{\sqrt{3}}{2} p_{y_8} \\ \pi_8'' &= \tfrac{1}{2\sqrt{3}} p_{x_8} + \tfrac{1}{6} p_{y_8} + \tfrac{2\sqrt{2}}{3} p_{z_8} \end{aligned} \tag{4.11}$$

Furthermore, some of these LPMO's are destabilized by mixing with σ MO's of proper symmetry. A CNDO/2 calculation[59] on the molecule, shows that the first three occupied σ orbitals are σ_{11a_+}, σ_{10b_-} and

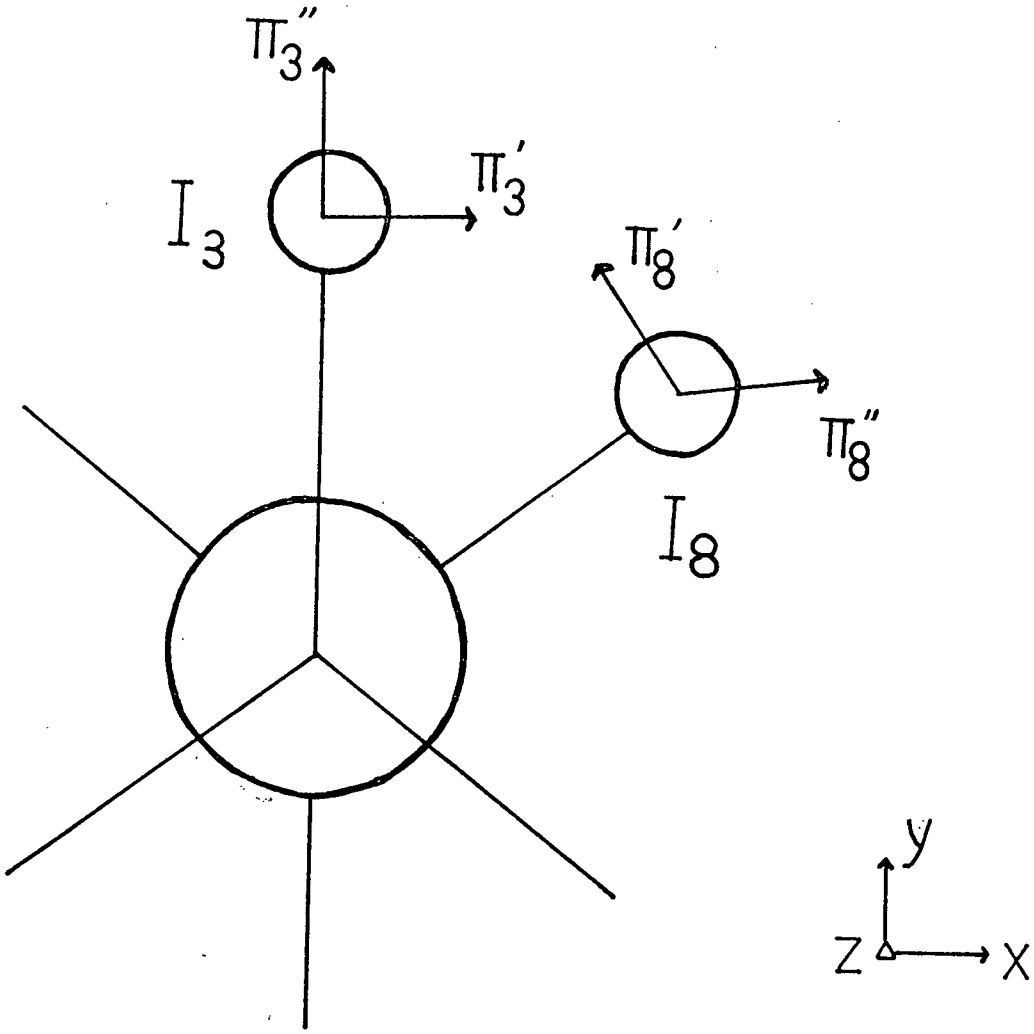

Figure 29. Molecular orbitals of halogen atoms in the gauche form of CF_2ICF_2I.

6_{10a_-} in order of increasing IP. Since it is difficult to distinguish the 6 IP's of the trans and gauche conformers owing to the overlapping nature of the PE bands in the spectrum, a MO treatment on trans $(CF_2X)_2$ is not applicable in this case. Therefore, the through bond interaction parameter is considered as a diagonal element in the secular equation given below. In addition, when the spin orbit coupling is taken into account, the following secular equation can be set up

$$\begin{vmatrix} 1.086\,\varepsilon_p + S_{a_+} - \varepsilon & 0 & 0 & i\zeta/6 \\ 0 & 0.984\,\varepsilon_p + S_{a_-} - \varepsilon & -i\zeta/6 & 0 \\ 0 & i\zeta/6 & 0.914\,\varepsilon_p - \varepsilon & 0 \\ -i\zeta/6 & 0 & 0 & 1.016\,\varepsilon_p + S_{b_-} - \varepsilon \end{vmatrix} = 0 \qquad (4.12)$$

for l_{12a_+}, l_{13a_-}, l_{12b_+} and l_{11b_-} respectively. The solutions of eqn. (4.12) with $\zeta = 0.0$, $\zeta_x/2$ and ζ_x are given in Table 19.

It is interesting to note that ε_p is smaller in the gauche isomer than in the trans (Tables 18 and 19). The same observation applies to cis and trans 1,2 diiodoethylene (section 4.4). It seems that the 'effective' electronegativity of the halogen increases with a larger through space interaction. This parallels the result of calculations on chloro- and bromo methanes[218].

In 1,2 dichloroethane, the trans isomer is found to be more stable than in both the gauche parent molecule[227] and the molecular ion. However, the energy difference between the two isomeric ions ΔH_{ion} is not known.

In $(CF_2I)_2$, both peaks arising from LPMO's of the trans and gauche rotamers are discernible in the PE spectrum. If the energies of the frontier MO's of both isomers are the same, the trans ion is found to be more stable than the gauche by 0.14 ev (ΔH_{mol} is equal to 0.04 ev from the previous discussion). Taking the difference in ε_p between trans and gauche isomers into account, ΔH_{ion} is estimated to be 0.06 ev, almost the same as ΔH_{mol}. This may be due to the delocalization of the positive charge over the whole cation by the fluorine atoms in $(CF_2I)_2$. In this respect, one would expect the difference $\Delta H_{ion} - \Delta H_{mol}$ to be larger in 1,2 dichloroethane, or 1,2 bromochloroethane, than in the corresponding fluorinated 1,2 dihaloethane.

In Tables 16 and 18, the quantity S_i for dibromoethane is greater for increasing replacement of hydrogen by fluorine. The same observation is applicable to the other dihaloethanes, and their respective fluorinated derivaties. This is probably due to more higher lying σ orbitals available for through bond interaction in the fluorinated compounds. This calculation indicates that the through bond interaction is not the same for the two isomers of $(CF_2I)_2$, but that the interaction is greater in the gauche form. If the inductive effect is predominant over other effects, and also if no rehybridization occurs in the C-X bond of both isomers, the iodine NMR chemical shift is expected to be larger for the gauche form, while the nuclear quadrupole coupling constant is greater for the trans. Unfortunately, no such measurements have been made.

In view of the quantity ε_p obtained for both trans and gauche $(CF_2I)_2$, force constant calculations in a simple Urey-Bradley force

field[112] are carried out on both isomers of $(CH_2Cl)_2$ and $(CH_2Br)_2$ using frequencies given in ref. 236. In this treatment, only C-C and C-X stretching, as well as CCX bending vibrations are considered. Both the Gs and Fs matrices used are the same as those given in ref. 226. Different sets of force constants are used for the two conformers. The force constants given in Table 20 reproduce the observed frequencies within 5%. In general, the nonbonded repulsive force constant F increases with shorter interatomic distances between two nonbonded atoms. However, the constant is found to be smaller in the gauche form than in the trans for both $(CH_2Cl)_2$ and $(CH_2Br)_2$. This reflects a greater attractive interaction of the halogen atoms in the gauche conformer. In $(CF_2I)_2$, ε_p of the gauche form is lower in the two conformers. This implies that the electron in the iodine is more delocalized over the C-I bond in the gauche form if we consider only the inductive effect. Therefore, the C-I bond should be stronger in the gauche form than in the trans. If the same situation occurs in the 1,2 dihaloethanes, one would expect a higher C-X stretching force constant in the gauche isomer. In fact, the calculated values of K_{CX} (table 20) parallels the above observation.

4.4 Dihaloethylenes

4.4.1 Introduction

The electronic structures of the dihaloethylenes $C_2H_2X_2$ have received considerable attention owing to their chemical and physical properties. PES has been employed by several workers[208,209,215,258-262] to elucidate the electronic structure of these molecules. From the IP's obtained, and hence the orbital energies (assuming Koopmans' theorem[37]

Table 20. Urey-Bradley Force Constants[a] (mdyn/Å) of Trans and Gauche $(CH_2Cl)_2$ and $(CH_2Br)_2$

	Trans $(CH_2Cl)_2$	Gauche $(CH_2Cl)_2$	Trans $(CH_2Br)_2$	Gauche $(CH_2Br)_2$
K_{CC}	2.99	3.21	2.93	2.96
K_{CX}	2.71	2.28	1.97	1.93
H_{CCX}	0.19	0.25	0.16	0.15
F_{XX}	0.39	0.23	0.43	0.38

[a] K_{CC}, K_{CX}, H_{CCX} and F are the C-C stretch, C-X stretch, CCX bending and and nonbonded repulsive force constants respectively. $F_{XX}' = -0.1\ F_{XX}$.

to hold), various parameters such as the Coulomb integrals ε_p and $\varepsilon_{c=c}$, resonance integrals between carbon and halogen β, as well as the through bond and through space parameters have been deduced[208,261] for the trans, cis 1,2 and also gem dihaloethylenes in the Huckel MO approximation. Inclusion of spin orbit coupling interaction is found to be necessary for the interpretation of the PE spectra of the iodoethylenes[209]. In this section, we again apply a one electron model, similar to that described in section 4.2, including spin orbit coupling, conjugative effects, as well as through bond and through space interactions, to all the dihaloethylenes except gem diiodoethylene and the fluoroethylenes. Qualitative correlation between the calculated MO parameters, the electronegativity of the halogen atom, the carbon and proton chemical shifts, δ_c and δ_H respectively, and the nuclear quadrupole coupling constant e^2Qq of the ethylene derivatives studies, is discussed. Throughout this work, the assignment of the valence orbitals of these molecules is based on the work of Wittel and Bock[208].

4.4.2 Method of Calculation

(a) One Electron Model for the Dihaloethylenes

Fig. 30 shows schematically the mixing of carbon π and σ orbitals, and halogen LPMO's in the gem and cis 1,2 dihaloethylenes by various kinds of interactions. First, case b, where the degeneracy of the unperturbed LPMO's is completely removed by the through space interaction[78] which gives rise to the orbitals l_{4b_2}, l_{1a_2}, l_{1b_1} and l_{5a_1} with different energies. (The orbital symmetry used is the same as that of Wittel and

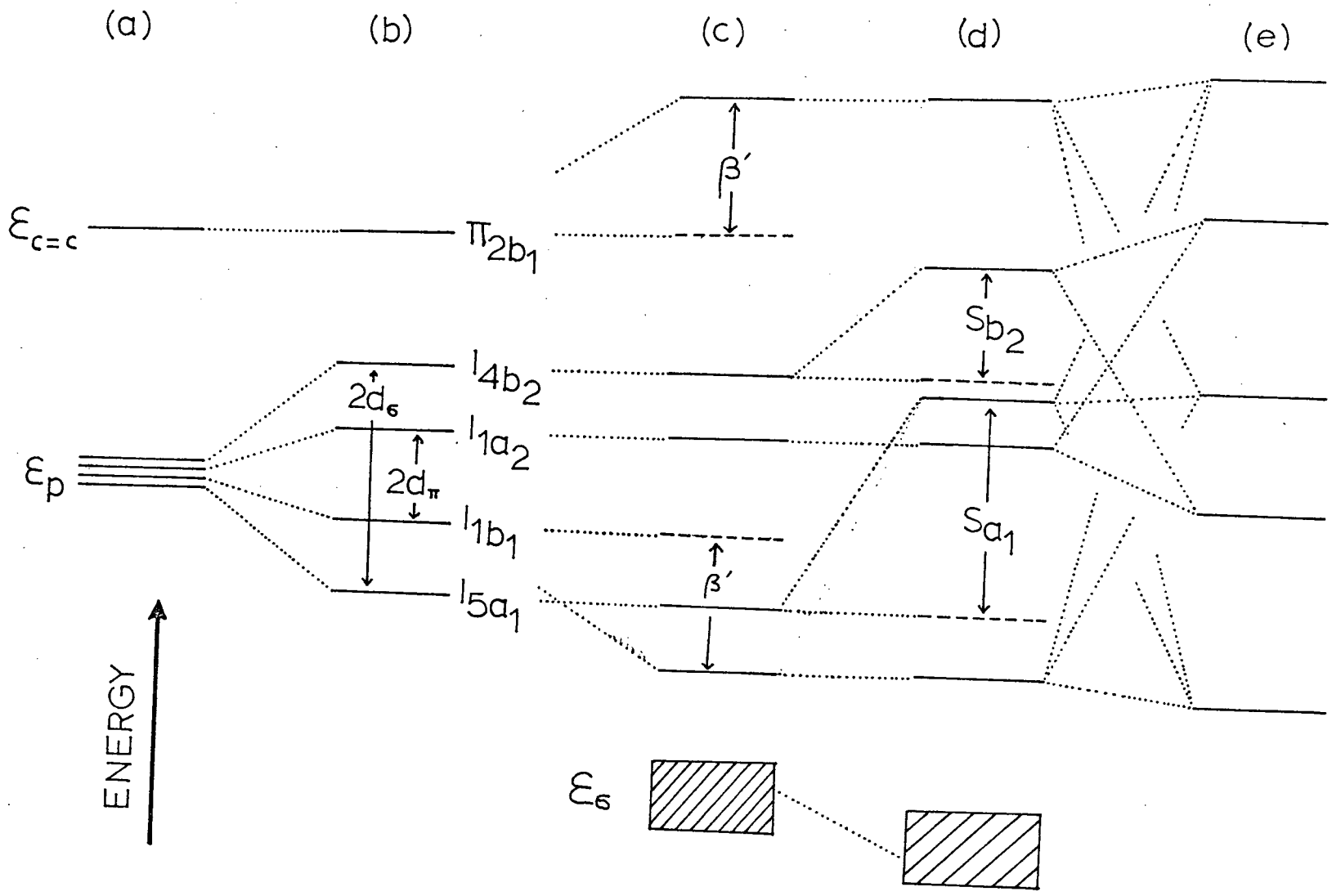

Figure 30. Qualitative MO diagram of cis 1,2 and gem dihaloethylene (a) no perturbation, (b) through space interaction, (c) conjugative effect added, (d) through bond interaction added, and (e) spin orbit coupling added.

Bock[208].) The quantities d_σ and d_π measure the through space energy shifts of the orbitals l_{4b_2} and l_{5a_1} and l_{1a_2} and l_{1b_1}, respectively, from the unperturbed energy ε_p. In addition to the through space interactions, conjugative effects between the carbon π orbital π_{2b_1} and the LPMO l_{1b_1} shift the former orbital up, and the latter down by an amount β' with $|\varepsilon_{c=c}| < |\varepsilon_{1b_1}|$. However, the reverse is true for diiodoethylene where $|\varepsilon_{c=c}| > |\varepsilon_{1b_1}|$. The relation between β and β' can be expressed mathematically as

$$\beta = -[|\beta'|(|\beta'| + |\varepsilon_p - \varepsilon_{c=c}| + d_\pi)]^{1/2} \qquad (4.13)$$

where β is the resonance integral.

The operation of through bond interactions on the l_{5a_1} and l_{4b_2} orbitals by the σ orbitals of the same symmetry (the first four highest occupied σ MO's of cis and gem isomers are of symmetry b_2 and a_1 [208]) destabilizes the two orbitals by energies S_{a_1} and S_{b_2} respectively. Further mixing between the LPMO's themselves with the same subscript 1 or 2 in the symmetry representation is allowed by the introduction of spin orbital coupling. The coupling constant ζ in dihaloethylenes should be smaller than that in dihaloethanes owing to the interaction between the π orbitals and the LPMO's in the ethylene derivatives. Consequently, the secular equation corresponding to all the perturbations mentioned above can be expressed as

$$\begin{vmatrix} \varepsilon_{c=c} - \beta' - \varepsilon & 0 & 0 & 0 & -i\varsigma/2\sqrt{2} \\ 0 & \varepsilon_p + d_\sigma + S_{b_2} - \varepsilon & -i\varsigma/2 & 0 & 0 \\ 0 & i\varsigma/2 & \varepsilon_p + d_\pi - \varepsilon & 0 & 0 \\ 0 & 0 & 0 & \varepsilon_p - d_\pi + \beta' - \varepsilon & i\varsigma/2\sqrt{2} \\ i\varsigma/2\sqrt{2} & 0 & 0 & -i\varsigma/2\sqrt{2} & \varepsilon_p - d_\sigma + S_{a_1} - \varepsilon \end{vmatrix} = 0 \qquad (4.14)$$

for π_{2b_1} , l_{4b_2} , l_{1a_2} , l_{1b_1} and l_{5a_1} respectively. The x axis is defined to be perpendicular to the molecular plane. The factor $\sqrt{2}$ in the matrix elements with ς arises from the assumption of equal mixing between the π and the LPMO's.

Similarly, a 5 x 5 secular determinant can be set up for trans 1,2 dihaloethylene including all kinds of interactions mentioned previously for the cis isomer. However, in this case, d_σ is identical to d_π and also the symmetry representations b_2 , a_1 , a_2 and b_1 in eqn. (4.14) and Fig. 30 are replaced by a_g , b_u , b_g and a_u respectively for the conversion to C_{2h} symmetry. The four frontier σ orbitals are of b_u and a_g symmetry[208] only.

In a secular equation such as (4.14), there are totally six independent unknown variables, $\varepsilon_{c=c}$, ε_p , β' , S_{a_1} , S_{b_2} and ς with only five IP's available. Since the value of ς should be in the range of 0.0 to ς_x , so it is constrained to have values 0, $\varsigma_x/2$ and ς_x again. Then the other five variables are determined in a trial and error fashion to reproduce the observed IP's. In all cases except $C_2H_2I_2$ with $\varsigma = \varsigma_x$, the calculated IP's fit exactly the observed ones and the parameters used are given in Tables 21 - 23. It is found that besides S_i , $\varepsilon_{c=c}$, ε_p , d_σ , d_π and β' are rather insensitive to ς . So comparison of

Table 21. Calculated MO Parameters (ev)[a] of Cis 1,2 Dihaloethylenes $C_2H_2X_2$

	$C_2H_2Cl_2$	$C_2H_2Br_2$	$C_2H_2I_2$[b]	$C_2H_2Cl_2$	$C_2H_2Br_2$	$C_2H_2I_2$	$C_2H_2Cl_2$	$C_2H_2Br_2$	$C_2H_2I_2$
ς	0.07	0.33	0.63	0.035	0.165	0.315	0.00	0.00	0.00
d_σ	0.34	0.52	0.66	0.34	0.53	0.67	0.34	0.53	0.67
d_π	0.06	0.10	0.14	0.06	0.10	0.14	0.06	0.10	0.14
$\varepsilon_{c=c}$	-10.97	-10.79	-10.05	-10.97	-10.76	-9.89	-10.96	-10.76	-9.86
ε_p	-12.53	-11.60	-10.51	-12.53	-11.62	-10.66	-12.53	-11.63	-10.69
S_{a_1}	0.87	0.89	1.11	0.87	0.92	1.22	0.87	0.93	1.25
S_{b_2}	0.55	0.30	0.03	0.55	0.35	0.37	0.55	0.37	0.42
β'	-1.17	-1.15	-1.07	-1.17	-1.13	-0.94	-1.16	-1.13	-0.92
β	-1.81	-1.54	-1.34	-1.80	-1.54	-1.32	-1.80	-1.54	-1.32

[a] Reproduce observed IP's within experimental error.

[b] Reproduce observed IP's within ± 0.08 ev.

Table 22. Calculated MO Parameters(ev)[a] of Trans 1,2 Dihaloethylenes $C_2H_2X_2$

	$C_2H_2Cl_2$	$C_2H_2Br_2$	$C_2H_2I_2$[b]	$C_2H_2Cl_2$	$C_2H_2Br_2$	$C_2H_2I_2$	$C_2H_2Cl_2$	$C_2H_2Br_2$	$C_2H_2I_2$
ς	0.07	0.33	0.63	0.035	0.165	0.315	0.00	0.00	0.00
d_{xx}	0.004	0.007	0.008	0.004	0.007	0.008	0.004	0.007	0.008
$\varepsilon_{c=c}$	-10.94	-10.92	-10.51	-10.94	-10.88	-10.35	-10.94	-10.87	-10.30
ε_p	-12.64	-11.52	-10.26	-12.64	-11.56	-10.41	-12.64	-11.58	-10.46
S_{a_g}	0.82	0.42	0.20	0.32	0.50	0.50	0.82	0.53	0.59
S_{b_u}	0.64	0.49	0.18	0.64	0.53	0.32	0.64	0.54	0.36
β'	-1.14	-1.36	-1.33	-1.14	-1.33	-1.42	-1.14	-1.32	-1.38
β	-1.80	-1.64	-1.45	-1.80	-1.64	-1.46	-1.80	-1.64	-1.46

[a]Reproduce observed IP's within experimental error.

[b]Reproduce observed IP's within ± 0.04 ev.

Table 23. Calculated MO Parameters (ev)[a] of Gem Dihaloethylenes $C_2H_2X_2$

	$C_2H_2Cl_2$	$C_2H_2Br_2$	$C_2H_2Cl_2$	$C_2H_2Br_2$	$C_2H_2Cl_2$	$C_2H_2Br_2$
ς	0.07	0.33	0.035	0.165	0.00	0.00
d_σ	0.42	0.40	0.42	0.40	0.42	0.40
d_π	0.17	0.17	0.17	0.17	0.17	0.17
$\varepsilon_{c=c}$	-11.08	-10.88	-11.07	-10.85	-11.07	-10.84
ε_p	-12.65	-11.73	-12.65	-11.76	-12.65	-11.77
S_{a_1}	0.87	0.90	0.87	0.93	0.87	0.94
S_{b_2}	0.61	0.57	0.61	0.63	0.61	0.65
β'	-1.08	-1.09	-1.07	-1.06	-1.07	-1.06
β	-1.74	-1.52	-1.74	-1.51	-1.74	-1.51

[a]Reproduce observed IP's within experimental error.

these quantities from molecule to molecule is possible even though the exact value of ς is not known.

(b) One Electron Model for the Vinyl Halides

The bonding nature of the vinyl halides (C_s) is similar to that of the dihaloethylenes in some aspects. Therefore, it is desirable to compare parameters such as $\varepsilon_{c=c}$, ε_p and β between these two types of ethylene derivatives.

In the vinyl halides (Fig. 31), one of the halogen LPMO's, $l_{1a''}$ can be combined with the π orbital $\pi_{2a''}$ (conjugative effect), while the other LPMO, $l_{7a'}$ interacts with the remaining carbon and hydrogen framework. Furthermore, these LPMO's mix with each other by spin orbit coupling. The overall interaction may be summarized in the following secular determinant

$$\begin{vmatrix} \varepsilon_p + S_{a'} - \varepsilon & -i\varsigma/2\sqrt{2} & i\varsigma/2\sqrt{2} \\ i\varsigma/2\sqrt{2} & \varepsilon_p - \varepsilon & \beta \\ -i\varsigma/2\sqrt{2} & \beta & \varepsilon_{c=c} - \varepsilon \end{vmatrix} = 0 \qquad (4.15)$$

for $l_{7a'}$, $l_{1a''}$ and $\pi_{2a''}$ respectively. $S_{a'}$ measures the energy change of $l_{7a'}$ through the mixing of a'' σ orbitals. The factor $\sqrt{2}$ in the determinant is again due to the equal mixing of $\pi_{2a''}$ and $l_{1a''}$.

The number of unknown parameters ε_p , $\varepsilon_{c=c}$, ς , β and $S_{a'}$ in eqn. (4.15) exceeds the number of observed IP's. Therefore, ς is assigned to have values of 0, $\varsigma_x/2$ and ς_x , and β is varied from zero to a value which gives a reasonable physical result. Then the other para-

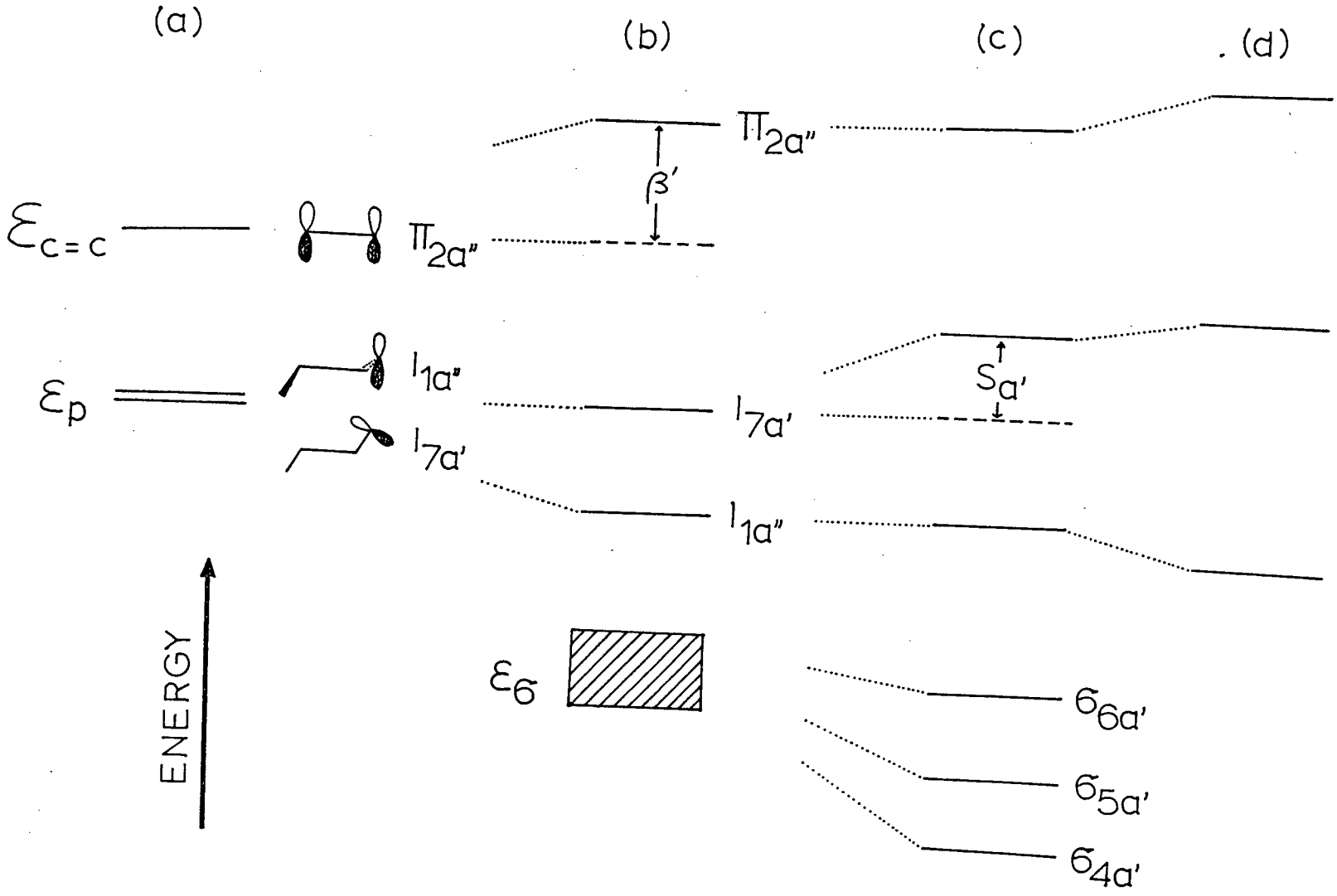

Figure 31. Qualitative MO diagram of vinyl halide (a) no perturbation, (b) conjugative effect, (c) through bond interaction added, and (d) spin or b it coupling added.

meters are adjusted to give agreement between the calculated and observed orbital energies[208]. The result of the calculation indicates that ε_p, $\varepsilon_{c=c}$, β and $S_{\alpha'}$ are rather insensitive to the value of ς. Also ε_p increases but both $\varepsilon_{c=c}$ and $S_{\alpha'}$ decrease with diminishing values of β. Table 24 lists the calculated MO parameters with $\varsigma = \varsigma_x/2$. It is obvious that β in the vinyl halides is less than that in the dihaloethylenes (Tables 21 - 23). The higher resonance energy in the latter molecules is probably due to an increase in electronegativity of the carbon atom by one more electron withdrawing halogen atom, in comparison to the former molecules. The choice of an appropriate β and hence other parameters is not obvious and will be discussed later in individual cases.

4.4.3 Results and Discussion

(a) Correlation between Huckel Parameters of Dihaloethylenes and the Chemical Shift in Carbon-13 and Proton NMR

There is a growing interest in the application of carbon-13 NMR to many aspects of chemistry. From the NMR spectrum of a molecule, valuable information about the bonding properties of a particular carbon atom, and the electron distribution within the atom can be deduced. For instance, the carbon chemical shift δ_c reflects the shielding by the electrons of a carbon nucleus from itself, or from its neighbours. The chemical shifts of some halogenated ethylenes are listed in Table 25 for convenience in comparison.

The difference in electronegativity between the halogen and carbon atoms in halogenated ethylenes leads to an inductive effect which will reduce the shielding of the carbon atom and thus increase the binding energy of the

Table 24. Calculated MO Parameters (ev)[a] of Vinyl Halides C_2H_3X with $\varsigma = \varsigma_x/2$

	β	$\varepsilon_{c=c}$	ε_p	$S_{\alpha'}$
C_2H_3Cl	-0.80	-10.39	-12.83	1.22
	-1.00	-10.55	-12.67	1.06
	-1.20	-10.78	-12.44	0.83
	-1.32	-10.99	-12.23	0.62
	-1.35	-11.05	-12.17	0.56
	-1.40	-11.20	-12.02	0.41
C_2H_3Br	-0.80	-10.17	-12.00	1.13
	-1.00	-10.39	-11.18	0.91
	-1.20	-10.89	-11.28	0.41
	-1.215	-11.09	-11.09	0.22
C_2H_3I	-0.80	-9.73	-11.21	1.15
	-1.00	-10.02	-10.91	0.86
	-1.05	-10.16	-10.77	0.72

[a]Reproduce observed IP's within experimental error.

Table 25. Carbon NMR Chemical Shifts (ppm)[a] δ_c, bond angles[b] and Nuclear Quadrupole Coupling Constants e^2Qq [c] (Mc/s) of Halogenated Ethylenes

	X	C_2H_3X	Gem $C_2H_2X_2$	Cis 1,2 $C_2H_2X_2$	Trans 1,2 $C_2H_2X_2$
δ_c	Cl	126.1[d]	127. [d]	121.3	119.4
	Br	114.7[d]	97.0[d]	116.4	109.4
	I	85.3[d]		96.5	79.4
∢CCX	Cl		122.8°	123.8°	123°
	Br			124.1°	121°
e^2Qq	Cl	67.23	73.67	70.00	71.17

[a]From ref.263. TMS is used as internal standard.

[b]See refs. 150, 193-195. [c]Refs. 266 and 267.

[d]The chemical shift of carbon attached to halogen.

π electrons of the carbon double bond. Conversely, the shielding of the halogen atom will be increased, and thus the binding energy of the electrons associated with it will be decreased.

The absolute magnitude of the parameter $\varepsilon_{c=c}$ in the dihaloethylenes (Tables 21-23) is found to be gem > cis > trans in decreasing order. This indicates that the carbon atom is more deshielded in the gem isomer than in the others providing that the bonding nature of the σ bonds is almost the same for these molecules. In fact, the observed chemical shifts parallel the above trend for $\varepsilon_{c=c}$.

In the case of the dibromoethylenes, such agreement is not obtained. δ_c is predicted to be the greatest for trans and the least for cis, in contrast to the observation [263] cis > gem > trans. According to a recent theoretical investigation on difluoroethylenes[264], diminution in the s character along the C-F bond will result in the widening of the CCF angle. This relation may probably hold for other dihaloethylenes also. The augmentation of s character in the C-C σ bond causes reduction in the same orbital along the C-Br bond and hence an increase in the shielding of the carbon atom and a deschielding of the hydrogen atom. If this effect predominates over that from π electrons, the observed trend in δ_c can be reproduced with higher s character along the C-C bond of cis than gem or trans. In fact, the CCBr angle[150,195] is found to be greater in cis than in trans by 3°. The result from proton NMR measurements[265], that the shielding of the proton is less in the cis than in the trans form further supports the explanation offered. The constancy of the CCCl angle[193,194] in the dichloroethylenes reflects that only small variation in s character occurs in the C-C σ bond.

In diiodoethylenes, the calculated value of $\varepsilon_{c=c}$ again fails to give the correct ordering of δ_c for cis and trans isomers. This may still arise from the different composition of the s orbital in the C-Br bond for the two isomers. The proton NMR data[265] for these molecules also favors this reasoning.

All the halogens except fluorine have commonly occurring isotopes with a quadrupole moment. The nuclear quadrupole coupling constant e^2Qq obtained from radio-frequency spectroscopy for these halogens in a molecule provides ample information about the electronic structure of the halogen atom and its environment. Usually, the more the ionic character of a halogen atom or the higher the electron density around the halogen nucleus, the lower the e^2Qq value obtained. The e^2Qq for the chloroethylenes[266,267] (see also Table 25) decreases from gem to trans and then cis. This shows that the electron cloud in chlorine is more concentrated in the cis isomer, and the least concentrated in the gem form. Then, the absolute magnitude of ε_p for these isomer should be gem > trans > cis. In fact, this parallels our calculated values of ε_p (Tables 21-23). Since the NQR data is incomplete for bromo- and iodoethylenes, no such comparison can be made. However, the relation between the calculated parameter ε_p and the observed value e^2Qq of these compounds may not be so straightforward owing to the variation in composition of the s character along the C-X bond.

It has been mentioned before that the choice of a reasonable set of ε_p , $\varepsilon_{c=c}$, β and S_a is not easy and depends on the criteria used. However, carbon MNR and NQR data are useful in this aspect. If the σ bonding in the chloroethylenes is similar to each other, $\varepsilon_{c=c}$ of

vinyl chloride should be somewhere between -11.07 and -10.97 ev in accordance with the observed chemical shifts for cis and trans 1,2 dichloroethylene and vinyl chloride. Then, β is in the range of -1.32 and -1.35 ev (Table 24), and the value of ε_p is the smallest among the chloroethylenes studied here. This in consistent with an NQR study[266,267] which gives the e^2Qq value of vinyl chloride less than all the dichloroethylenes.

It has been mentioned that[265] the difference $\delta_c^{cis} - \delta_c^{trans}$ for the dihaloethylenes increases from a chlorine to iodine substituent. Consideration of both resonance and anisotropy effects alone seems inadequate to explain the difference. A theoretical treatment of carbon chemical shifts[263] shows that the contribution from paramagnetic shielding is more important than that from diamagnetic shielding or anistropy effect. The paramagnetic shielding approximately depends on the energy gap between the highest occupied and the lowest unoccupied orbital. The decreasing energy difference between the π and π^* levels[268] from dichloroethylene to diiodoethylene may at least offer an explanation for part of the difference in the observed chemical shift.

(b) Correlation Between Huckel's Parameters in Dihaloethylene and Electronegativity of the Halogen.

The replacement of a hydrogen atom by a halogen in ethylene will change the bonding property of the attached carbon. A halogen atom with a strong electron withdrawing effect gives a low value for $\varepsilon_{c=c}$. Tables 21 - 23 show the general trend of the influence of this inductive effect on the Coulomb integral $\varepsilon_{c=c}$ by different halogens. In Dewar's approach[269,270], the influence of $\varepsilon_{c=c}$ by the electronegativity of the halogen can be expressed quantitatively as

$$\Delta\varepsilon_{c=c} = \delta\,[\,\varphi_M(X) - \varphi_M(C)\,] \qquad (4.16)$$

where δ is the auxiliary inductive parameter. $\varphi_M(X)$ is the Mulliken electronegativity of the halogen X, with $\varphi_M = 2.82\ \varphi_{Pauling}$. If we calculate $\Delta\varepsilon_{c=c}$ with $\delta = 1/3$[269], $\Delta\varepsilon_{c=c}$ is found to be 0.43, 0.71 and 1.41 ev for the dibromo-, dichloro- and difluoroethylenes respectively. Assuming that $\Delta\varepsilon^{obs}_{c=c}$ is equal to the difference between $\varepsilon_{c=c}$ of any halogen and that of iodine (which is chosen as a reference), then the $\Delta\varepsilon^{obs}_{c=c}$'s are 0.53, 0.59 and 1.79 for trans 1,2 dibromo-, dichloro- and difluoroethylene (section 4.5.2) respectively. With regard to the cis isomers with bromine, chlorine and fluorine substituents, $\varepsilon^{obs}_{c=c}$ has values of 0.87, 1.08 and 2.33 ev respectively. The large discrepancy between the calculated $\Delta\varepsilon_{c=c}$ and $\Delta\varepsilon^{obs}_{c=c}$ for the cis isomer is due to the surprisingly low value of $\varepsilon_{c=c}$ obtained for the cis diiodoethylene (the reference compound).

In the Huckel MO treatment, the parameters ε_p and β of a heteroatom are usually related to the standard value for ε°_p and $\beta_\circ$ by the equation[270],

$$\begin{aligned} \varepsilon_p &= \varepsilon^\circ_p + h_p\beta_\circ \\ \beta &= k_p\beta_\circ \end{aligned} \qquad (4.17)$$

The constants h_p and k_p refer to $C_2H_2X_2$. If ethylene is used as a standard with $\beta_\circ = -1.22$ ev[85], and hence $\varepsilon^\circ_p = -9.29$ ev evaluated from the first IP of ethylene[271], then both k_p and h_p are found to be constant over all the isomers of a dihaloethylene for a particular halogen. The calculated values are 1.3, 1.5, 2.8, 1.9, 2.7 and 6.4 for k_{Br}, k_{Cl}, k_F, h_{Br}, h_{Cl}, and h_F respectively. In addition the ratio of

h_{Br} , h_{Cl} and h_F to one another is almost equal to that of $\rho_M(x) - \rho_M(c)$.

Recently, the PE spectrum[272] of trans 1,2 dicyanoethylene has been obtained. Using the observed IP's and the above MO treatment (ς = 0 for this molecule), $\varepsilon_{C\equiv N}$, β , S_{b_u} , S_{a_g} and $\varepsilon_{C=C}$ are found to have values of -13.67, -0.74, 0.57, 0.89 and -11.89 ev respectively with d_π equal to zero. Owing to the higher electron withdrawing power of the cyano group in comparison to the halogens (except fluorine), values of $\varepsilon_{C=C}$ for the cyanoethylene studied are expected to be lower than that of the dihaloethylenes. The electronegativity of the cyano group evaluated through eqn. (4.17) is 3.3, compared to 3.0 predicted from a group electronegativity calculation[273].

An extended Huckel calculation on the π orbital of the CN radical using expression (2.7) for the exchange integral gives the orbital energy of the highest occupied MO to be -14.84 ev. Destabilization of the π orbital of the cyano group in the dicyanoethylene (-13.67 ev) with respect to the CN radical originates because of the delocalization of the π orbital onto the carbon skeleton.

Application of the same approach as above to trans 1,2 dimethyl-thioethylene[274] with a negligible contribution of spin orbit coupling as well as through bond and through space interactions gives -9.20, -1.49 and -9.50 ev for ε_{SCH_3} , β and $\varepsilon_{C=C}$ respectively. The magnitude of $\varepsilon_{C=C}$ obtained for the trans 1,2 dimethylthioethylene is indicative of the electron donating power of the $-SCH_3$ group but the value seems to be too high. This is probably because of our assumption that the through bond interaction is unimportant in this case.

4.5 Cis and Trans 1,2 Difluoroethylene

4.5.1 Interpretation of the Photoelectron Spectra of Cis and Trans 1,2 Difluoroethylene

The He I PE spectra of cis (I) and trans (II) 1,2 difluoroethylene are shown in Figs. 32 - 34 and the derived IP's and associated vibrational levels are given in Table 26. The first two IP's of both I and II are the same as those given by Brundle et al[41].

The frontier occupied orbitals of the fluoroethylenes studied are mainly of carbon π bonding character and destabilized by interaction with one of the LPMO's of the fluorine atoms l_{1b_1} (I) and l_{1a_u} (II) (conjugative effect). However, the electronegative nature of the fluorine atoms tends to withdraw electron density from their neighbours and thus the π orbital is stabilized (inductive effect). These two effects work in opposition to each other. In chloroethylenes[208,215,259], bromoethylenes[208,258] and iodoethylenes[209], the conjugative effect dominates, resulting in an overall destabilization of the π orbital relative to ethylene[271]. However, the situation may be different in the fluoroethylenes owing to the electronegativity of the fluorine atom. The first IP of the compounds studies, which corresponds to the removal of an electron from the π orbital should provide information of this sort. In addition, from the energy shifts of the σ orbitals of I and II, the perfluoro effect[41,42] which operates on the ethylene molecule may be investigated.

The first PE band of I (Fig. 33a) with a vertical IP of 10.42 ev and adiabatic IP 10.23 ev exhibits extensive vibrational structure which can be interpreted as being due to excitation of ν_2, ν_4 and ν_5 modes with values of 1595, 1360 and 234 cm^{-1} respectively. A reduction in the C-C stretching frequency and an increase in the C-F symmetric stretching mode

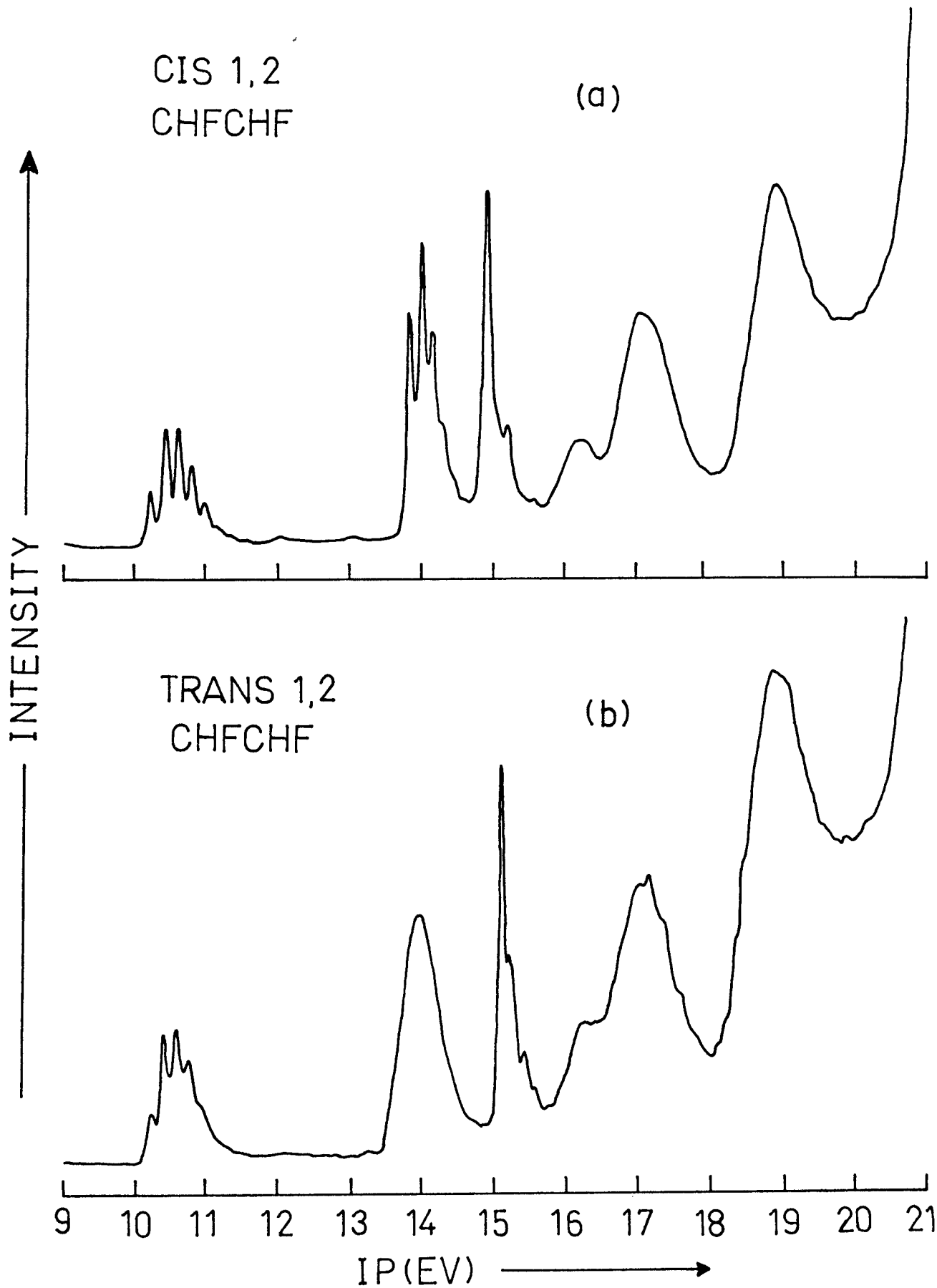

Figure 32. The PE spectra of (a) cis, and (b) trans 1,2 difluoroethylene.

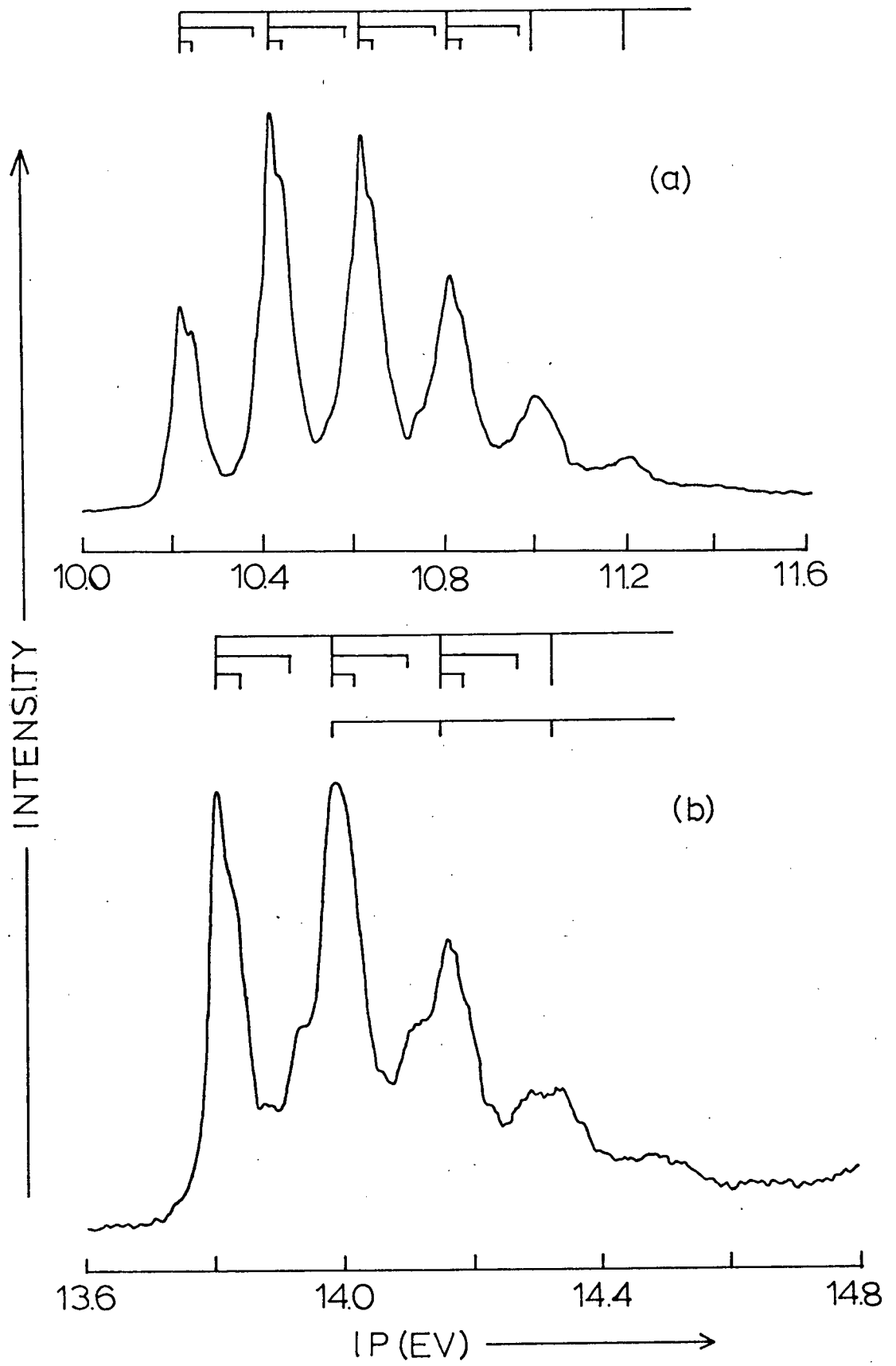

Figure 33. The PE spectra of cis 1,2 difluoroethylene (a) the first band, and (b) the second and the third band.

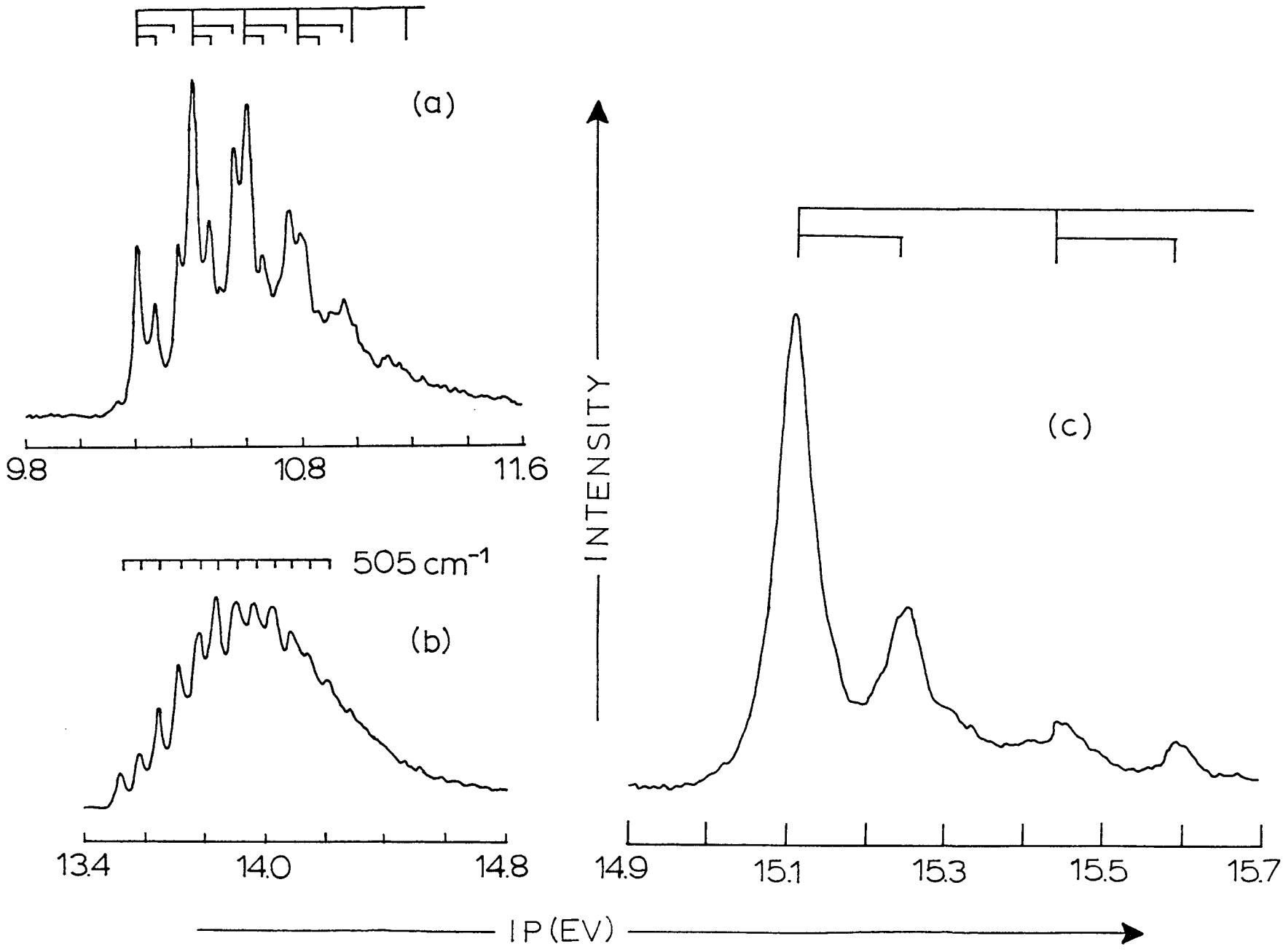

Figure 34. The PE spectra of trans 1,2 difluoroethylene (a) the first band, (b) the second and the third band, and (c) the fourth band.

Table 26. Ionization Potentials[a] and Symmetric Vibrational Frequencies[b] of the Molecular Ions of Cis and Trans 1,2 Difluoroethylene

	Orbital	Vertical IP(ev)	Adiabatic IP(ev)	Vibrational Frequencies (cm^{-1})[c]				
				ν_1	ν_2	ν_3	ν_4	ν_5
Cis 1,2 $C_2H_2F_2$	Ground[d] Neutral State			3122	1716	1263	1015	237
	π_{2b_1}	10.42	10.23		1595		1360	234
	6_{5a_1}	13.81	13.81		1438		992	331
	6_{4b_2}	13.99	13.99		1438			
	6_{3b_2}	14.89	14.89	2653		1185		
	l_{1a_2}	17.10						
	l_{1b_1}, l_{4a_1}	18.91						
Trans 1,2 $C_2H_2F_2$	Ground[d] Neutral State			3111	1694	1286	1123	548
	π_{2a_u}	10.41	10.21		1591	1234		533
	6_{5a_g}, 6_{4a_g}	13.84	13.52					505
	6_{4b_u}	15.11	15.11	2815			1125	
	l_{1b_g}	17.08						
	l_{1a_u}, l_{3b_u}	18.82	18.09		1791		920	

[a] The experimental error is ± 0.01 ev except the vertical IP's of the first and the fourth band, ± 0.02 ev.

[b] The assignment of ionic frequencies is based on the result of the FCF calculation in section 3.3.

[c] ν_1 is the C-H stretching, ν_2 C-C stretching, ν_3 and ν_5 angle bending and ν_4 C-F stretching mode.

[d] Ref. 185.

in comparison to those of the neutral molecule[185] (Table 26) is consistent with the fact that the corresponding π orbital possess C-C bonding and C-F antibonding character. With regard to II (the trans isomer), the first vertical and adiabatic IP's are 10.41 and 10.21 ev respectively, and there are three associated vibrational modes of frequencies 1591, 1234 and 533 cm^{-1}. These may be assigned to the ν_2, ν_3 and ν_5 vibrations in accord with a FCF calculation in section 3.3.

In the region of 17-20 ev in the PE spectrum of either I or II (Fig. 32), there are two bands with a higher intensity for the lower energy one. According to a CNDO/2 calculation[59], these bands are related to the fluorine LPMO's. These orbitals can combine with each other to give $1a_2$, $1a_2$, $1b_1$ and $4a_1$, for I (Fig. 35) and $3a_g$, $3b_u$, $1b_g$ and $1a_u$ for II. The symmetry notation used for I are the same as that for cis 1,2 dihaloethylene in the previous section. All these orbitals except $1b_g$ and $1a_2$ are stabilized to a different extent through either mixing with σ orbitals of the same symmetry, or with the carbon π orbital. Therefore, the orbital that gives rise to the peak at around 17.10 ev for I or II is assigned to either $1a_2$ (I) or $1b_g$ (II).

The other PE band at about 19 ev is a composite of two overlapping peaks with almost the same IP on the basis of its intensity and bandwidth compared to the other band (17.10 ev). One of these two peaks should be related to the $1b_1$ of I, or the $1a_u$ of II which posses both C-C and C-F bonding character from the results of a CNDO/2 calculation[59]. This is in accord with the observed frequency change in the ν_2 mode of II (Table 26). Hence the second peak can readily be assigned to correspond to $4a_1$ (I),

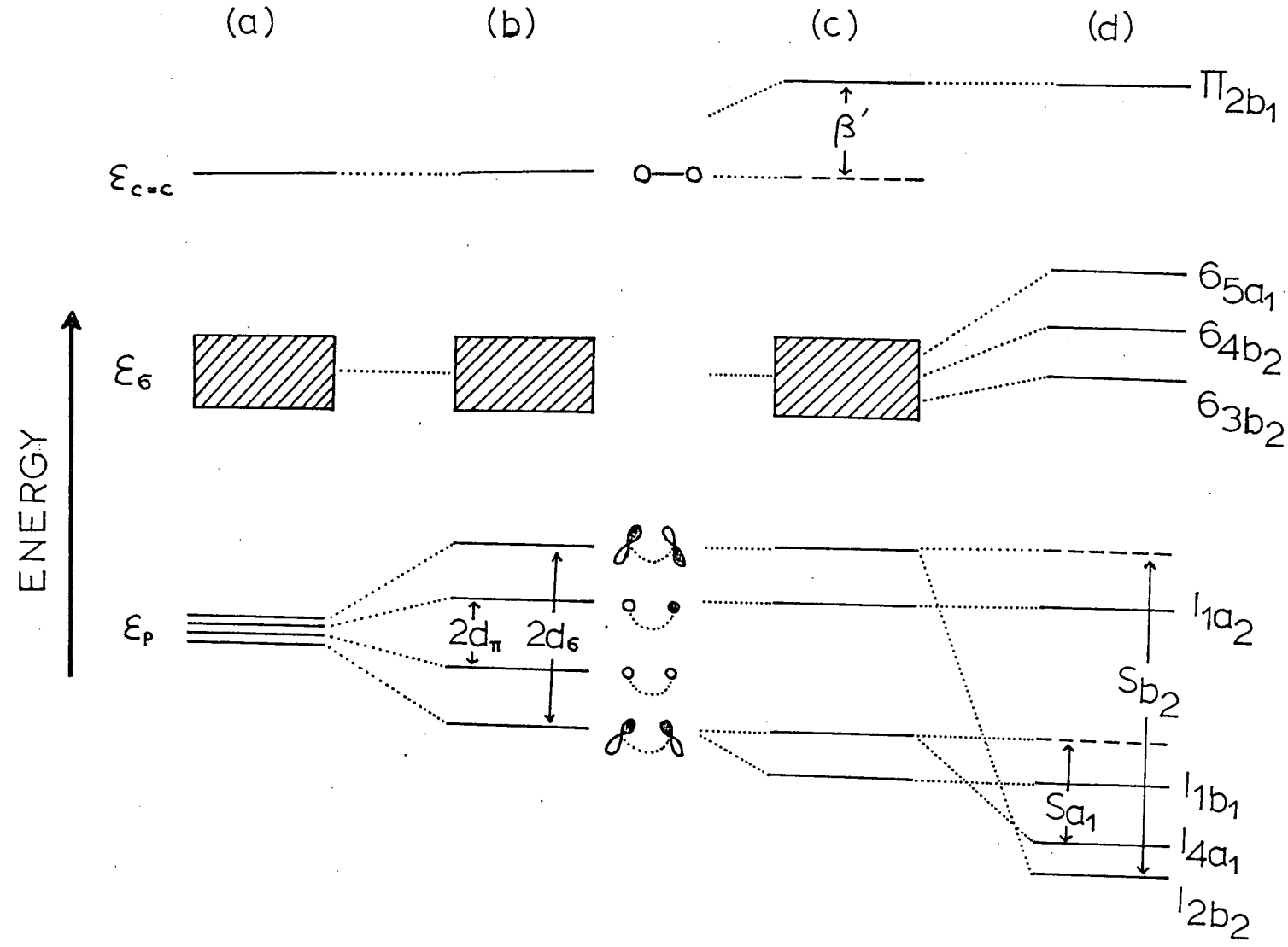

Figure 35. Qualitative MO diagram of cis 1,2 difluoroethylene (a) no perturbation, (b) through space interaction, (c) conjugative effect added, and (d) through bond interaction added.

or l_{3b_u} (II) due to a smaller through bond interaction exerted in this orbital compared to the other LPMO l_{3b_2} (I) or l_{3a_g} (II) (see discussion later).

Between 13 and 16 ev, the PE spectra of the two isomers each show two peaks with resolvable fine structure (Figs. 33b, 34b and 34c and Table 26). CNDO/2 calculations[59] on both isomers give three σ orbitals σ_{5a_1}, σ_{3b_2} and σ_{4b_2} for I, and σ_{4a_g}, σ_{5a_g} and σ_{4b_u} for II in decreasing energy (these σ orbitals have a high mixture of fluorine atomic orbitals) with IP's lower than those of l_{1a_2} (I) and l_{1b_g} (II). In I, the second PE band consists of two overlapping bands instead of only one. This is exemplified by both the results of a FCF calculation on this state (section 3.3), and the relative intensity. The vertical IP's are 13.81 and 13.99 ev for the two bands. An MO calculation[59] indicates that the σ_{5a_1} possesses C-C and C-F bonding character. In view of the reduction in the ν_2 and ν_4 modes observed in the 13.81 ev band, it is assigned to come from σ_{5a_1}. The remaining peaks with vertical IP's 13.99 (excitation of ν_2 is observed) and 14.89 ev (excitation of both ν_1 and ν_3 is observed) are simply related to the orbitals σ_{3b_1} and σ_{4b_1} respectively.

In the case of II, the assignment for the second and the third PE bands is not so obvious even though the intensity of the second band is high compared to that of the third one. It is, therefore, difficult to distinguish the IP's σ_{4a_g} and σ_{5a_g}, which possibly give rise to the second band, because only a single ν_5 progression is observed. The third band, consisting of ν_1 and ν_4 progressions, should be related to σ_{4b_u} in parallel with the orbital sequence predicted from a MO calculation[59], as well as the correlation between the bonding nature of the C-H bond and the observed reduction in the C-H stretching frequency.

According to the assignment given above, the small peak at 16.2 ev in the PE spectrum of either I or II may arise from an impurity. However, this is not conclusive since the lower IP regions are 'clean'. It is improbable for an impurity to have a first IP of about 16.2 ev. Also, no variation in intensity was observed in this peak for different scans of the spectrum. It is probable that this band corresponds either to a fluorine lone pair or to a σ orbital shifted up to 16.2 ev from one of the σ orbital in ethylene. The former possibility can be ruled out since the intensity of this peak is small (ca. one-third) of the other fluorine lone pairs. If the latter situation is the case, then the band in both the cis and trans isomers at 14 ev is due to only one ionization. However, no definite assignment can be made at this stage.

4.5.2 One Electron Model for the Cis and Trans 1,2 Difluoroethylenes

The four fluorine LPMO's of I can interact with each other spatially to give l_{1a_2} , l_{1b_1} , l_{4a_1} and l_{2b_2} with different energies (Fig. 35 case b). In addition, the conjugative effect destabilizes the C-C π orbital π_{2b_1} with an unperturbed energy $\varepsilon_{c=c}$, but stabilizes the l_{1b_1} by the same amount β' . Furthermore, l_{2b_2} and l_{4a_1} are 'repelled' by σ orbitals of the same symmetry[78]. Usually the greater the number of σ orbitals available for interaction, as well as the smaller the energy gap between the σ orbital and l_i , the larger the energy shift S_i . Therefore, l_{4a_1} , is considered to be less repelled by the σ moiety than l_{2b_2} does, i.e. S_{b_2} is greater than S_{a_1} .

A Huckel type MO calculation similar to that for the dihaloethylenes was carried out with $\varsigma = 0$. In this way, $\varepsilon_{c=c}$, ε_p, S_{a_1}, β', σ_{5a_1}, d_π and d_σ are found to be -12.22, -17.10, 1.85, -1.80, -15.66, 0.01 and 0.04 ev respectively, and reproduce the observed IP's exactly. The fact that only three orbitals with IP's lower than 17 ev are found in cis 1,2 dichloro- and 1,2 dibromoethylene[208] further supports our assignment that there are three bands in the region of 13-16 ev in the PE spectrum of I.

A similar treatment is applied to II and gives $\varepsilon_{c=c}$, ε_p, S_{b_u}, β', σ_{4b_u} and d_{xx} to be -12.14, -17.08, 1.73, -1.73, -16.84 and 0.00 ev respectively. The resonance integral β evaluated through expression (4.13) is found to be greater in I than in II. This agrees with a calculation[275] on the mesomeric effect of fluorine which shows that the conjugative effect is more important in I.

It is interesting to note that the 'effective' electronegativity of the fluorine atom seems to be different for the two isomers. This is probably due to a different degree of electron delocalization between the fluorine lone pairs, carbon π orbitals and the σ orbitals. The first IP of both isomers is close to that of ethylene[271] and this indicates that the inductive effect and the conjugative effect are nearly the same. The shortening of the C-C bond in both I and II in comparison to that of ethylene[276] parallels the electronegative nature of the fluorine atom.

The large difference in electronegativity between the fluorine and carbon atoms reduces the shielding of the carbon atom and thus enhances the binding energy of the π electrons of the C-C bond. Conversely, the shielding of the fluorine atom will be increased and the binding energy of electrons

associated with it will be decreased. Information about the electron distribution around the carbon and fluorine nuclei can be obtained from the chemical shifts in carbon and fluorine NMR.

The chemical shifts δ_F of I and II in the fluorine NMR spectra are found to be -165.0 and -186.25 ppm respectively. The lower value of δ_F in II than in I reflects the fact that the electron cloud is more dense around the carbon nucleus in the former molecule. In fact, the calculated MO parameters ε_p agree with this observation.

The absolute value of $\varepsilon_{c=c}$ is found to be greater in I. If the σ framework is nearly the same for both isomers, the chemical shift δ_c in the carbon NMR should be greatest for I. However, the reverse is observed. A recent ab inito calculation[264] on the fluoroethylenes shows that the contribution of the carbon s orbital along the C-C bond is different in these two molecules. The higher the s character involved in the C-C bond, i.e. the more shielding around the carbon nucleus, the wider is the CCF angle. Actually, the CCF angle is found to be greater in I than II[191]. This implies that the electron density around the carbon nucleus is greater in I. Thus the observed trend in δ_c can be reproduced, providing that the electronic effect arising from the σ orbitals predominates over that from the π orbital. The fact that the chemical shift[277] in proton NMR is greater in II further supports the above argument.

The PE spectrum of gem difluoroethylene[215] was reported, but no assignment was made on the observed IP's. We have remeasured the spectrum of this molecule and the vertical IP's of π_{2b_1}, σ_{5a_1}, σ_{4b_2}, σ_{3b_2}, l_{1a_2} and l_{1b_1} are assigned to have values -10.64, -14.91, -15.75, -16.06, -18.31 and -19.87 ev respectively based on a CNDO/2 calculation[59], peak

intensities and a comparison with cis 1,2 difluoroethylene. Application of an MO treatment similar to that for I gives ε_p , β' and $\varepsilon_{c=c}$ as -18.37, -1.43 and -12.08 ev respectively. The smallness of $|\varepsilon_{c=c}|$ in the gem isomer compared with the other difluoroethylenes is in parallel with the largest observed elctron shielding[278] around the carbon nuclei of this molecule.

4.6 1,2 Dibromocyclohexane

4.6.1 Introduction

Trans 1,2 dibromocyclohexane may exist in two different forms with both bromine atoms at either the equatorial position (ee), or the diaxial position (aa). The conformational equilibrium between the isomers has been well investigated by various methods[279-282], and the aa conformer is found to be more stable than the ee despite the non-bonded repulsions between the axial bromines and the axial hydrogens.

The population of the aa and ee forms in the vapor phase has been studied using electron diffraction[281]. Both conformers were found to exist in nearly equal amounts. Recently, however, by using the dilute solution method, Ul'yanova and his coworkers[282] estimate the mole fraction of the aa form in the gas phase to be 0.95. The result of these latter authors may be more reliable in view of the technique used at that (1946) for measurement of the intensities in electron diffraction experiments. In this section, we report the He I PE spectrum of 1,2 dibromocyclohexane (Fig. 36), and,

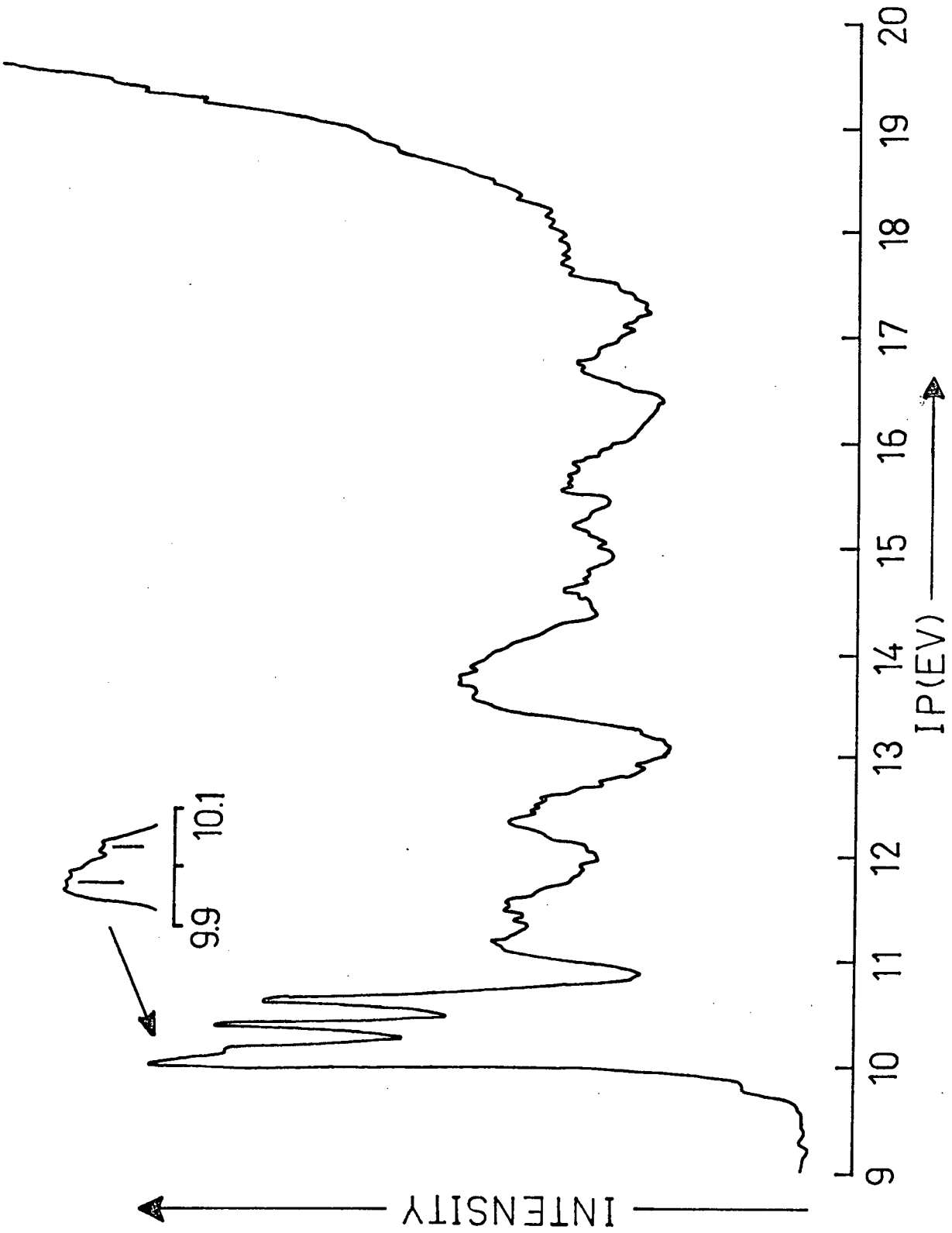

Figure 36. The PE spectrum of trans-1,2-dibromocyclohexane.

assuming the validity of Koopmans' theorem, the interpretation of the spectrum is based on the assumption that the aa conformers of this molecule exists almost exclusively in the vapor state. The observed IP's are given in Table 27.

4.6.2 Results and Discussion

(a) Interaction between the Lone Pair Orbitals of Bromine Atoms in Diaxial 1,2 Dibromocyclohexane (C_2)

Fig. 37 shows schematically the splitting of the bromine LPMO's by spin orbit coupling, and the through bond and through space interactions. In case a, there is no perturbation operating on all four LPMO's, namely p_x and p_y which are degenerate orbitals. The x axis is taken to be perpendicular to the BrC_1C_2Br plane while the y axis is perpendicular to both the x and z (along C-Br bond) axes. However, the degeneracy is partly removed with the introduction of a through space interaction by which these orbitals combine to give l_{13a_x}, l_{12a_y}, l_{11b_y} and l_{10b_x} of a, a, b and b symmetry under the C_2 point group. l_{a_i} implies that the lone pair orbital of a symmetry is contributed from the i^{th} (p_x or p_y) atomic orbital. $l_{a_i} = (i_1 + i_2)/\sqrt{2}$ and $l_{b_i} = (i_1 - i_2)/\sqrt{2}$. with j of i_j the number of the halogen atom.

The bromine LPMO's can further mix with each other through orbitals of the same symmetry (case c). Thus, the degeneracy is completely removed and all these orbitals are destabilized to different extents. According to the result[59] of CNDO/2 calculations on diaxial 1,2 dichlorocyclohexane, the p_x and p_y orbitals of the chlorine atoms combine mainly with the p_x and p_y orbitals of the cyclohexane. In view of the similarity

Table 27. Observed and Calculated Vertical IP's (ev) of Trans 1,2 Dibromocyclohexane

Molecular Orbital	Obs. IP[a] (This Work)	Obs. IP (ref. 283)	Cald. IP (Set 1)	Cald. IP (Set 2)
χ_1[b]	10.06	10.02	10.05	10.05
χ_2	10.19		10.20	10.20
χ_3	10.41	10.42	10.40	10.42
χ_4	10.65	10.66	10.64	10.65
σ_{11a}	11.21		11.21	11.21
σ_{10a}	11.56		11.64	11.59
σ_{9b}	12.46		12.50	12.53
σ_{8b}, σ_{9a}	13.75			13.74
σ_{7b}	14.63			
σ_{8a}	15.24			
σ_{7a}	15.70			
σ_{6b}	16.74			
σ_{5b}	17.75			

[a] Experimental error is within ± 0.01 ev for the first four IP's and within ± 0.03 ev for all other IP's.

[b] χ_i represents the i^{th} bromine LPMO.

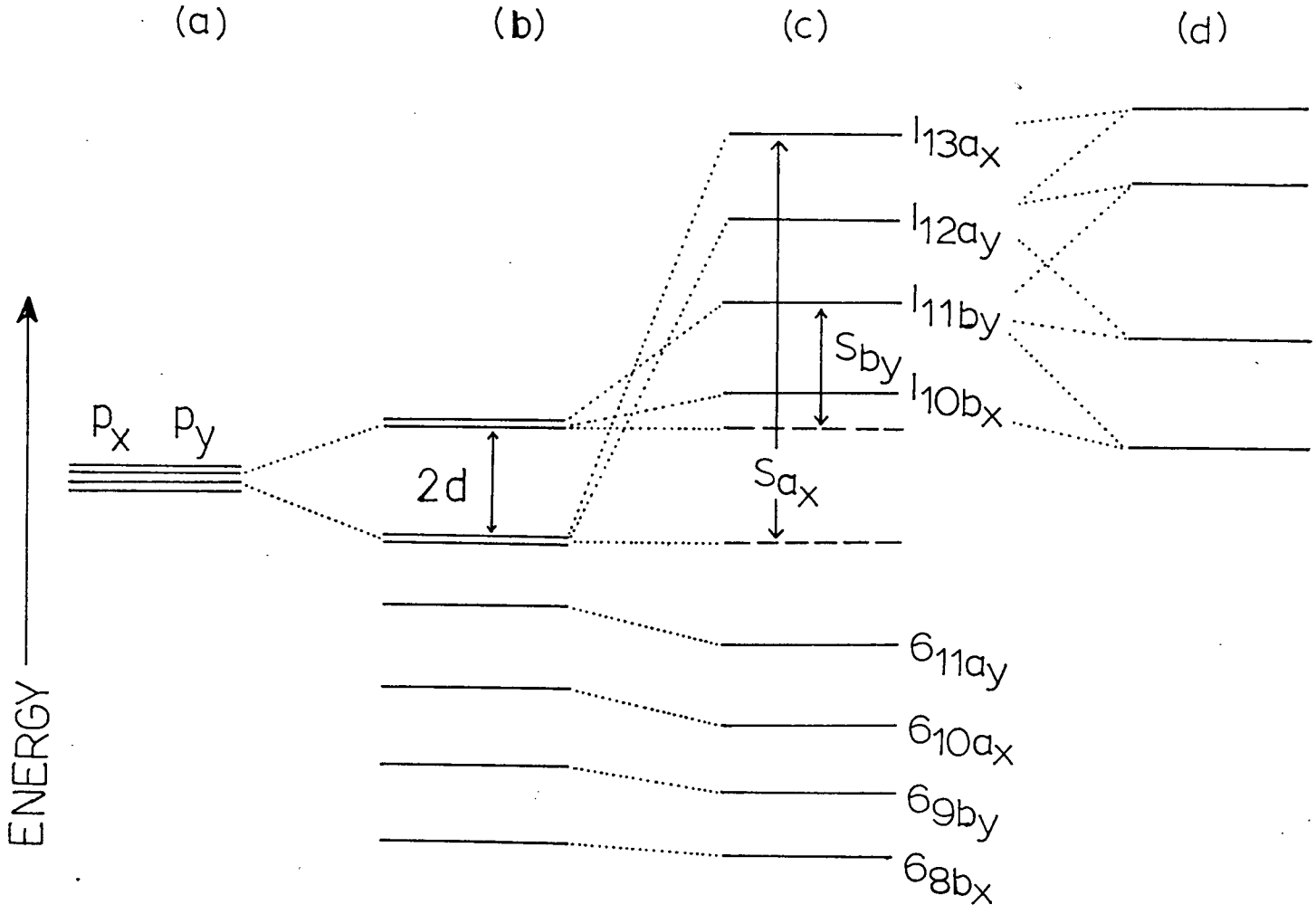

Figure 37. Effects of interaction on molecular orbitals of trans-1,2 dibromocyclohexane (a) no perturbation, (b) through space interaction, (c) through bond interaction added, and (d) spin orbit coupling added.

of the bonding nature between this molecule, and diaxial 1,2 dibromo-cyclohexane, only a LPMO with appropriate symmetry and direction (x or y axis) is allowed to combine with a particular orbital.

The presence of spin orbit coupling enables LPMO's of the same symmetry to mix with one another. Using the operator described in section 2.1.5, the following secular equation corresponding to the overall interaction can be

$$\begin{vmatrix} \varepsilon_p - d - \varepsilon & 0 & i\zeta/2 & 0 & 0 & 0 & 0 & S'_{a_y} \\ 0 & \varepsilon_p + d - \varepsilon & 0 & i\zeta/2 & 0 & 0 & S'_{b_y} & 0 \\ -i\zeta/2 & 0 & \varepsilon_p + d - \varepsilon & 0 & S'_{b_x} & 0 & 0 & 0 \\ 0 & -i\zeta/2 & 0 & \varepsilon_p - d - \varepsilon & 0 & S'_{a_x} & 0 & 0 \\ 0 & 0 & S'_{b_x} & 0 & \varepsilon_{b_x} - \varepsilon & 0 & 0 & 0 \\ 0 & 0 & 0 & S'_{a_x} & 0 & \varepsilon_{a_x} - \varepsilon & 0 & 0 \\ 0 & S'_{b_y} & 0 & 0 & 0 & 0 & \varepsilon_{b_y} - \varepsilon & 0 \\ S'_{a_y} & 0 & 0 & 0 & 0 & 0 & 0 & \varepsilon_{a_y} - \varepsilon \end{vmatrix} = 0 \qquad (4.18)$$

obtained for l_{12a_y}, l_{11b_y}, l_{10b_x}, l_{13a_x}, σ_{8b_x}, σ_{10a_x}, σ_{9B_y} and σ_{11a_y} respectively. ε_p, ε_{b_x}, ε_{a_x}, ε_{b_y} and ε_{a_y} denote the energies of the unperturbed lone pairs, σ_{8b_x}, σ_{10a_x}, σ_{9b_y} and σ_{11a_y} respectively. ζ the spin orbit coupling constant of bromine is taken to be 0.33 ev (section 4.2.2a).

In the secular equation (4.18), the number of unknown parameters (totally nine) exceeds the number of observed quantities. So it is impossible to get a unique solution for the determinant. Assuming that S_{b_x} is equal to zero, ε_p, S_{a_y}, S_{a_x} and S_{b_y} are found to be -10.67, 0.41, 0.53 and 0.27 ev respectively (set 1). Increasing S_{b_x} by 0.02 ev, ε_p and S_{a_y}

remain the same, while S_{a_x} and S_{b_y} increase to 0.59 and 0.29 ev (set 2). The calculated IP's for the first eight highest occupied orbitals from set 1 and set 2 are listed in Table 27. The values of the parameters deduced from set 1 may be considered as the lower bound for these quantities, and they are found to be greater than those of 1,2 dibromoethane (Table 16). Thus the through bond interaction has a greater influence in 1,2 dibromocyclohexane than in 1,2 dibromoethane owing to a smaller energy gap between the σ MO's and the LPMO's in the former molecule. In other words, the more paths available for through bond interaction, the stronger the interaction between the σ MO and the LPMO.

(b) Discussion on the Stability of Trans and Cis 1,2 Dibromocyclohexane

Recently, PE spectra of a series of trans and cis 1,2 disubstituted cyclohexanes $C_6H_{10}BrX$ with X = F, Cl and Br, have been reported by Botter et al[283]. From the sign and magnitude of the difference $IP_{trans} - IP_{cis}$ of this series, the authors[283] concluded that the trans ion of $C_6H_{10}BrX$ is less stable than the cis ion. In this work, different conclusions are drawn for 1,2 dibromocyclohexane.

The non-bonded distance between the two bromine atoms in trans ee 1,2 dibromocyclohexane is shorter than that in the aa form of trans 1,2 dibromocyclohexane, and, hence, the through space interaction is stronger in the former molecule. However, the difference is small, only 0.01 ev as estimated through expression (2.5). By considering the enthalpy difference between the cis and trans conformers in the neutral ground state ($\backsim$ 0.08 ev[283]) and their first lowest IP, the trans ion is found to be more stable

by 0.05 ev on the assumption of the insensitivity of the through bond interaction to the position of the bromine atoms. This is not unreasonable because of a stronger dipole-dipole interaction in the cis form compared to the trans.

The He I PE spectra of trans 1,2 dichlorocyclohexane has also been recorded. However, the band corresponding to the chlorine LPMO's is not resolvable owing to the overlapping of bands arising from both aa and ee conformers as well as the small energy gap between these LPMO's.

CHAPTER V

CONCLUSION

The results described in this thesis have demonstrated the usefulness of photoelectron spectroscopy for the measurement of ionization potentials, and hence via Koopmans' theorem[37], the orbital energies of many molecules exhibiting cis-trans isomerism or various conformers.

The assignment of the PE spectra of the molecules studied is based on the results of CNDO calculations[59,221] and Franck-Condon factor calculations, band shapes, vibrational fine structures and the associated ionic frequencies, relative intensities of PE bands, and comparison with other related molecules. In the substituted ethanes studied, their PE spectra are complicated by the existence of two stable conformers, the trans and the gauche forms in the vapor phase. The interpretation of the spectra is based on the relative population of the two isomers from other spectroscopic techniques, e.g. infrared and Raman spectroscopies as well

as the constancy of the photionization cross sections for these rotamers. In all the ethanes studies, the trans form is found to be more stable than the gauche and has a higher concentration in the vapor phase. Hence the main features of the spectra of these substituted ethanes are assumed to derive from the trans form. In this manner, the frontier orbitals of the gauche diiodotetrafluoroethane are observed. However, determination of the conformational energy difference between the trans and gauche ions cannot be estimated with high accuracy owing to the presence of vibrational fine structure on bands of the trans isomer. In general, the trans ion is found to be more stable than the gauche even though a quantitative result has not been obtained.

From the IP's obtained from a series of halogenated organic molecules, some molecular orbital properties such as the Coulomb energies, resonance energies, and through bond and through space interaction parameters have been deduced using one electron models with the inclusion of spin orbit coupling and through bond and through space interactions between halogen lone pair orbitals. This treatment enables one to determine the through bond and through space interactions quantitatively, such parameters not being previously available. Naturally, the method can also be applied to organic molecules containing heteroatoms other than a halogen, e.g. nitrogen, oxygen or sulfur and hence one may deduce valuable information about the bonding properties in such molecules.

The relation between orbital energies, MO parameters from the above treatment, force constants, bond lengths, nuclear quadrupole coupling constants, NMR chemical shifts and electronegativity of the halogen atom is discussed

for the dihaloethanes, dihaloethylenes and halotrifluoromethanes. It has been found that the calculated MO parameters are useful in explaining some physical properties, such as NMR chemical shifts, nuclear quadrupole coupling constants and bonding properties of dihaloethylenes. It would be fruitful to apply a similar MO treatment to the halogenated benzenes to know more about the nature of the ortho effect and the carbon and halogen NMR chemical shifts.

PE bands of molecules sometimes exhibit vibrational fine structure from which the vibrational transition probabilities can be evaluated. From these transition probabilities, the ionic geometries of molecules may be determined by means of two current methods, the generating function method and the method developed by Coon et al[33]. These methods have been applied to the group VI hydrides, nitrous oxide, dihaloethylenes, 1,2 dichloroethane and bromofluoromethane. The results show that these methods are powerful for determination of the ionic geometry and helpful in assigning ionic frequencies observed in a PE band e.g. in the cis and trans 1,2 difluoroethylenes. Also, the results of calculations give a better picture of the changes in bonding properties during an ionization process. Although the technique has not been widely employed by PE spectroscopists, it will be used extensively in the near future when easier methods for FCF calculations are developed. Certainly the least squares fit technique described in section 2.2.2 simplifies the procedure of calculation. Recently, Dr. Chong[284] of this Department has developed a similar treatment which gives promising results.

In most current work, including the work described in this thesis, the vibrational transition probabilities during the ionization process are assumed to be proportional to the height of the corresponding components

in the PE band. This implies that the band widths at half height are constant within the progression. This approximation is good only when the vibrational components are well separated from each other. It becomes more difficult to use when the components are seriously overlapped by one another, e.g. this situation arises to some extent in the dihaloethylenes where many vibrational modes may be excited. In this case, resolution of these components using a Gaussian or Lorentzian band shape analysis should be effected to obtain a better estimation of the relative intensities. Application of a deconvolution technique[285-287] may further improve the date obtained. The transmission factor[288] of the particular spectrometer should also be considered. The above approaches are rather unexplored, and it would be well worthwhile to improve the accuracy of the vibrational intensity measurements by these mathematical techniques.

Recently, theoretical calculations using Rayleigh-Schrodinger perturbation theory[289] and Green's function techniques[290] have been carried out to reproduce the vibrational structure of the PE spectra of diatomic and triatomic molecules. The theoretical results are in satisfactory agreement with the experimental spectra. In principle, the treatment can be applied to other polyatomic molecules with more than three atoms. However, it is unfortunate that the time for computation increases rapidly with the number of atoms in the molecule under consideration.

In summary, the work discussed in this thesis has illustrated the potential of the methods described herein (the method of FCF calculation, and the Huckel MO treatment) to obtain information about the bonding properties, orbital energies, ionic geometries, through bond and through space

interactions of molecules. In particular, the extension of FCF calculations to larger polyatomic systems will further assist the investigation of the molecular parameters of molecules under consideration.

REFERENCES

1. L. Asbrink, Chem. Phys. Lett. 7, 549 (1970).

2. L.Asbrink and J. W. Rabalais, Chem. Phys. Lett. 12, 182 (1971).

3. T. E. H. Walker, P. M. Dehmer, and J. Berkowitz, J. Chem. Phys. 59, 4292 (1973).

4. K. Siegbahn, C. Nordling, A. Fahlman, R. Nordberg, K. Harmin, J. Hedman, G. Johansson, T. Bergmark, S. Karlsson, I. Lindgren, and B. Lindgren, Electron Spectroscopy For Chemical Analysis, Nova Acta Regiae Societatis Scientiorum Uppsaliensis Ser. IV, Vol. 20, 1967.

5. K. Siegbahn, C. Nordling, G. Johansson, J. Hedman, P. F. Heden, K. Harmin, U. Gelius, A. T. Bergmark, L. O. Werme, R. Manne, and Y. Baer, ESCA Applied to Free Molecules, North-Holland, Amsterdam, 1970.

6. F. I. Vilesov, B. L. Kurbatov, and A. N. Terenin, Sov. Phys.-Dokl. 6, 490 (1961).

7. M. E. Akopyan, F. I. Vilesov, and A. W.Terenin, Sov. Phys.-Dokl. 6, 883, 890 (1962).

8. B. L. Kurbatov and F. T. Vilesov, Sov. Phys.-Dokl. 6, 1091 (1962).

9. M. I. Al-Joboury and D. W. Turner, J. Chem. Soc. London 5141 (1963); 4434 (1965).

10. D. W. Turner and M. I. Al-Joboury, J. Chem. Phys. 37, 3007 (1962).

11. D. W. Turner, A. D. Baker, C. Baker, and C. R. Brundle, High Resolution Molecular Photoelectron Spectroscopy, Wiley-Interscience, N.Y., 1970.

12. A. D. Baker and D. Betteridge, Photoelectron Spectroscopy: Chemical and Analytical Aspects. Pergamon Press, Oxford, 1972.

13. A. D. Baker and C. R. Brundle, Ionizing Photon Impact Phenomena. Academic Press, in preparation.

14. D. W. Turner, in Molecular Spectroscopy (P. Hepple, ed.), p 209. Institute of Petroleum, London, 1968.

15. W. C. Price, in Molecular Spectroscopy (P. Hepple, ed.), p 221. Institute of Petroleum, London, 1968.

16. C. R. Brundle and M. B. Robin, in Determination of Organic Structure by Physical Methods (F. A. Nachod and J. J. Juckerman, eds.), p 1. Academic Press, N.Y., 1971.

17. D. W. Turner, Adv. Mass Spectrom. 4, 755 (1968).

18. D. W. Turner, Adv. Phys. Org. Chem. 4, 31 (1966).

19. D. W. Turner, in Physical Methods in Advanced Inorganic Chemistry, (H. A. O. Hill and P. Day, eds.), p 74. John Wiley, N.Y., 1968.

20. D. W. Turner, Chem. Brit. 4, 435 (1968).

21. W. C. Price, Endeavour 26, 78 (1967).

22. D. Betteridge and A. D. Baker, Anal. Chem. 42 43A (1970).

23. A. D. Baker, Acc. Chem. Res. 3, 17 (1970).

24. S. D. Worley, Chem. Rev. 71, 295 (1971).

25. C. E. Brion, in MTP Int. Rev. of Sci., Phys. Chem. (A. Maccol, ed.), Ser. 1, Vol. 5. Butterworth, London, 1972.

26. H. Bock and B. G. Ramsay, Angew. Chem. Internat. Edit. 12, 734 (1973).

27. A. D. Baker, C. R. Brundle, and M. Thompson, Quarterly Rev. p. 355, The Chem. Soc., London, 1972.

28. C. A. McDowell, in Recent Develop. Mass Spectrosc., Proc. Int. Conf. Mass Spectrosc. (K. Ogata, ed.), p 854. Univ. Park Press, Baltimore, 1970.

29. D. C. Frost, J. Electron Spectrosc. 5, 99 (1974).

30. A. W. Potts, H. J. Lempka, D. G. Streets, and W. C. Price, Phil. Trans. Roy. Soc. Lond. A 268, 59 (1970).

31. J. E. Collin and P. Natalis, Int. J. Mass Spectrom. Ion Phys. 1, 483 (1968).

32. J. Delwiche, P. Natalis, and J. E. Collin, Int. J. Mass Spectrom. Ion Phys. 2, 221 (1969).

33. J. B. Coon, R. E. De Wames, and C. M. Loyd, J. Mol. Spectrosc. 8, 285 (1962).

34. W. L. Smith and P. A. Warsop, Trans. Fara. Soc. 64, 1165 (1968).

35. T. E. Sharp and H. M. Rosenstock, J. Chem. Phys. 41, 3453 (1964).

36. D. P. Craig, J. Chem. Soc. 2146 (1950).

37. T. Koopmans, Physica 1, 104 (1933).

38. D. Chadwick, A. B. Cornford, D. C. Frost, F. G. Herring, A. Katrib, C. A. McDowell, and R. A. N. Mclean, in Electron Spectroscopy (D. A. Shirley, ed.), p 453. North-Holland, Amsterdam, 1972.

39. A. D. Baker, D. Betteridge, N. R. Kemp, and R. E. Kirby, Anal. Chem. 43,375 (1971).

40. J. C. Bunzli, D.C. Frost, and C. A. McDowell, J. Electron Spectrosc. 1, 481 (1972/73).

41. C. R. Brundle, M. B. Robin, N. A. Kuebler, and H. Basch, J. Amer. Chem. Soc. 94, 1451 (1972).

42. C. R. Brundle, M. B. Robin, and N. A. Kuebler, J. Amer. Chem. Soc. 94, 1466 (1972).

43. F. T. Chau and C. A. McDowell, to be published.

44. F. T. Chau and C. A. McDowell, J. Electron Spectrosc. 6, 365 (1975).

45. W. C. Price, A. W. Potts, and D. G. Streets, in Electron Spectroscopy (D. A. Shirley, ed.), p 187. North-Holland, Amsterdam, 1972.

46. M. B. Robin, N. A. Kuebler, and C. R. Brundle, in Electron Spectroscopy (D. A. Shirley, ed.), p 351. North-Holland, Amsterdam, 1972.

47. A. Schweig and W. Thiel, J. Chem. Phys. 60, 951 (1974).

48. W. Thiel and A. Schweig, Chem. Phys. Lett. 16, 409 (1972).

49. W. Thiel and A. Schweig, Chem. Phys. Lett. 12, 49 (1971).

50. L. L. Lohr and M. B. Robin, J. Amer. Chem. Soc. 92, 7241 (1970).

51. A. Schweig and W. Thiel, J. Electron Spectrosc. 3, 27 (1974).

52. J. T. J. Huang, F. O. Ellision, and J. W. Rabalais, J. Electron Spectrosc. 3, 339 (1974).

53. A. Katrib, T. P. Debies, R. J. Cotton, T. H. Lee, and J. W. Rabalais, Chem. Phys. Lett. 22, 196 (1973).

54. V. Fuchs and H. Hotop, Chem. Phys. Lett. 4, 71 (1969).

55. J. A. R. Samson, Chem. Phys. Lett. 4, 257 (1969).

56. C. R. Brundle, Chem. Phys. Lett. 5, 410 (1970).

57. R. B. Cairns, H. Harrison, and R. I. Schoen, Appl. Opt. 9, 605 (1970).

58. W. G. Richards, Int. J. Mass Spectrom. Ion Phys. 2, 419 (1969).

59. J. A. Pople and D. L. Beveridge, Approximate Molecular Orbital Theory. McGraw Hill, N.Y., 1970.

60. F. Brogli, P. A. Clark, E. Heilbronner, and M. Neuenschwander, Angew. Chem. Internat. Edit. 12, 422 (1973).

61. S. T. Lee, Ph.D. Thesis, The University of British Columbia, 1974.

62. L. S. Cederbaum, G. Hohlneicher, and S. Peyerimhoff, Chem. Phys. Lett. 11, 421 (1971).

63. F. Ecker and G. Hohlneicher, Theoret. Chim. Acta 25, 289 (1972).

64. G. Hohlneicher, F. Ecker, and L. S. Cederbaum, in Electron Spectroscopy (D. A. Shirley, ed.), p 647. North-Holland, Amsterdam, 1972.

65. L. S. Cederbaum, G. Hohlneicher, and W. Von Niessen, Chem. Phys. Lett. 18, 503 (1973).

66. L. S. Cederbaum, G. Hohlneicher, and W. Von Niessen, Mol. Phys. 26, 1405 (1973).

67. L. S.Cederbaum, Theoret. Chim. Acta 31, 239 (1973).

68. B. Kellerer, L. S. Cederbaum, and G. Hohlneicher, J. Electron Spectrosc. 3, 107 (1974).

69. L. S. Cederbaum, Chem. Phys. Lett. 25, 562 (1974).

70. R. D. Mattuck, A. Guide to Feynman Diagrams In The Many Body Problem. McGraw Hill, N.Y. 1967.

71. K. F. Freed, Ann. Rev. Phys. Chem. 22, 313 (1971).

72. B. T. Pickup and O. Govcinski, Mol. Phys. 26, 1013 (1973).

73. D. P. Chong, F. G. Herring, and D. McWilliams, J. Chem. Phys. 61, 78, 958, 3567 (1974).

74. D. P. Chong, F. G. Herring, and D. McWilliam, Chem. Phys. Lett. 25, 568 (1974).

75. J. O.Hirschfelder, W. B. Brown, and S. T. Epstein, Adv. Quant. Chem. 1, 255 (1964).

76. G. Herzberg, Electronic Spectra and Electronic Structure of Polyatomic Molecules. D. Van Nostrand Co., N.Y. 1967.

77. R. Hoffmann, A. Imamura, and W. J. Hehre, J. Amer. Chem. Soc. 90, 1499 (1968).

78. R. Hoffmann, Acc. Chem. Res. 4, 1 (1971).

79. C. J. Ballhausen and H. B. Gray, Molecular Orbital Theory. Benjamin, N.Y., 1965.

80. R. S. Mulliken, C. A. Rieke, D. Orloff, and H. Orloff, J. Chem. Phys. 17, 1248 (1949).

81. R. Hoffmann, J. Chem. Phys. 39, 1397 (1963).

82. L. Pauling and E. B. Wilson, Introduction to Quantum Mechanics. McGraw Hill, N.Y., 1935.

83. E. Heilbronner, in XXIIIrd. International Congress of Pure and Applied Chemistry, Vol. 7, p 9. Butterworth, London, 1971.

84. E. Heilbronner and H. D. Martin, Helv. Chim. Acta 55, 1490 (1972).

85. M. Beez, G. Bieri, H. Bock, and E. Heilbronner, Helv. Chim. Acta 56, 1028 (1973).

86. P. Bischof, J. A. Marshall, E. Heilbronner, and V. Hornung, Helv. Chim. Acta 52, 1745 (1969).

87. J. C. Bunzli, D. C. Frost, and L. Weiler, Tetrahedron Letters, 1159, (1973).

88. E. Haselbach and A. Schmelzer, Helv. Chim. Acta 54, 1575 (1971).

89. E. Haselbach and A. Schmelzer, Helv. Chim. Acta 55, 1745 (1972).

90. E. Haselbach and E. Heilbornner, Helv. Chim. Acta 53, 684 (1970).

91. R. Gleiter, E. Heilbronner, and V. Hornung, Helv. Chim. Acta 55, 255 (1972).

92. F. Brogli, E. Heilbronner, and T. Kobayashi, Helv. Chim. Acta 55, 274 (1972).

93. W. Kauzmann, Quantum Chemistry, p 351. Academic Press, N.Y., 1957.

94. F. Brogli and E. Heilbronner, Helv. Chim. Acta 54, 1423 (1971).

95. J. A. Hashmall and E. Helibronner, Angew. Chem. Internat. Edit. 9, 305 (1970).

96. H. A. Jahn and E. Teller, Proc. Roy. Soc. 161A, 220 (1937).

97. C. R. Brundle, M. B. Robin, and H. Basch, J. Chem. Phys. 53, 2196 (1970).

98. J. L. Ragle, I. A. Stenhouse, D. C. Frost, and C. A. McDowell, J. Chem. Phys. 53, 178 (1970).

99. J. W. Rabalais, L. Karlsson, L. O. Werme, T. Bergmark, and K. Siegbahn, J. Chem. Phys. 58, 3370 (1973).

100. R. N. Dixon, Mol. Phys. 20, 113 (1971); J. W. Rabalias, T. Bergmark, L. O. Werme, L. Karlsson, and K. Siegbahn, Physica Scripta. 3, 13 (1971).

101. C. R. Brundle and D. W. Turner, Proc. Roy. Soc. Ser. A 307, 27 (1968).

102. D. C. Frost, A. Katrib, C.A. McDowell, and R. A. N. Mclean, Int. J. Mass. Spectrom. Ion Phys. 7, 485 (1971).

103. D. W. Turner and D. P. May, J. Chem. Phys. 45, 471 (1966).

104. F. Duschinsky, Acta Physicochim. URSS 7, 551 (1937).

105. F. Ansbacher, Z. Naturforsch, 14a, 889 (1959).

106. E. Heilbronner, K. A. Muszkat, and J. Schaublin, Helv. Chim. Acta 54, 58 (1971).

107. R. S. Berry, M. Tamres, C. J. Ballhausen and H. Johanson, Acta Chem. Scand. 22, 231 (1968).

108. R. Botter and H. M. Rosenstock, J. Res. Nat. Bur. Stand. 73A, 313 (1969).

109. E. B.Wilson, J. C.Decius, and P. C. Cross, Molecular Vibrations. McGraw Hill, N.Y., 1955.

110. M. Tinkham, Group Theory and Quantum Mechanics. McGraw Hill, N.Y., 1964.

111. H. C. Urey and C. A. Bradley, Phys. Rev. 38, 1969 (1931).

112. T. Shimanouchi, J. Chem. Phys. 17, 245 (1949).

113. S. Mizushima and T. Shimanouchi, Infrared Absorption and The Raman Effect, Kyoritsu, Tokyo, 1958.

114. T. Shimanouchi, in Physical Chemistry (D. Henderson, ed.), Vol. IV, Chapter 6. Academic Press, N.Y., 1970.

115. W. Sawodny, A. Fadini, and K. Ballein, Spectrochim. Acta 21A, 995 (1965).

116. J. Herranz and F. Castano, Spectrochim. Acta 22A, 1965 (1966).

117. J. Overend and J. R. Scherer, J. Chem. Phys. 32, 1289 (1960).

118. J. R. Scherer and J. Overend, J. Chem. Phys. 32, 1720 (1960).

119. J. H. Schachtschneider and R. G. Snyder, Spectrochim. Acta 19A, 117 (1963).

120. F. T. Chau, M. Sc. Thesis, The Chinese University of Hong Kong, 1972.

121. Y. Itikawa, J. Electron Spectrosc. 2, 125 (1973).

122. J. Berkowitz and R. Spohr, J. Electron Spectrosc. 2, 143 (1973).

123. T. H. Lee and J. W. Rabalais, J. Chem. Phys. 61, 2747 (1974).

124. D. P. Craig and G.J. Small, J. Chem. Phys. 50, 3827 (1969).

125. A. Katrib, Ph.D. Thesis, The University of British Columbia, 1972.

126. D. A. Vroom, Ph.D. Thesis, The University of British Columbia, 1966.

127. D. W. Turner, Proc. Roy. Soc. London, A 307, 15 (1968).

128. J. A. R. Samson, Rev. Sci. Inst. 40, 1174 (1969).

129. M. M. Mann, A. Hustrulid, and J. T. Tate, Phys. Rev. 58, 340 (1940).

130. W. C. Price and T. M. Sugden, Trans Faraday Soc. 44, 168 (1948).

131. H. Neuert and H. Clasen, Z. Naturforsch, 7a, 410 (1952).

132. M. Cottin, J. Chim. Phys. 56, 1024 (1960).

133. A. Skerbele and E. N. Lassettre, J. Chem. Phys. 42, 395 (1965).

134. H. Sjogren, Ark. Fys. 33, 597 (1967).

135. P. H. Metzger and G. R. Cook, J. Chem. Phys. 41, 642 (1964).

136. K. Watanabe and A. S. Jursa, J. Chem. Phys. 41, 1650 (1964).

137. A. J. C. Nicholson, J. Chem. Phys. 43, 1111 (1965).

138. V. H. Dibeler, J. A. Walker, and H. M. Rosenstock, J. Res. Nat. Bur. Stand. 70a, 459 (1966).

139. V. H. Dibeler and S. K. Liston, J. Chem. Phys. 49, 482 (1968).

140. L. De Reilhac and N. Damany, Spectrochim. Acta 26A, 801 (1970).

141. R. B. Cairns, H. Harrison, and R. I. Schoen, J. Chem. Phys. 55, 4886 (1971).

142. A. D. Baker, C. R. Brundle, and D. W. Turner, Int. J. Mass Spectrom. Ion Phys. 1, 443 (1968).

143. J. Delwiche, P. Natalis, and J. E. Collin, Int. J. Mass Spectrom. Ion Phys. 5, 443 (1970).

144. J. Delwiche and P. Natalis, Chem. Phys. Lett. 5, 564 (1970).

145. A. D. Baker, C. R. Brundle, and D. W. Turner, Int. J. Mass Spectrom. Ion Phys. 2, 495 (1969).

146. S. Durmaz, G. H. King, and R. J. Suffolk, Chem. Phys. Lett. 13, 304 (1972).

147. A. W. Potts and W.C. Price, Proc. Roy. Soc. London A 326, 181 (1972).

148. H. Lew and I. Heiber, J. Chem. Phys. 58, 1246 (1973).

149. R. N. Dixon and G. Duxbury, M. Horani and J. Rostas, Mol. Phys. 22, 977 (1971).

150. Tables of Interatomic Distances and Configurations in Molecules and Ions and Supplementary Volumes (L. E. Sutton, ed.). The Chemical Society, Burlington House, London, 1958.

151. W. S. Benedict, N. Gailar, and E. K. Plyler, J. Chem. Phys. 24, 1139 (1956).

152. B. Brehm, Z. Naturforsch, 21a, 196 (1966).

153. H. C. Allen, Jr. and E. K. Plyler, J. Chem. Phys. 25, 1132 (1956).

154. Itaru Gamo, J. Mol. Spectrosc. 30, 216 (1969).

155. R. E. Miller and D. F. Eggers, Jr., J. Chem. Phys. 45, 3028 (1966).

156. R. E. Miller, G. E. Leroi, and D. F. Eggers, Jr., J. Chem. Phys. 46, 2292 (1967).

157. R. A. Hill and T. H. Edwards, J. Chem. Phys. 42, 1391 (1965).

158. E. D. Palik, J. Mol. Spectrosc. 3, 259 (1959).

159. K. Rossman and J. W. Straley, J. Chem. Phys. 24, 1276 (1956).

160. K. Nakamoto, Infrared Spectra of Inorganic and Coordination Compounds. John Wiley and Sons, N.Y., 1963.

161. V. H. Dibeler, J. A. Walker, and H. M. Rosenstock, J. Res. Nat. Bur. Stand. 70A, 459 (1966).

162. D. Kivelson and E. B. Wilson, Jr., J. Chem. Phys. 21, 1229 (1953).

163. J. H. Meal and S. R. Polo, J. Chem. Phys. 24, 1119 (1956).

164. J. H. Meal and S. R. Polo, J. Chem. Phys. 24, 1126 (1956).

165. S. J. Cyvin, Molecular Vibration and Mean Square Amplitude. Elsevier Publishing Company, Amsterdam, 1968.

166. R. T. Hall and J. M. Dowling, J. Chem. Phys. 47, 2454 (1967).

167. S. J. Cyvin, B. N. Cyvin, and G. Hagen, Z. Naturforsch, 23A, 1949 (1968).

168. J. W. C. Johns, Can. J. Phys. 41, 209 (1963).

169. J. W. C. Johns, Can. J. Phys. 49, 944 (1971).

170. S. Bell, J. Mol. Spectosc. 16, 205 (1965).

171. R. M. Badger, J. Chem. Phys. 2, 128 (1934); ibid 3, 710 (1935).

172. D. R. Herschach and V. W. Laurie, J. Chem. Phys. 35, 458 (1961).

173. T. Oka and Y. Morino, J. Mol. Spectrosc. 8, 9 (1962).

174. H. M. Rosenstock, Int. J. Mass Spectrom. Ion Phys. 7, 33 (1971).

175. J. H. Callomon and F. Creutzberg, Phil. Trans. Roy. Soc. London A277, 157 (1974) and private communication.

176. J. Pliva, J. Mol. Spectrosc. 27, 461 (1968).

177. E. K. Plyler, E. D. Tidwell, and A. G. Maki, J. Res. Nat. Bur. Stand. 68A, 79 (1964).

178. A. Anderson and T. S. Sun, Chem. Phys. Lett. 8, 537 (1971).

179. J. L. Griggs, K. N. Rao, L. H. Jones, and R. M. Potter, J. Mol. Spectrosc. 18, 212 (1965).

180. J. L. Griggs, K. N. Rao, L. H. Jones, and R. M. Potter, J. Mol. Spectrosc. 25, 24 (1968).

181. R. J. Boyd, Can. J. Chem. 51, 1151 (1973) and private communication.

182. W. C. Richardson and E. B. Wilson, Jr., J. Chem. Phys. 18, 644 (1950).

183. L. H. Jones, Coord. Chem. Rev. 1, 351 (1966).

184. C. A. Coulson and Z. Luz, Trans. Faraday Soc. 64, 2884 (1968).

185. N. C. Craig and J. Overend, J. Chem. Phys. 51, 1127 (1969).

186. J. R. Scherer and J. Overend, J. Chem. Phys. 33, 1681 (1960), and references therein cited.

187. J. M. Dowling, P. G. Puranik, and A. G. Meister, J. Chem. Phys. 26, 233 (1957).

188. R. A. R. Pearce and I. W. Levin, J. Chem. Phys. 59, 2698 (1973).

189. S. Jeyapandian and G. A. Savari Raj, J. Mol. Struct. 8, 97, 325 (1971); ibid 14, 17 (1972).

190. K. Tanabe and S. Saiki, Bull. Chem. Soc. Japan 47, 2545 (1974).

191. E. J. M. Van Schaick, F. C. Mijlhoff, G. Renes, and H. J. Geise, J. Mol. Struct. 21, 17 (1974).

192. I. L. Karl and J. Karl, J. Chem. Phys. 18, 963 (1950).

193. M. I. Davis and H. P. Hanson, J. Phys. Chem. 69, 4091 (1965).

194. R. L. Livingston, C. N. Ramachandra Rao, L. H. Kaplan, and L. Rocks, J. Amer. Chem. Soc. 80, 5368 (1958).

195. M. I. Davis, H. A. Kappler, and D. J. Cowan, J. Chem. Phys. 68, 2005 (1964).

196. J. S. Ziomek, A. G. Meister, F.F. Cleveland, and C. E. Decker, J. Chem. Phys. 21, 90 (1953).

197. J. M. Freeman and T. Henshall, Can. J. Chem. 47, 935 (1969).

198. D. E. Mann, T. Shimanouchi, J. H. Meal, and L. Fano, J. Chem. Phys. 27, 43 (1957).

199. L. S. Bartell and K. Kuchitsu, J. Chem. Phys. 37, 691 (1962).

200. J. H. Schachtschneider and R. G. Snyder, Spectrochim. Acta 19, 117 (1963).

201. S. Enomoto and S. Echinohe, Nippon Kagaku Zasshi 79, 1343 (1958).

202. H. J. Bernstein and D. A. Ramsay, J. Chem. Phys. 17, 556 (1949).

203. J. Charrette, dissertation, University of Louvain, 1954.

204. M. DeCroes, M. Perlinghi, and R. Van Riete, Bull. Classe Sci. Acad. Roy. Belg. 42, 379 (1956).

205. J. C. Evans and H. J. Bernstein, Can. J. Chem. 33, 1171 (1955).

206. R. H. Krupp, E. A. Piotrowski, F. F. Cleveland, and S. I. Miller, Develop. Appl. Spectrosc. 2, 52 (1963).

207. S. I. Miller, A. W. Weber, and F. F. Cleveland, J. Chem. Phys. 23, 44 (1955).

208. K. Wittel and H. Bock, Chem. Ber. 107, 317 (1974) and private communication.

209. K. Wittel, H. Bock and R. Manne, Tetrahedron 30, 651 (1974).

210. T. Shimanouchi, J. Chem. Phys. 26, 594 (1957).

211. N. C. Craig, G. Y. Lo, C. D. Needham, and J. Overend, J. Amer. Chem. Soc. 86, 3232 (1964).

212. C. A. Coulson, Proc. Roy. Soc. A 169, 413 (1939).

213. Handbook of Chemistry and Physics, 52nd ed. The Chemical Rubber Co., Cleveland, 1971-72.

214. A. L. McClellan, Tables of Experimental Dipole Moments. W. H. Freeman and Company, San Francisco, 1963.

215. R. F. Lake and H. Thompson, Proc. Roy. Soc. Lond. A 315, 323 (1970).

216. Y. Morino, K. Kuchitsu, and T. Shimanouchi, J. Chem. Phys. 20, 726 (1952).

217. D. E. Mann, L. Fano, J. H. Meal, and T. Shimanouchi, J. Chem. Phys. 27, 51 (1957).

218. R. N. Dixon, J. N. Murrell, and B. Narayan, Mol. Phys. 20, 611 (1971).

219. S. Katsumata and K. Kimura, Bull. Chem. Soc. Japan 46, 1342 (1973).

220. A. G. Meister, S. E. Rosser, and F. F. Cleveland, J. Chem. Phys. 18, 346 (1950).

221. R. J. Boyd and M. A. Whitehead, J. Chem. Soc. Dalton Trans 73, (1972).

222. H. H. Claasen, J. Chem. Phys. 22, 50 (1954).

223. P. J. Bassett and D. R. Lloyd, J. Chem. Soc. Dalton Trans. 278 (1972).

224. K. Kimura, S. Katsumata, Y.Achiba, H. Matsumoto, and S. Nagakura, Bull. Chem. Soc. Japan 46, 373 (1973)

225. J. Doucet, P. Sauvageau, and C. Sandorfy, J. Chem. Phys. 58, 3708 (1973).

226. S. Mizushima, Structure of Molecules and Internal Rotation. Academic Press, N.Y., 1954.

227. N. Sheppard, Advan. Spectry. 1, 288 (1959).

228. K. Tanabe, Spectrochim. Acta 28A, 407 (1972).

229. J. Ainthworth and J. Karle, J. Chem. Phys. 20, 425 (1952).

230. J. Y. Beach and A. Turkevich, J. Amer. Chem. Soc. 61, 303 (1939).

231. E. B. Wilson, Jr., Proc. Nat. Acad. Sci. Wash. 43, 816 (1957).

232. E. B. Wilson, Jr. and D. R. Lide, Determination of Organic Structures by Physical Methods, Vol. I, Academic Press, N.Y., 1955.

233. F. Ehrhardt, Physik. Z. 33, 605 (1932).

234. R. A. Boschi and D. R. Salahub, Mol. Phys. 24, 289 (1972).

235. J. L. Ragle, I. A. Stenhouse, D. C. Frost and C. A. McDowell, J. Chem. Phys. 53, 178 (1970).

236. T. Shimanouchi, Table of Molecular Vibrational Frequencies, Nat. Bur. Stand. Part 1, NSRDS-NBS6, 1967.

237. A. D. Baker, D. Betteridge, N. R. Kemp, and R. E. Kirby, Int. J. Mass Spectrom. Ion Phys. 4, 92 (1970).

238. J. D. Cox and G. Pilcher, Thermochemistry and Organic and Organometallic Compounds. Academic Press, London, 1970.

239. T. Wu, J. Chem. Phys. 7, 965 (1939).

240. G. Herzberg, Spectra of Diatomic Molecules ,D. Van Nostrand Co., N.Y., 1950.

241. T. Wentink, Jr., J. Chem. Phys. 30, 105 (1959).

242. J. L. Duncan, J. Mol. Spectrosc. 18, 62 (1965).

243. T. Shimanouchi, I. Nakagawa, J. Hiraishi, and M. Ishii, J. Mol. Spectrosc. 19, 78 (1966).

244. P. Labonville, J. R. Ferraro, M. C. Wall, S.M.C., and L. J. Basile, Coord. Chem. Rev. 7, 257 (1972).

245. A. B. Cornford, Ph.D. Thesis, The University of British Columbia, 1971.

246. D. C.Frost, S. T. Lee, and C. A. McDowell, J. Chem. Phys. 59, 5484 (1973).

247. H. J. Haink, E. Heilbronner, V. Hornung, and Else Kloster-Jensen, Helv. Chim. Acta 53, 1073 (1970).

248. R. J. Boyd and M. A. Whitehead, J. Chem. Soc. A 3579 (1971).

249. R. J. Boyd, Ph.D. Thesis. McGill University, 1970.

250. G. R. Hunt and M. K. Wilson, J. Chem. Phys. 34, 130 (1961).

251. H. P. Bucker and J. R. Nielsen, J. Mol. Spectrosc. 11, 47 (1963).

252. R. E. Kagarise, J. Chem. Phys. 26, 380 (1957).

253. R. E. Kagarise and L. W. Daasch, J. Chem. Phys. 23, 130 (1955).

254. K. R. Crook, P. J. D. Park, and E. Wyn-Jones, J. Chem. Soc. A 130 (1969).

255. M. Iwasaki, Bull. Chem. Soc. Japan 31, 1071 (1958).

256. M. Iwasaki, Bull. Chem. Soc. Japan 32, 205 (1959).

257. J. Doucet, P. Sauvageau, and C.Sandorfy, J. Chem. Phys. 62, 355 (1975).

258. D. Chadwick, D. C. Frost, A. Katrib, C. A. McDowell, and R.A. N. McLean, Can. J. Chem. 50, 2642 (1972).

259. N. Jonathan, K. Ross, and V. Tomlinson, Int. J. Mass Spectrom. Ion Phys. 4, 51 (1970).

260. H. Bock and G. Wagner, Angew. Chem. Internat. Edit. 11, 150 (1972).

261. H. Bock and K. Wittel, J. C. S. Chem. Comm. 602 (1972).

262. A. Katrib, T. P. Debies, R. J. Colton, T. H. Lee, and J. W. Rabalais, Chem. Phys. Lett. 22, 196 (1973).

263. G. C. Levy and G. L. Nelson, Carbon-13 Nuclear Magnetic Resonance for Organic Chemists. Wiley Interscience, N.Y., 1972.

264. P. Kollman, J. Amer. Chem. Soc. 96, 4363 (1974).

265. G. B. Savitsky and K. Namikawa, J. Phys. Chem. 67, 2754 (1963).

266. I. P. Biryukov, M. G. Voronkov, and I. A. Safin, Tables of Nuclear Quadrupole Resonance Frequencies, translated by J.Schmorak. Israel Program for Scientific Translation Ltd., 1969.

267. E. A. C. Lucken, Nuclear Quadrupole Coupling Constants. Academic Press, London, 1969.

268. H. Kato, K. Hirao, H. Konishi and T. Yonezawa, Bull. Chem. Soc. Japan 44, 2062 (1971).

269. M. J. S. Dewar, J. Chem. Soc. 463 (1949).

270. A. Streitwieser, Jr., Molecular Orbital Theory. Wiley, London, 1961.

271. G. R. Branton, D. C. Frost, T. Makita, C. A. McDowell, and I. A. Stenhouse, J. Chem. Phys. 52, 802 (1972).

272. H. Bock and H. Stafast, Chem. Ber. 105, 1158 (1972).

273. S. Chandra and S. Chandra, Tetrahedron 22, 3403 (1966).

274. H. Bock, G. Wagner, K. Wittle, J. Sauer, and D. Seebach, Chem. Ber. 107, 1869 (1974).

275. D. G. Streets, Chem. Phys. Lett. 28, 555 (1974).

276. K. Kuchitsu, J. Chem. Phys. 44, 906 (1966).

277. M. Fukuyama, Reports Govt. Chem. Ind. Res. Inst. Tokyo, 61, 129 (1966).

278. R. Ditchfield and P. D. Ellis, Chem. Phys. Lett. 17, 342 (1972).

279. E. L. Eliel, N. L. Allinger, S. J.Angyal, and G.A. Morrison, Conformational Analysis, 2nd ed. Wiley, N.Y., 1966.

280. M. Hanack, Conformational Theory, translated by H. C. Newmann. Academic Press, N.Y., 1965.

281. O. Bastiansen and O. Hassel, Tidsskr. Kjemi, Bergresen Met. 6, 96 (1946).

282. O. D. Ulyanova and Yu. A. Pentin, Zh. Fiz. Khim. 41, 2675 (1967).

283. R. Botter, F. Menes, Y. Gounelle, J. M. Pechine, and D. Solgadi, Int. J. Mass Spectrom. Ion Phys. 12, 188 (1973) and private communication.

284. D. P. Chong, private communication.

285. R. G. Dromey, J. D. Morrison, and J. B. Peel, Chem. Phys. Lett. 23, 30 (1973).

286. J. D. Morrison, J. Chem. Phys. 39, 200 (1963).

287. R. G. Dromey and J. D. Morrison, Int. J. Mass Spectrom. Ion Phys. 4, 475 (1970).

288. J. Berkowitz, P.-M. Guyon, Int. J. Mass Spectrom. Ion Phys. 6, 302 (1971).

289. D. P. Chong, F. G. Herring, and D. McWilliams, to be published.

290. L. S. Cederbaum and W. Domcke, J. Chem. Phys. 60, 2878 (1974).

```
C
C
C
C                                   APPENDIX I
C
C
C     PROGRAM TO CALCULATE FRANCK-CONDON FACTORS OF COMBINATION BANDS
C     OR OVERTONES          BY F.T. CHAU    7 MAY 1974
C     THE METHOD WAS DEVELOPED BY H.M. ROSENSTOCK
C     T.E. SHARP AND H.M.ROSENSTOCK     J.CHEM.PHYS. 41,P3453(1964)
C     ERRATUM: R.BOTTER,V.H.DIBELER,J.A.WALKER,AND H.M.ROSENSTOCK
C              J.CHEM.PHYS. 44,P1271(1966)
C
C     ND              DIMENSION OF THE LS, FREQUENCY MATRICES  (=3N-6)
C     RLS(I,J)        LS MATRIX IN GROUND STATE (AMU**(-1/2)) ;
C                     INPUT IN ROW
C     RLP(I,J)        LS MATRIX IN UPPER STATE OR EXCITED STATE  (=3N-6)
C                     INPUT IN ROW  MAX=10
C     FF(I)           FREQUENCY IN GROUND STATE (IN CM**-1)  MAX=10 (=3N-6)
C     FP(I)           FREQUENCY IN EXCITED STATE (IN CM**-1) MAX=10 (=3N-6)
C     RS(I)           CHANGE IN STRUCTURAL PARAMETERS IN INTERNAL SYMMETRY
C                     COORDINATES  (IN ANGSTROM)  (=S'-S)
C     TAU(I,J)        TAU MATRIX IN LOWER STATE    AMU**-1 A**-2
C     TAUP(I,J)       TAU MATRIX IN UPPER STATE    SAME UNIT
C     RJ(I,J)         J MATRIX  NO UNIT
C     RK(I,J)         K MATRIX    AMU**(1/2)*A
C     RJTJ(I,J)       (JT)(TAUP)(J)+TAU
C     RJTJI(I,J)      INVERSE OF MATRIX RJTJ(I,J)
C     RE(I,J)         IDENTITY MATRIX   3N-6
C     A(I,J)          A MATRIX   3N-6 X 3N-6
C     B(I)            B MATRIX   3N-6
C     C(I,J)          C MATRIX   3N-6 X 3N-6
C     D(I)            D MATRIX   3N-6
C     E(I,J)          E MATRIX   3N-6 X 3N-6
C     IOVER(I)        ARRAY WITH ELEMENTS (ORDER EQUAL TO ND)
C                     0    NO CALN. WILL BE DONE ON OVERTONE
C                     1    CALN. WILL BE DONE ON OVERTONE
C     MOVER(I)        MAXIMIUM NO. OF OVERTONE CALD. FOR THE CORRESPONDING
C                     IOVER(I) IF IT IS NONZERO. INPUT NUMBER OF V
C     ICOMB(I)        ARRAY WITH ELEMENTS (ORDER EQUAL TO ND)
C                     0    NO CALN. WILL BE DONE ON COMBINATION BAND
C                     1    CALN. WILL BE DONE
C     TPC(I,J)        MATRIX WITH ELEMENTS AS TRANSITION PROBABILITY OF
C                     COMBINATION BAND OF I AND J TH MODE
C     REMEMBER THE ORDERING OF OVERTONE IN SUCH WAY (1,1),(2,1),(3,1)...
C     ICOMB3(I)       ARRAY WITH NO. OF ELEMENTS = ND
C                     0    NO. CALN. WILL BE DONE ON EXCITATION OF THREE
C                          VIBRATIONAL MODES
C                     1    CALN. WILL BE DONE
C     SO(I)           ARRAY TO STORE ALL FCF'S FOR PLOT
C     FSO(I)          ARRAY TO STORE ALL FREQUENCIES FOR PLOT
C
      DIMENSION TITLE(20),RLS(10,10),RLP(10,10),FF(10),FP(10),L(15)
      DIMENSION RS(10),TAU(10,10),TAUP(10,10),RLPI(10,10),RI(225),M(15)
      DIMENSION RJ(10,10),RK(10),RW(10,10),RJTJ(10,10),RX(10,10)
      DIMENSION RJTJI(10,10),RE(10,10),A(10,10),RR(10,10),B(10)
      DIMENSION C(10,10),D(10),E(10,10),FI(20),TPC(4,4),TPT(2,1,1)
      DIMENSION IOVER(10),MOVER(10),ICOMB(10),NIN(10),TC3(2,1,1)
C
```

```
C
C
      DIMENSION ICOMB3(10),RZ(10),S1(300),FS1(300)
C     INPUT DATA
      IR=5
      IW=6
      READ(IR,10) TITLE
   10 FORMAT(20A4)
      WRITE(IW,20) TITLE
   20 FORMAT(1H1,///,10X,20A4)
      WRITE(IW,30) TITLE
   30 FORMAT(//,10X,20A4)
      READ(IR,40) ND
   40 FORMAT(I5)
      DO 60 I=1,ND
   60 READ(IR,50) (RLS(I,J),J=1,ND)
   50 FORMAT(10F8.4)
      DO 70 I=1,ND
   70 READ(IR,50) (RLP(I,J),J=1,ND)
      READ(IR,80) (FF(I),I=1,ND)
   80 FORMAT(10F8.2)
      READ(IR,80) (FP(I),I=1,ND)
      READ(IR,85) (IOVER(I),I=1,ND)
      READ(IR,85) (MOVER(I),I=1,ND)
      READ(IR,85) (ICOMB(I),I=1,ND)
      READ(IR,85) (ICOMB3(I),I=1,ND)
   85 FORMAT(10I5)
      WRITE(IW,90)(I,FF(I),I=1,ND)
   90 FORMAT(////,5X,'FUNDAMENTAL FREQUENCIES IN LOWER STATE (IN CM**-1)
     2'//,10(2X,I2,F8.2))
      WRITE(IW,100)(I,FP(I),I=1,ND)
  100 FORMAT(//,5X,'FUNDAMENTAL FREQUENCIES IN EXCITED STATE (IN CM**-1)
     2'//10(2X,I2,F8.2))
      READ(IR,110) (RS(I),I=1,ND)
  110 FORMAT(10F8.5)
      WRITE(IW,120) (RS(I),I=1,ND)
  120 FORMAT(///,5X,'CHANGE IN STRUCTURAL PARAMETERS (=SP-S)'//,5X,
     210F10.5)
      WRITE(IW,130)
  130 FORMAT(///,4X,'L MATRIX IN GROUND STATE'/)
      DO 140 I=1,ND
  140 WRITE(IW,162)(RLS(I,J),J=1,ND)
      WRITE(IW,150)
  150 FORMAT(///,4X,'L MATRIX IN EXCITED STATE'/)
      DO 160 I=1,ND
  160 WRITE(IW,162) (RLP(I,J),J=1,ND)
  162 FORMAT(2X,10F8.4)
C
C     EVALUATION OF TAU AND TAUP MATRICES
      DO 170 I=1,ND
      DO 170 J=1,ND
      TAU(I,J)=0.0
      TAUP(I,J)=0.0
  170 CONTINUE
      DO 180 I=1,ND
      TAU(I,I)=0.029681*FF(I)
      TAUP(I,I)=0.029681*FP(I)
  180 CONTINUE
      IK=1
      DO 190 J=1,ND
```

```
C
C
C
      DO 190 I=1,ND
      RI(IK)=RLP(I,J)
      IK=IK+1
  190 CONTINUE
      CALL MINV(RI,ND,DD,L,M)
      IK=1
      DO 200 J=1,ND
      DO 200 I=1,ND
      RLPI(I,J)=RI(IK)
      IK=IK+1
  200 CONTINUE
C
C     EVALUATION OF J AND K MATRICES
      DO 220 I=1,ND
      DO 220 J=1,ND
      RJ(I,J)=0.0
      DO 210 K=1,ND
      RJ(I,J)=RJ(I,J)+RLPI(I,K)*RLS(K,J)
  210 CONTINUE
  220 CONTINUE
      DO 240 I=1,ND
      RK(I)=0.0
      DO 230 K=1,ND
      RK(I)=RK(I)+RLPI(I,K)*RS(K)
  230 CONTINUE
  240 CONTINUE
C
C     EVALUATION OF A,B,C,D AND E MATRICES
      DO 270 I=1,ND
      DO 270 J=1,ND
      RW(I,J)=0.0
      DO 260 NN=1,ND
      DO 250 K=1,ND
      RW(I,J)=RW(I,J)+RJ(NN,I)*TAUP(NN,K)*RJ(K,J)
  250 CONTINUE
  260 CONTINUE
  270 CONTINUE
C
      DO 280 I=1,ND
      DO 280 J=1,ND
      RJTJ(I,J)=RW(I,J)+TAU(I,J)
  280 CONTINUE
      IK=1
      DO 290 J=1,ND
      DO 290 I=1,ND
      RI(IK)=RJTJ(I,J)
      IK=IK+1
  290 CONTINUE
      CALL MINV(RI,ND,DD,L,M)
      IK=1
      DO 300 J=1,ND
      DO 300 I=1,ND
      RJTJI(I,J)=RI(IK)
      IK=IK+1
  300 CONTINUE
C
C     CALCULATION OF TRANSITION PROBABILITY OF OVERTONES
```

```
C
C
C
      NSO=1
      CALL ABCDE(ND,RJ,TAUP,TAU,RJTJI,RK,A,B,C,D,E)
      DO 730 I=1,ND
      IF(IOVER(I).EQ.0) GO TO 730
      MM=MOVER(I)+1
      I1=I-1
      CALL INTSIM(C,D,MM,I,FI)
      WRITE(IW,720) I,FP(I),MOVER(I)
  720 FORMAT(////,5X,'FREQP(',I2,') =',F10.2/5X,'NO. OF OVERTONES(FROM 0
     2 TO MM =',I3//,5X,'V',5X,'TRANSITION PROBABILITES FOR OVERTONES'/)
      DO 721 J=1,MM
      J1=J-1
  721 WRITE(IW,723) J1,FI(J)
  723 FORMAT(4X,I2,14X,F10.4)
      DO 722 J=1,MM
      SO(NSO)=FI(J)
      FSO(NSO)=FP(I)*FLOAT(J)
  722 NSO=NSO+1
  730 CONTINUE
C
C     CALCULATION OF TRANSITION PROBABILITIES OF COMBINATION BANDS
      ND1=ND-1
      DO 760 I=1,ND1
      IF(ICOMB(I).EQ.0) GO TO 760
      J=I+1
  740 CONTINUE
      IF(ICOMB(J).EQ.0) GO TO 750
      CALL COMBIN (C,D,I,J,TPC)
      WRITE(IW,1010) I,FP(I),J,FP(J)
 1010 FORMAT(////,5X,'TRANSITION PROBABILITY OF COMBINATION BANDS WITH'/
     25X,'EXCITATION OF TWO VIB. MODES'/5X,'FREQP(',I2,') =',F10.4,5X,
     3'FREQP(',I2,') =',F10.4//5X,'I',2X,'J',3X,'TRANSITION PROBABILITIE
     4S OF COMB. BANDS'/)
      DO 1015 N=1,4
 1015 WRITE(IW,1020) N,TPC(N,1)
 1020 FORMAT(4X,I2,2X,'1',4X,F10.4)
      DO 1030 N=2,3
 1030 WRITE(IW,1035) N,TPC(N,2)
 1035 FORMAT(4X,I2,2X,'2',4X,F10.4)
      DO 745 LL=1,4
      SO(NSO)=TPC(LL,1)
      FSO(NSO)=FP(J)+FP(I)*FLOAT(LL)
  745 NSO=NSO+1
      DO 747 LL=2,3
      SO(NSO)=TPC(LL,2)
      FSO(NSO)=2.*FP(J)+FP(I)*FLOAT(LL)
  747 NSO=NSO+1
  750 CONTINUE
      IF(J.EQ.ND) GO TO 760
      J=J+1
      GO TO 740
  760 CONTINUE
C
C     CALCULATION OF TRANSITION PROBABILITIES OF THREE VIB. MODES
C     EXCITED AT THE SAME TIME
      ND2=ND-2
      DO 900 I=1,ND2
```

```
C
C
C
      IF(ICOMB3(I).EQ.0) GO TO 900
      J=I+1
  910 CONTINUE
      IF(ICOMB3(J).EQ.0) GO TO 920
      K=J+1
  930 CONTINUE
      IF(ICOMB3(K).EQ.0) GO TO 940
      CALL COMBTH(C,D,I,J,K,TPT)
      DO 934 LL=1,2
      SO(NSO)=TPT(LL,1,1)
      FSO(NSO)=FP(J)+FP(K)+FP(I)*FLOAT(LL)
  934 NSO=NSO+1
      WRITE(IW,2010) I,FP(I),J,FP(J),K,FP(K)
 2010 FORMAT(////,5X,'TRANSITION PROBABILITIES OF COMBINATION WITH'/5X,
     2'EXCITATION OF THREE VIB. MODES'/5X,'FREQP(',I2,') =',F10.2,5X,
     3'FREQP(',I2,') =',F10.2,5X,'FREQP(',I2,') =',F10.2//5X,'I',2X,'J',
     42X,'K',3X,'TRANSITION PROBABILITIES'/)
      WRITE(IW,2020) TPT(1,1,1),TPT(2,1,1)
 2020 FORMAT(5X,'1',2X,'1',2X,'1',10X,F10.4/5X,'2',2X,'1',2X,'1',10X,
     2F10.4//)
  940 CONTINUE
      IF(K.EQ.ND) GO TO 920
      K=K+1
      GO TO 930
  920 CONTINUE
      IF(J.EQ.ND1) GO TO 900
      J=J+1
      GO TO 910
  900 CONTINUE
C     NORMALIZATION OF CALCULATED FCF
      NSO=NSO-1
      BIG=SO(1)
      GR=FSO(1)
      DO 1068 JJ=1,NSO
      IF(SO(JJ).LE.BIG) GO TO 1066
      BIG=SO(JJ)
 1066 CONTINUE
 1068 CONTINUE
      DO 1073 JJ=1,NSO
      IF(FSO(JJ).LE.GR) GO TO 1072
      GR=FSO(JJ)
 1072 CONTINUE
 1073 CONTINUE
      DO 1074 JJ=1,NSO
      SO(JJ)=SO(JJ)/BIG
 1074 CONTINUE
      XMAX=GR+1000.
      CALL ALSCAL(-1000.,XMAX,0.0,1.2)
      CALL ALGRAF(FSO,SO,NSO,-3)
      CALL PLOTND
      STOP
      END
C
C
C
C     SUBROUTINE TO EVALUATE A,B,C,D AND E MATRICES
C     ND            DIMENSION OF MATRICES (3N-6)
```

```
C
C
C
C      RJ              J MATRIX
C      TAUP            TAU' MATRIX FOR EXCITED STATE
C      TAU             TAU  MATRIX FOR GROUND STATE
C      RJTJI           INVERSION MATRIX OF JTJ
C      RK              D MATRIX
C      A,B,C,D,E       OUTPUTED MATRICES
C
       SUBROUTINE ABCDE(ND,RJ,TAUP,TAU,RJTJI,RK,A,B,C,D,E)
       DIMENSION RW(10,10),RJ(10,10),TAUP(10,10),RJTJ(10,10),TAU(10,10)
       DIMENSION RE(10,10),RJTJI(10,10),A(10,10),RR(10,10),RZ(10)
       DIMENSION RX(10,10),RK(10),B(10),NIN(10),C(10,10),D(10),E(10,10)
C      EVALUATION OF A MATRIX ND*ND
       IW=6
       DO 310 I=1,ND
       DO 310 J=1,ND
       RE(I,J)=0.0
  310 CONTINUE
       DO 320 I=1,ND
       RE(I,I)=1.0
  320 CONTINUE
       DO 370 I=1,ND
       DO 370 J=1,ND
       RW(I,J)=0.0
       DO 360 L=1,ND
       DO 350 N=1,ND
       DO 340 M=1,ND
       DO 330 K=1,ND
       RW(I,J)=RW(I,J)+SQRT(TAUP(I,L))*RJ(L,N)*RJTJI(N,M)*RJ(K,M)*SQRT(TA
      2UP(K,J))
  330 CONTINUE
  340 CONTINUE
  350 CONTINUE
  360 CONTINUE
  370 CONTINUE
       DO 380 I=1,ND
       DO 380 J=1,ND
       A(I,J)=2.0*RW(I,J)-RE(I,J)
  380 CONTINUE
       DO 382 I=1,10
  382 NIN(I)=I
       WRITE(IW,390) (NIN(I),I=1,ND)
  390 FORMAT(///,5X,'A MATRIX',5X,'A MATRIX'//7X,10(I2,9X)/)
       DO 400 I=1,ND
  400 WRITE(IW,410) NIN(I),(A(I,J),J=1,ND)
  410 FORMAT(I3,10F11.6)
C
C      EVALUATION OF B MATRIX ND*1
       DO 450 I=1,ND
       DO 450 J=1,ND
       RW(I,J)=0.0
       DO 440 N=1,ND
       DO 430 M=1,ND
       DO 420 K=1,ND
       RW(I,J)=RW(I,J)+RJ(I,N)*RJTJI(N,M)*RJ(K,M)*TAUP(K,J)
  420 CONTINUE
  430 CONTINUE
  440 CONTINUE
```

```
C
C
C
  450 CONTINUE
      DO 460 I=1,ND
      DO 460 J=1,ND
      RR(I,J)=RW(I,J)-RE(I,J)
  460 CONTINUE
      DO 490 I=1,ND
      RZ(I)=0.0
      DO 480 M=1,ND
      DO 470 K=1,ND
      RZ(I)=RZ(I)+SQRT(TAUP(I,M))*RR(M,K)*RK(K)
  470 CONTINUE
  480 CONTINUE
  490 CONTINUE
      DO 500 I=1,ND
      B(I)=-2.0*RZ(I)
  500 CONTINUE
C
C     EVALUATION OF C MATRIX  ND*ND
      DO 530 I=1,ND
      DO 530 J=1,ND
      RW(I,J)=0.0
      DO 520 M=1,ND
      DO 510 K=1,ND
      RW(I,J)=RW(I,J)+SQRT(TAU(I,M))*RJTJI(M,K)*SQRT(TAU(K,J))
  510 CONTINUE
  520 CONTINUE
  530 CONTINUE
      DO 540 I=1,ND
      DO 540 J=1,ND
      C(I,J)=2.0*RW(I,J)-RE(I,J)
  540 CONTINUE
      WRITE(IW,550) (NIN(I),I=1,ND)
  550 FORMAT(///,5X,'B MATRIX',5X,'B MATRIX'/4X,10(I2,9X))
      WRITE(IW,552) (B(I),I=1,ND)
  552 FORMAT(10F11.6)
      WRITE(IW,560) (NIN(I),I=1,ND)
  560 FORMAT(///,5X,'C MATRIX',5X,'C MATRIX'/7X,10(I2,9X))
      DO 570 I=1,ND
  570 WRITE(IW,410) NIN(I),(C(I,J),J=1,ND)
C
C     EVALUATION OF D MATRIX   ND*1
      DO 620 I=1,ND
      RZ(I)=0.0
      DO 610 L=1,ND
      DO 600 N=1,ND
      DO 590 M=1,ND
      DO 580 K=1,ND
      RZ(I)=RZ(I)+SQRT(TAU(I,L))*RJTJI(L,N)*RJ(M,N)*TAUP(M,K)*RK(K)
  580 CONTINUE
  590 CONTINUE
  600 CONTINUE
  610 CONTINUE
  620 CONTINUE
      DO 630 I=1,ND
      D(I)=-2.0*RZ(I)
  630 CONTINUE
      WRITE(IW,640) (NIN(I),I=1,ND)
```

```
C
C
C
  640 FORMAT(///,5X,'D MATRIX',5X,'D MATRIX'/4X,10(I2,9X))
      WRITE(IW,552) (D(I),I=1,ND)
C
C     EVALUATION OF E MATRIX ND*ND
      DO 680 I=1,ND
      DO 680 J=1,ND
      RW(I,J)=0.0
      DO 670 N=1,ND
      DO 660 M=1,ND
      DO 650 K=1,ND
      RW(I,J)=RW(I,J)+SQRT(TAU(I,N))*RJTJI(N,M)*RJ(K,M)*SQRT(TAUP(K,J))
  650 CONTINUE
  660 CONTINUE
  670 CONTINUE
  680 CONTINUE
      DO 690 I=1,ND
      DO 690 J=1,ND
  690 E(I,J)=4.0*RW(I,J)
      WRITE(IW,700) (NIN(I),I=1,ND)
  700 FORMAT(///,5X,'E MATRIX',5X,'E MATRIX'/7X,10(I2,9X))
      DO 710 I=1,ND
  710 WRITE(IW,410) NIN(I),(E(I,J),J=1,ND)
      RETURN
      END
C
C
C
      FUNCTION FACT(I)
      IF(I.GT.0) GO TO 5
      FACT=1.
      GO TO 20
    5 IFACT=1
      DO 10 N=1,I
      IFACT=IFACT*N
   10 CONTINUE
      FACT=FLOAT(IFACT)
   20 CONTINUE
      RETURN
      END
C
C
C
C     SUBROUTINE TO CALCULATE TRANSITION PROBABILITY OF OVERTONES
C     METHOD USED BASED ON T.E.SHARP AND H.M.ROSENSTOCK
C     J.CHEM.PHYS. 41,P3454(1964)  SEE ALSO CORRECTION
C     C(I,J) AND D(I) ARE INPUTED MATRICES
      SUBROUTINE INTSIN(C,D,MZ,N,FI)
C     M=MAXIMUM NO. OF OVERTONE CAL'D.
C     N=N TH VIBRATIONAL MODE
C     FI(I) = TRANSITION PROBABILITY OUTPUTED
      DIMENSION C(10,10),D(10),FI(20)
      FI(1)=1.
      FI(2)=(D(N)**2)/2.
      FI(3)=(2.*C(N,N)+D(N)**2)**2/8.
      FI(4)=(6.*D(N)*C(N,N)+D(N)**3)**2/48.
      FI(5)=(12.*(C(N,N)**2)+12.*(D(N)**2)*C(N,N)+D(N)**4)**2/384.
C
```

```
C
C
      FI(6)=(60.*D(N)*(C(N,N)**2)+20.*(D(N)**3)*C(N,N)+D(N)**5)**2/3840.
      FI(7)=(120.*(C(N,N)**3)+120.*(D(N)**2)*(C(N,N)**2)+
     230.*(D(N)**4)*C(N,N)+D(N)**6)**2/46080.
      IF(MZ.LE.7) GO TO 20
      IK=8
    5 FFI=0.
      IK1=IK-1
      MX=IK1/2+1
      FI(IK)=0.
      DO 10 I=1,MX
      IQ=I-1
      MQ=IK1-2*IQ
      FFI=FFI+(C(N,N)**IQ)*(D(N)**MQ)/(FACT(IQ)*FACT(MQ))
   10 CONTINUE
      FI(IK)=FFI*FFI*FACT(IK1)/(2.**IK1)
      IF(IK.EQ.MZ) GO TO 20
      IK=IK+1
      GO TO 5
   20 CONTINUE
      RETURN
      END
C
C
C
C     SUBROUTINE TO CALCULATE THE TRANSITION PROBABILITIES OF
C     COMBINATION BANDS
      SUBROUTINE COMBIN(C,D,I,J,TPC)
C     C AND D MATRICES FROM MAIN PROGRAM
C     I AND J REFER TO ITH AND JTH MODE OF VIBRATIONS THAT GIVE
C     RISE TO OBSERVABLE COMBINATION BANDS
C     TPC(I,J)  MATRIX WITH ELEMENT AS TRANSITION PROBABILITY OF
C     COMBINATION BANDS
      DIMENSION C(10,10),D(10),TPC(4,4)
      TPC(1,1)=(2.0*C(I,J)+D(I)*D(J))**2/4.0
      TPC(2,1)=(4.0*D(I)*C(I,J)+2.0*D(J)*C(I,I)+(D(I)**2)*D(J))**2/16.0
      TPC(3,1)=(12.*C(I,I)*C(I,J)+6.0*(D(I)**2)*C(I,J)+12.*D(I)*D(J)*C(I
     2,I)+(D(I)**3)*D(J))**2/96.0
      TPC(4,1)=(12.*D(J)*(C(I,I)**2)+48.*D(I)*C(I,I)*C(I,J)+12.*D(J)*(D(
     2I)**2)*C(I,I)+8.0*(D(I)**3)*C(I,J)+(D(I)**4)*D(J))**2/763.
      TPC(2,2)=(4.0*C(I,I)*C(J,J)+8.0*(C(I,J)**2)+2.0*(D(I)**2)*C(J,J)+2
     2.0*(D(J)**2)*C(I,I)+8.0*D(I)*D(J)*C(I,J)+(D(I)*D(J))**2)**2/64.
      TPC(3,2)=(24.0*D(J)*C(I,I)*C(I,J)+12.*D(I)*C(I,I)*C(I,J)+24.0*D(I)
     2*(C(I,J)**2)+6.0*D(I)*(D(J)**2)*C(I,I)+2.0*(D(I)**3)*C(J,J)+12.0*(
     3D(I)**2)*D(J)*C(I,J)+(D(I)**3)*(D(J)**2))**2/384.
      RETURN
      END
C     SUBROUTINE TO CALCULATED TRANSITION PROBABILITIES OF
C     EXCITATION OF THREE VIB. MODES
      SUBROUTINE COMBTH(C,D,I,J,K,TPT)
C     C AND D MATRICES INPUTED FROM MAIN PROGRAM
C     I,J AND K REFER TO I,TH, J TH AND K TH MODE OF VIB. THAT GIVE
C     RISE TO OBSERVABLE COMBINATION BANDS
C     TPT(I,J,K)  MATRIX GIVES THE TRANSITION PROBABILITIES OF
C     COMBINATION BANDS
      DIMENSION C(10,10),D(10),TPT(2,1,1)
      TPT(1,1,1)=(2.0*D(I)*C(J,K)+2.0*D(J)*C(I,K)+2.0*D(K)*C(I,J)+
     2D(I)*D(J)*D(K))**2/8.
      TPT(2,1,1)=(4.0*C(I,I)*C(J,K)+8.0*C(I,J)*C(I,K)+4.0*(D(I)**2)*
```

```
C
C
C
C
      2C(J,K)+4.0*D(I)*D(J)*C(I,K)+4.0*D(I)*D(K)*C(I,J)+(D(I)**2)*D(J)*
     3D(K))**2/32.0
       RETURN
       END
C          SUBROUTINE  MINV
C          PURPOSE
C            INVERT A MATRIX
C          USAGE
C            CALL MINV(A,N,D,L,M)
C          DESCRIPTION OF PARAMETERS
C            A - INPUT MATRIX, DESTROYED IN COMPUTATION AND REPLACED BY
C                RESULTANT INVERSE
C            N - ORDER OF MATRIX A
C            D - RESULTANT DETERMINANT
C            L - WORK VECTOR OF LENGTH N
C            M - WORK VECTOR OF LENGTH N
C
C          REMARKS
C          MATRIX A MUST BE A GENERAL MATRIX
C          SUBROUTINE AND FUNCTION SUBPROGRAMS REQUIRED
C            NONE
C          METHOD
C            THE STANDARD GAUSS-JORDAN METHOD IS USED. THE DETERMINANT
C            IS ALSO CALCULATED. A DETERMINANT OF ZERO INDICATES THAT
C            THE MATRIX IS SINGULAR
C
C     ..................................................................
C
      SUBROUTINE MINV(A,N,D,L,M)
      DIMENSION A(225),L(15),M(15)
      D=1.0
      NK=-N
      DO 80 K=1,N
      NK=NK+N
      L(K)=K
      M(K)=K
      KK=NK+K
      BIGA=A(KK)
      DO 20 J=K,N
      IZ=N*(J-1)
      DO 20 I=K,N
      IJ=IZ+I
      X = ABS(BIGA)-ABS(A(IJ))
10    IF(X) 15,20,20
15    BIGA=A(IJ)
      L(K)=I
      M(K)=J
20    CONTINUE
C
C     INTERCHANGE ROWS
C
      J=L(K)
      IF(J-K)35,35,25
25    KI=K-N
      DO 30 I=1,N
      KI=KI+N
      HOLD=-A(KI)
```

```
C
C
C
      JI=KI-K+J
      A(KI)=A(JI)
30    A(JI)=HOLD
C
C          INTERCHANGE COLUMNS
C
35    I=M(K)
      IF(I-K)45,45,38
38    JP=N*(I-1)
      DO 40 J=1,N
      JK=NK+J
      JI=JP+J
      HOLD=-A(JK)
      A(JK)=A(JI)
40    A(JI)=HOLD
C
C          DIVIDE COLUMN BY MINUS PIVOT (VALUE OF PIVOT ELEMENT IS
C          CONTAIND IN BIGA
C
45    IF(BIGA)48,46,48
46    D=0.0
      RETURN
48    DO 55 I=1,N
      IF(I-K)50,55,50
50    IK=NK+I
      A(IK)=A(IK)/(-BIGA)
55    CONTINUE
C
C          REDUCED MATRIX
C
      DO 65 I=1,N
      IK=NK+I
      HOLD=A(IK)
      IJ=I-N
      DO 65 J=1,N
      IJ=IJ+N
      IF(I-K)60,65,60
60    IF(J-K)62,65,62
62    KJ=IJ-I+K
      A(IJ)=HOLD*A(KJ)+A(IJ)
65    CONTINUE
C
C          DIVIDE ROW BY PIVOT
C
      KJ=K-N
      DO 75 J=1,N
      KJ=KJ+N
      IF(J-K)70,75,70
70    A(KJ)=A(KJ)/BIGA
75    CONTINUE
C
C          PRODUCT OF PIVOTS
C
      D=D*BIGA
C
C          REPLACE PIVOT BY RECIPROCAL
C
```

```
C
C
C
      A(KK)=1.0/BIGA
80    CONTINUE
C
C          FINAL ROW AND COLUMN INTERCHANGE
C
      K=N
100   K=(K-1)
      IF(K)150,150,105
105   I=L(K)
      IF(I-K)120,120,108
108   JQ=N*(K-1)
      JR=N*(I-1)
      DO 110 J=1,N
      JK=JQ+J
      HOLD=A(JK)
      JI=JR+J
      A(JK)=-A(JI)
110   A(JI)=HOLD
120   J=M(K)
      IF(J-K)100,100,125
125   KI=K-N
      DO 130 I=1,N
      KI=KI+N
      HOLD=A(KI)
      JI=KI-K+J
      A(KI)=-A(JI)
130   A(JI)=HOLD
      GO TO 100
150   RETURN
      END
```

```
$SIG
```

```
C
C
C                                   APPENDIX II
C
C
C     COMPUTER PROGRAM FOR CALCULATION OF D, DISPLACEMENT OF NORMAL
C     COORDINATE, DURING ELECTRONIC TRANSITION OR IONIZATION
C     REFINEMENT OF D BY USING JACABIAN METHOD.
C     F.T. CHAU  CHEM DEPT  UBC      6TH,JUNE,1974
C     THIS PROGRAM CAN HANDLE VIBRATIONAL PROGRESSION UP TO QUANTUM
C     NUMBER, V, 19
C     OFCF(I)        OBSERVED FCF
C     CFCF(I)        CALCULATED FCF
C     P(I)           WEIGHING MATRIX
C     DF(I)          ERROR MATRIX   OFCF(I) - CFCF(I)
C     AJ(I)          JACOBIAN MATRIX
C     ND             NO. OF PROGRESSION CALCULATED.  =V+1    MAX. 19
C     MAX            NO. OF LARGEST FCF    V(MAX)+1
C     PP             POWER FOR P(I) MATRIX
C                    < 1     FCF WITH LOW VALUE IS EMPHASISED
C                    = 0     ALL FCF'S GIVE SAME WEIGHT
C                    1 <     FCF WITH HIGH VALUE IS EMPHASISED
C     NSET           NO. OF SETS CALCULATED
C     NC             NO. OF CYCLES DESIRED DURING ITERATION
C                    1   FOR ONLY TWO FCF'S IMPUTED
C     SCAL           SCALING FACTOR
C     SDL            THE DESIRED UPPER LIMIT FOR ELEMENTS OF ERROR MATRIX
C     NCN            INTEGER FOR CHECKING NO. OF CYCLE DURING ITERATION
C     NW             0     READ PP,SCAL ETC. AGAIN
C                    1     READ FROM THE VERY BEGINNING
C     FF             FREQUENCY IN GROUND STATE
C     FP             FREQUENCY IN EXCITED STATE
C     SD             WEIGHTED STANDARD DEVIATION OF THE ERROR MATRIX
C     DDX            INPUT VALUE OF D
C     NF             VIBRATIONAL QUANTUM NO. FIXED AS STANDARD
C                    0  ALL THE FCF'S WILL BE CALCULATED WITHOUT ITERATIO
C     BETA           = FF/FP     SAME AS PRO IN HEILBRONNER'S NOTATION
C                                DIFFERENT FROM SMITH AND WARSOP'S NOTATIO
C
      DIMENSION TITLE(20),OFCF(40),CFCF(40),P(20),DF(20),AM(20),CM(20)
      DIMENSION NW(15),AJ(20),BJ(20)
      IR=5
      IW=6
      NT=1
      READ(IR,1) NSET
    1 FORMAT(15I5)
      READ(IR,1) (NW(I),I=1,NSET)
    5 READ(IR,10) TITLE
   10 FORMAT(20A4)
      WRITE(IW,20) TITLE
   20 FORMAT(1H1,///,10X,20A4/7X,'FRANCK-CONDON CALCULATION'/7X,'FRANCK-
     2CONDON CALCULATION'/)
      READ(IR,1) ND,MAX
      ND1=ND-1
      MAX1=MAX-1
      WRITE(IW,50) ND1,MAX1
   50 FORMAT(///,5X,'NO. OF OBSERVED FCF =',I3/5X,'NO. OF THE MAXIMUM
     2CF =',I3)
      READ(IR,60) (OFCF(I),I=1,ND)
```

```
C
C
   60 FORMAT(10F8.4)
C
C      NORMALIZATION OF OBSERVED FCF AND WEIGHING MATRIX
       IF(ND.LE.16) GO TO 430
       NDX=ND
       ND=16
  430 DMAX=OFCF(1AX)
       DO 85 I=1,ND
   85 OFCF(I)=OFCF(I)/DMAX
C      ESTIMATION OF GAMA FROM OBSERVED OFCF(1) AND OFCF(2)
       READ(IR,90) FF,FP
   90 FORMAT(10F8.2)
       BETA=FF/FP
       WRITE(IW,610) FF,FP,BETA
  610 FORMAT(/,5X,'FREQUENCY IN GROUND STATE =',F9.2/5X,'FREQUENCY IN E
      2CITED STATE =',F9.2/5X,'BETA =',F9.6,2X,' SAME AS PRO IN HEILBRON
      2ER NOTATION')
   98 IF(OFCF(1).EQ.0.) GO TO 910
       GAMA=(OFCF(2)/OFCF(1))*(1.+BETA)/(1.4142136*BETA)
       DELTA=0.5*GAMA
  910 BETA1=BETA+1.
       CX=-2.0*BETA/BETA1
       DO 710 M=1,ND
       MM=M-1
  710 AM(M)=(BETA**0.25)*SQRT(FACT(MM))/SQRT(BETA1*(2.**(MM-1)))
   93 READ(IR,95) NC,PP,SCAL
   95 FORMAT(I5,2F5.2)
       READ(IR,411) DDX,NF
  411 FORMAT(F9.6,I6)
       IF(DDX.EQ.0.) GO TO 420
       GAMA=DDX*SQRT(FP*0.017877)
       DELTA=0.5*GAMA
  420 CONTINUE
       IF(NF.GT.0) GO TO 422
       ND=NDX
       GO TO 440
  422 CONTINUE
       WRITE(IW,96) PP,SCAL
   96 FORMAT(5X,'POWER FOR WEIGHING MATRIX =',F5.2/5X,'SCALING FACTOR =
      2,F5.2)
       WRITE(IW,870) NF
  870 FORMAT(5X,'NF =',I3)
       NCN=1
       DO 86 I=1,ND
       IF(OFCF(I).GT.0.) GO TO 81
       P(I)=0.0
       GO TO 86
   81 P(I)=OFCF(I)**PP
   86 CONTINUE
       SUM=0.0
       DO 87 I=1,ND
   87 SUM=SUM+P(I)
       DO 89 I=1,ND
   89 P(I)=P(I)/SUM
C
C      CALCULATE AND NORMALIZE FCF FROM GAMA OBTAINED ABOVE
   97 CFCF(1)=1.
       CFCF(2)=1.4142136*BETA*GAMA/(1.+BETA)
```

```
C
C
C
      IF(ND.LT.3) GO TO 152
  440 DO 100 M=3,ND
      M1=M-1
      M2=M-2
  100 CFCF(M)=CFCF(M1)*(1.4142136*BETA*GAMA/((1.+BETA)*SQRT(FLOAT(M)))+
     2SQRT(FLOAT((M-1)/M))*(CFCF(M2)/CFCF(M1))*((1.-BETA)/(1.+BETA)))
C
      IF(NF.EQ.0) GO TO 450
      DMA=OFCF(NF)/CFCF(NF)
      DO 110 M=1,ND
  110 CFCF(M)=CFCF(M)*DMA
C
C     CALCULATION OF ERROR MATRIX USING FORMULA BY CHAU
      DO 102 I=1,ND
  102 DF(I)=OFCF(I)-CFCF(I)
  450 DM=CFCF(MAX)
      DO 103 I=1,ND
  103 CFCF(I)=CFCF(I)/DM
      IF(NF.GT.0) GO TO 460
      WRITE(IW,470)
  470 FORMAT(//,5X,'V',6X,'OBS FCF',6X,'CALC FCF'/)
      DO 480 I=1,ND
      N1=I-1
  480 WRITE(IW,490) N1,OFCF(I),CFCF(I)
  490 FORMAT(4X,I2,5X,F8.4,5X,F8.4)
      GO TO 170
  460 IF(BETA+1.) 104,104,200
  104 DO 120 I=1,ND
      I1=I-1
  120 AJ(I)=CFCF(I)*(2.*AM(I)*GAMA+2.*I*BB*CFCF(I1)/CFCF(I)*CM(I)/
     2CM(I1)*EXP(AM(I)-AM(I1)))
      SJ=0.0
      DO 800 I=1,ND
      IF(OFCF(I).EQ.0.) GO TO 800
      SJ=SJ+P(I)*AJ(I)*AJ(I)
  800 CONTINUE
      DO 820 I=1,ND
  820 AJ(I)=P(I)*AJ(I)/SJ
      WRITE(IW,130)
  130 FORMAT(//,5X,'V',6X,'OBS FCF',6X,'CALC FCF',6X,'JACOBIAN',6X,
     2'P(I)',3X,'NO. OF CYCLE'/)
      DO 140 I=1,ND
      N1=I-1
  140 WRITE(IW,150) N1,OFCF(I),CFCF(I),AJ(I),P(I),NCN
  150 FORMAT(4X,I2,5X,F8.4,5X,F8.4,5X,F8.4,5X,F8.4,6X,I2,2F12.4)
      SDD=0.
      DO 920 I=1,ND
      IF(OFCF(I).EQ.0.) GO TO 920
      SDD=SDD+DF(I)*DF(I)*P(I)
  920 CONTINUE
      SD=SQRT(SDD)
      WRITE(IW,930) SD
  930 FORMAT(5X,'STD DEVIATION =',F9.6)
  152 DD=GAMA/SQRT(FP*0.017877)
      WRITE(IW,155) GAMA,DD,OFCF(1),OFCF(2)
  155 FORMAT(//,5X,'GAMA =',F9.6,10X,'D =',F9.6,' 10**-20 GM**+0.5*CM**-
     21'/5X,'OFCF(1) =',F8.4,5X,'OFCF(2) =',F8.4)
```

```
C
C
C
      IF(NCN.GT.NC) GO TO 170
      NCN=NCN+1
      DGAMA=0.0
      DO 160 I=1,ND
      IF(OFCF(I).EQ.0.) GO TO 160
      DGAMA=DGAMA+DF(I)*AJ(I)
  160 CONTINUE
      GAMA=GAMA+SCAL*DGAMA
      GO TO 97
C
C     BETA GREATER THAN 1, HEILBRONNER'S FORMULA IS ADOPTED  HEL CHEM
C     ACTA VOL 54, P58 (1971)
  200 DELTA=0.5*GAMA
      BX=-4.*BETA*DELTA/BETA1
      DO 210 M=1,ND
      MM=M-1
      CALL SUMAT(BETA,MM,DELTA,SUM,SUX)
      AC=AM(M)*EXP(CX*(DELTA**2))
  210 AJ(M)=BX*AC*SUX+AC*SUM/DELTA
      SS=0.0
      DO 810 I=1,ND
      IF(OFCF(I).EQ.0.) GO TO 810
      SS=SS+P(I)*AJ(I)*AJ(I)
  310 CONTINUE
      DO 830 I=1,ND
  830 AJ(I)=P(I)*AJ(I)/SS
      WRITE(IW,130)
      DO 570 I=1,ND
      N1=I-1
  570 WRITE(IW,150) N1,OFCF(I),CFCF(I),AJ(I),P(I),NCN
      GAMA=2.*DELTA
      DD=GAMA/SQRT(EP*0.017877)
      SDD=0.
      DO 560 I=1,ND
      IF(OFCF(I).EQ.0.) GO TO 560
      SDD=SDD+DF(I)*DF(I)*P(I)
  560 CONTINUE
      SD=SQRT(SDD)
      WRITE(IW,600) GAMA,DD,SD
  600 FORMAT(//,5X,'GAMA =',F9.6,10X,'D =',F9.6,' 10**-20 GM**+0.5*CM**
     21'/5X,'STD DEVIATION =',F9.6)
      IF(NCN.GT.NC) GO TO 170
      NCN=NCN+1
      DDELTA=0.
      DO 550 I=1,ND
      IF(OFCF(I).EQ.0.) GO TO 550
      DDELTA=DDELTA+DF(I)*AJ(I)
  550 CONTINUE
      DELTA=DELTA+SCAL*DDELTA
      GAMA=2.*DELTA
      GO TO 97
  170 CONTINUE
      NT=NT+1
      IF(NT.GT.NSET) GO TO 180
      IF(NW(NT).GT.0) GO TO 5
      GO TO 93
  180 CONTINUE
```

```
C
C
C
      STOP
      END
C
C
      FUNCTION FACT(I)
      IF(I.GT.0) GO TO 5
      FACT=1.
      GO TO 20
    5 IFACT=1
      DO 10 N=1,I
      IFACT=IFACT*N
   10 CONTINUE
      FACT=FLOAT(IFACT)
   20 CONTINUE
      RETURN
      END
C
C     SUBTOUTINE USED TO CALCULATE SUMATION OF HERMITE POLYNOMIALS
      SUBROUTINE SUMAT(BETA,M,DELTA,SUM,SUX)
      DD=-4.*DELTA*SQRT(BETA)/(1.+BETA)
      IF(M.GT.0) GO TO 3
      SUM=0.
      SUX=1.
      GO TO 60
    3 CONTINUE
      IF(MOD(M,2).GT.0) GO TO 40
      MX=M/2
      SUX=(((BETA-1.)/(BETA+1.))**MX)/FACT(MX)
      SUM=0.
      DO 30 IP=2,M,2
      MP=(M-IP)/2
      SUX=SUX+(DD**IP)*(((BETA-1.)/(BETA+1.))**MP)/(FACT(IP)*FACT(MP))
   30 SUM=SUM+IP*(DD**IP)*(((BETA-1.)/(BETA+1.))**MP)/(FACT(IP-1)*FACT(
     JP))
      GO TO 60
   40 SUM=0.
      SUX=0.
      DO 50 IP=1,M,2
      MP=(M-IP)/2
      SUX=SUX+(DD**IP)*(((BETA-1.)/(BETA+1.))**MP)/(FACT(IP)*FACT(MP))
   50 SUM=SUM+IP*(DD**IP)*(((BETA-1.)/(BETA+1.))**MP)/(FACT(IP-1)*FACT(
     UP))
   60 CONTINUE
      RETURN
      END


$SIG
```

APPENDIX III. Approximation Method for Evaluation of Force Constants of Ions.

The $\underline{Fs}$, $\underline{Ls}$ and $\underline{\Lambda}$ matrices in the ground state are related to one another by[109]

$$\underline{\Lambda} = \underline{L_s^t}\ \underline{F_s}\ \underline{L_s} \tag{A1}$$

In the ionic state, a similar relation is obtained

$$\underline{\Lambda'} = (\underline{L_s'})^t\ \underline{F_s'}\ \underline{L_s'} \tag{A2}$$

Upon subtracting eqn. (A2) by eqn. (A1), expanding and regrouping, one obtains

$$\underline{\Delta\Lambda} = (\underline{L_s^t}\ \underline{F_s} + \underline{L_s^t}\ \underline{\Delta F_s} + \underline{\Delta L_s^t}\ \underline{F_s} + \underline{\Delta L_s^t}\ \underline{\Delta F_s})\ \underline{\Delta L_s} +$$

$$(\underline{L_s^t} + \underline{\Delta L_s^t})\ \underline{\Delta F_s}\ \underline{L_s} + \underline{\Delta L_s^t}\ \underline{F_s}\ \underline{L_s} \tag{A3}$$

where $\underline{\Delta\Lambda} = \underline{\Lambda'} - \underline{\Lambda}$, $\underline{\Delta F_s} = \underline{F_s'} - \underline{F_s}$, and $\underline{\Delta L_s} = \underline{L_s'} - \underline{L_s}$

Usually $\underline{\Delta Ls}$ is very small compared to $\underline{\Delta F_s}$. By neglecting terms with $\underline{\Delta Ls}$, a simple relation is arrived at for $\underline{\Delta\Lambda}$ and $\underline{\Delta F_s}$

$$\underline{\Delta\Lambda} = \underline{L_s^t}\ \underline{\Delta F_s}\ \underline{L_s} \tag{A4}$$

or

$$\underline{\Delta F_s} = (\underline{L_s^t})^{-1}\ \underline{\Delta\Lambda}\ (\underline{L_s})^{-1} \tag{A5}$$

The expression (A5) provides a method to calculate $\underline{Fs}'$ if $\underline{Fs}$, $\underline{Ls}$, $\underline{\Lambda}$ and $\underline{\Lambda}'$ are known.

In order to check the validity of the method, calculations were performed on both the $^2B_1$ and $^2A_1$ states of H_2O. Values of f_r and f_α thus obtained are, respectively, 5.725 and 0.551 mdyn/Å for the $^2B_1$ state and 7.690 and 0.273 mdyn/Å for the $^2A_1$ state which agree well with those from the rigorous method (Table 6).

It should be noted that the approximation method enables one to estimate values for the force constants of an ion even though the geometry is unknown. If the number of observed frequencies is less than that of the force constants to be determined, computation of f_r or f_α or both, still can be done by assuming that the interaction force constants and the difference in the unobserved frequency $\Delta\lambda_i$ are zero. The numerical values of f_r for H_2Se and H_2Te in the $^2B_1$ state were obtained in this way.